REPORT DOCUMENTATION PAGE

Form Approved
OMB No. 0704-0188

1. AGENCY USE ONLY (Leave blank)	2. REPORT DATE	3. REPORT TYPE AND DATES COVERED
		FINAL 01 Dec96 to 30 Nov 97

4. TITLE AND SUBTITLE
INTERNATIONAL CONFERENCE ON ORGANIC NONLINEAR OPTICS III

5. FUNDING NUMBERS
F49620-97-1-0039
1651/01
62173C

6. AUTHOR(S)
Dr Mark G. Kuzyk

AFOSR-TR-97
0516

7. PERFORMING ORGANIZATION NAME(S) AND ADDRESS(ES)
Dept of Physics,
Washington State University
Pullman WA 99164-2814

9. SPONSORING / MONITORING AGENCY NAME(S) AND ADDRESS(ES)
AFOSR/NL
110 Duncan Ave Room B115
Bolling AFB DC 20332-8050

Dr Charles Y-C. Lee

10. SPONSORING / MONITORING AGENCY REPORT NUMBER

11. SUPPLEMENTARY NOTES

12a. DISTRIBUTION / AVAILABILITY STATEMENT

Approved for public release;
distribution unlimited.

19971021 249

E

13. ABSTRACT *(Maximum 200 words)*

The objective of ICONO'3 was to bring together top researchers - whose expertise spans materials design, material characterization, device fabrication, and integrated device architectures - to the captive setting of a small island to discuss and assess progress in the field of organic nonlinear optics (meeting headquarters on Marco Island, Florida). AFOSR funds were used to partially offset the travel expenses of U.S. invited speakers and students. This conference was motivated by 2 previous AFOSR-supported conference sessions that were held in Val Thorens, France in the Winter of 1994 (ICONO'1); and in Kusatsu, Japan in the summer of 1995 (ICONO'2). The demand for such a meeting was evidenced by full-capacity attendance at the last three meetings (ICONO'1 ICONO'2 and ICONO'3). The meeting has succeeded in bringing together a group of internationally distinguished researchers to the United States to rigorously discuss and asses the field. (a majority of attendees were from abroad).

14. SUBJECT TERMS			15. NUMBER OF PAGES
			16. PRICE CODE
17. SECURITY CLASSIFICATION OF REPORT (U)	18. SECURITY CLASSIFICATION OF THIS PAGE (U)	19. SECURITY CLASSIFICATION OF ABSTRACT (U)	20. LIMITATION OF ABSTRACT (UL)

International Conference on Organic Nonlinear Optics III (ICONO'3)- Final Report

Mark G. Kuzyk
Department of Physics, Washington State University, Pullman, WA 99164-2814

October 1, 1997

GRANT # F496209710039

FINAL REPORT TO AFOSR

REPORT PERIOD: 01 Dec 96 - 30 Nov 97

Summary

The objective of ICONO'3 was to bring together top researchers - whose expertise spans material design, material characterization, device fabrication, and integrated device architectures - to the captive setting of a small island to discuss and assess progress in the field of organic nonlinear optics (meeting headquarters on Marco Island, Florida). AFOSR funds were used to partially offset the travel expenses of U.S. invited speakers and students. This conference was motivated by 2 previous AFOSR-supported conference sessions that were held in Val Thorens, France in the Winter of 1994 (ICONO'1); and in Kusatsu, Japan in the Summer of 1995(ICONO'2). The demand for such a meeting was evidenced by full-capacity attendance at the last three meetings (ICONO'1, ICONO'2 and ICONO'3). The meeting has succeeded in bringing together a group of internationally distinguished researchers to the United States to rigorously discuss and asses the field. (A majority of attendees were from abroad.)

Technical Information

The symposium provided a forum for discussion of recent developments in studies of nonlinear-optical processes in organic and polymeric systems and their applications in pho-

tonic technologies. The topics focused on fundamental issues in nonlinear-optical experiments and theory and on novel optical guided-wave devices and architectures.

Specifically, areas of discussion included:

- Theory of molecular hyperpolarizabilities
- Design and synthesis of new molecules for nonlinear optics
- Characterization of linear and nonlinear optical properties
- Oriented thin film preparation and characterization
- Thermal stability issues
- Electroluminescence and photoluminescence
- Thin film processing for nonlinear waveguiding applications
- Photorefractive effects in organic materials
- Temporal response in organic systems
- Organic single crystal growth for parametric conversion
- Electrooptic measurements
- Device applications including image processing and recognition, electrooptic modulation, switching, nonlinear couplers, optical bistability, etc.

Publications

A copy of the conference proceedings is enclosed. Full conference papers were submitted to a special issue of the Journal of the Optical Society of America B that is dedicated to organic nonlinear optics. The volume is being edited by Professors Kuzyk, Singer, and Twieg. The papers were reviewed according to the Optical Society's high standards and has resulted in a high-quality two-issue set with 4 dozen papers. These two volumes are slated to appear in January and February of 1998. The last such issue appeared in 1986.

Impact

The interdisciplinary interactions and exchanges between internationally renowned leaders in the field resulted in new perspectives that can be brought to bear to develop a

nonlinear-optics-based technology. Furthermore, because this conference attracted a large international group, this gave us the opportunity to better asses the status of our foreign competitors. Our overseas colleges have made many scientific leaps since the last meeting.

Student Training

Many students participated at ICONO'3 as attendees and as poster/oral authors. They had the opportunity to meet with researchers in their own area of specialty and in areas that are not as familiar to them. These interactions gave students first-hand experience in the importance of multidisciplinary interactions and collaborations. Note that many students have coauthored papers that will appear in the special issue of JOSA B.

ICONO'3

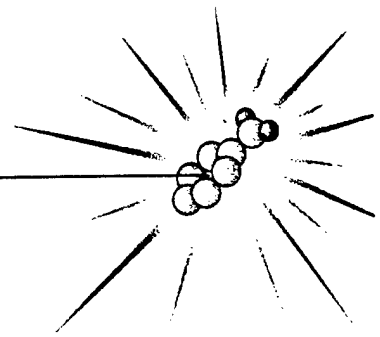

Third International Conference on Organic Nonlinear Optics

Marco Island, Florida
December 16-20, 1996

Conference Location

Marriot's Marco Island Resort and Golf Club
400 South Collier Boulevard
Marco Island, Florida 33937

Tel: 1-941-394-2511 Fax: 1-941-642-2682

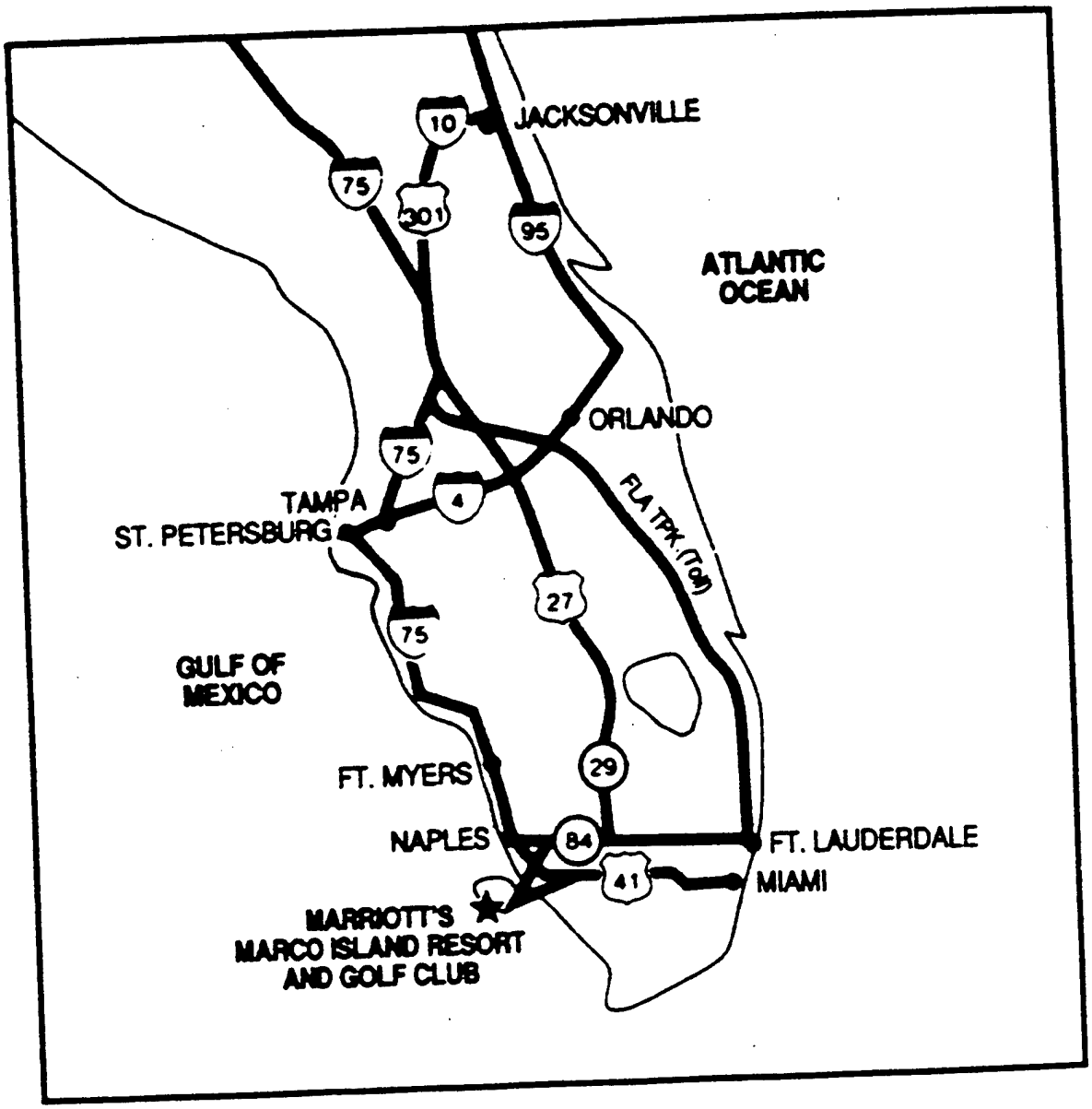

Organizing Committee

Mark G. Kuzyk, Conference Chair
Department of Physics
Washington State University
Pullman WA 99164-2814
Tel: 1-509-335-4672
Fax: 1-509-335-7816
e-mail: mark_kuzyk@wsu.edu

François Kajzar, European Chair
Commissariat A L'Energie Atomique
DEIN/SPE, bât 451, CEN de Saclay
F-91191 Gif-sur-Yvette Cedex, France
Tel: 33-1-69-08-6810
Fax: 33-1-69-08-7679
e-mail: kajzar@serin.cea.fr

Siezo Miyata, Pacific Chair
Tokyo University of Agriculture and Technology
Koganei, Tokyo, 184
Japan
Tel: 81-423-88-7054
Fax: 81-423-86-1084
e-mail: miyata@cc.tuat.ac.jp

Local Organizing Committee

Jamie O'Neal
CREOL
University of Central Florida
P.O. Box 162700
4000 Central Florida Blvd.
Orlando, FL 32816-2700
Tel: 1-407-823-6916
Fax: 1-407-823-6955
e-mail: jamie@creol.ucf.edu

George Stegeman
CREOL
University of Central Florida
P.O. Box 162700
4000 Central Florida Blvd.
Orlando, FL 32816-2700
Tel: 1-407-823-6915
Fax: 1-407-823-6955
e-mail: george@creol.ucf.edu

Kenneth Wynne
Organic and Polymeric Materials - 331
Office of Naval Research
800 N. Quincy St.
Arlington, VA 22217-5660
Tel: 1-703-696-4315
Fax: 1-703-696-6887
e-mail: wynnek@onrpo2.onr.navy.mil

Program Committee

Kenneth Singer, Program Chair
Department of Physics
Case Western Reserve University
Cleveland, OH 44106-7079
Tel: 1-216-368-4017
Fax: 1-216-368-4671
e-mail: kds4@po.cwru.edu

Acknowledgements

Conference Sponsors

National Science Foundation
Office of Naval Research
Allied Signal
Lockheed
Hitachi
AKZO

Coffee Break Sponsors

Center for Research and Education in Optics and Lasers (CREOL)
Molecular Opto-Electronic, Corp (MOEC)
Coherent Laser Group, Inc.
Spectra Physics Lasers

Third International Conference on Organic Nonlinear Optics
December 16 - 20, 1996 Marco Island, Florida

Agenda

Thanks to AFOSR for supporting the
Symposium on Polymers and Photonic Materials
Tuesday December 17

Time	Monday	Tuesday	Wednesday	Thursday	Friday
7:30		Breakfast	Breakfast	Breakfast	Breakfast
8:30		I-1	I-6	I-15	I-23
8:55		O-1	O-5	O-11	O-18
9:15		O-2	O-6	O-12	I-27
9:35		I-2	O-20	I-16	I-24
10:00		Coffee	Coffee	Coffee	Coffee
10:30		I-3	I-8	I-17	I-25
10:55		O-3	O-7	O-13	I-7
11:15		O-4	O-8	O-14	O-21
11:35		I-4	I-9	I-18	O-22
11:55		I-5	I-10	I-19	I-26
12:20		Lunch	Lunch	Lunch	Lunch
13:30		FREE	FREE	FREE	
14:30		FREE	FREE	FREE	
15:30		FREE	FREE	FREE	
16:40			O-9	O-15	
17:00	Hors d'oeuvres	Posters and Hors d'oeuvres	I-11	I-20	
17:25			I-12	O-16	
17:45			I-13	I-21	
18:10	Plenary		O-10	O-17	
18:30			I-14	I-22	
18:55	Dinner	Dinner	Dinner	Dinner	

Session Chairs

	Tuesday	Wednesday	Thursday	Friday
Breakfast to Break	S. Miyata	Charles Lee	Francois Kajzar	Joe Zyss
Break to Lunch	Hiro Sasabe	N.J. Kim	Ken Wynne	K. Sasaki
Evening	W. Haase	Warren Herman	Andre Knoesen	

Table of Contents

Nonlinear Optics of Organics; Fundamentals and Devices

N. Bloembergen
Harvard University

A broad historical review of the use of organic and polymeric materials in nonlinear optics is presented, based on their second and third order complex nonlinear susceptibilities. Guided wave structures, quasi-phase matching, symmetry and pulse propagation characteristics will be among the properties reviewed.

Bandwidth Limitations of Current Plastic Optical Fiber

C. Koeppen, G. Jiang, W. D. Chen, R. F. Shi, and A. F. Garito

Department of Physics and Astronomy, University of Pennsylvania, Philadelphia PA 19104

Plastic optical fibers (POF) continue to attract study for possible applications in short distance communication systems such as local area networks (LANs), data links, and multi-noded bus networks. In our presentation, we will discuss results of our theoretical and experimental studies of POFs, centering on the relationship between the observed refractive index profile and optical bandwidth.

With advances in polymer materials and fabrication techniques, the optical loss typically observed for POFs has dropped considerably. For example, we have measured PMMA-based step index (SI) POF samples at 650 nm that have an optical loss of 110 dB/km, which is approaching the theoretical limit of 106 dB/km. The main issue has now become the attainable optical bandwidth, which in POFs is limited primarily by intermodal dispersion.

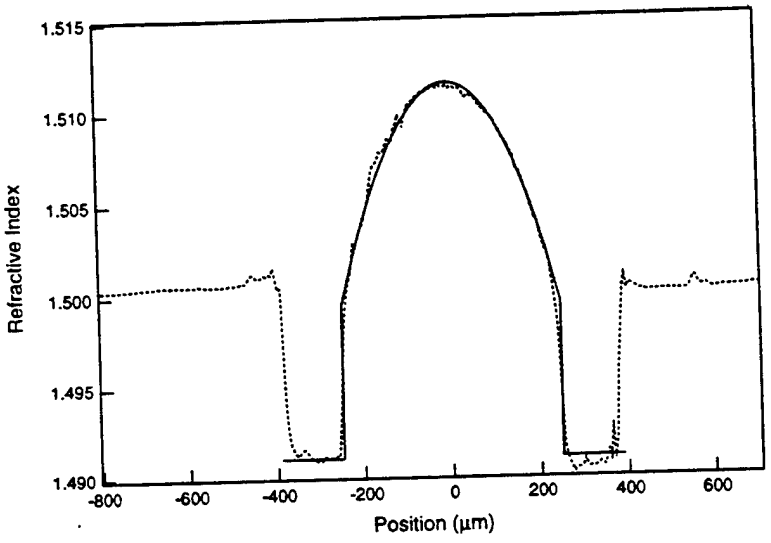

Figure 1. Refractive index profile of GI POF: Exp. (dotted) and Theo. (solid).

The large core diameter and large numerical aperture typical of POF results in millions of guided modes, all traveling at their own characteristic speed. Such dispersion is most severe in SI POF, which is the only widely available POF today. It has long been known for optical fibers that by making the refractive index a smoothly varying gradient, the intermodal dispersion can be greatly reduced. We have studied this relationship between refractive index profile and optical bandwidth in considerable detail with experimental measurements and theoretical calculations. Our theoretical studies are based on finite element analysis and the WKB approximation in addition to power series methods.

We have measured the bandwidth behavior for a variety of POFs using time domain methods. GI POF samples made by a co-polymerization method show an impressive bandwidth of 3 GHz for a 100 meter length. However, what we have found in our studies is that the 3 GHz-100 m bandwidth-length product is still far below the potential of an optimal GI fiber and that the origin of this limited bandwidth is the actual refractive index profile itself. We have developed a near field refractive measurement technique especially suited for POF that enables us to perform highly accurate measurements of the refractive index profile of GI POF. Using our theoretical methods, we identify prominent features typically seen in the refractive index profile of current SI and GI POFs that are likely responsible for the observed bandwidth performances.

Our theoretical models based on the measured profile quantitatively explain the reduced bandwidth observed compared to that of the ideal profile. Additionally, these models reveal the regions of the current GI POF index profile that must be improved for optimal performance. By comparing the theoretically calculated bandwidths with experimental measurements, we further have found strong evidence that the mode distribution is inhomogenous and that there exists mode coupling which strongly affects the observed bandwidth. Work is now underway here at Penn to develop high speed optical fiber for data communications.

POLYMER OPTICAL FIBER AND AMPLIFIER

Yasuhiro Koike, Eisuke Nihei, Takaaki Ishigure, Takeyuki Kobayashi and Keisuke Sasaki

Faculty of Science and Technology, Keio University, Yokohama 223, Japan
Kanagawa Academy of Science and Technology, Yokohama 236, Japan

1. High-speed and Low-loss Polymer Optical Fiber

We have proposed a high bandwidth graded-index polymer optical fiber (GI POF), and have demonstrated several giga bit per second (Gbit/s) transmission in the 100 m GI POF link[1]. The attenuation of transmission of the PMMA base GI POF is shown in Fig. 1. The minimum attenuation was about 150 dB/km at 0.65-μm wavelength which was almost the same as that of the step-index type POF commercially available.

However, the attenuation of PMMA base POF was abruptly increased from about 0.6-μm wavelength to the infrared region due to the absorption loss of overtones of carbon-hydrogen stretching vibration. The attenuation spectra of perdeuterated (PD) and perfluorinated (PF) polymer GI POFs measured by conventional cut-back method are also shown in Fig. 1. It is quite noteworthy that the PF polymer base GI POF has no serious absorption peak in the range of 0.5 - 1.3 μm wavelength and the attenuation even at 1.3-μm wavelength is about 50 dB/km.

Theoretical attenuation spectrum of the PF polymer base POF was estimated by the summation of scattering and absorption losses. The result is shown in Fig. 2. Here, it was assumed that the absorption peak at 1.361 μm was the Gaussian profile with 0.020-μm full width half maximum. It is indicated that the attenuation limit of the PF polymer base GI POF at 1.3-μm wavelength is approximately 0.3 dB/km which is comparable with that of silica fiber (0.2 dB/km).

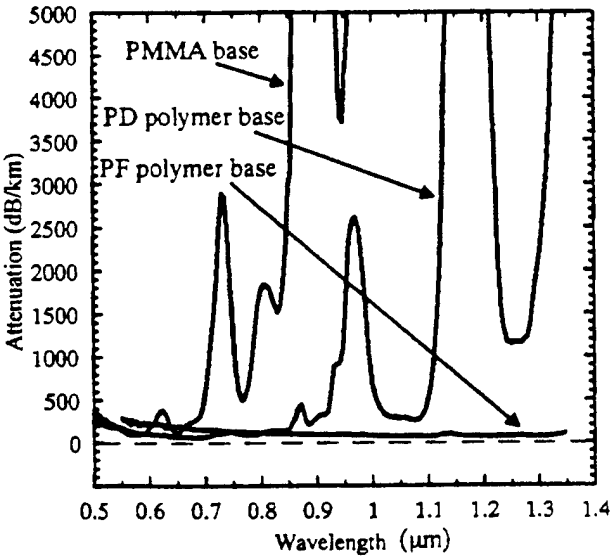

Fig. 1
Experimental attenuation spectra of GI POFs.

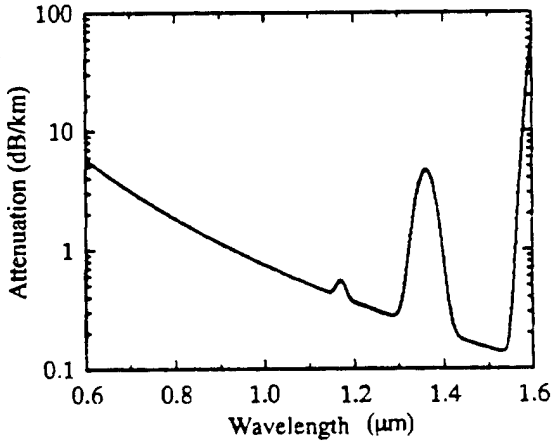

Fig. 2
Calculated attenuation spectrum of PF polymer base POF.

2. Polymer Optical Fiber Amplifier

In quest of high-power, compact and coherent light sources in the visible, we incorporated organic dyes into polymer optical fibers by means of the interfacial-gel polymerization technique[2]. Organic dyes were chosen as gain media because of the physical properties they exhibit: a large emission cross section, which allows the achievement of high gains in a short length, and a broadband fluorescence spectrum that provides wide tunability (Fig. 3).

A Rhodamine B-doped polymer optical fiber amplifier, 1 m in length and 300 μm in core diameter, has exhibited 36 dB signal gain and 1200 W output power when optically pumped at a wavelength of 532 nm. Furthermore, we have obtained the optical amplification covering most of the spectral range from 560 nm to 650 nm (Fig. 4). The prospect is that the spectral range in the visible can be continuously covered with the polymer optical fiber amplifiers doped with several selected dyes.

We successfully combined the excellent properties of polymer optical fibers (large core diameter) and organic dyes (large emission cross section) to generate high-power light pulses. The organic dye-doped polymer optical fiber amplifiers offer a high-power coherent light source with minimum maintenance and an easy change of wavelengths, and are currently under further investigation with a view to applications in such diverse fields as medicine and industry.

References

1. Y. Koike, T. Ishigure, E. Nihei, *IEEE J. Lightwave Technol.*, **13**, 1475 (1995)
2. A. Tagaya, S. Teramoto, T. Yamamoto, K. Fujii, E. Nihei, Y. Koike, and K. Sasaki, *IEEE J. Quantum Electron.*, **31**, 2215 (1995)

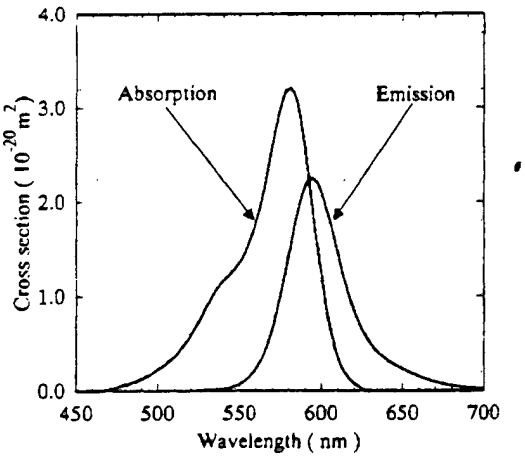

Fig. 3
Absorption and emission spectra of Rhodamine 101 in PMMA.

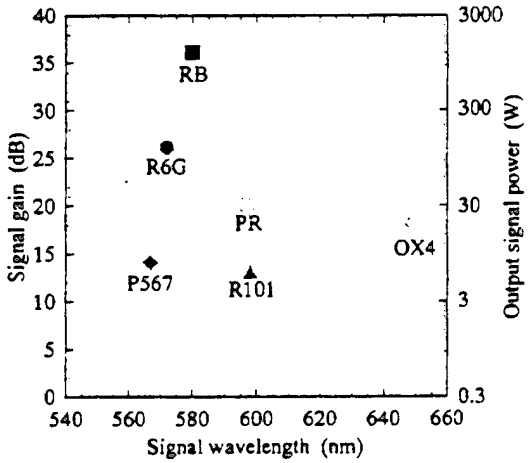

Fig. 4
Measured signal gain and output power against signal wavelengths for Rhodamine B (RB)-doped, Rhodamine 6G (R6G)-doped, Rhodamine 101 (R101)-doped, Pyrromethene 567 (P567)-doped, Perylene red (PR)-doped, and Oxazine 4 (OX4)-doped polymer optical fiber amplifiers.

A Highly Luminous Interface-Controlled EL device

S. Miyata, T. Iihama, H. Suzuki, R. Tethui, H. Yamamoto, T. Watanabe
Graduate School of Bio-Applications &Systems Engineering
Tokyo University of Agriculture & Technology
2-24-16 Nakamachi Koganei-shi, Tokyo 184, Japan

1. INTRODUCTION

Organic materials have been expected to be applicable for practical electroluminescent (EL) devices because of their high fluorescence efficiency and semiconducting properties. The adoption of organic heterostructure to the EL devices was very effective in the improvements of carrier confinement in the emission region in organic EL devices.[1] One of problems for EL devices is the peeling of the cathode electrode from organic layers which cause the shortening of the life time. In order to improve this problem metal organic interface was prepared by co-evaporating technique. In this presentation, we investigate the effect of controlling of the metal organic interface on EL characteristic.

2. EXPERIMENTAL

For the hole transport layer (HTL), poly(N-vinyl carbazole) PVCz was used. The cell structure was Mg/electron transport and emitting layer/hole transport layer/ITO. The all layers except PVCz were prepared by vacuum deposition. In order to improve the hole drift mobility, N,N'-diphenyl-N,N'-bis(3-methylphenyl)-1,1-biphenyl-4,4-diamne (TPD) was doped into PVCz layer. The weight ratio between TPD and PVCz was 1:1. The PVCz film was prepared by dip-coating method onto ITO glass plate. The thickness of obtained film was about 50 nm. Tris(8-quinolinolate)aluminum (III) complex (Alq_3) was deposited onto PVCz layer with 30 nm thick. In order to improve the metal organic interface, the co-evaporating technique was applied to the preparation of cathode electrode. The 3 nm thick magnesium/Alq_3 composite layer (20:1 of weight ratio) was prepared on an emitting layer as shown in Figure 1(b). Finally 300 nm

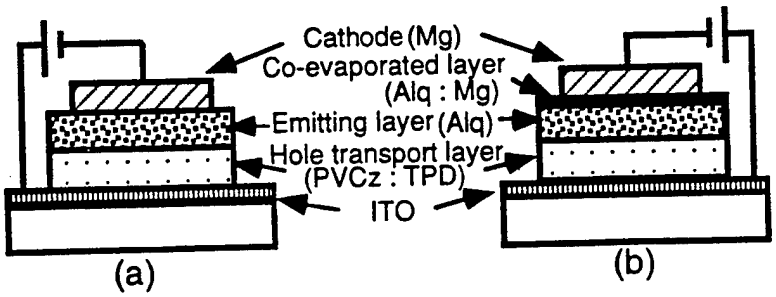

Fig. 1 Configuration of the EL devices.
(a) : Conventional multi-layer EL device
(b) : Interface-controlled EL device

of magnesium was deposited as cathode electrode. For the comparison the conventional EL devices without co-evaporated metal-organic layer were also prepared as shown in Figure 1(a). Current-voltage characteristics were measured by an electrometer.

3. Results and Discussions

Figure 2 shows the current-voltage characteristics of the EL device which used Alq_3 as an emitter material. The TPD doped PVCz layer can transport only holes and inject them efficiently into the emitting layer. The EL emission threshold of interface-controlled device is slightly smaller than that of conventional multi-layer EL devices. Brightness and color were uniform over the whole emitting area, and no discharge was found till bias voltage of 12 V. Green EL emission was observed only in forward bias which is ascribed to the Alq_3. Above bias voltage of 8 V, the difference of current-voltage and EL characteristic between two EL cells clearly observed. The current and EL intensity of interface-controlled EL device is 1.4 and 2 times larger than that of conventional multi-layer EL devices, respectively. The interface-controlled EL device shows the highest brightness 25,000 cd/m^2 at the condition of 1000 mA/cm^2. The luminance efficiency of interface-controlled EL device was found to be 2.3 lm/W. These results suggest that the co-evaporation of magnesium and Alq_3 assists the electron injection from cathode electrode. The morphology of normal magnesium surface and co-evaporated Alq_3/ magnesium surface was observed by scanning probe microscope. The surface of co-evaporated metal-organic layer seems to be more smooth than that of normal vacuum deposited magnesium electrode. This result indicates that the co-evaporated Alq3 may help the nucleation of magnesium which results in the formation of toughened and smooth magnesium electrode. The decay of the emission intensity was also improved by the introduction of co-evaporating metal-organic layer.

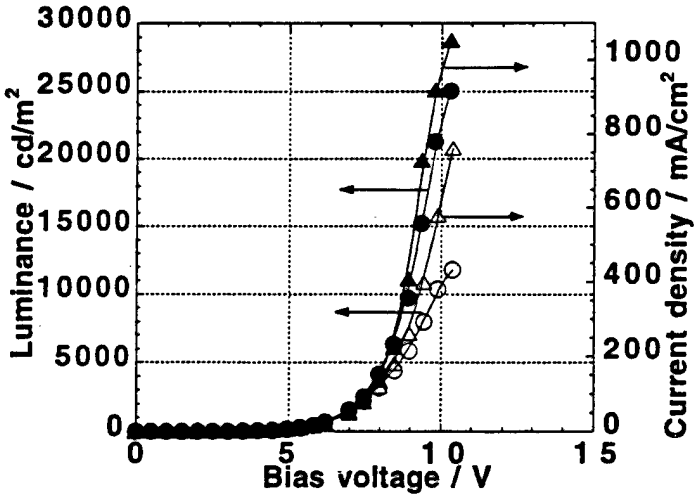

Fig. 2. Luminance and current density of EL devices as a function of voltage. (Filled marks : Interface-controlled EL device, Open marks : Conventional multi-layer EL device)

4. Reference

[1] C. W. Tang and S. A. Vanslyke, Appl. Phys. Lett., **51**, 913(1987).

NONLINEAR OPTICAL PROPAGATION

IN

BULK ORGANIC CRYSTALS

William E. Torruellas
Department of Physics
Washington State University
Pullman, WA 99164

Joseph Zyss
C.N.E.T., 196 Av. Henri Ravera
92220 Bagneux, France

David J. Hagan, Eric W. VanStryland
C.R.E.O.L., University of central Florida
Orlando, Florida 32826

ABSTRACT

Parametric second order nonlinear optical effects resulting in temporal and spatial self-action will be presented in bulk NLO organic crystals. In particular the case of NPP, a molecular single crystal with one of the largest phase-matchable second order nonlinear coefficients known has been investigated.

The nonlinear phase front distortion imposed on the propagation of a fundamental plane wave as it propagates in a phase-matched quasi resonant second order structure is represented in the low depletion approximation by the following expression:

$$n_2^{eff} = \frac{2\omega d_{eff}^2}{c^2 \varepsilon_o n_1^2 n_2} \frac{[1-\mathrm{sinc}(\Delta k.L)]}{\Delta k.L} L \qquad \text{Eq.1}$$

From a materials point of view, the figure of merit $d^2/n_1{}^2 n_2$ is the same one used for second-harmonic generation. Under that consideration alone, organic materials being well known for their large figures of merit among phase-matchable second order nonlinear optical structures should be well suited for all optical applications based on "cascading". Indeed NPP, for example, is known to possess one of the largest phase-

matchable coefficients known, approximately 85 pm/V, resulting in an excellent figure of merit both for SHG and cascaded nonlinear optical effects.

We will present experimental results showing strong cascaded second order contributions to the nonlinear propagation in NPP. For example, nonlinear switching experiments at 1064nm have been performed. In all cases Eq.1 fails to accurately predict the nonlinear phase distortion accumulated by the fundamental beam and scale properly the effective nonlinearities. To accurately predict such cascaded nonlinear interactions we have developed a spatio-temporal beam propagation code which takes into account diffraction and group velocity dispersion. More importantly in the case of highly dispersive materials such as NPP our modeling includes the effects of spatial and temporal walk-off induced by dispersion of the refractive indexes and natural birefringence. Because of the length dependence of the effective nonlinearity, Eq.1, the effect of walk-off in time or space will be discussed as an important designing factor for the implementation of future devices based on cascaded nonlinear interactions. Device concepts and requirements will be presented.

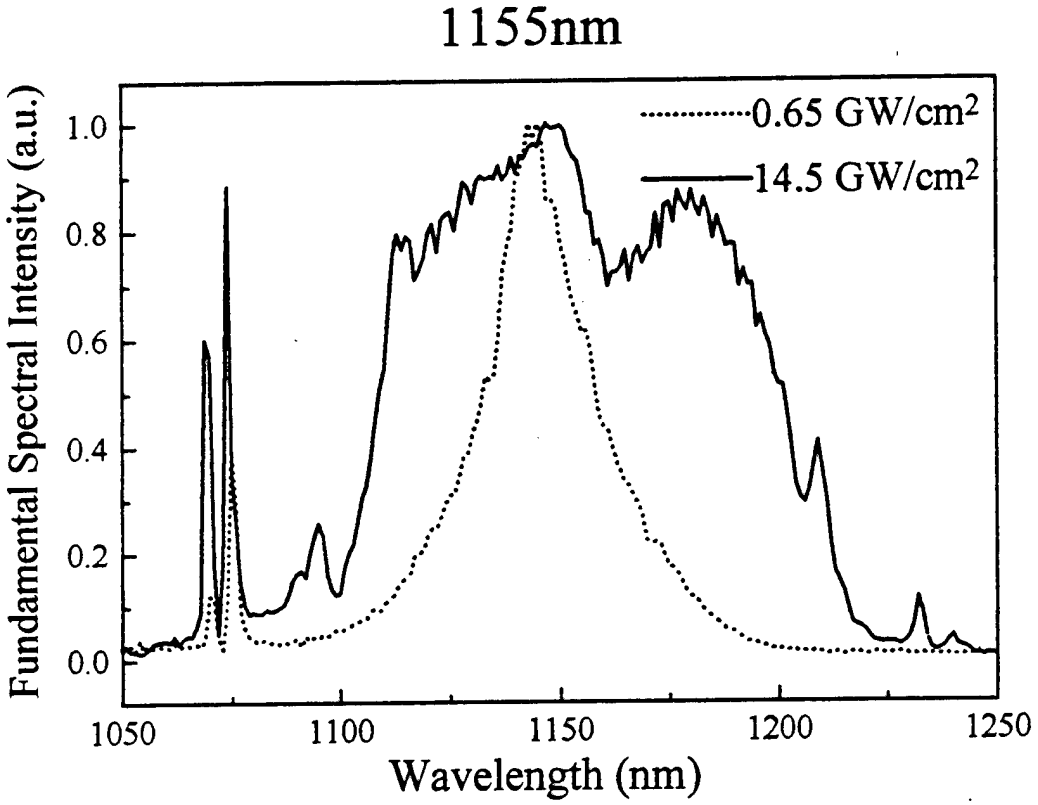

The above figure shows the cascaded effect on the spectrum of a femtosecond fundamental beam close to the non-critical-phase-matching wavelength of NPP. Large self-phase-modulation and self action effects were observed.

HYPER-STRUCTURED MOLECULES FOR PHOTONIC APPLICATIONS

Tatsuo Wada, Yadong Zhang and Hiroyuki Sasabe
Frontier Research Program, The Institute of Physical and Chemical Research (RIKEN)
2-1 Hirosawa, Wako, Saitama 351-01, Japan

A great deal of interest surrounds development of organic photorefractive materials because of their potential application for real-time holography.[1] The requirements for photorefractivity are usually achieved by using multicomponents, each of which fulfill a single requirement. On the other hand, we have applied multifunctional chromophores to a new class of organic photorefractive materials. The multifunctional chromophores fulfill all the requirements and enable the development of "monolithic" photorefractive materials. In this paper, we present novel molecular architecture of hyper-structured molecules for photonic applications as a multifunctional material and also discuss their optical image processing applications using photorefractive effects.

New class of opto and electroactive materials: hyper-structured molecules have been developed as shown in Figure 1. Star burst dendrimers and cyclic oligomers etc. have sparked new development in both organic and macromolecular chemistry.

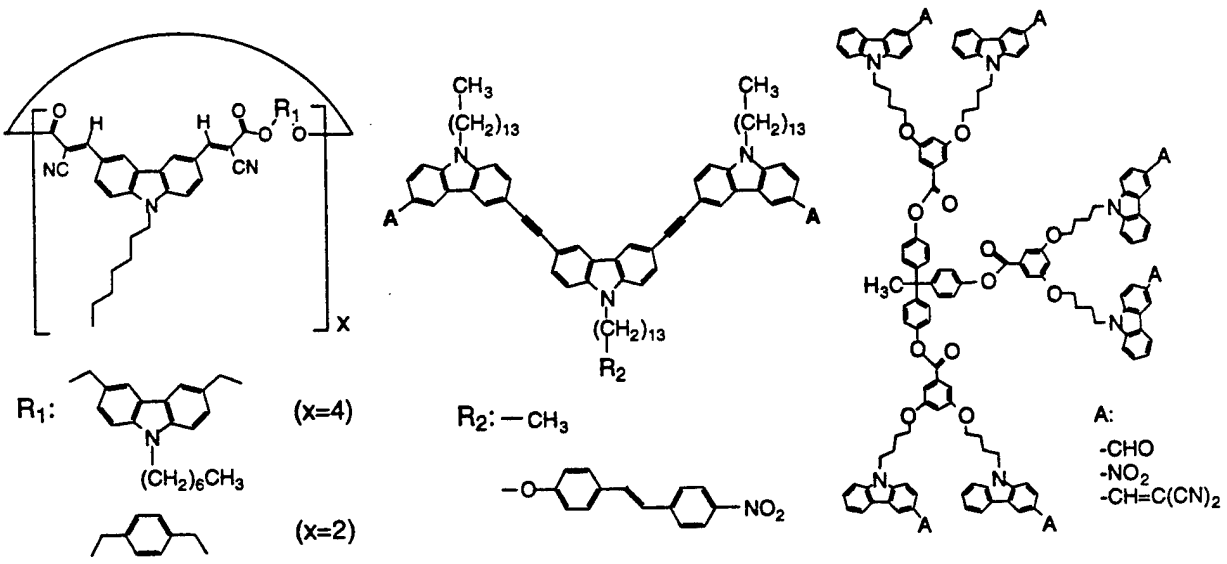

Figure 1. Hyper-structured molecules: carbazole cyclic oligomers, conjugated trimers and dendrimers.

Recently we synthesized a cyclic carbazole oligomer[2] besides head-to-tail carbazole dimers, trimers and main-chain polymers. This cyclic oligomers have alternating units of acceptor-substituted carbazole and arene moieties connected through 3, 6-linkages of carbazole. Acceptor-substituted carbazoles appeared to be very promising for second-order nonlinear optical chromophores.[3] We also synthesized carbazole dendrimers and conjugated trimers as a hyper-structured molecule.[4] Although functionalized polymers have been developed as a macroscopic material, they have distributions of molecular weight, number and size of free volume, and structures. On the other hand these carbazole oligomers can be considered as a perfectly defined structure.

Carbazole dendrimers can be formed molecular solid films by spin-coating and these films can be poled at an elevated temperature. We observed an asymmetric optical energy exchange in the two beam coupling in the poled dendrimer film at a wavelength of 532 nm. Unlike multicomponent photorefractive materials, the phase shift without any external electric field was determined to be 90 °. We also obtained efficient photorefractive effects on conjugated carbazole trimers. Spectral response of photorefractivity can be sensitized by formation of charge-transfer complexes between cental carbazole moiety and an electron-acceptor. Electric field-induced alignment and thermal relaxation of hyper-structured molecules can be controlled by the molecular-level tuning of the size, shape, surface chemistry and topology. These functionalized hyper-structured molecules with well-defined structures are one of the promising materials which exhibit high performance for photonic applications.

REFERENCES

1. W. E. Moerner and S. M. Silence, *Chem. Rev.*, **94**, 127 (1994).
2. Y. Zhang, T. Wada and H. Sasabe, *Chem. Commun.*, 621 (1996).
3. T. Wada, Y. D. Zhang, Y. S. Choi and H. Sasabe, *J. Phys. D: Appl. Phys.*, **26**, B221 (1993).
4. T. Wada, L. Wang, Y. Zhang, M. Tian and H. Sasabe, *Nonlinear Optics,* **15**, 103 (1996).

POLYMER ELECTRO-OPTIC WAVEGUIDES - FABRICATION & PERFORMANCE

S. Ermer, D. G. Girton, W. W. Anderson, T. E. Van Eck, J. Marley, S. M. Lovejoy, D.S. Leung, A. Harwit and Lee-Yin Liu[i]

Lockheed Martin Missiles & Space Co.
Advanced Technology Center
3251 Hanover Street
Palo Alto, CA 94304-1191

Abstract

This presentation will describe recent work performed in the area of electro-optically active polymer based materials and devices at the Lockheed Martin Advanced Technology Center in Palo Alto, CA. We have designed and built devices using a core layer mixture of 4-(Dicyanomethylene)-2-methyl-6-(p-dimethyl-aminostyryl)-4H-pyran (DCM) and Amoco 4212, a commercial polyimide. We have also synthesized and characterized a series of chromophores which are chemically related to DCM. These chromophores are photobleachable. We are now investigating the photobleaching process to optimize device fabrication.

Applications and Performance

Application areas for polymer based EO devices include RF signal distribution, phased array antenna control and digital data distribution. Gain, noise figure and bandwidth considerations for RF applications have led us to focus our efforts on improving device sensitivity, i.e., lowering V_π.

In the past two years we have successfully reduced the switching voltage V_π of our DCM-polyimide Mach-Zehnder modulators from 25V to 5V. More recently we have demonstrated Mach-Zehnder modulators with switching voltages of 3.5V and extinction ratios over 20 dB optical and over 40 dB RF. This shows that EO polymer based devices can exhibit performance levels comparable or superior to that of $LiNbO_3$ based devices. Our ongoing work is aimed at improving this performance while simultaneously addressing packaging and manufacturing cost issues for this technology. The dominant cost for $LiNbO_3$ based electro-optic components is packaging. The polymer based devices are fabricated on silicon substrates using low cost VLSI and fiber-optic connector technologies. Component reliability and stability issues remain to be addressed in detail.

---

[i] present address: Gemfire, Inc., 2440 Embarcadero Way, Palo Alto, CA 94303

Fabrication - Investigation of Photobleaching

A key process step in the fabrication of our EO devices is photobleaching, used to lower core layer index of refraction for waveguide definition (Figure 1b). Advantages of photobleaching include ease of fabrication, the ability to precisely tailor index, and broad applicability to a range of dyed polymeric materials including guest-host, side-chain, and cross-linked systems. Polymeric channel waveguides fabricated by photobleaching and active waveguide devices incorporating photobleached waveguides have been extensively reported in the literature and are the focus of our work. Although devices have been successfully fabricated using photobleaching, precisely controlling the index profile should improve the performance of electro-optic devices and is especially important for design-sensitive devices such as directional couplers. For this reason we have decided to investigate the photobleaching process in greater detail, especially the effect of atmosphere on the kinetics of the process.

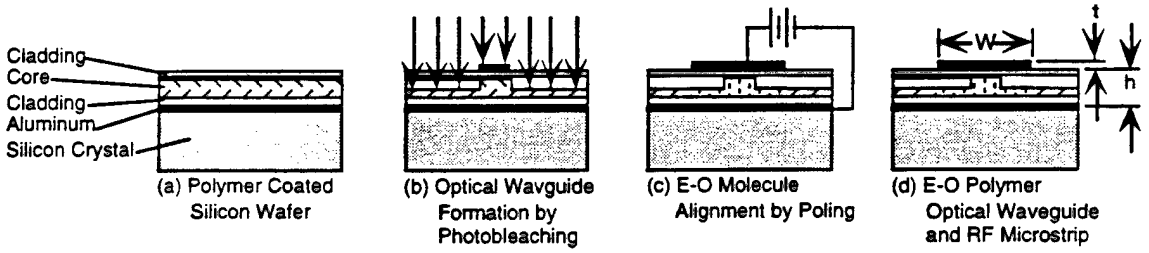

Figure 1. Electro-Optically Active Polymer Waveguide Fabrication

Our observations to date indictate that oxygen is required in the process of photobleaching films DCM-doped polyimide. Initial tests show that photobleaching does not occur if the DCM film is in a nitrogen environment or under vacuum. A series of tests have been carried out which show that a pure oxygen environment enhances the photobleaching rate over an air ambient. Oxygen may be required in the photobleaching process for most of the polymer-dye systems currently in use today.

PACKAGED POLYMER-WAVEGUIDE DIGITAL OPTICAL SWITCHES

Anthony J. Ticknor

Akzo Nobel Electronic Products Inc.

1257 C Tasman Drive, Sunnyvale, CA

408-752-1809, FAX: 480-752-1818

ticknor@akzochip.com

There is a rapidly growing interest in transparent optical switching for reconfiguring and managing diverse fiber communications networks. At the photonics group of Akzo Nobel we have designed, fabricated, and packaged a family of single-mode optical switches based upon the use of the thermo-optic effect in polymer waveguides. The basic switching element is a 1x2 branching waveguide[1,2] and switching is achieved through the thermo-optic effect by applying a thermal gradient across the branching region via thin-film metal heaters deposited on the device surface. Ultralow loss polymers have been developed for these components. The absorption losses for the materials used for the devices to be described are 0.06 dB/cm and 0.15 dB/cm at 1.31 μm and 1.55 μm, respectively. Configurations of 1x2, 1x4, 1x8, and 2x2 have been produced using monolithic integration to interconnect multiple switching elements in a single optical circuit. These solid-state switch arrays are realized from the polymer Optoboard technology developed at Akzo Nobel Photonics[2].

In order to integrate the larger switches such as the 1x8s, the index contrast of the RIE waveguides is optimized with respect to device crosstalk, insertion loss, and active length. The resulting waveguides have an index contrast of 0.005 and an initial divergence angle of 0.1° at the waveguide branch.

The "optochips" are bonded to a glass submount for mechanical support and single fibers or fiber arrays are aligned and attached to each end to make a pigtailed switch. The switch is then fixed into a package body and the heater electrodes are bonded to electrical pins mounted in the package to give a standard single-inline or dual-inline pinout. Each end of each heater element is individually connected to an input pin so that 4 pins are required for each branch. A standard 1x8 has 7 switch branches (figure 1) and hence 28 active pins, but is packaged into a 48-pin dual-inline package (DIP) body that can accommodate circuits with an even higher number of switch branches.

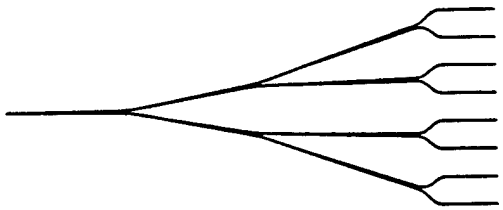

Figure 1. Waveguide Layout for a 1x8 Switch

Because of the digital response of the switching element, switching performance specifications can be met simply by applying a voltage across the appropriate electrode within a margin of the specified voltage. Operating voltage is determined at design time and we have produced switches specified for nominal drive voltages ranging from 5 to 8 volts with margins typically at least +/- 1V.

A finished switch provides fully transparent reconfiguration for single-mode fibers carrying optical signals in either or both the 1310nm and 1550nm bands. A fully packaged standard 1x8 is expected to have 5dB or less fiber-to-fiber insertion loss for the on channel and 17dB or more extinction in all off channels for either wavelength range. Polarization-dependent loss is specified to be less than 0.5db and is typically less than 0.2dB and back-reflection should be less than -30dB. Switches with significantly higher performance have also been demonstrated with this technology. Figure 2 shows the insertion loss at 1530nm of a typical 1x8 switch for each of the ouput states.

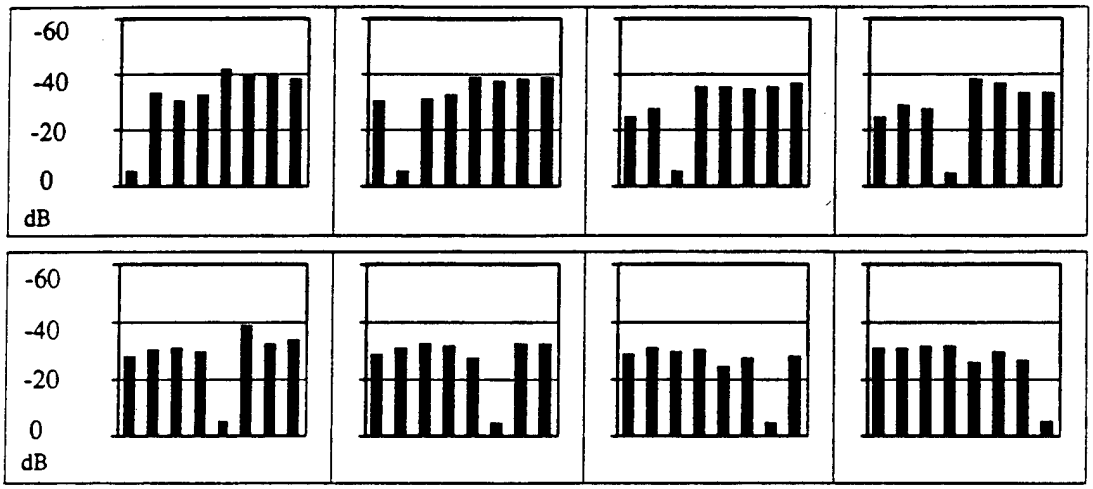

Figure 2. Measured insertion loss (in dB) of output channels in all 8 switched states of 1x8 switch at 1530 nm.

Since handling and interfacing of packaged switches is easy and straightforward, they can be flexibly used in the integration of larger switching networks. For example, eight 1x8 switches and their drivers can easily be mounted on a circuit card. By using two such cards and appropriately interconnecting the 128 output fibers, one could construct a full 8x8 router-selector cross-connect in a volume less than 12-inches x 12-inches x 2-inches with less than 10dB insertion loss and better than 34dB isolation, transparent for all optical signals at both 1.3μ and 1.55μ.

1. H.M.M.Klein Koerkamp et. al, "Design and fabrication of a pigtailed thermo-optic 1x2 switch", Proc. Integrated Photonics Research (San Francisco, CA 1994), pp. 274-276.

2. M.B.J. Diemeer et. al, "Low loss (non)linear optical polymeric waveguide materials and devices", Proc. SPIE (San Diego, CA 1995), to be published.

I-8

Polymeric EO Modulators: From Chromophore Synthesis to Integration with VLSI Electronics and Silica Fibers

Larry R. Dalton
Loker Hydrocarbon Research Institute, University of Southern California, Los Angeles, CA 90089-1661

The realization of polymeric electro-optic waveguides characterized by electro-optic coefficients (at 1.3 mm) of greater than 30 pm/V which exhibit reasonable thermal stability (greater than 95% retention of optical nonlinearity for 1000 hours at 100°C) is a critical objective. The vast majority of research has involved donor-acceptor charge transfer materials with a π-electron connective segment (consisting typically of polyene, azo, or heteroaromatic moieties) separating electron donating and electron accepting groups. The research discussed here has focused upon the exploration of alkyl and aryl amine and ketene dithioacetal donor groups and a variety of electron acceptor groups including thiobarbituric acids, isoxazolones, parazolone, cyanovinyls, sulfoximines, tetracyanoindanes, and Sandoz-type (cyanosulfone) acceptors. Improvements in μβ values by factors of 3-20, relative to the values observed for commonly used stilbenes and azobenzene chromophores, have been realized. Covalent incorporation of more than one hundred such chromophores into processable polymer lattices has been carried out and the stability of the chromophores incorporated in polymers under corona poling, polymer hardening, and optical illumination (at 1.3 mm) conditions has been evaluated. Of chromophore-containing polymeric materials which can be poled to yield electro-optic coefficients greater than 30 pm/V, those containing isoxazolone, parazolone, and tetracyanoindane acceptors appear to exhibit the best stability to conditions of corona poling and optical irradiation (in the presence of atmospheric oxygen).

A crucial aspect of our research has been the *in situ* monitoring of second harmonic generation efficiency and electro-optic activity during poling and aging experiments. We have also coordinated measurements of optical loss with measurements of optical nonlinearity to gain insight into crystallization effects associated with interaction between chromophores exhibiting large dipole moments. During poling, an effort has been made to carefully monitor the temperature and electrical conductivity of the sample and to continuously correlate these measurements with those of linear and nonlinear optical properties.

With high μβ chromophores it is no simple matter to realize high chromophore loading and a large order parameter. Indeed, due to the problem of centrosymmetric crystallization, these latter two quantities are not independent and typically a maximum is observed in the graph of electro-optic coefficient versus number density reflecting the fall-off of order parameter at higher number densities due to centrosymmetric crystallization. Chromophore crystallization can be understood in terms of London theory. If we neglect chromophore-polymer electrostatic interactions and steric effects, chromophore-electric poling field and chromophore-chromophore interactions can be expressed as

$$U = \mu E_p f(0)\cos\theta - W\cos\theta' \quad (1)$$

where U is the total potential energy, μ is the dipole moment of the chromophore, E_p is the applied electrical poling field, f(0) is the local field factor, θ is the angle between the chromophore principal axis and the poling field, W is the intermolecular interaction potential, and θ' is the angle between the chromophore principal axis and the intermolecular interaction direction. The intermolecular interaction potential is composed of the orientation force, the induction force, and the dispersion force. NLO chromophores are typically prolate ellipsoidal molecules characterized by molecular volumes (estimated from crystallographic data or Van der Waal radii) ranging from 200 to 700 cubic angstroms. For example, a typical azobenzene chromophore has molecular axes of 15, 5.5, and 4 angstroms. This suggests a 4 angstrom closest approach distance--a value which varies only slightly from chromophore to chromophore unless special chromophore derivatization is employed. The major axis shows the greatest variation for the various chromophores considered and is responsible for significant steric hindrance to molecular reorientation for the longest high μβ chromophores. Dipole moments vary from 5 to 10 Debye. Using London theory, an approximate poling-induced order parameter can be calculated:

$$\langle\cos^3\theta\rangle = (\mu E_p f(0)/5kT)[1 - L^2(W/kT)] \quad (2)$$

where L(W/kT) is the Langevin function, L(W/kT) = coth(W/kT) - (kT/W). The term in brackets will vary from 1 to 0 reflecting the competition of poling induced noncentrosymmetric ordering and chromophore centrosymmetric crystallization. This "attenuation" factor accounts for the decrease in both optical transparency and electro-optic activity with increasing chromophore loading due to increasing chromophore crystallization. Detailed analysis suggests that the picture just presented is too simple and that both chromophore-polymer electrostatic interactions and steric effects play important roles in quantitatively defining order parameters. The above analysis does yield the appropriate functional form for understanding changes in optical loss and optical nonlinearity with chromophore

loading and does provide useful qualitative insights into chromophore crystallization phenomena which currently limit realizable electro-optic coefficients. Of the chromophores evaluated, the most serious centrosymmetric crystallization problems were observed for those containing tetracyanoindane, Sandoz, and thiobarbituric acid acceptor groups reflecting steric and electrostratic interactions associated with those groups. The least serious crystallization problems were observed for disperse red type chromophores and for high $\mu\beta$ chromophores containing isooxazolone and parazolone acceptor groups--chromophores which also exhibited superior stability to conditions of electric field poling and operation of fabricated modulators. However, it should be kept in centrosymmetric crystallization can be dramatically reduced by derivatization with groups which increase the distance of closest approach.

The fabrication of buried channel active polymeric waveguides and tapered transitions between active polymer and passive silica waveguides by multi-color photolithography has been evaluated for several new chromophores. The problem of interfacing silica and polymer waveguides can be summarized as follows. At 1.3 microns communication wavelength, a silica fiber has a core of approximately 10 microns. To avoid mode size mismatch would require a polymer waveguide of approximately 10 microns. For single mode operation, this polymer waveguide core would have to be surrounded by a graded index cladding. The size requirements on core and cladding would lead to unacceptably large electrode spacings and drive voltage, V_π. The requirement of digital voltage levels demands active polymer waveguides on the order of 1-2 microns which permit single mode guiding with step-index cladding layers. To avoid a coupling loss on the order of 4-5 dB due to mode size mismatch, a tapered transition region between the silica and polymer waveguides is required. Precisely defined index of refraction tapers can be prepared by multi-color photolithography which employs a photochromic chromophore with well characterized photochemical kinetics and wavelength dependent absorption coefficient. Controlled time and wavelength exposure permits the generation of virtually any desired waveguide structure and a stepping of the photolithographic operation along the waveguide structure permits precise generation of tapers. The multi-color photolithographic process is quantitatively modeled using a modification of the photoresist response model developed by Dill and coworkers. Tapered transitions were developed according to the theory of Sakai and Maracatili. In addition to dramatically reducing optical losses associated with mode mismatch and surface roughness of the polymer waveguide generated during the cladding deposition, multi-color photolithography dramatically reduces the steps required for waveguide fabrication. Four steps (spin coat bottom cladding, spin coat NLO polymer, first exposure at λ_1, second exposure at λ_2 using a mask) are required for multi-color photolithography as compared to nine steps (spin coat bottom cladding, spin coat photoresist, soft bake, expose photoresist to UV using mask, wet process photoresist, plasma etch, strip photoresist, spin coat NLO polymer, spin coat top cladding layer) for conventional waveguide processing.

Reactive ion etching (RIE) and electron cyclotron resonance (ECR) etching has been used to investigate the fabrication of active waveguide structures and to develop v-grooves in silicon substrates for the coupling of silica optical fibers to polymer waveguides. In particular, we have demonstrated that the greater control over reactive ions afforded by ECR etching results in smoother wall surfaces and reduced optical losses. An example of reduction in waveguide losses by systematic control of the conditions of reactive ion etching is given in Table 1 for a PU-DR19 nonlinear optical material described previously. Optical loss is obtained by measuring the distance dependent intensity of outcoupled light when the waveguide is immersed into an index matching fluid.

Table 1. Optical loss at 1.3 mm wavelength due to waveguide surface roughness as a function of the conditions of reactive ion etching

Oxygen Flow Rate sccm	Oxygen Pressure mT	Rf power Watts	Optical Loss dB/cm
25	50	95	0.93
25	175	100	0.74
25	175	60	0.41
25	400	15	0.05
50	400	12	0.01

Both vertical and horizontal integration of polymeric electro-optic modulators with VLSI semiconductor electronics has been explored. Vertical integration was accomplished by first deposition of a planarizing polymer layer on top of the VLSI wafer, depositing a thin film of nonlinear optical polymer, poling and processing the material as describe above with care taken to isolate the VLSI circuit as much as possible (e.g., by appropriate grounding).

Laser action in solutions and films containing semiconducting polymer and titanium dioxide nanocrystals

María A. Díaz-García, Fumitomo Hide, Benjamin J. Schwartz and Alan J. Heeger

Institute for Polymers and Organic Solids
University of California, Santa Barbara
Santa Barbara, California 93106-5090, USA
Telephone: 805-893-2576; Fax: 805-893-4755

Semiconducting conjugated polymers have shown to present very interesting properties for their use as the active medium in a variety of optoelectronic devices, such as light emitting diodes (LEDs)[1,2], photodiodes[3] and light emitting electrochemical cells (LECs)[4]. These thin film devices have the advantages of a very good processability and solubility.

In this work we present the first steps towards a new approach for producing solid state polymer laser diodes in the absence of any external cavity. Our idea is based in the recent work of Lawandy *et al.*[5], who demonstrated isotropic laser emission from optically pumped dye solutions containing colloidally suspended titanium dioxide (TiO_2) particles. Our initial experiments[6] report laser action from both solutions and solid state dilute blend films of poly(2-methoxy,5-(2'-ethyl-hexoxy)-1,4-phenylene-vinylene) (MEH-PPV) in polystyrene (PS), which contain suspended titania particles. This is the first demonstration of lasing with a semiconducting polymer in the solid state as the active medium.

Photoluminescence experiments have been performed by pumping the samples at a 30° angle with 532 nm excitation wavelength provided by a frequency doubled Q-switched Nd:YAG Laser. The emitted light was then collected from the front face of the sample, frequency dispersed in a monochromator and detected by a Peltier-cooled CCD array. We investigated the changes in the PL spectrum as a function of the excitation energy per pulse.

Firstly, the effect of introducing titania particles on the PL of MEH-PPV in solutions was investigated. As shown in Fig. 1, the PL spectrum of MEH-PPV is characterized by a central peak at around 570 nm, with shoulders due to vibronic structure present at both higher and lower wavelengths. This spectrum remains essentially constant with increasing energy, as indicated in Figure 1a (solid curve). In the presence of $\sim 10^{10}$ cm^{-3} titania particles, however, dramatic gain narrowing is observed (Fig. 1a, dashed curve and 1b) when pumped above the threshold for stimulated emission, indicative of laser action. The polymer and titania particle concentration dependence of the line narrowing has been studied.

Experiments were also performed in dilute blends (0.6-1.6 %) of MEH-PPV in PS with $\sim 10^{11}$ cm^{-3} titania particles. Again, line narrowing was observed in a similar manner that for the solutions, although for the films the final linewidth is slightly narrower and the red luminescence tail is better suppressed.

In summary, we have used scattering from titanium dioxide nanocrystals to produce laser action from optically pumped solutions and free-standing dilute blend films of the conducting polymer MEH-PPV. Gain narrowing was observed above a critical pump threshold for several polymer and particle concentrations. We believe this is the first demonstration of lasing from a conjugated polymer in the solid state. The isotropic nature of the narrowed emission and the straightforward extension of adding titania particles to polymer EL devices are promising for the eventual production of scattering solid state polymer laser diodes.

Further work in this field is in progress. The role of the thickness of the polymer film is being investigated in more detail, as well as the performance of different types of polymers.

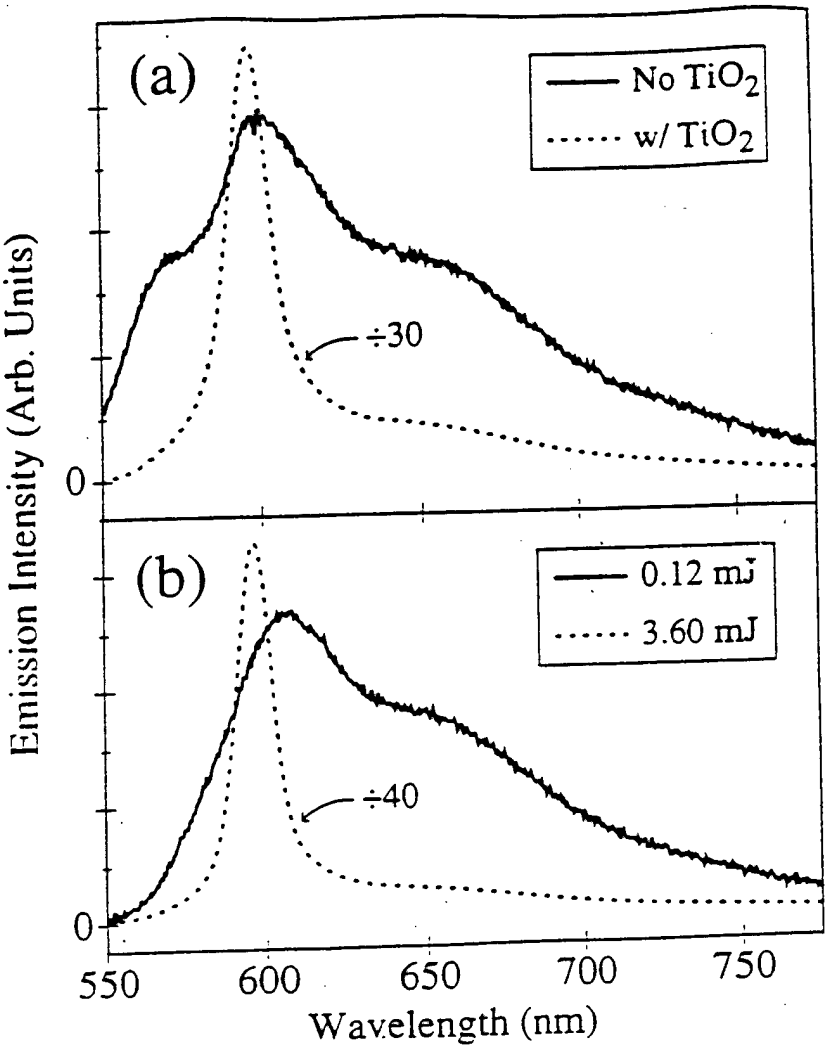

Figure 1.- Luminescence of MEH-PPV in cyclohexanone solution (a) (0.6% w/w) pumped with 4.5 mJ/pulse of 532 nm light without TiO_2 particles (solid curve) and after addition of ~ 10^{10} cm^{-3} TiO_2 particles (dashed curve). (b) (1% w/w) with ~ 10^{11} cm^{-3} TiO_2 particles pumped at 0.12 and 3.60 mJ/pulse (solid and dashed line respectively).

References.

1. J.H. Burroughes, D.D.C. Bradley, A.R. Brown, R.N. Marks, K. MacKay, R.H. Friend, P.L. Burns, A.B. Holmes, Nature 347 (1990) 539.
2. G. Gustafsson, Y. Cao, G.M. Treacy, F. Klavetter, N. Colaneri, A.J. Heeger. Nature 357 (1992) 477.
3. G. Yu, J. Gao, J.C. Hummelen, F. Wudl, A.J. Heeger, Science 270 (1995) 1789.
4. Q. Pei, G. Yu, C. Zhang, Y. Yang, A.J. Heeger, Science 269 (1995) 1086.
5. N.W. Lawandy, R.M. Balachandran, A.S.L. Gomes, E. Sauvain, Nature 368 (1994) 436.
6. F. Hide, B. J. Schwartz, M.A. Diaz-Garcia, A. Heeger, Chem. Phys. Lett. in the press.

Organic Nonlinear Optical Crystals for Device Applications

Toshikuni Kaino

Institute for Chemical Reaction Science, Tohoku University

Katahira, Aoba-ku, Sendai-shi, Miyagi, 980-77 Japan

In this presentation, organic nonlinear optical (NLO) crystals for practical optical system applications are discussed. As future telecommunication systems will use ultrafast electrical and optical signals, they need ultrafast signal diagnosing systems. These kinds of systems have already attracted considerable attention as key techniques in realizing ultra-high speed time division-multiplexed (TDM) transmission systems. Exploiting second-order NLO effects such as second-harmonic generation (SHG) and electro-optical (EO) effects offer great potential for wide tunability and agile response time. The high-speed signal measurement to evaluate optical transmission systems and electronic circuits uses an optical sampling (OS)[1] and electro-optical sampling (EOS)[2] through SHG or sum-frequency generation (SFG) or EO effect. Compared with inorganic materials such as $LiNbO_3$, it is recognized that organic NLO materials with π-electron conjugation will be useful substances with higher NLO susceptibility, increased operating speed, and higher laser damage threshold. However, in spite of a large number of potentially interesting NLO and EO characteristics, only a few of the organic material could so far be crystallized in reasonable crystal size with high optical quality required for possible applications. SHG or SFG applications need crystals grown for phase-matched direction.

To reveal the potential of the organic materials, an EO crystal and an organic SFG crystal are investigated of their applicability to signal diagnosis use.

Electro-optical sampling:

For use in EO applications, 4-dimethylamino-N-methystilbazorium tosylate (DAST) which is reported to have an EO coefficient r_{11} of larger than 160 pm/V[3,4]. Figure 1 shows the DAST chemical structure. Thin crystal of DAST, less than 1 mm thick with 2x2 mm^2 in size, was fabricated from methanol solution by slow cooling. To utilize the largest electro-optical coefficient r_{11}, transverse electric field sensing is adequate where electric field is parallel to IC substrates and perpendicular to incident laser light. Figure 2 shows the schematic diagram of transverse electric field sensing system. Using a polarization microscope, a-axis and b-axis are decided for as-grown DAST crystal. The crystal was set on the 60 μm wide co-planer electrodes with 40 μm gap between the electrodes, fabricated on the dielectric mirror. Semiconductor laser light of 1.55 μm wavelength was irradiated between the center of the two electrodes then the reflected light from the mirror was detected using the EOS optical system. As a reference, 0.5 mm thick KTP crystal, polished for both sides of its surface, was used.

4.8 Gbit/s electric signal was applied to the electrode then the EO signal from the DAST crystal was detected. The signal/noise (S/N) ratio was larger than 50 dB and the signal intensity of about 4 times higher than that from the KTP crystal was obtained. The intensity is a little bit low compared with the theoretical value, 10 times higher than KTP, calculated from the reported EO coefficient, r_{11} of 160 pm/V. The reason will be that the r_{11} at 1.55 μm is lower than 80 pm/V. By increasing the sensitivity 4 times higher than KTP, EO measurement time will be reduced to 1/16-th. So, DAST crystal is very effective for use as a sensing material for practical EOS system.

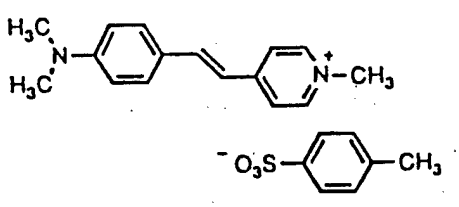

Fig.1 Chemical structure of DAST

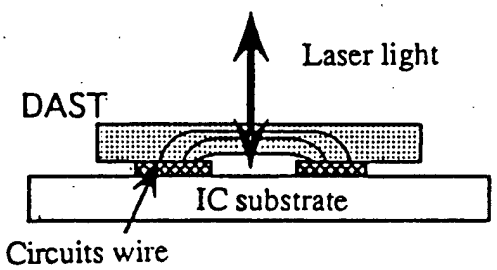

Fig.2 Experimental set-up of EO sampling

Optical sampling:

We chose 2-adamantylamino-5-nitropyridine (AANP) for OS study whose chemical structure is illustrated in Fig. 3. AANP been reported to have a large second-order optical nonlinearity of d31 80= pm/V and the possibility of angle-tuned phase-matched SHG in the wavelength region between 1.06 and 1.55 μm[5]. To fabricates a single crystal long enough in a phase matched direction, we have applied indirect laser heater pedestal growth (ILHPG) method[6]. In this crucible-less method, a CO_2 laser is used to melt the end of a rod of feed material in a 360 axially symmetric irradiance. A schematic of the modified LHPG method for organic materials is shown in Fig. 4. The source rod and seed crystals are inserted into the glass tube from opposite sides of the tube. The tip of the rod melts due to radiation from the glass tube, forming a molten zone into which the oriented seed crystal is dipped. Then the crystal is grown by pulling it out of the melt while simultaneously introducing fresh feed materials into the molten zone. The orientation and characteristics of them are identified with a Buerger-precession camera. It is confirmed that the orientation of the seed crystal and that of the grown crystal are the same.

Figure 5 shows the configuration of optical sampling system where waveform sampling is made all-optically by ultrafast SFG[7]. An 1.8 mm AANP crystal was used for the SFG measurement from 100 Gbit/s optical sibnal. The OS signal from the crystal obtained by this technique is about two orders higher than conventional inorganic crystal, KTP.

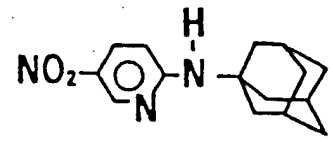

Fig.3 Chemical structure of AANP

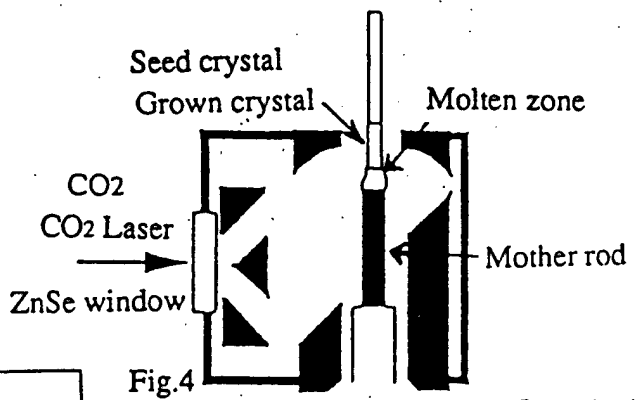

Fig.4 Schematic of the modified LHPG method

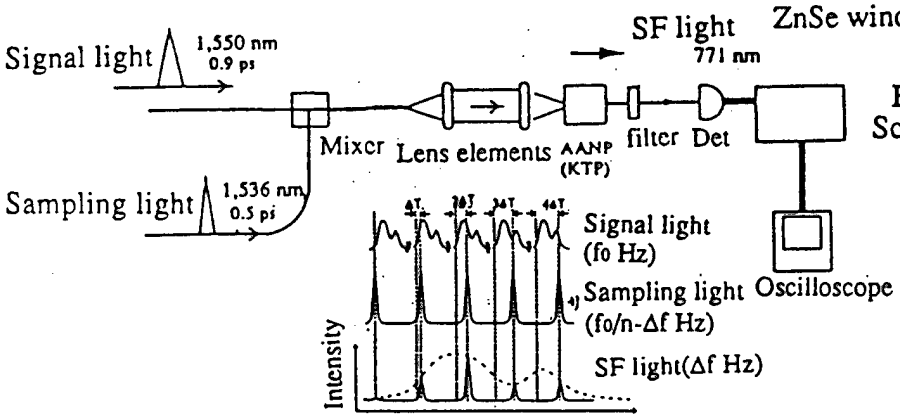

Fig.5 Configuration of optical sampling system

In conclusion, high sensitivity electro-optical sampling is effectively attained using an organic electro-optical crystal. We have the eye-diagram of a 100 Gbit/s optical signal waveform is successfully measured by using SFG sampling oscilloscope through organic nonlinear optical crystal. This is the first example of the NLO organic crystal which is applied in actual ultra-fast signal diagnosing systems. Finally I would like to thank A.Yokoo, S.Tomaru, T.Takara, N.Nagatsuma and other researchers in NTT Laboratories for their discussions.

References

1. H.Takara et al, IEJCE, B-1, J75-B-I, 372 (1992)
2. T.Nagatuma et al, IEJCE Annual Society Meeting Proc., (Sept. 1996)
3. K.Sakai et al, SPIE, 1337, 307 (1990)
4. J.W.Perry et al, SPIE, 1560, 302 (1991)
5. S.Tomaru et al,, Appl.Phys.Lett, 58(13), 2563 (1991)
6. A.Yokoo et al, J. Cryst. Growth, 156, 279 (1995)
7. H.Takara et al, ECOC '96 Proc. (Sept. 1996)

Organic Monomer Glass Nonlinear Optical Materials

R. Twieg, R. Wortmann, C. Moylan, P. Lundquist,
V. Lee, M. Jurich, C. Geletneky, D. Burland

IBM Almaden Research Center
San Jose, CA 95120-6099

The glass forming properties of organic monomers have been neither widely appreciated nor often exploited. This situation is in stark contrast to the substantial efforts already undertaken to study and utilize inorganic glasses and glassy organic polymers for numerous applications including those as nonlinear optical (NLO) media. It seems worthwhile to ask the question: "Just why are polymers employed in NLO media at all?" In the case of most $\chi^{(3)}$ systems the answer is simple as the polymers themselves are highly conjugated and clearly possess critical intrinsic nonlinear properties. In contrast, in most $\chi^{(2)}$ systems the polymer has little, if any, direct electronic contribution to the nonlinear function (except when it is functionalized with chromophores wherein this contribution is highly localized). Polymers overall can and do imbue these systems with some very valuable mechanical and processing properties and do make a profound (but indirect and again often overlooked) contribution to the $\chi^{(1)}$ properties which are often critical to the overall net NLO function.

In the course of some earlier studies of organic chromophores intended for single crystal frequency doubling (SHG) and electro-optic (E-O) waveguide applications glassy behavior was occasionally observed but hardly ever pursued. For example, the single crystal NLO molecule MBANP could also be poled as a monomer glass to produce a small and unstable bulk nonlinearity.[1] The class of triarylazoles studied as high temperature E-O chromophores included numerous examples such as PSPEO with novel glassy properties.[2,3] Very recently, during the development of organic chromophores as holographic storage media two new classes of chromophores with valuable glassy properties were discovered. In the first case of photochromic systems the dicyanopolyene class including DCPT were studied in much detail and are attractive candidates for multiplexed write-once read-many (WORM) applications.[4] In the second case of photorefractive (PR) chromophores a very valuable new class of glass forming monomers in the methylenedihydropyridine family including 2BNCE were discovered. These latter compounds exhibit a really remarkable array of useful properties (large ground state dipole moment, small first hyperpolarizability, large refractive index anisotropy, good thermal stability, intrinsic transport character) in addition to their propensity for glass formation which permits polymer-free and solvent-free PR sample preparation.[5]

It appears that glassy monomers may have a valuable role to play as organic NLO media just as crystals and polymers already do but first the molecular properties and processing variables which influence the temperature and dynamics of phase transitions must be identified and improved upon.[6] Currently it is of particular general importance to enhance glass transition temperatures (T_g) and to produce glasses with better stability and less prone to crystallization. The glassy properties of organic monomers will be reviewed here with special focus on the chemistry and physical properties of the new optical storage chromophores. The question we seek to answer is: "Can we design and implement specialized glassy monomers which reduce or even ultimately eliminate the need for polymers in nonlinear optical media?"

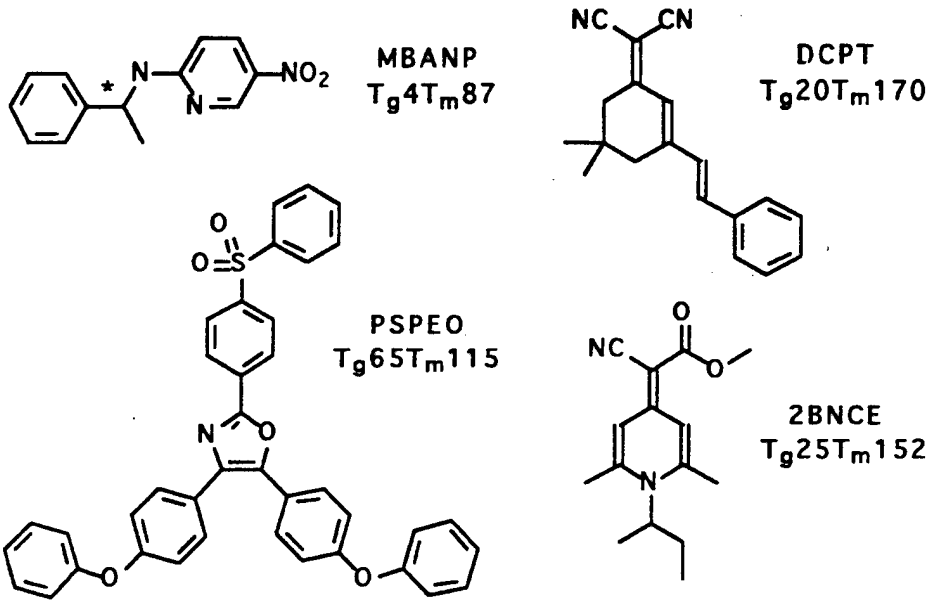

References:

[1] M. Eich, H. Looser, D. Yoon, R. Twieg, G. Bjorklund, C. Baumert, J. Opt. Soc. Am. B: Opt. Phys., **6**, 1590 (1989)

[2] S.-J. Kim, T. E. Karis, R. J. Twieg, J. Mat. Sci. Lett., **14**, 901 (1995).

[3] C. R. Moylan, R. D. Miller, R. J. Twieg, K. M. Betterton, V. Y. Lee, T. J. Matray, C. Nguyen, Chem. Mater., **5**, 1499 (1993).

[4] R. Wortmann, P. M. Lundquist, R. J. Twieg, C. Geletneky, C. R. Moylan, Y. Jia, R. G. DeVoe, D. M. Burland, M.-P. Bernal, H. Coufal, R. K. Grygier, J. A. Hoffnagle, C. M. Jefferson, R. M. Macfarland, R. M. Shelby, G. T. Sincerbox, submitted.

[5] R. Twieg, R. Wortmann, C. Moylan, P. Lundquist, V. Lee, M. Jurich, C. Geletneky, D. Burland, manuscript in preparation.

[6] R. Twieg, C. Dirk, "Organic Nonlinear Optical Chromophores" in "Organic Thin Films for Waveguiding Nonlinear Optics", F. Kajzar, J. D. Swalen, Eds., (Gordon & Breach, 1996)

I-12

One and two-dimensional functional dyes for nonlinear optics and photorefractive organic composites

Rüdiger Wortmann

Institute for Physical Chemistry, University of Mainz,

Jakob Welder-Weg 11, D-55099 Mainz, Germany

A series of one (1D) and two-dimensional (2D) nonlinear optical chromophores was studied by polarization and temperature (T) dependent electrooptical absorption (EOAM), electric field induced second harmonic generation (EFISH) and Hyper-Rayleigh-Scattering (HRS) experiments. The EOAM experiment yields information on dipole moment μ^g and polarizability α^g of the electronic ground state g, the change of dipole moment $\Delta\mu$ and polarizability $\Delta\alpha$ upon electronic excitation to state a, and the direction of the transition dipole μ^{ag} in the molecule-fixed frame. EFISH and HRS measurements yield linear combinations of tensor components of the second order polarizability β. T-dependent measurements can be used to seperate orientational from isotropic effects in EFISH and EOAM.

The combined evaluation of these experiments is possible only by using a consistent theoretical framework for their description. To this end, a scheme based on Liptay's concept of partial molar quantities and model molar quantities is introduced. Onsager's reaction field approach is extended to nonlinear optics and the frequently applied Lorentz correction is demonstrated to be systematically incorrect for SHG.

Some fundamental results on 1D NLO chromophores could be obtained with this unique combination of experimental tools. The validity of the two-level approximation $\beta_{zzz} \sim \Delta\mu_z\,(\mu_z^{ag})^2\,\Omega$, where Ω is a dispersion function, could be demonstrated by comparative EFISH and EOAM studies of β and $\Delta\mu$, respectively, for the standard 4-nitroaniline (pNA) [1], pyridine-N-oxides (NPO and POM) as well as push-pull substituted oligothiophenes [2] and carotinoides [3]. NPO is one of the rare examples for which a simultaneous determination of $\Delta\mu$ and $\Delta\alpha$ could be achieved, β of NPO could be measured by T-dependent EFISH. EOAM measurements on push-pull carotinoides reveal giant dipoles in their excited states.

1D chromophores in the charge-resonance (CR) limit are introduced as promising functional dyes for photorefractive (PR) materials. These chromophores combine large dipole moments μ with large anisotropies $\delta\alpha$ of the linear polarizability in their electronic ground

state which optimize the PR Kerr effect of organic composites with low T_g. The CR transition of the chromophores occurs in the UV region and does not solvatochromically shift in a polar environment since $\Delta\mu \sim 0$. Highly transparent and efficient PR materials can therefore be devised on the basis of functional dyes in the CR limit.

NLO chromophores of type 3,5-dinitroaniline (3,5-DNA), 3,5-diaminonitrobenzene, N,N'-dihexyl-1,3-diamino-4,6-dinitrobenzene (DHANB) and derivatives of these structures which are conjugationally elongated through phenylethinyl units exhibit a pronounced 2D character of β. All three independent and non-negligible tensor components β_{zzz}, β_{zyy} and $\beta_{yzy} = \beta_{yyz}$ of these C_{2v} symmetric compounds can be determined by a combination of polarization dependent EFISH and HRS measurements. A significant deviation $\beta_{zyy} \neq \beta_{yyz}$ from index (Kleinman) permutation symmetry is observed for many of these chromophores. This effect can be ascribed to low-lying electronic bands having a transition dipole perpendicular to the C_2 axis z: $\beta_{zyy} \sim \Delta\mu_z \, (\mu_y^{ag})^2 \, {}^1\Omega$ and $\beta_{yzy} \sim \Delta\mu_z \, (\mu_y^{ag})^2 \, {}^2\Omega$. ${}^2\Omega$ exhibits a two-photon resonance which is lacking for ${}^1\Omega$. Therefore $\beta_{yyz} = \beta_{yzy} > \beta_{zyy}$ in the preresonance regime, as could be verified quantitatively by experimental EOAM determination of $\Delta\mu_z$ and μ_y^{ag} for several chromophores such as 3,5-DNA. The second-order polarizability of DHANB is observed to be governed by the orthogonal components, $\beta_{yyz} = \beta_{yzy} > \beta_{zyy} >> \beta_{zzz}$. An EOAM study of DHANB reveals a sequence of three y, z and y polarized electronic bands a, b and c whose dipole changes and transition dipoles could be determined. It is found that only 1/3 of β is due to dipolar two-level contributions $\Delta\mu \, (\mu^{ag})^2$ while non-dipolar three-level contributions of type μ^{ga} μ^{ab} μ^{bg} contribute to 2/3. The latter is the only source for β in non-dipolar chromophores with threefold symmetry axes such as conjugationally elongated s-triazines and cyaninium cations which were studied by polarization dependent HRS.

References

[1] R. Wortmann, P. Krämer, C. Glania, S. Lebus und N. Detzer, Chem. Phys. 173 (1993) 99.

[2] F. Würthner, F. Effenberger, R. Wortmann und P. Krämer, Chem. Phys. 173 (1993) 305.

[3] M. Blanchard-Desce, R. Wortmann, S. Lebus, J.-M. Lehn, P. Krämer, Chem. Phys. Lett. 43 (1995) 526.

RECENT DEVELOPMENT OF HIGH PERFORMANCE ELECTRO-OPTIC MATERIALS FOR DEVICE APPLICATIONS

Alex K-Y. Jen*[1], Tian-An Chen[1], Yue Zhang[1], Yue-Jin Liu[1],
XuanQi Zhang[1], John T. Kenney[1] and Larry R. Dalton[2]
1. ROI Technology, 2000 Cornwall Rd. Monmouth Junction, NJ 08852
2. Loker Hydrocarbon Institute, University of Southern California,
Los Angeles, CA 90089-1661

Introduction

Organic polymeric electro-optic (E-O) materials have recently attracted significant attention because of their potential use as fast and efficient components of integrated photonic devices. However, the practical application of these materials in optical devices is somewhat limited by the stringent material requirements imposed by the device design, fabrication processes and operating environments. Among the various material requirements, the most notable ones are large electro-optic coefficients (r_{33}), low optical loss and high thermal stability. The factors that affect the material thermal stability are a) the inherent thermal stability of the NLO chromophores, b) the chemical stability of the NLO chromophores during polymer processing, and c) the long-term dipolar alignment stability at high temperatures. This paper highlights our new approaches in the optimization of molecular and material nonlinear optical and thermal properties.

Thermally and Chemically Stable NLO Chromophores Derived From the 1,1-Dicyanovinyl Electron Acceptor

Our earlier research has clearly shown that incorporation of easily delocalizable conjugating units such as thiophene in donor-acceptor substituted systems results in large molecular nonlinearity ($\beta\mu$). By combining thiophene conjugating units with a highly electron-deficient tricyanovinyl group, dramatically enhanced $\beta\mu$ values have been achieved in compounds **1** and **2**.

Although the compounds **1** and **2** possess high $\beta\mu$ and good thermal stability their use in polyimide based electro-optic materials is somewhat limited by the sensitivity of the tricyanovinyl group to the processing solvents and curing conditions. It was found that the cyano group on the vinylcarbon-2 of the tricyanovinyl acceptor was responsible for the chemical sensitivity of compounds **1** and **2**. For this reason, we modified these tricyanovinyl derivatives with an objective of achieving excellent tradeoffs among many useful properties such as thermal stability, molecular nonlinearity and stability to solvent and acid-base enviroments.

We discovered that a modification involving the replacement of the cyano group on the vinyl carbon-2 of the tricyanovinyl acceptor with aromatic/heteroaromatic rings, produces high thermal stability and excellent chemical stability. However, the replacement of the cyano group with a phenyl moiety resulted in a significant blue shifted charge-transfer absorption and a lower $\beta\mu$ value. The loss of activity caused by the replacement of cyano group can be partially compensated for by adding an electron-donor to the phenyl ring and increasing the conjugation length. These modified compounds **3**-**6**, despite their higher molecular weight, possess very good solubility. The better solubility allows us to increase significantly higher weight content in polyimide matrices to achieve high E-O coefficients.

Electro-Optic Polymers: Side-chain Polyquinolines

Although the preliminary results reported in the literature for NLO polyimides are quite encourging, there are some drawbacks. For example, a highly reactive environment during the imidization process severaly limits the selection of usable chromophores. Recently, we have explored a new optical polymer system, polyquinolines, for second-order NLO applications. The studies of their electro-ptic properties have shown very promising results for both guest/host and side-chain polyquinoline systems. Here we describe a generally applicable synthetic approach of making side-chain NLO polyquinolines with broad variety of NLO chromophores covalently attached onto the polymer backbones. These side-chain NLO polyquinolines were prepared via the direct polymerization of a bis(*ortho*-aminoketone) monomer, such as **8**, with a chromophore- containing bis(ketomethylene) monomer **9**. The copolymerization of side-chain NLO polyquinolines could also be achieved by adjusting the ratio of fluorinated bis(ketomethylene) monomer **7** to chromophore containing bis(ketomethylene) monomer **9** as shown in Scheme 1.

The synthesized side-chain NLO plyquinolines were all soluble in common organic solvents, such as cyclopentanone, cyclohexanone, chloroform, cresol, *N*-methyl-pyrrolodinone, *N,N*-dimethylacetamide, pyridine, and tetrahydrofuran. Typical weight average molecular weight M_w for the side-chain polyquinolines are 40,000 - 50,000 with polydispersity index of 1.5 - 2.0 determined by GPC (relative to polystyrene standard). The glass transition temperature (Tg) of the polymers are higher than 200°C by DSC. All the polymers have a thermal stability of < 1% weight loss up to 300°C by TGA.

Optical-quality thin films (1 - 3 μm) of the polyquinolines were obtained by spin-coating of the polymer

solutions onto an ITO glass substrate. The electro-optic coefficients r_{33} of these poled polymer films were typically between 10 to 20 pm/V at 0.83 μm. The r_{33} values typically retained ~90% of their original values at 100°C for more than 1000 hours.

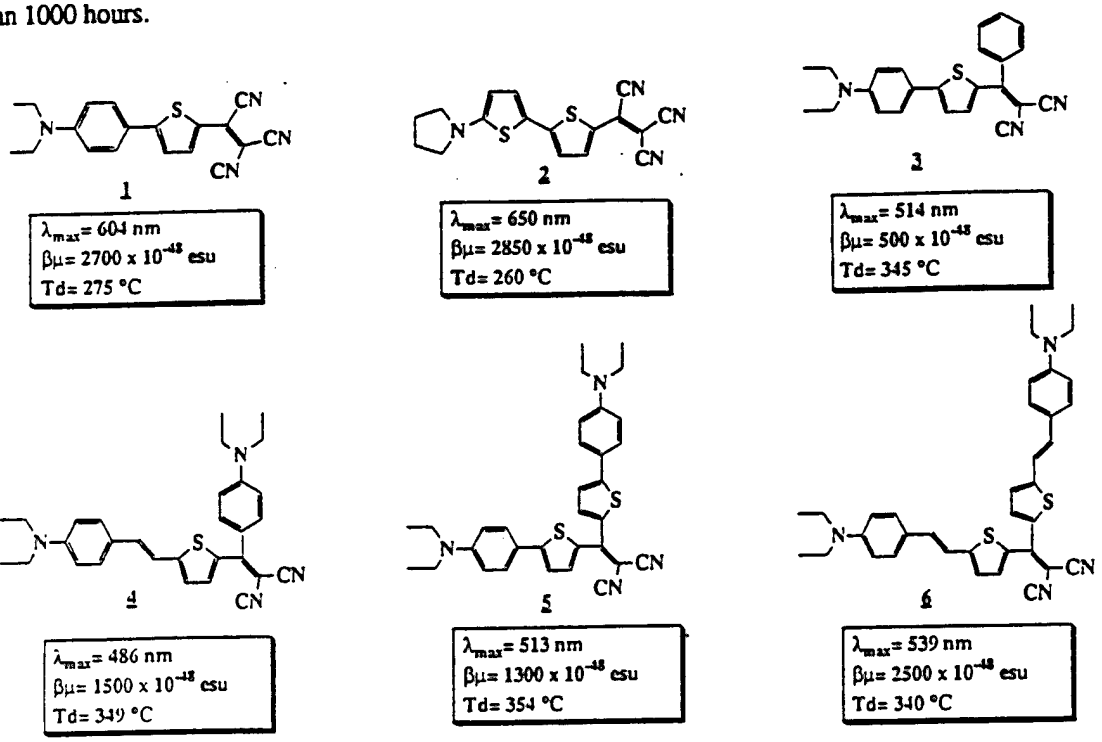

Scheme 1

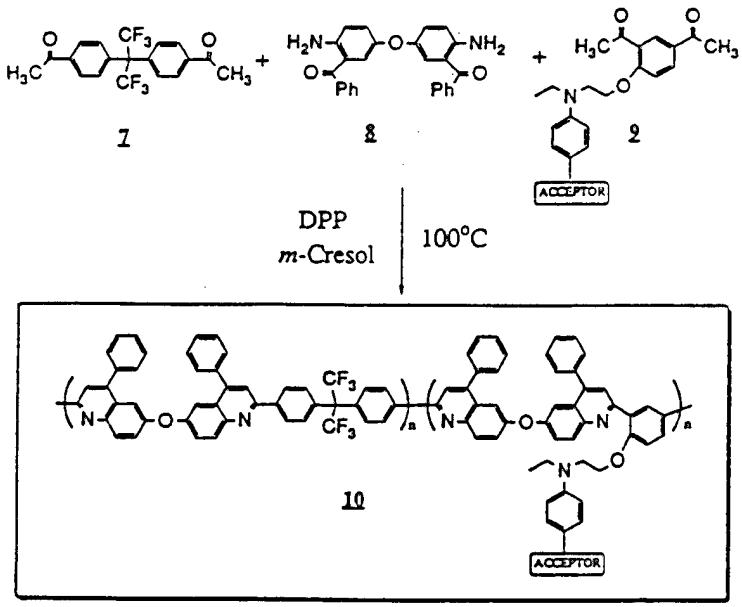

Acceppt: Disperse red, Dicyanovinyl-, Tricyanovinyl-, and DCM-type

Acknowledgements

This research was supported by the Air Force Office of Scientific Research under contract F49620-94-C-0064 and Office of Naval Research under contract N00014-95-C-0321.

PHOTOINDUCED SECOND HARMONIC GENERATION IN MOLECULAR MEDIA : FROM FUNDAMENTALS TO APPLICATIONS

Céline Fiorini, Jean-Michel Nunzi, Fabrice Charra, Witold Chalupczak and Paul Raimond
Commissariat à l'Energie Atomique, Leti/Technologies Avancées,
DEIN-SPE, Organic Devices Group, Centre d'Etudes de Saclay,
91191 GIF-SUR-YVETTE Cedex, FRANCE
Tel. : +33 (1) 69 08 52 34
Fax : +33 (1) 69 08 76 79
e-mail : fiorini@serin.cea.fr

Light-induced second-harmonic generation was first observed in glass optical fibers [1,2]. The method consists in a seeding-type experiment : thanks to dual-frequency interference processes, it can be shown that the coherent superposition of two beams at fundamental and second-harmonic frequencies can result in the breaking of the initial centrosymmetry of a medium [3,4]. In addition to its relative ease of processing, one of the fundamental advantage of such method is that the spatial period of the induced $\chi^{(2)}$ susceptibility satisfyes automatically the phase-matching condition for second-harmonic generation.

Compared to optical fibers, where the induced nonlinearities remain relatively small, the use of organic molecules is quite interesting because of the large benefit which can be derived from molecules with high second-order polarizabilities β. Molecular engineering together with the large potential of organic synthesis make it possible to design and synthetize molecules with optimized linear and nonlinear properties. Additionally, side chain polymers containing organic hyperpolarisable moieties may combine the large nonlinearities with the attractive processing properties of polymers.

Using a six-wave mixing configuration in a picosecond regime, we have demonstrated the possibility of photoinducing second-order susceptibilities $\chi^{(2)}$ in solutions of dye molecules [5]. The physical origin of the effect was attributed to an orientational hole-burning in the isotropic distribution of molecules [5,6]. More recently, experiments performed with spin-coated films of azo-dye doped polymers proved that it was possible to achieve an efficient and quasi-permanent poling of the molecules [7,8]. More precisely, it can be shown that it is possible to induce the same orientational efficiency as with the more standard poling methods which use a dipolar orientation of the molecules under a strong DC field (such as the Corona poling method). Indeed, identification of the physical mechanisms responsible for the organized polar arrangement enables optimization of the preparation conditions of the sample [9]. It can be shown that the crucial parameter of an efficient all-optical poling is appropriate relative energies of the seeding beams at fundamental and second-harmonic frequencies. Typically, this requirement consists only in the use of a high enough peak power density of the beam at fundamental frequency (about 100 MW/cm2) to enable the second-harmonic generated signal to be detected. Such power density can be delivered even from relatively low power sources by use of tight focussing. We have demonstrated recently efficient all-optical poling of an azo-dye copolymer using a low power microsecond laser [10].

In addition to the automatic fulfilment of the phase matching condition, the all-optical poling technique opens prospects that are not permitted with Corona poling such as

orientation of molecules without a permanent dipole moment in the ground state, such as octupolar molecules. It can indeed be shown that the resulting field of the coherent superposition of two beams at fundamental and second-harmonic frequencies presents a component of octupolar symmetry in addition to the polar one, thus allowing for the coupling of this field with an octupolar molecule. After the first experimental evidence of light-induced second-harmonic generation in solutions of the planar octupolar Ethyl Violet molecule [11], we reported a quasi-permanent light-induced second order susceptibility in a solgel matrix doped with Ethyl Violet [12] and more recently in a PMMA rod doped with a tetrahedral organotin molecule. In both cases, the tensorial analysis of the induced $\chi^{(2)}$ is in good agreement with the microscopic symmetries of the molecules and confirms the octupolar symmetry of the photoinduced order. It can also be shown that the use of particular combinations of beams' polarization may permit an enhancement of the light-matter interactions and could lead to an enlargement of the achievable poled geometries. It is also noteworthy that the method of all-optical induction of non-centrosymmetry can be applied to solutions of ionic salts or polyelectrolyte glasses.

Erasure mechanisms following a monochromatic irradiation appear to be a major problem preventing the use of such systems. However, experiments are currently in progress with sol-gel systems or crosslinkable polymers. These could provide an attractive route to improve the stability of the photoinduced polar order. Another limitation to be overcome concerns the absorption of the nonlinear chromophores at the SH frequency : with such molecules as DR1, although it was shown that it was possible to induce locally high second-order susceptibilities $\chi^{(2)}$, because of absorption, it appears impossible to achieve phase-matching over long distances and to reach higher harmonic efficiencies. The studies reported here have however lead to a good understanding of the different mechanisms involved in the process of all-optical induction of noncentrosymmetry in organics. More recently, we have demonstrated light-induced $\chi^{(2)}$ in highly transparent materials.

The aim of the talk is to show that this technique opens new directions towards the design of devices for free or guided-wave frequency conversion while offering broad possibilities in the field of molecular photophysics and nonlinear spectroscopy. After a detailled theoretical analysis of the particular mechanism of polar and octupolar coupling between light and molecules, we illustrate our theoretical study by results obtained in different molecular systems.

REFERENCES :

1. U. Osterberg and W. Margulis, *Opt.Lett.* **11**, 516 (1986);
2. R.H. Stolen and H.W.K Tom, *Opt.Lett.* **12**, 585 (1987).
3. N.B.Baranova et B.Ya. Zeldovich, *JETP Lett.*, **45**, 717, (1987).
4. B.Ya. Zeldovich and Yu.E. Kapitskii, *JETP Lett.*, **51**, 441, (1990).
5. F. Charra, F. Devaux, J.M. Nunzi and P. Raimond, *Phys.Rev.Lett.*, **68**, 2440 (1992).
6. C.Fiorini, F.Charra et J.M.Nunzi, *J. Opt. Soc. Am. B*, **11**, 12, 2347 (1994).
7. F. Charra, F. Kajzar, J. M. Nunzi, P. Raimond and E. Idiart, *Opt. Lett.*,**18**, 941,(1993).
8. C. Fiorini, J.M. Nunzi, F. Charra and P. Raimond, *Nonlinear Optics*, **9**, 339 (1995).
9. J.M.Nunzi et al., *ACS Symposium Series* **601**, G. Lindsay and K. Singer Eds, p. 240, (1995).
10. W. Chalupczak et al., *Opt. Comm.*, **126**, 103, (1996)
11. J.M. Nunzi, F. Charra, C. Fiorini, J. Zyss, *Chem. Phys.Lett.*, **219**, 349 (1994).
12. C. Fiorini et al., *Opt. Lett.*, 20, **24**, 2469, (1995).

CHIRAL EFFECTS IN SECOND-ORDER NONLINEAR OPTICS OF THIN FILMS

André Persoons, Martti Kauranen, Thierry Verbiest, Jeffery J. Maki, and Sven Van Elshocht
Laboratory of Chemical and Biological Dynamics and
Center for Research on Molecular Electronics and Photonics,
University of Leuven, Celestijnenlaan 200 D, B-3001 Heverlee, Belgium
Tel. +32-16-327197, Fax. +32-16-327982
e-mail: andre@lcbdiris.fys.kuleuven.ac.be

Abstract

Nonlinear optical properties of chiral materials have experienced a surge of experimental activity over the past few years. In particular, second-order nonlinear properties of chiral surfaces and thin films have been studied by several groups. Compared to linear optical properties of chiral materials, the second-order properties of chiral surfaces have several similarities but also important differences.

The key property of second-harmonic generation from chiral surfaces is its different response to left- and right -hand circularly-polarized fundamental light. Compared to the work of other groups, which have used this circular-difference (CD) effect to investigate model systems of chiral molecules using this technique, we have concentrated on understanding and separating the various physical mechanisms that can give rise to the CD response.

In our experiments, we have utilized thin films of chiral poly(isocyanide)s functionalized with nonlinear-optical chromophores. The CD response of second-harmonic generation from chiral surfaces can occur within the electric-dipole approximation. However, our experimental results can not be explained within the electric-dipole approximation. Chiral molecules are known to possess also significant magnetic-dipole transitions. Hence, we have developed a technique that can be used to separate the electric and magnetic contributions to the surface nonlinearity. The technique relies on measuring several second-harmonic signals as functions of the rotation angle of a quarter wave-plate that controls the state of polarization of the fundamental beam. It is sufficient to measure only normalized lineshapes of each signal, hence, the technique is limited only by the accuracy of a single measurement. For the case of poly(isocyanide) thin (35 nm) films and properly accounting for linear optical effects, the largest components of the surface susceptibility tensor including magnetic transitions were found to be of the order of 20% of the electric-dipole-only components.

The CD response of surface second-harmonic generation is analogous to the linear optical activity effects. However, we have shown that appropriately chosen linear input polarizations can also be used to probe surface chirality. The measured difference effects between the appropriate linear polarizations are comparable to the CD effects. The fundamental origin of the linear-difference effects is the broken symmetry between the *s*- and *p*-polarized components of the fundamental light in the surface geometry.

The poly(isocyanide) films have in-plane isotropy. For such samples these nonlinear optical activity effects can occur only for chiral surfaces, i.e., for surfaces that have no mirror planes (perpendicular to the surface). However, we have also used these techniques to investigate anisotropic achiral surfaces. As an anisotropic sample we have used Langmuir-Blodgett films of DCANP (2-docosylamino-5-nitropyridine) with the achiral C_{1h} symmetry.

These samples were also found to exhibit nonlinear optical activity (circular-difference and linear-difference response). However, in this case the optical activity arises from the chirality of the experimental setup. For most orientations of the sample, the experimental arrangement possesses no mirror planes, because the sample director, surface normal, and the wave vector of the fundamental beam are not coplanar, i.e., a coordinate system based on these vectors possesses a definite handedness. The optical activity was found to vanish for sample orientations that make the experimental geometry achiral. Furthermore, the optical activity effects were found to reverse sign as the handedness of the experiment was reversed.

I-16

NONLINEAR ANISOTROPY IN MULTIPOLAR NONLINEAR SYSTEMS

Sophie BRASSELET, Irène CAZENOBE, Isabelle LEDOUX and Joseph ZYSS
France Telecom, Centre National d'Etudes des Télecommunications
Laboratoire de Bagneux
196, Avenue Henri Ravera, 92225-Bagneux, FRANCE

A simple and experimentally accessible parameter can be introduced to account for the spatial anisotropy of quadratic nonlinear optical properties by way of extension of the usual linear birefringence. At the molecular level, the *nonlinear anisotropy* is defined as the ratio $u=\|\beta_{J=3}\|/\|\beta_{J=1}\|$ of the norms of the octupolar over dipolar contributions to the hyperpolarizability tensor β. This parameter can be infered from the depolarization ratio in HyperRayleigh scattering and will be discussed for different molecular systems. In particular, one can prove, based on a simple intrinsic tensorial formalism that the depolarization ratio expressed as a function of the nonlinear anisotropy exhibits two extrema corresponding respectively to purely octupolar ($u=\infty$) and purely dipolar ($u=0$) molecular systems. Along similar lines, a general formalism capable of handling in a rotationally invariant way the averaged $\beta\otimes\beta$ *squared* hyperpolarizability tensor as well as the corresponding *nonlinear field tensor* $E^{2\omega*}\otimes E^{\omega}\otimes E^{\omega}$ will be shown to be applicable to both HyperRayleigh and optical poling induced SHG processes.

The multidimensional structure and related multipolar nature of the polarizability properties of multiple charge transfer systems bears stringent implications on their quantum mechanical description. In particular, their spectral dispersion properties cannot be accounted for by the usual two-level quantum model applicable to paranitroaniline and related quasi one dimensional polar molecules. As expected by symmetry considerations, the existence of a third level as well as its geometric and spectroscopic features have been evidenced in the case of a planar C_{2v} (mm2) multipolar aromatic molecule. Linear and nonlinear optical studies of this system in guest-host poled polymer films exhibit specific features which can be accounted for by the existence of an angle between $\Delta\vec{\mu}_j$ and $\vec{\mu}_{0j}$ standing respectively for the difference between dipole moments of excited state $|j\rangle$ ($j=1,2$) and ground state $|0\rangle$ and the transition dipole moment connecting ground and excited states. In the simpler but illustrative case of C_{2v} planar molecules, the transition dipole moments towards excited states are respectively parallel and perpendicular to the permanent dipole, leading respectively in the former case to the usual decrease of the in-plane polarized linear absorption in contrast with a less familiar increase in the latter case.

Based on an intimate combination of tensorial and quantum mechanical considerations, linear and nonlinear spectroscopic studies of guest-host poled polymer films will be shown to provide interesting insights on the excited state properties of multidimensional conjugated molecular systems.

Figure 2 shows a cross-section of the ring formation occurring in the same crystal and the accompanying simulation for the same initial conditions as in figure 1, but with an intensity of 9 GW/cm^2 (power = 43 kW). Complete ring formation does not occur due to the pulsed nature of the beam, whereby the higher intensity, center portion of the beam forms the ring, and the lower intensity, temporal wings stay trapped as a solitary wave on axis. The experimental results agree very well with the numerical simulations. Both the solitary wave in figure 1 and the ring in figure 2 have a background that results from portions of the beam that do not form a solitary wave, but instead diffract away, either as portions of the temporal wings of the pulse that are below the threshold for self-trapping or scattering off of defects in the crystal.. To our knowledge, these results are the first experimental demonstration of a quintic nonlinearity, independent of saturation, in a solid-state material system.

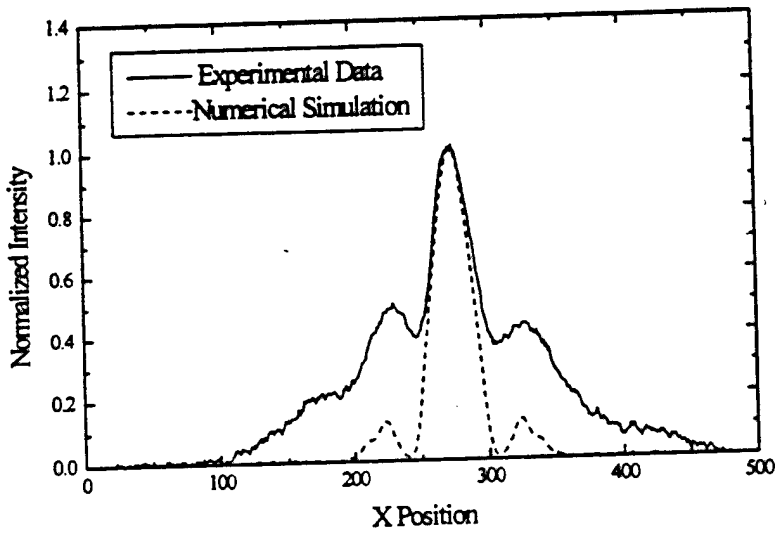

Figure 2: Experimental data (solid line) and numerical calculation (dashed line) of ring formation in a 1.7 mm PTS crystal at 1600 nm, with an input waist of 16 μm, at an intensity of 9 GW/cm^2 (power = 36 kW).

References:

1. P. L. Kelley, Phys. Rev. Lett. **15**, 1005 (1965)

2. J. E. Bjorkholm and A. Ashkin, Phys. Rev. Lett. **32**, 129 (1974)

3. V. E. Zakharov, V. V. Sobolev, and V. C. Synakh, Sov. Phys. JETP **33**, 77 (1971)

4. V. M. Malkin, Physica D **64**, 251 (1993)

5. B. L. Lawrence, M. Cha, J. U. Kang, W. Torruellas, G. Stegeman, G. Baker, J. Meth, and S. Etemad, Electron. Lett. **30**, 447 (1994)

6. E. M. Wright, B. L. Lawrence, W. E. Torruellas, G. I. Stegeman, Opt. Lett., **20**, 2478 (1995)

Due to the high refractive index modulation amplitudes that can be achieved in these highly efficient photorefractive polymers (Δn = 0.007), the recording of thick phase grating in these materials can also lead to non-Bragg diffraction orders.[9] This effect is different from higher diffraction orders observed in the Raman-Nath diffraction on thin gratings. For instance, diffraction is not obtained for beams incident at arbitrary angles like in thin gratings and the higher diffraction orders can not be described by Bessel functions. Observation of such non-Bragg diffraction orders will be reported and their properties including phase-conjugation and phase-doubling will be demonstrated.

Finally, to illustrate the technological potential of photorefractive polymers for optical processing applications we will demonstrate an all-optical, all-polymeric correlator for security applications. In this correlator, a highly efficient PVK-based polymer is used as the nonlinear medium for security verification of documents such as credit cards optically encoded with pseudo-randomly generated phase masks. The use of a low cost photorefractive polymer as active medium keeps the overall manufacturing cost of the device sufficiently low to make it technologically viable. We will discuss its technical merits and its advantages over previous designs that greatly increase its potential to be used in wide-spread security applications.

Acknowledgments: This work was supported by ONR through the Center for Advanced Multifunctional Nonlinear Optical Polymers and Molecular Assemblies (CAMP), by NSF, by AFOSR, and by an NSF-CNRS collaboration program. We acknowledge O. Savina for her help during sample preparation, and collaboration with Drs. K. Meerholz, N. V. Kukhtarev, B. Javidi, and CAMP members.

References:

[1] Moerner, W. E.; Silence, S. M. *Chem. Rev.* 1994, *94*, 127.

[2] Meerholz, K.; Volodin, B. L.; Sandalphon; Kippelen, B.; Peyghambarian, N. *Nature* 1994, *371*, 497.

[3] Liphard, M.; Goonesekera, A.; Jones, B. E.; Ducharme, S.; Takacs, J. M.; Zhang, L. *Science* 1994, *263*, 367.

[4] Zhang, Y.; Cui, Y.; Prasad, P. N. *Phys. Rev. B* 1992, *46*, 9900.

[5] Volodin, B. L.; Sandalphon; Meerholz, K.; Kippelen, B.; Kukhtarev, N.; Peyghambarian, N. *Opt. Eng.* 1995, *34*, 2213.

[6] Kippelen, B.; Peyghambarian, N. In *Chemistry & Industry*, 1995, *22*, 917.

[7] Moerner, W. E.; Silence, S. M.; Hache, F.; Bjorklund, G. C. *J. Opt. Soc. Am. B* 1994, *11*, 320.

[8] Kippelen, B.; Sandalphon; Meerholz, K.; and Peyghambarian, N. *Appl. Phys. Lett.* 1996, *68*, 1748.

[9] Volodin,B. L.; Kippelen, B.; Meerholz, K.; Kukhtarev, N. V.; Caulfield, H. J.; and Peyghambarian, N. *Opt. Lett.* 1996, *21*, 519.

Mechanisms of Photorefractivity in Polymer Composites

W. E. Moerner, A. Grunnet-Jepsen, and C. Thompson

Department of Chemistry and Biochemistry
University of California San Diego, La Jolla, California 92093-0340

In the past few years, a new class of polymeric materials for photonic applications has appeared called photorefractive (PR) polymers. Photorefractivity is defined as modulation of the index of refraction in an electro-optic material by internal electric fields produced by optical redistribution of charge carriers. In principle, such materials can be used for many optical processing, holographic, optical limiting, phase conjugation, and storage applications, but to date, no widespread applications have attained practicality due to materials limitations.

Until very recently, all materials showing the PR effect were inorganic crystals. Polymers exhibiting the photorefractive effect have attracted interest since their first discovery in 1991 [1] because this new class of photorefractive materials offers potentially large improvements in photorefractive figures of merit due to the low dielectric constant [2]. They also possess other advantages over inorganic materials, such as compositional flexibility and relative ease of sample preparation and processability. Moreover, the performance of the newest PR polymers is beginning to be competitive with the conventional inorganic crystals for some applications.

Several recently-reported materials show very large diffraction efficiency and index modulations approaching 10^{-3} or larger [3][4]. In almost all cases, the large signals have been shown to be due to an orientational enhancement mechanism described in 1994 [5]. According to this model, in low glass-transition materials, the orientational mobility of the chromophores allows both the hyperpolarizability as well as the polarizability anisotropy (birefringence) of the chromophore to become important in determining the index of refraction change.

Special Properties and Design of PR Polymers

In general, to make a PR polymer composite, functional moieties are provided which produce the required properties of charge generation, charge transport, charge trapping, and electro-optic behavior. Although the basic mechanism of generation of the space-charge field, the hopping of photogenerated charges to trapping sites under the influence of a nonuniform light distribution, is similar between PR polymers and the conventional inorganics, there are some essential differences. First, in organics the quantum efficiency for generation of mobile charge, ϕ, is highly field dependent [6] due to Onsager geminate recombination, which means that high fields are generally necessary for facile charge generation. Second, the mobility is also highly field-dependent, often varying as $\log\sqrt{E}$, a behavior that has been widely observed in many molecularly doped polymers [7] as well as in the few PR polymers in which mobility measurements have been completed [8][9]. Thus, in cases where the mobility may be limiting the speed of response, higher fields are necessary to increase the speed of charge transport. Finally, in many PR polymer composites, the glass transition temperature T_g is low so that the nonlinear chromophores have sufficient rotational mobility as to be oriented by the total local electric field at ambient temperatures. This means in particular that the optical nonlinearity of the material is a function of the applied field, and moreover that the readout of a stored space-charge-field can be turned on and off by controlling the externally applied electric field. (Note that low T_g is not an essential requirement, as some PR polymers have been studied which are permanently poled at high temperature in the usual fashion[10]).

The Orientational Enhancement Mechanism

The greatly improved performance of many new photorefractive polymer composites is too large to be explained by the simple electro-optic photorefractive effect alone. In a recently presented a theoretical model [5], a new orientational enhancement mechanism is described in which both the birefringence and the electro-optic coefficient are periodically modulated by the space-charge field, due to the orientational mobility of the NLO chromophores at ambient temperatures. This effect is responsible for more than an order of magnitude increase in diffraction efficiency or more, depending upon the actual molecular parameters of the chromophore. This mechanism should be important in any system in which the NLO chromophores have sufficient orientational mobility and dipole moment so as to be oriented by the space charge field itself.

Due to the orientational enhancement effect, chromophores may now be compared by the following two parameters: $\mu\beta$, which describes the ability to field-orient the chromophore with hyperpolarizability β with ground-state dipole moment μ, and $\mu^2\Delta\alpha$, where $\Delta\alpha$ is the polarizability anisotropy difference parallel and perpendicular to the molecular axis. Optimization of chromophores may now be done by optimizing either of these quantities, and in many cases, it may be easier to optimize the birefringence instead of the hyperpolarizability.

Conclusion

Photorefractive polymer composites have shown impressive gains in performance in just a few years of research, and it is clear that the actual limits to the performance of this new class of photorefractive materials are not known at present. However, as is the case with any new materials class vying for applications, the ultimate utility of PR polymers may rest on difficult issues which have not yet been considered in detail such as fatigue and optical quality. In particular, the tendency of the researcher to dope a polymer with higher and higher concentrations of a nonlinear optical chromophore can lead to problems with sample stability and crystallization.

Acknowledgment:

This work was supported in part by the Air Force Office of Scientific Research.

References

1. S. Ducharme, J. C. Scott, R. J. Twieg, and W. E. Moerner, *Phys. Rev. Lett.* **66**, 1846 (1991).
2. For a review, see W. E. Moerner and S. M. Silence, *Chem. Revs.* **94**, 127 (1994), and S. M. Silence, D. M. Burland, and W. E. Moerner, Chap. 5 of *Photorefractive Effects and Materials*, edited by D. D. Nolte, (Kluwer Academic, Boston, 1995), pp. 265-309.
3. K. Meerholz, B. L. Volodin, Sandalphon, B. Kippelen, and N. Peyghambarian, *Nature* **371**, 497 (1994).
4. O. Zobel, M. Eckl, P. Strohriegl, and D. Haarer, *Adv. Mater.* **7**, 911 (1995).
5. W. E. Moerner, S. M. Silence, F. Hache, and G. C. Bjorklund, *J. Opt. Soc. Am. B* **11**, 320 (1994).
6. P. J. Melz, *J. Chem. Phys.* **57**, 1694 (1972).
7. L. B. Schein, *Phil. Mag. B* **65**, 795 (1992).
8. J. C. Scott, L. Th. Pautmeier, and W. E. Moerner, *J. Opt. Soc. Am. B* **9**, 2059 (1992).
9. J. C. Scott, L. Th. Pautmeier, W. E. Moerner, C. A. Walsh, S. M. Silence, T. J. Matray, and R. J. Twieg, *Proc. Mat. Res. Soc.* **277**, 135 (1992).
10. S. M. Silence, F. Hache, M. C. J. M. Donckers, C. A. Walsh, D. M. Burland, G. C. Bjorklund, R. J. Twieg, and W. E. Moerner, *Proc. Soc. Photo-Opt. Instrum. Engr.* **1852**, 253 (1993).

Excited-state electronic structure and nonlinear optical response of long donor-acceptor conjugated molecules

J.L. Brédas [a], J. Li [a], T. Kogej [a], D. Beljonne [a], V. Geskin [a], S. R. Marder [b,c], and R. Silbey [d,a]

a: Center for Research on Molecular Electronics and Photonics, Université de Mons-Hainaut, Place du Parc 20, B-7000 Mons, Belgium

b: The Beckman Institute, California Institute of Technology, Pasadena, California 91125.

c: The Jet Propulsion Laboratory, California Institute of Technology, Pasadena, California 91109.

d: Department of Chemistry, Massachusetts Institute of Technology, Cambridge, Massachusetts 02139.

We are exploring various routes to strongly enhanced second-order and third-order optical nonlinearities. To do so, we evaluate the electronic structure in the excited state and the nonlinear optical tensor components by means of quantum-chemical calculations including correlation effects. We focus on:

(i) β-apocarotenals. Such molecules, that contain 11 double bonds along the polyene segment and are substituted with strong acceptors, have been recently demonstrated to exhibit exceptionally large third-order optical nonlinearities. We discuss the origin of enhancement of the NLO properties with respect to β-carotene and show that such long compounds can sustain more than a single electron transfer to the acceptor end. We also describe results obtained on molecules derivatized with multiple donor/acceptor functionalities.

(ii) spacer-containing donor-acceptor polyenes. The presence of a spacer moiety in the middle of the conjugated segment constitutes, upon application of an external electric field, the origin of an abrupt change in molecular dipole moment as charge transfer takes place from the donor part to the acceptor part; as a result, very large second-order and third-order optical responses are predicted. By varying the nature of the spacer, a good compromise can be found between enhancement of the NLO properties and optical transparency.

(iii) compounds with large two-photon or photo-induced absorption. Here, via a detailed characterization of the electronic structure in the excited state, we describe the mechanisms that lead to large TPA or PA intensities. We address organic as well as metallo-organic (porphyrin-based) systems.

Recent Advances in the Design and Use of the Real and Imaginary Third-Order Optical Nonlinearities of Organic Dyes.

M. Barzoukas[a], M. Blanchard-Desce[b,c], S. Boxer[d], G. Bublitz[d], J.-L. Brédas[e], J. Ehrlich[f], A. Fort[a], A. Heikal[f], Z.-Y. Hu[c], K. Kustedjo[c], J. Li[e], J. Mendez[c], S. R. Marder[c,f], F. Meyers[c], A. Oseroff[g], J. W. Perry[c,f], W. Potter[g], V. Ricci[h], W.Torruellas[h,i], G. Stegeman[h], X. L. Wu[c], and R. Zowada[g]

a: IPCMS (UM 046 CNRS), 23, rue du Loess, F-67037, Strasbourg Cedex France.

b: Ecole Normale Supérieure, Département de Chimie (URA 1679 CNRS), 24 rue Lhomond 75231 Paris Cedex 05, France.

c: The Beckman Institute, California Institute of Technology, Pasadena, CA 91125, USA.

d: Department of Chemistry, Stanford University, Stanford, CA 94305, USA.

e: Center for Research on Molecular Electronics and Photonics, Université de Mons-Hainaut, Place du Parc 20, B-7000 Mons, Belgium.

f: The Jet Propulsion Laboratory, California Institute of Technology, Pasadena, CA 91109, USA.

g: Roswell Park Cancer Institute, Elm and Carlton Street, Buffalo, NY, 14263, USA.

h: Center for Research on Electro-optic and Lasers, University of Central Florida, Orlando FL 32826, USA.

i: Department of Physics, Washington State University, Pullman, WA 99164, USA.

ABSTRACT

We have been developing mechanisms to enhance both the real and imaginary parts of the second-hyperpolarizability tensor, γ. It had been predicted by several groups including ours that dipolar molecules possessing a large change in dipole between the ground and a charge-transfer excited state could exhibit enhanced γ. This enhancement was demonstrated in model systems however, there have not been reports of exceptionally large nonlinearities exploiting this design strategy. In this paper, we will report on systems derived from β-apo 8'-carotenal, substituted with strong acceptors that exhibit exceptionally large third-order optical nonlinearities. EFISH and Stark spectroscopy coupled with INDO-SDCI calculations provide insight into the origin of the nonlinearity.

We are also interested in systems that exhibit strong two-photon absorption and fluorescence for a variety of applications that include *in vivo* imaging of cancer tumors. One requirement for such imaging is that the molecules must have large two-photon

induced fluorescence quantum yields. For imaging of tumors *in vivo*, when irradiating with 1.064 μm light, it is additionally important that the dye which should absorb at 532 nm exhibit a significant Stokes shift, for efficient penetration of emitted light through tissue. Furthermore, the dye must preferentially accumulate in the tumor and must have low toxicity at dosages required to obtain images. In this paper, we will present some results from our preliminary studies geared at understanding how to attack this problem.

Preparation and in-situ electro-optical investigation of poling structures for phase-matched second-harmonic generation in waveguides

S. Yilmaz, W. Wirges, W. Brinker, S. Bauer-Gogonea, and S. Bauer*
Heinrich-Hertz-Institute, Einsteinufer 37, 10587 Berlin, Germany

M. Jäger and G. I. Stegeman
CREOL, University of Central Florida
12424 Research Parkway, Orlando, FL 32826, USA

M. Ahlheim, M. Stähelin, B. Zysset, and F. Lehr
Sandoz Optoelectronics, Av. de Bale, F-68330 Huningue, France

M. Diemeer and M. C. Flipse
Akzo Nobel Electronic Products, Arnhem, The Netherlands

Recently second-harmonic generation (SHG) of light in waveguides has gained new attention, as the cascading of second-order nonlinearities gives rise to large, nonresonant third-order-like optical nonlinearities for all-optical switching, spatial solitons etc /1/. Nonlinear optical (NLO) polymers seem to be very interesting materials for waveguide SHG due to large second order nonlinearities after poling. Efficient SHG requires phase matching (PM) so that the harmonic fields generated in different parts along the waveguide interfere constructively at the output. PM is possible via different routes, such as anomalous dispersion PM /2/, quasi-phase-matching (QPM) /3/, and modal dispersion PM /4/. Anomalous dispersion PM suffers from the limited transaprency, while periodical poling for QPM leads to significant surface deformations /5/. Therefore modal dispersion PM seems to be an interesting alternative for efficient SHG.

Modal dispersion PM was demonstrated in a multilayer waveguide with a guiding layer consisting of a passive and a nonlinear optically active polymer film /4/. Another technique is based on a step-like dipole orientation profile across the thickness of the waveguide and has been demonstrated by using the Langmuir-Blodgett technique /6/.

Our proposal uses the waveguide geometries in Fig. 1 and the two step-poling process of Fig. 2 /7/.

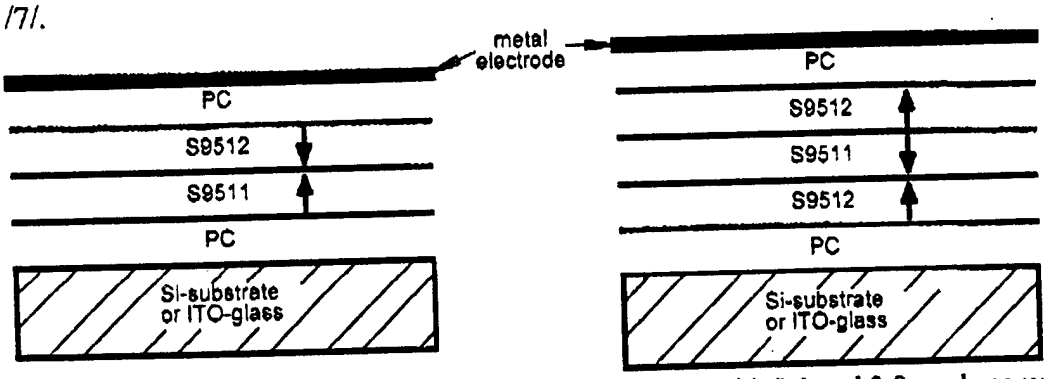

Fig. 1: (left) and (right): waveguide geometries for PM-SHG with 0-1 and 0-2 mode conversion.

* Present address: Institute of Solid State Physics, University of Potsdam, Am Neuen Palais 10, D-14469 Potsdam, Germany

Dynamics of Two-Photon Processes and their Applications

P. N. Prasad, J. D. Bhawalkar, G. S. He, P. C. Cheng,* S. J. Pan,* A. Shih,* and W. S. Liou*
Photonics Research Laboratory, Dept. of Chemistry
*Advanced Microscopy and Imaging Laboratories, Dept. of Electrical and Computer Engineering,
State University of New York at Buffalo, Buffalo, NY 14260

In the decades following their discovery, two-photon processes have found limited applications other than in spectroscopy, due to the relatively small two-photon absorption cross-sections of most materials. However, recent work in our laboratory has resulted in a new class of organic molecules with enhanced two-photon properties. These materials are multifunctional, combining strong two-photon absorption with other properties, such as efficient fluorescence. These multifunctional materials have opened up a a range of novel applications in photonics and biophotonics.

Two of the new chromophores, trans-4-[P-(N-ethyl-N-hydroxylethyl-amino)styryl]-N-methylpyridinium tetraphenylborate (ASPT), and 4-[N-(2-hydroxyethyl)-N-(methyl) amino phenyl]-4′-(6-hydroxyhexyl sulfonyl)stilbene (APSS) have two-photon absorption cross-sections (ASPT: $\sigma_2=1.2\times10^{-46}cm^4s$, in a hydroxyethyl methacrylate polymer matrix at 1064 nm, and APSS: $\sigma_2=3.8\times10^{-47}cm^4s$, in dimethyl formamide solution at 800 nm) that is much larger than the reported literature values for commercial dyes such as Rhodamine 6G ($\sigma_2=1\times10^{-49}cm^4s$ in hexafluoroisopropanol solution at 1054 nm). They exhibit strong fluorescence with emission maxima at about 600 nm and 520 nm, respectively, and also have excellent lasing properties. We have demonstrated two-photon pumped lasing from both the chromophores in different geometries at very low pump energies (< 0.1 mJ).

We reported efficient solid-state two-photon pumped cavity lasing in ASPT-doped polymer rods, sol-gel glass, and VYCOR (a commercially available porous glass), when pumped with 1064 nm laser pulses. The feasibility and advantage of two-photon pumped lasing in confined structures was demonstrated using the dye APSS in a hollow fiber geometry. A 15-cm long, 100 μm inner diameter hollow quartz fiber filled with a solution of APSS in dimethyl sulfoxide served as the gain medium. The input 800-nm pump IR laser beam was provided by a pulsed nanosecond dye laser. Under excitation from the pump beam, a strong TPA induced green fluorescence emission could be seen from the hollow fiber. When the input pump intensity exceeded a threshold level, an intense green laser emission was observed at the output. The net conversion efficiency from the absorbed pump energy to the lasing output was 2.3%.

Optical power limiting is an area of growing interest due to applications such as eye and sensor protection against intense light. Several mechanisms such as reverse saturable absorption, multiphoton absorption, free carrier absorption in semiconductors, nonlinear refraction, and optically-induced scattering have been suggested and used for passive optical limiting. Multiphoton absorption-induced optical limiting has desirable features such as low attenuation at low incident intensities, and an instantaneous response to the incident light. The dye, ASPT is ideally suited for optical limiting at 1064 nm, because it has a very strong two-photon absorption at 1064 nm. The sample used in the study of the optical limiting behavior of this dye was a 0.02 m-long epoxy rod doped with ASPT at a concentration of 4×10^{-3} M/L. The source at 1064 nm was a 10 ns Q-switched Nd:YAG laser. The beam was focused on the sample by a f=0.3 m lens, and the incident intensity was varied from zero to about 225 MW/cm^2. It was observed that at an incident intensity of around 200 MW/cm^2, the transmissivity dropped to about 25% of its initial value. It is likely that in conjunction with other mechanisms, multiphoton absorption can be used in a practical optical limiter.

Optical data storage in bulk media (three-dimensional) has received a lot of attention in recent years. Several approaches to 3D optical data storage, such as, holographic recording on photorefractive media, hole burning, and photon echo, are currently being investigated. There have also been some recent reports on two-photon based optical data storage in polymer systems. The advantages of two-photon based memory systems are, (1) volume storage with high data storage densities of over 10^{12} $bits/cm^3$, (2) fast read/write times, (3) random access, and (4) low cost. The basic components of a two-photon memory are, a medium which exhibits a change in its optical properties (absorbance, fluorescence, refractive index, etc.) after two-photon absorption, an appropriate read and write beam, and a mechanism to precisely access any volume element in the medium. We have demonstrated permanent data storage (Write Once, Read Many times- WORM) in the bulk of a dye-doped polymer. A confocal laser scanning microscope (CLSM) operating in the fluorescent mode enabled read/write with high accuracy and precision. Using red or near infrared excitation followed by two-photon absorption induced upconverted fluorescence, the CLSM offers advantages over conventional one-photon pumped fluorescence

microscopy, especially to read and write data in a photoactive medium. Since two-photon excitation has a strong dependence on the pump intensity, the writing process occurs only in the near vicinity of the focal point. In a polymer doped with a chromophore, an infrared beam can penetrate deeper due to a low linear absorption at that wavelength. Thus writing and reading in the volume are possible. The excitation source was a mode-locked Ti:Sapphire laser oscillator producing a train of 798 nm pulses of duration 90 fs each, at a frequency of 92 Mhz. The average power measured at the sample was only about 0.3 mW. A 3×5×3 mm HEMA (hydroxyethyl methacrylate) polymer block doped with APSS was used as the data storage medium. When a focused infrared beam from the Ti:Sapphire laser is incident in the sample, there is a strong two-photon induced green fluorescence at the focal point, and with sufficiently strong pumping, photobleacing occurs at that point. It should be noted that the z dimension of the photobleached spot was only about 0.8μm. This is in contrast to the single-photon case where photobleaching occurs in the entire cone of illumination. To read these planes, the same laser source was used but the illumination dose per unit area was reduced by over two orders of magnitude compared to the writing process. We wrote a set of photobleached planes with different contrast separated from each other by 5 μm in the z-direction. As another example, bitmap images of different frames from an animated movie were stored in planes one behind the other, separated by 5 μm. The sequence of images could then be read back with the confocal microscope.

Multiphoton confocal laser scanning microscopy can be a useful tool to study surface, interface, and fractures in polymer or glass specimens. We have also demonstrated its use to nondestructively probe multilayered coatings and paints. The major advantage of using two-photon excitation arises from the fact that the fluorescence intensity of a two-photon process is quadratically dependent on the illumination intensity. Therefore, the fluorescence emission is limited to the vicinity of the focal point and drops off sharply on all sides. This makes it possible to achieve depth discrimination even without a confocal aperture in front of the photo-detector. The two-photon excitation beam experiences very little absorption along its path except near the focal point allowing deeper penetration. The background scattered light in the two-photon excited system is also lower because the excitation light has a longer wavelength than in the linear excitation process, and well separated from the emission wavelength.

Multiphoton processes appear to be promising for biophotonic applications also. Photodynamic therapy (PDT) is a technique that uses a photosensitizer in the presence of light to produce a cytotoxic effect on cancerous cells. PDT requires three elements: a photosensitizer, oxygen, and light. The photosensitizer is selected to have tumor localizing properties. Upon absorption of light, the photosensitizer is excited to a short lived singlet state. From this state, it undergoes an intersystem crossing (ISC) to a long lived triplet state. In the presence of atmospheric oxygen, which has a triplet ground state, triplet-triplet annihilation occurs. This restores the ground state of the photosensitizer, and generates singlet oxygen which is highly reactive and causes irreversible damage to living tissue. In currently used photosensitizers, with Photofrin® as their most commonly used representative, the peak of excitation is about 400-500 nm. However, the penetration depth of light at those wavelengths in tissue is minimal. Thus, there is a trade-off between penetration depth and efficiency of photosensitizer excitation. The increase of light penetration is considered to be an important factor in increasing the clinical efficacy of PDT. Using two-photon absorption, it may be possible to use near infra-red light for excitation of the photosensitizer. The spectral window for transmission through tissue lies around 800-1100 nm. Using one of the efficient new two-photon pumped upconverting dyes in conjunction with the photosensitizer used in PDT, we have proposed a novel approach to PDT using infra-red laser light for treatment. In this approach, an efficient two-photon absorbing dye is excited by short laser pulses. The dye molecules de-excite and transfer the energy to the photosensitizer which is in proximity to the photosensitizer (or covalently bonded to it). The photosensitizer is thus excited to the singlet state from which the same sequence of energy transfer occurs as described earlier to produce the singlet oxygen.

The initial two-photon absorption of the dye molecules requires high intensity IR laser pulses. These can be easily generated by ultrashort pulse lasers even with relatively low pulse energy. Low pulse energy is highly desirable because it minimizes thermal side effects. An added advantage of using two-photon absorption arises from the quadratic dependence of the efficiency of such a process on the incident light. Therefore the photodynamic effect is restricted to a small area around the focal point. Such spatial selectivity is important in many treatments such as PDT of brain cancers. Preliminary *in vitro* and *in vivo* studies have yielded very promising results.

EFFECT OF STRUCTURAL RELAXATION ON THERMAL AND TEMPORAL STABILITY OF GUEST-HOST SECOND ORDER NONLINEAR OPTICAL POLYMERS

G.A. Medvedev, S.-J. Lee, J.M. Caruthers, H.S. Lackritz
School of Chemical Engineering, Purdue University
West Lafayette, Indiana 47907-1283

It has been shown that second order nonlinear optical methods such as second harmonic generation (SHG) are sensitive to local mobility in guest-host (chromophore doped) polymer systems. This work reports on a model based on stochastic nonlinear constitutive equations to predict structural relaxation in these guest-host systems, including the effects of temporal and thermal stability of the chromophore orientation as a function of processing. Second order nonlinear properties in chromophore doped polymers can be observed when the chromophore is oriented noncentrosymmetrically in the polymer host by electric field poling. When an electric field is applied, the polar chromophore is torqued into the poling induced orientation; when the field is removed, thermal rotation of the chromophores in regions of sufficient mobility will cause the NLO signal to drop. This disorientation is related to the local mobility and structural relaxation in the polymer host as well as fluctuations of the local field.

The rotational Brownian motion of a chromophore in a polymer matrix modeled as a viscous medium can be described in terms of the diffusion equation. Generally rotational diffusion coefficient depends on the local and instantaneous density and temperature in the polymer matrix surrounding the chromophore. Thus, for chromophores embedded in a polymer glass that contains domains of different mobility, there exists a distribution of diffusion coefficients. The physical reason for the heterogeneity is that the local fluctuations of the specific volume appear to be frozen as a result of the dramatic increase in relaxation times. To take into account the time- and specific volume- dependence of the diffusion coefficient, the rotary diffusion equation should be completed using a stochastic equation governing polymer structural relaxation.

Recently developed stochastic model for the specific volume relaxations is used to describe structural relaxation in glassy polymers. The stochastic model naturally incorporates the effect of density fluctuations on the relaxation time and is able to qualitatively predict experimentally observed thermorheological behavior of polymers for a variety of thermal histories as well as long term physical aging. The solution of stochastic differential equation (SDE) for volume relaxation corresponds to an individual realization of the specific volume history; it describes the evolution of the local environment around a single chromophore. The NLO response from the sample is obtained as a statistical average over an ensemble of realizations.

Chromophore rotation in sample consisting of domains with fluctuating specific volumes is modeled. The smaller the value of specific volume, the less able the polymer chains belonging to a given domain to change their configurations, Physically, implying that at that any instant in time, not all the chromophores are allowed to rotate, especially when the temperature is well below T_g. Only those chromophores located in domains of sufficient local volume have freedom to rotate through large angles. This mechanism of local relaxation behavior has significant impact on the characteristics of the SHG intensity decay.

The result of a simulation of chromophore orientational relaxation obtained by averaging over 2000 realizations of SDE is presented in Fig. 1c. The curves display nonexponential behavior, and residual orientation persists for all numerically accessible times. The difference between curves results from the fact that the SHG decay starts after different amount of volume relaxation (Fig. 1b) occurred in the system for different thermal histories (Fig. 1a).

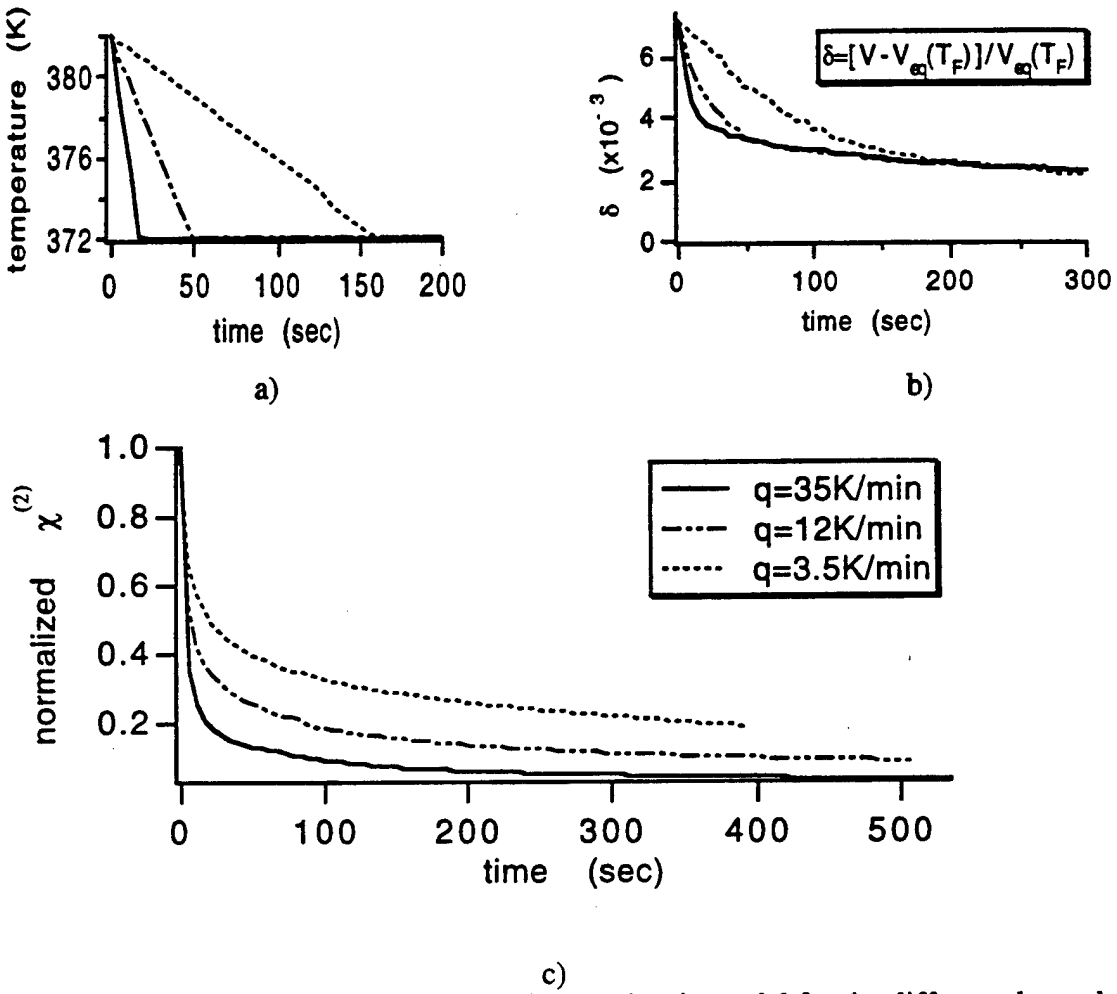

Figure 1. Simulation of the SHG decay using stochastic model for the different thermal histories. Material parameters for PMMA (Tg= 378K); q= cooling rate.; T_F= 372K; δ= average specific volume deviation from the equilibrium value. Poling field is removed after temperature reaches T_F for each thermal history.

It can be concluded that the demonstrated model qualitatively describes main features of SHG signal temporal behavior at the temperatures near and below T_g that have been observed experimentally. Quantitative agreement will be obtained when comparisons are made with series of NLO relaxation data[1]. It has been shown here that the nonexponential character of the chromophore orientational relaxation and its dependence on thermal history can be explained by the coupling between rotary diffusion of chromophores and structural relaxation of polymer matrix.

Acknowledgment
The authors gratefully acknowledge financial support by the National Science Foundation and the Office of Naval Research.

References

1. Medvedev, G. A.; Lee, S.-J.; Caruthers, J. M.; Lackritz, H. S. paper in preparation.

Novel High Nonlinearity Organic Crystals

Peter Günter
Nonlinear Optics Laboratory
ETH-Zürich, Switzerland

We will present most recent results on the growth and characterization of novel high quality molecular crystals for nonlinear optics. These crystals are based on ionic or hydrogen bonding of new and known chromophores with large first-order hyperpolarizabilities.

Detailed results of linear optical, electro-optical and nonlinear optical properties of high quality and large size DAST crystals, of hydrazone derivatives, and new co-crystals will be presented. It will be shown, that optimized parallel alignment of chromophores as well as optimum structures for phase-matched frequency mixing have been realized. In addition we report on the measurement of the highest known phase-matchable nonlinear susceptibility coefficient of 200 pm/V determined recently in our laboratory.

Full Optical Characterization of Highly Nonlinear Organic Material, 3-Methyl-4-methoxy-4'-nitrostilbene(MMONS)

Hyung-Ki Hong and Choon Sup Yoon

Department of Physics, KAIST, Taejon, Korea, 305-701

Tiejun Xia and E.W.Van Stryland

CREOL, University of Central Florida, Orlando, Florida 32826, U.S.A.

Organic material 3-Methyl-4-methoxy-4'-nitrostilbene(MMONS) exhibits one of the largest powder second harmonic signals and has a great potential in frequency doubling and parametric conversion. The large second order nonlinear optical effect in this material attracts great interests because the phase shifts due to the second-order cascading effect can be utilized for the practical switching device.

The single crystals of MMONS of a large size ($40 \times 40 \times 30$ mm^3) and of high quality were successfully grown by solution growth method. Crystal perfection was characterized by white beam synchrotron X-ray topography, which shows a perfection of high degree.

The full coefficients of the second order nonlinear susceptibility tensor were measured by using the Maker fringe technique and d_{31} component was determined for the first time (Fig.1). However the measured value of d_{33} (80 pm/V) is smaller than that of Bierlein's[(1)] and this is probably due to the fact that Bierlein et al used the wrong d_{33} value of KTP as a reference. Utilizing the birefringence of the crystal, the type I and II collinear phase matching conditions were exploited. Maximum conversion efficiencies of 2.5 % for the type I and 13 % for the type II were obtained at 1064 nm (Fig.2). The laser damage threshold was measured to be 56 MW/cm^2 for 8 nsec Nd:YAG laser beam, while the threshold goes up as high as 17 GW/cm^2 for the beam of 30 ps pulse width.

The second order nonlinear refractive indices and absorption coefficients were measured by Z-scan technique at 532 nm and 1064 nm for b- and c- polarizations (Fig.3). The observed large nonlinear absorption coefficient in the c-polarization at 532 nm is about 5 times larger than that of b-polarization, which clearly indicates that the nonlinear effect occurs predominantly along the molecular charge transfer direction.

Also optical parametric conversions of MMONS are presented and a comparison is made for the theory and experiments for type I and type II phase matchings.

Reference

(1) J.D. Bierlein, L.K.Cheng, Y.Wang and W.Tam, *Appl.Phys.Lett.*, **56**, 423(1990).

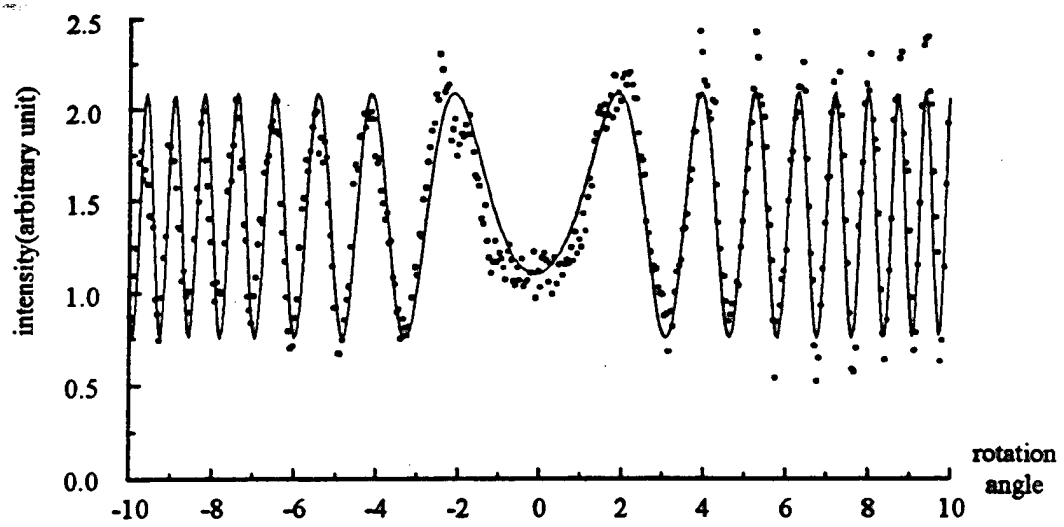

Fig.1 Maker fringe of a-cut MMONS sample. The points represent measured values and the curve calculated one.

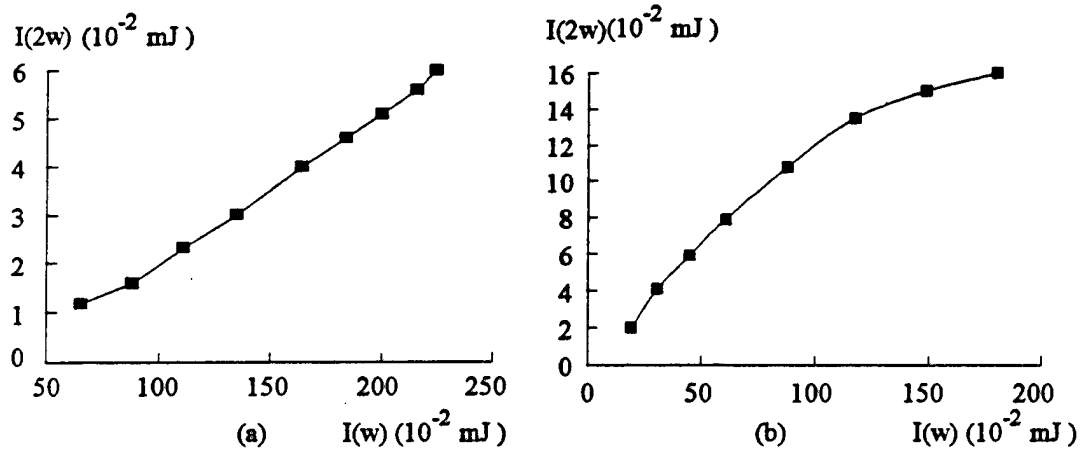

Fig.2 The energy of the second harmonic wave as a function of the fundamental energy for (a) the type I and (b) the type II phase matching.

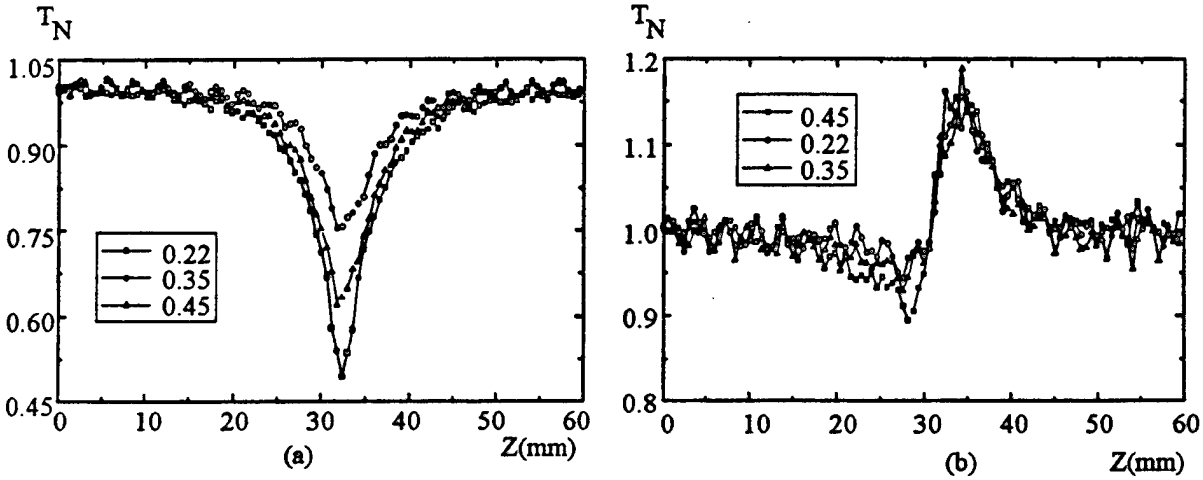

Fig.3 Z-scan transmission for the c-polarization at 532 nm for (a) open aperture and (b) closed aperture.

CONTROLLING THE STRUCTURE OF LANGMUIR-BLODGETT FILMS FOR SECOND-HARMONIC GENERATION

Geoffrey J. Ashwell
Centre for Molecular Electronics, Cranfield University
Cranfield MK43 0AL (UK)

Interest in LB films for second-harmonic generation (SHG) stems, in part, from the requirement that the structure must be non-centrosymmetric and, in part, from the fact that the LB technique allows control of the packing at the molecular level. Conventional materials, which comprise a hydrophilic head and a hydrophobic alkyl tail, may be aligned at the air-water interface prior to deposition but, when transferred to a solid substrate, the molecules frequently invert to give a centrosymmetric bilayer arrangement in which the layers pack head-to-head and tail-to-tail (Y-type). Few single-legged dyes form non-centrosymmetric multilayers in which the molecules pack in a head-to-tail manner (Z-type) unless interleaved by compatible spacer layers. However, the addition of a second hydrophobic group at the opposite end of the hydrophilic chromophore facilitates Z-type deposition and there is a narrow range of alkyl chain lengths which allows the films to be non-centrosymmetric. Improved deposition and nonlinear optical properties have been realised by using a two-legged cationic dye (a hemicyanine) and an amphiphilic anion (octadecylsulphate). For such dyes, the position of the absorption band may be finely tuned by systematically varying the donor and acceptor parts of the molecule and transparency has been achieved.

The paper will mainly concern the fabrication of thick (>100 layers) Z-type film structures, their stability and the ease of non-centrosymmetric deposition by using the unconventional two-legged materials. Data from grazing incidence synchrotron X-ray diffraction studies on floating monolayers and deposited films will be reported. These studies have confirmed that the molecules adopt a "stretched" rather than a "U-shaped" configuration and pack at the air/water interface with one of the hydrophobic groups adjacent to the subphase. The molecules retain their alignment when deposited and the second-harmonic intensity has been found to increase quadratically with the number of LB layers to thicknesses of *ca.* 1 μm.[1,2] Several micron-thick LB films have now been deposited. The best of these have moderately high second-order susceptibilities of $\chi^{(2)}_{zzz}$ = 40 pm V^{-1} at 1.064 μm when transparent and $\chi^{(2)}_{zzz}$ > 100 pm V^{-1} when coloured.

The second-order properties of a series of squaraine dyes with centrosymmetric donor-acceptor-donor structures will also be discussed. Their LB films exhibit strong SHG whereas, until recently, it had been assumed that molecular asymmetry was a prerequisite of dipolar second-order effects. However, the criteria may be satisfied if there is an intermolecular charge transfer contribution to the susceptibility and if the materials aggregate in a non-centrosymmetric manner. For example, charge transfer between the terminal donor and central acceptor of adjacent squaraine molecules can give rise to acentric "T-shaped" dimers and these are perceived as the "molecular" building blocks for SHG. Interestingly, recent work has shown that LB films of the centrosymmetric squaraine dyes exhibit strong SHG[3] comparable with the intensities from films of conventional donor-(π-bridge)-acceptor materials. The results suggest that intermolecular processes play an important role and, from this work, it is clear that the range of useful LB film-forming materials for SHG could be broadened. Intermolecular charge transfer is particularly relevant to the design of donor-(π-bridge)-acceptor materials where interlayer interactions may be exploited to improve the long-range structural order as well as the nonlinear optical properties. Such materials form part of our current activity at Cranfield and their properties will be reported.

1 G.J.Ashwell, G.Jefferies, C.D.George, R.Ranjan, R.B.Charters and R.P.Tatam, *J. Mater. Chem.*, 1996, **6**, 131-136.

2 G.J.Ashwell, P.D. Jackson, G.Jefferies, I.R.Gentle and C.H.L.Kennard, *J. Mater. Chem.*, 1996, **6**, 137-141.

3 G.J.Ashwell, G.Jefferies, D.G.Hamilton, D.E.Lynch, M.P.S.Roberts, G.S.Bahra and C.R.Brown, *Nature*, 1995, **375**, 385-388.

Enhancement of Cerenkovian SHG Powers in Channel Guide due to NLO $\chi^{(2)}$ Corrugations Formed by UV Irradiation

Heihachi Sato and Hiroaki Matsuno*

Department of Electrical Engineering, National Defense Academy, Yokosuka 239, Japan.
*Japan Self-Defense Air Force, Sayama, Saitama 350-13, Japan.

In a sequence of our recent works the authors et al have proposed that the Cerenkov-radiative SHG power can be much enhanced with introducing a periodic or chirped NLO $\chi^{(2)}$, instead of uniform distribution, onto a guiding layer, and have successfully demonstrated its validity with organic copolymer (VDCN/VAc), together with theoretical treatments.[1,2] Through this demonstration the method of contact electrode has been used to induce the corrugated NLO $\chi^{(2)}$ configuration. On the other hand, the organic polymer above has a strong absorption peak near 200 nm and it is also believed that UV irradiation corresponding to this peak usually reduces both NLO $\chi^{(2)}$ and refractive index n. Thus, in the present paper we shall attempt to induce the NLO $\chi^{(2)}$ corrugation with UV irradiation through metallic mask instead of the electric-poling method, and shall compare the SHG power obtained by the UV irradiation and the method of contact-electrode poling. Additional SHG enhancement due to the UV induced channel-guide will also be described.

In Fig. 1 the experimental schematics are depicted:(a) configuration process of a periodic or chirped NLO $\chi^{(2)}$ structure and channel waveguides and (b) setup for the Cerenkovian SHG observation. First, UV source (ArF 193nm) was irradiated onto a uniformly poled VDCN/VAc copolymer through a metallic mask (chirped pattern mask is shown) to induce sinusoidal periodic or chirped NLO $\chi^{(2)}$ corrugation. For uniform poling the Au electrode on the substrate is remained to force be asymmetric waveguide. A periodic structure with the period 20 μm and a chirped structure with the average period 20 μm and the chirping period 200 μm were prepared by irradiating the UV source for 5 minutes. Then, after taking off the mask, the UV source was again irradiated through tiny metallic wires (60, 100 and 150 μm), resulting in channel waveguide with a periodic or chirped NLO $\chi^{(2)}$ structure. The setup for observing the SHG power is the same as in works[3] with Nd:YAG 1.06 μm as a fundamental wave and a prism coupling scheme as in the figure (b).

In Fig. 2 the SHG power enhancement observed are depicted:(a) channel-guide and (b) its dependence on channel-width w, where $w=\infty$ corresponds to a slab-guide. It is seen that the SHG power is increased in inverse-proportional to the channel-guide width as expected. Enhancements of the SHG power with UV irradiation (UV) are

compared with those obtained by the contact-electrode poling (EL) in Fig. 3, telling us that the SHG power obtained with UV irradiation is slightly small but almost comparable to those with the method of contact electrode. Since UV irradiation to induce NLO $\chi^{(2)}$ corrugation is much simpler than the method of contact electrode, this is quite promising for the Cerenkov-radiative SHG scheme with periodic or chirped NLO $\chi^{(2)}$ corrugation. Physical interpretation about why the Cerenkov-radiative SHG power is enhanced with a periodic or chirped NLO $\chi^{(2)}$ corrugation will also be discussed.

References

1. H. Sato and Y. Azumai, Opt. Lett. **19**, 93-94 (1994).
2. H. Sato and Y. Azumai, Nonlinear Optical Properties of Proc. of SPIE, Vol. **2285**, 272-281 (1994).
3. H. Sato, H. Matsuno and I. Seo, in Organic Thin Films for Photonics Applications, 1995 OSA Tech. Digest Series, Vol. **21**, ThB-1, p. 400.

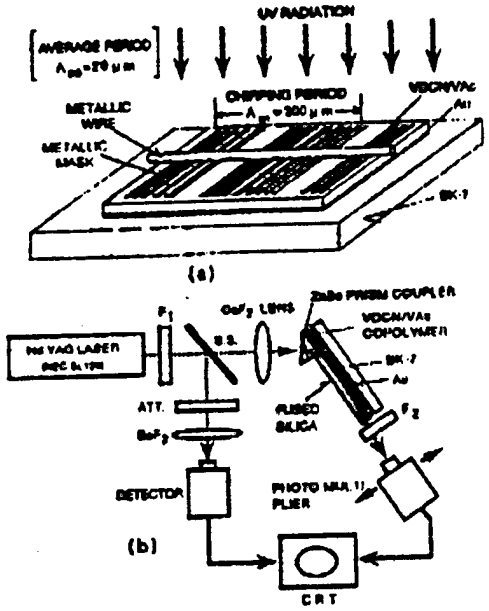

Fig. 1 Experimental schematics : (a) forming process of NLO $\chi^{(2)}$ corrugation and (b) setup for SHG observation.

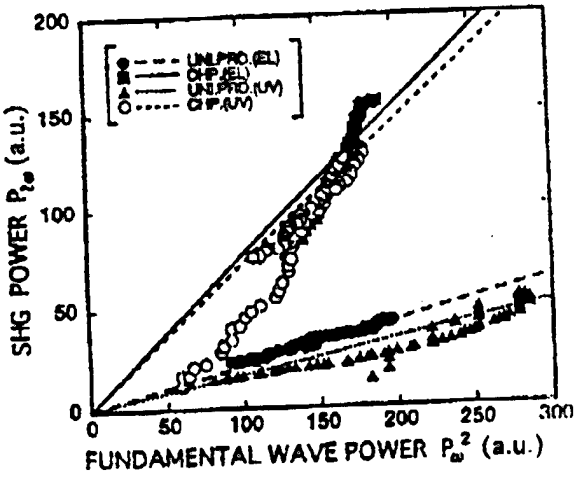

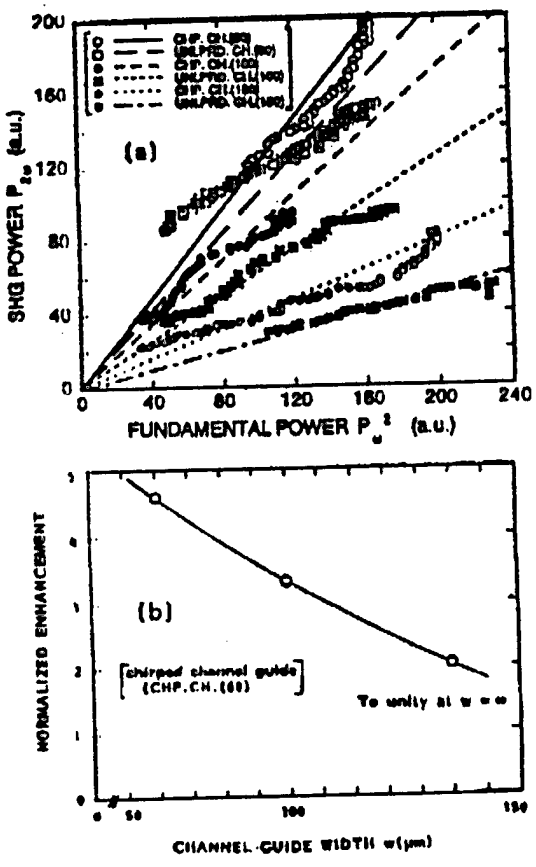

Fig. 2 Enhanced SHG powers (a) for various NLO $\chi^{(2)}$ corrugations and (b) for various channel-widths.

Fig. 3 Comparison of SHG power obtained with UV irradiation scheme (UV) and contact electrode method (EL).

Modal Dispersion Phase-Matching over 7 mm Length in Overdamped Polymeric Channel Waveguides

Matthias Jäger, George I. Stegeman, CREOL, University of Central Florida
P.O. Box 162700, Orlando, FL 32816-2700, U.S.A.

Mart Diemeer, Marinus C. Flipse, AKZO Nobel Electronic Products
Arnhem, The Netherlands

Nonlinear frequency conversion and the possibility of employing cascaded $\chi^{(2)}$-effects for all-optical switching, spatial solitary waves, etc[1] have created a strong interest in efficient Second Harmonic Generation (SHG). Even though poled polymers have very large nonlinear coefficients, high efficiencies have been demonstrated only in ferroelectric crystals to date.[2] We demonstrate phase-matched SHG in a channel waveguide made of 4-dimethylamino-4'-nitrostilbene (DANS) polymer. Our SHG figure of merit $\eta=P_{2\omega}/(P_{\omega}L)^2$= 14 %/W-cm^2 is an improvement of 40% over our previously reported result[3] and is competitive with those of the best inorganic crystals[4]. Phase-matching was demonstrated for up to 7 mm.

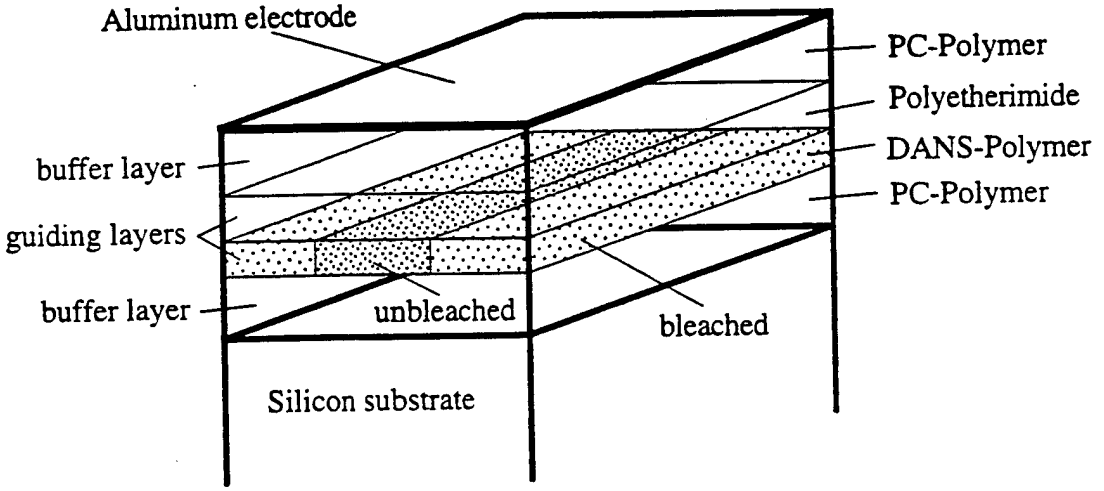

Fig 1 Sample construction of the poled polymer channel waveguide

In our case phase-matching is achieved between the TM_{00}^{ω} and $TM_{10}^{2\omega}$ modes using the modal dispersion of the waveguide. To optimize the efficiency, the guiding region consists of a linear polyetherimide layer and a nonlinear DANS-layer (figure 1), therefore eliminating the destructive interference which would normally drastically reduce the overlap integral. The samples were fabricated by multi-layer spin-coating, subsequently poled (≈ 180 V/µm nominal poling field), and diced into pieces of different lengths for end-fire coupling. Finally, channel waveguides of various widths were fabricated by photo-bleaching through a mask.

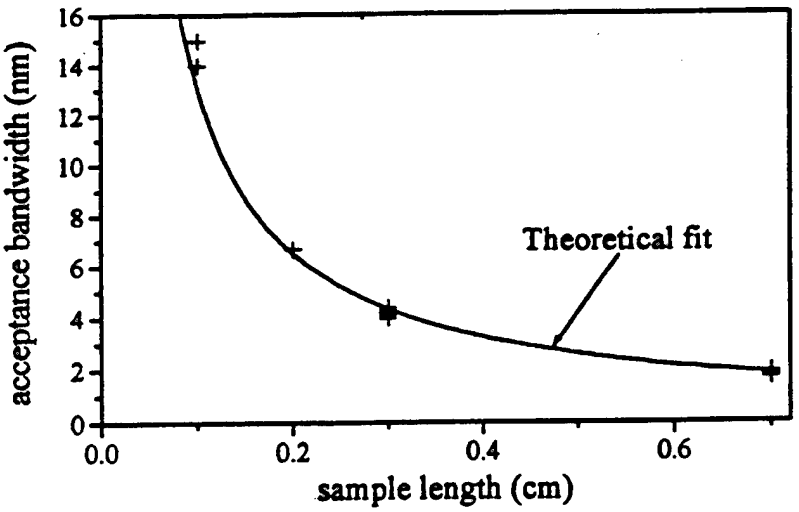

Fig. 2 SHG acceptance bandwidth (measured data and theoretical fit)

A tunable color center laser was used for the SHG experiments, in which the SHG power was recorded versus the fundamental wavelength. The highest figure of merit 14%/W-cm^2 was measured for a 1 mm long channel. For longer samples, this number drops due to the presence of waveguide losses α (α_ω=6.5 dB/cm, $\alpha_{2\omega}$=20 dB/cm due to DANS-absorption). In this loss configuration (where $\Delta\alpha=\alpha_{2\omega}-2\alpha_\omega$ is small), the SHG tuning curve retains a $\mathrm{sinc}^2(\Delta\beta L)$-like dependence for propagation lengths longer than the individual loss lengths $L_{\omega,2\omega}=1/\alpha_{\omega,2\omega}$, where $\Delta\beta L$ is the net phase detuning from phase-matching. Experimental tuning curves exhibit this dependence for up to L=7mm, suggesting phase-matching is maintained over the sample length L. This conclusion is also supported by an investigation of the acceptance bandwidth versus the propagation length, which shows the expected peak narrowing for longer samples up to 7 mm (figure 2).

In conclusion, we have demonstrated an SHG figure of merit η=14 %/W-cm^2 for a 1 mm long waveguide, comparable to the 22 %/W-cm^2 reported in $LiNbO_3$.[4] Phase-matching could be demonstrated for up to 7 mm with reduced efficiencies. For applications an alternative chromophore has to be used with less SHG absorption. We would like to thank AKZO for providing the DANS and PC polymers and MOEC for the polyetherimide. The research was sponsored by AFOSR and NSF.

References:

1. G.I. Stegeman, R. Schiek, G. Krijnen, W. Torruellas, M. Sundheimer, E. VanStryland, C. Menyuk, L. Torner and G. Assanto, Proceedings of the 4'th WRI *International Conference on Guided Wave Optoelectronics*, edited by T. Tamir, H. Bertoni and G. Griffel, (Plenum , New York 1995), pp. 371-379.
2. best cases reviewed in G.I. Stegeman, Proceedings of ICONO'2, J. Nonlinear Optics, **15**, 469 (1996).
3. M. Jäger, G.I. Stegeman, M. Diemeer, G.R. Möhlmann, M.C. Flipse, ACS/OSA Symposium: Polymeric and Organic Materials for Optical Applications, Orlando 1996
4. M.L. Bortz, M.A. Arbore, M.M. Fejer, Opt. Lett. **20**, 49 (1995).

Quasi-Phase Matched Surface Emitting Second Harmonic Generation in Poled Polymer Waveguides

A. Otomo
Kansai Advanced Research Center (KARC)
Communications Research Laboratory
Ministry of Posts and Telecommunications
588-2 Iwaoka, Nishi-ku, Kobe 651-24 Japan

G.I. Stegeman
Center for Research and Education in Optics and Lasers (CREOL)
University of Central Florida
4000 Central Florida Blvd., Orlando, FL 32816-2700

W.H.G. Horsthuis and G.R. Möhlmann
Akzo Electronic Products
Arnhem, The Netherlands

Surface emitting second harmonic generation (SE-SHG) by the mixing of counter propagating guided waves in poled polymers has been demonstrated in 4-dimethylamino-4'-nitrostilbene (DANS) side-chain polymer waveguides. Although the poling fields available at that time were small (50 V/μm), large second harmonic conversion was observed compared to inorganic and semiconductor single layer devices. This is due to the large polymer second order nonlinearities and small refractive indices at the second harmonic wavelength. However, in the last few years, several experiments in GaAs based waveguides were reported and the conversion efficiency was improved dramatically by using a form of quasi-phase matching (QPM) in the transverse direction. A large efficiency improvement is also expected in organic polymers by employing both transverse QPM and the large poling fields now available.

Phase matching is one of the most essential requirements for efficient harmonic generation of co-propagating fundamental and harmonic beams. In the case of mixing of two counter directed guided beams, the phase matching condition is always satisfied along the propagation direction, since the harmonic field is radiated out from the film surface. However, large phase mismatches occur along the transverse direction, *i.e.* perpendicular to the film surface. Transverse phase matching is often represented by maximizing the overlap integral S which is expressed for the counter propagating case as

$$S=\int_{-\infty}^{\infty}\frac{d_{22}(x')f_y(x')^2}{\tilde{n}_f^{(2\omega)}(x')}\exp\left[ik_0^{(2\omega)}\tilde{n}_f^{(2\omega)}(x')x'\right]dx'$$

Where f_y is the guided field distribution of the counter propagating fundamental beams, $\tilde{n}_f^{(2\omega)}$ is the complex refractive index of the film, and d_{22} is the second order nonlinearity. The exponential term represents the spatial distribution of the phase of the generated second harmonic field. Since the generated second harmonic intensity is quadratic in S, the expected second harmonic signal can be estimated by investigating the overlap integral. The integrand oscillates across the waveguide varying from positive to negative values with a period corresponding to the second harmonic wavelength. In a single layer waveguide for which d_{22} is constant, the resultant integral is small due to the destructive interference between the second harmonic waves generated from the different depths corresponding to successive half wavelength regions (Fig. 1). The destructive interference can be partially compensated by modulating d_{22} along the film depth, a form of quasi phase matching. In previous semiconductor QPM experiments, the Al concentration (and therefore d_{22}) was modulated in AlGaAs waveguides. For poled polymer devices, three possible modulation methods have been proposed, specifically a) a nonlinear/linear (NL/L) multilayer, b) a reverse poling multilayer, and c) a hetero-phase multilayer. We fabricated NL/L multilayer films as shown in Fig. 2 successfully and QPM enhanced SHG was observed in poled polymer based SE-SHG devices. In a quasi phase matched structure, the SH light grows monotonically towards the radiating film surface and an order of magnitude efficiency enhancement is expected compared to the single layer device, as shown in Fig. 1. Here A^{NL} is the nonlinear cross-section coefficient defined by $P^{(2\omega)}=A^{NL}(L/W)P_+^{(\omega)}P_-^{(\omega)}$ where $P^{(2\omega)}$ is the radiated SH power,

$P^{(\omega)}$ are the counter directed fundamental powers, and L and W are the device interaction length and the channel waveguide width respectively. Although complete phase matching is not achievable along the transverse direction, the maximum possible efficiency is one order of magnitude larger than for the NL/L QPM device.

The measured nonlinear cross section of the NL/L multilayer device is $A^{NL}=2.3\times10^{-6}W^{-1}$ and the conversion efficiency is $\eta=P^{(2\omega)}/LP_{+}^{(\omega)}P_{-}^{(\omega)}=0.6\%/Wcm$. With the hetero-phase multilayer QPM, more efficiency improvement is expected since nonlinearity is fully modulated. Moreover with the larger nonlinearities available near resonance and a narrower waveguide such as W = 1μm, a power conversion efficiency η = 100 %/Wcm can be obtained. The measured cross section is 20 % of the theoretically calculated value. Since the waveguide propagation losses used to evaluate the cross section were characterized for the single layer device, there can be increased losses due to the multilayer structure. Another possible reason for the discrepancy is inhomogeneity of the nonlinearity across the poling electrode gap. Although the inhomogeneity and the influence of the charge injection were found to be small for the film poled at 50 V/μm, a larger influence of charge injection can occur for films poled at higher fields. Since the measured nonlinearity for the parallel poled film is the averaged value across the gap, the nonlinearity in the middle of the gap where the channel waveguide is located can be overestimated. We have not investigated the life time of device activity in detail, however SH efficiency measured for films 11 months after poling decreased less than 15% from the original value.

Figure Captions:

Fig. 1 Second harmonic growth through the film. — NL/L multilayer film; --- Single layer film; ···· Perfectly phase-matched film.

Fig. 2 Schematic of the cross section of the NL/L multilayer waveguide.

Fig. 1

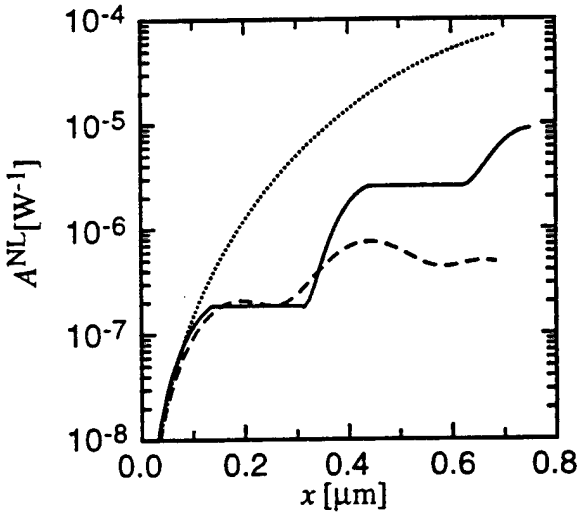

Fig. 2

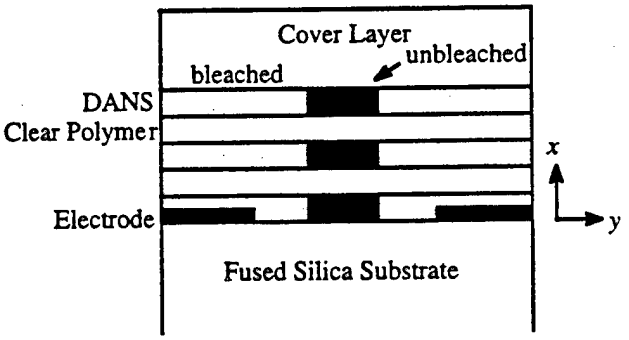

Supramolecular Architecture and Nonlinear Optical Materials

DeQuan Li, Xiaoguang Yang, and Duncan McBranch

Chemical Sciences and Technology Division (CST-4)
Mail Stop G755
Los Alamos National Laboratory
Los Alamos, NM 87545 (U.S.A.)
Telephone: 505-665-1158
Fax: 505-667-8021

The design and construction of artificial supramolecular architectures on surfaces are of great interest and represent an important aspect of supramolecular science. Molecular self-assembly technique is one of the useful tools for constructing mesoscale structures with desired chemical functionalities and physical properties. The fabrication of polar molecular superstructures proves particularly challenging; our approach here is to fix dipole orientation by structurally locking of chromophores into a polar cone conformation for second order nonlinear optical applications. Here, we discuss the molecular design of calixarene-based, molecular "pyramids", their monolayer self-assemblies on oxide surfaces, and their spectroscopic second order properties.

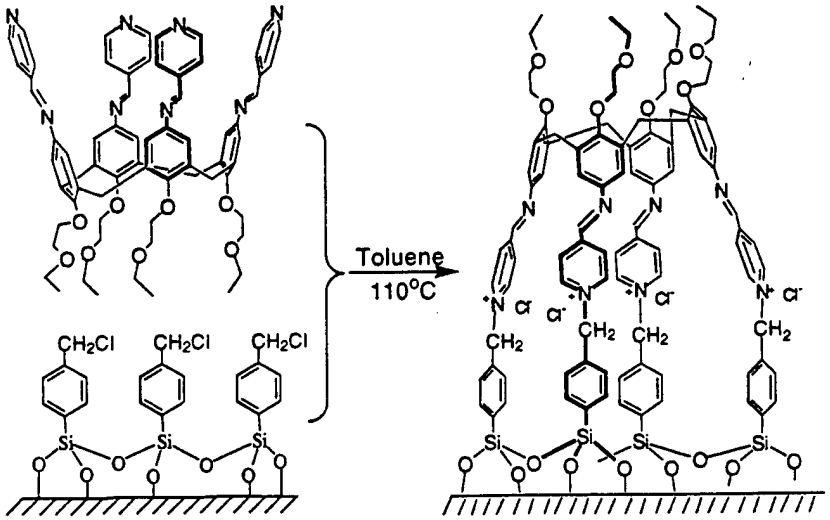

Figure 1. A robust monolayer of molecular pyramids is formed on silica surfaces.

The supramolecular chromophore—calix[4]stilbazole imine—was synthesized by coupling p-aminocalix[4]arene with p-pyridylcarboxaldehyde. The subunits of this supermolecule, 4-hydroxyl stilbazole, are extremely efficient frequency doublers with extremely large β value. The advantages of using these supermolecules are that they are pre-aligned, and have better thermal and chemical stabiltities comparing to their monomeric units. These cone-shaped molecular pyramids were self-assembled on silica surfaces via a quaternization reaction which was summarized in Figure 1. The reaction forms an efficient electron withdrawing center (pyridinium) which actually enhances the second order nonlinear optical properties. The formation of C-N bonds was also manifested in the surface-infrared spectroscopy as a new pyridinium mode replaces the old pyridyl mode; the absorption red-shift in the UV-vis also confirms the formation of this covalent pyridinium bond.

In order to study the molecular orientation and the NLO response on glass surfaces, spectroscopic second harmonic generation (SHG) was carried out on the monolayers of these calixarene-based chromophores. These measurements were performed using a modelocked

Ti:sapphire laser in either femtosecond (150 fs autocorrelation width) or picosecond (2 ps width) mode with 100 MHz repetition rate. Results using picosecond pulses to generate *p*-polarized SHG from both *p*- and *s*-polarized fundamental are shown in Figure 2 for a fundamental wavelength of 890 nm. An average molecular orientation of $\psi \sim 35 \pm 5^{o}$ was deduced by modeling the angular dependent SHG response ($n_{film} = 1.7$); an absolute magnitude of $d_{33} \sim 80$ pm/V for monolayers of calixarene chromophores was deduced by calibrating to reference Y-cut quartz. The solid lines in Figure 2 are best fits, modulated by an interference term, which has the same physical origin and angular dependence as the well-known Maker fringes in bulk samples.

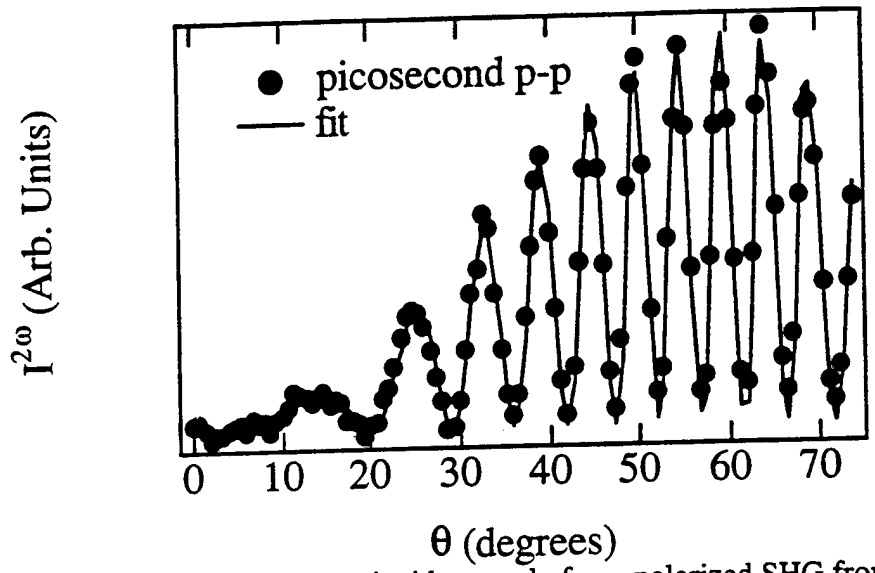

Figure 2. SHG signal *vs.* incident angle for *p*-polarized SHG from *p*-polarized (solid circles) fundamental at a wavelength of 890 nm and 2 ps pulsewidth, and best theoretical fit (solid line).

Spectroscopic second harmonic generation was measured form 890 nm to 750 nm for fundamental wavelength (harmonic $\lambda = 445$-375 nm). The nonlinear optical spectrum closely resembles the linear optical absorption spectrum, which is fairly featureless. The wavelength dependence indicates a gradual increase of d_{33} as the fundamental moves to shorter wavelength, consistent with normal refractive index dispersion in this spectral region approaching the charge transfer resonance at 390 nm. The charge transfer resonance is fairly broad; the measured value for d_{33} at the longest wavelength (60 pm/V at 890 nm) is still somewhat resonantly enhanced. We find a value of $d_{33} \sim 110$ pm/V at $\lambda = 775$ nm, indicating a nearly twofold two photon resonant enhancement at the peak of the charge transfer band.

To summarize, we have made a significant step forward in the construction of supramolecular architecture by demonstrating the formation of self-assembled monolayers with "pyramid"-like molecular building blocks. Structural interlocking via the bridging methylene groups among the dipolar units yields films with extremely large second-order nonlinearities ($d_{33} \sim 60$ pm/V; $\lambda = 890$ nm), and robust molecular dipole alignment.

IMPROVED ACCORDION POLYMERS FOR $\chi^{(2)}$ NONLINEAR OPTICS

G. A. Lindsay, J. D. Stenger-Smith, R. A. Hollins, A. P. Chafin, R. Y. Yee, M. J. Roberts, P. Zarras, L. H. Merwin, G. Ostrom, E. G. Nickel[1], M. E. Wright[2], R. F. Gratz[3], P. R. Ashley[4], W. N. Herman[5], K. J. Wynne[6]

U.S. Navy, Research & Techn. Div., NAWC-474220D, China Lake, CA 93555
1 now at Dept. of Chemistry & Biochemistry, Georgia Tech, Atlanta, GA 30332
2 Dept. of Chemistry, Utah State Univ., Logan, UT 84322-0300
3 Dept. of Chemistry, Mary Washington College, Fredericksburg, VA 22401
4 U.S. Army, AMSMI-RD-WS-CM, Redstone Arsenal, AL 35898
5 U.S. Navy, Code 455650R07, Warminster, PA 18974
6 U.S. Navy, Code 331, Office of Naval Research, Arlington, VA 22217-5000

Extended Abstract: Advances in accordion polymers designed for second-order nonlinear optics (NLO) will be reported. Accordion NLO polymers are comprised of asymmetric chromophores linked head-to-head and tail-to-tail to form the main chain (the backbone).

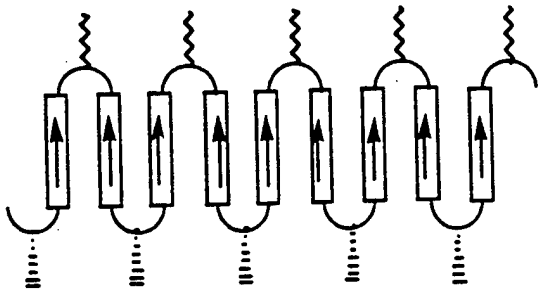

The accordion polymer architecture makes it possible to have a very large density of chromophores in an amorphous nonlinear optical film. The sierrulate topology of the backbone prevents chromophore aggregation and crystallite formation which would scatter light in the film. The bulk NLO coefficients of the film increase linearly with concentration of the chromophore (assuming the same degree of alignment can be maintained). The chromophoric content of these new polymers is over 80 weight percent.

New polymers have been made that have higher nonlinear optical coefficients than the first generation of accordion NLO polymers. The molecular designs attempted for increasing the optical nonlinearity include thienylene,

thienylene-vinylene, and butadienylene extensions of the chromophore. Results were obtained on the optical properties of EO films made by conventional spin-coating, blade-coating, and corona poling techniques. Using second-harmonic generation to measure d_{33} as a screening technique, a resonance-enhanced value of 120 pm/V at 1.06 microns was achieved for one polymer containing the thienylene vinylene extended chromophore. Advances have also been made in the synthesis of more thermally stable bridging groups which link the chromophores. The molecular designs for increasing thermal stability include triaryl amine electron-donating groups and heterocyclic electron-accepting groups.

In order to make these accordion polymers, a bis-aldehyde containing the electron donating groups is heated in solvent with a bis-cyanoacetamide containing the electron accepting groups. Polymer forms by a Knoevenagel condensation reaction. It has been found that in addition to polymer, varying amounts of cyclic dimers are formed. The cyclic dimers are comprised of two chromophores in parallel juxtaposition. The ratio of cyclic dimer to polymer formed during the polymerization reaction depends upon the structure of the bridging groups, the aspect ratio of the chromophores, and the polymerization conditions. An extraction processes for removing residual cyclomer from the polymer has been developed. Single crystals of the polar cyclomer have been made, and are in the process of being characterized.

Utilizing a complementary bilayer approach, electric-field poling is not necessary to achieve NLO films having desirable $\chi^{(2)}$ properties. These films can be formed by low temperature self-ordering processes, such as the Langmuir-Blodgett-Kuhn (LBK) method. The optical performance of a buried Mach-Zehnder interferometer was measured in which the core EO film was fabricated by the LBK technique from 618 molecular layers (309 complementary bilayers) of accordion polymers. The preliminary r_{33} = 1.1 pm/V. It is believed that this is the first optical modulator to be fabricated in an LBK film.

Aging of 25-nm thick LBK films (10 complementary bilayers) under nitrogen in the dark compared to aging in air in the dark demonstrated that oxidation can occur at room temperature with essentially no photo activation. The aging behavior of four different pairs of accordion polymers was compared. It was found that aging is a function of the length and number of aliphatic hydrophobic chains per chromophore.

In-line Fiber Electro-optic Modulator using Decal Deposition of Poled Nonlinear Polymers

A. Knoesen, S. A. Hamilton, and D. R. Yankelevich
Department of Electrical and Computer Engineering
University of California, Davis CA 95616

R. A. Hill and G. C. Bjorklund
Optivision, Inc., Palo Alto CA

The predominant external modulator technology is based on integrated optical technology which suffer from the need for fiber pigtailing, which raises cost, increase insertion losses, and causes mechanical fragility. We will report on the application of a decal deposition technique, first developed for fabricating quasi-phasematched polymeric structures for second-harmonic generation by Khanarian et. al. [1], to implement electro-optic fiber modulators by decal depositing high quality poled films selectively onto substrates without spin coating [2].

The fiber modulator consists of a fiber half coupler with a multimode waveguide overlay consisting of an electro-optic polymer whose index of refraction is controlled by the modulating electrodes [3-4]. Modulation is achieved by altering the phase-matching conditions between the fiber and the polymer waveguide. This is achieved via the linear electro-optic effect in the nonlinear polymer, and the modulation in this modualtor is limited only by the electrode structure of the device. We deposit the nonlinear polymer by the decal deposition technique.

The decal technique can easily be adapted to other devices and allows the deposition of high-quality, corona-poled, nonlinear polymer films onto structures without subjecting them to spin coating, large electrostatic fields, and other nonlinear polymer processing steps that may damage the underlying device. Another distinct advantage of the decal deposition for devices where the film thickness determines the optical spatial resonances, such as Fabry Perot structures or waveguides, is that the thickness of the film is determined prior to deposition on the final substrate.

Devices were made to operate in the 1.3 micron window using a poly(Disperse Red 1 methacrylate-co-methyl methacrylate) poled polymer. With a 15 V amplitude modulating voltage, we obtained a maximum modulation in transmission of 40% up to 100 MHz. These devices are mechanically rugged, due to the selfpigtailed design, and could be fabricated at a fraction of the cost of other integrated optical modulators.

References:

1) G. Khanarian, M. A. Mortazavi, A. J. East, "Phase-matched second-harmonic generation from free-standing periodically stacked polymer films", Appl. Phys. Lett., 63, 1462-1464 (1993).
2) R. A. Hill, G. C. Bjorklund, S. A. Hamilton, D. R. Yankelevich, A. Knoesen, "Polymeric in-line fiber modulator using novel processing techniques", OFC'96, vol. 2, 166-167, 1996.
3) M. Wilkinson, J. R. Hill nad S. A. Cassidy, "Optical fibre modulator using electro-optic overlay," Electron. Lett. 27, 979-981 (1991).
4) G. Fawcett, W. Johnstone, I. Andovic, D. J. Bone, T. G. Harvey, N. Carter, and T. G. Ryan, "In-line fibre-optic intensity modulator using electro-optic polymer," Electron. Lett. 28, 985-986 (1992).

DESIGN, SYNTHESIS AND OPTICAL NONLINEARITY OF CROSSLINKED POLYURETHANES WITH HEMICYANINE-TYPE CHROMOPHORE

[1]Kwang-Sup Lee, [2]Ki-Jeong Moon and [2]Hong-Ku Shim
[1]Department of Macromolecular Science, Hannam University, Taejon 300-791, Korea
[2]Department of Chemistry, KAIST, Taejon 305-701, Korea

Relaxation of molecular dipoles in poled NLO polymeric systems has been the major problem for the photonics applications[1,2]. Two approaches to minimize the relaxation have been proposed. In the first approach, NLO chromophores are introduced using high Tg polymers (such as a polyimide) producing a material with enhanced temporal and thermal stability[3,4]. In the second approach, a main chain NLO polymers are combined with thermally or photochemically crosslinkable chemical unit[2]. Yet, these two methods present some drawbacks with respect to level of chromophore doping, optical quality, processability, etc.

In order to solve these problems we have developed a polyurethane with covalently linked side chain moieties containing a highly active NLO chromophore[5]. The main reason we selected the polyurethane as a matrix was that an extensive formation of hydrogen bonds between the urethane linkage is expected, thus increasing the rigidity of the matrix and to prevent the relaxation process of the oriented NLO chromophore dipoles. In addition, we have also developed crosslinked polyurethanes with a excellent long-term stability and optical quality. In these systems, NLO chromophore were covalently attached to the parallel, vertical, or parallel/vertical direction in polymer chains.

In the part of our work devoted to the material design we decided to take the advantage of the high second order susceptibility of hemicyanine chromophore. It is well-known that the nonlinear activity of hemicyanine is strongly dependent on the properties of the counter ions and it usually increases when big, 'softer' anions are used. Thus, we have chosen, as the counter ion for the hemicyanine-type chromophore, the bulky tetraphenylborate anion. In addition to increasing the nonlinear activity of the chromophore, it was expected to reduce the ion mobility in the strong electric field during the poling process. Also, they may slow down the relaxation process of aligned molecular dipoles after the removal of the electric field.

In this presentation, we report design, synthesis and characterization of polyurethane-based NLO system. We also discuss the details of its optical second order activity in terms of electric field poling, and temporal and thermal stability.

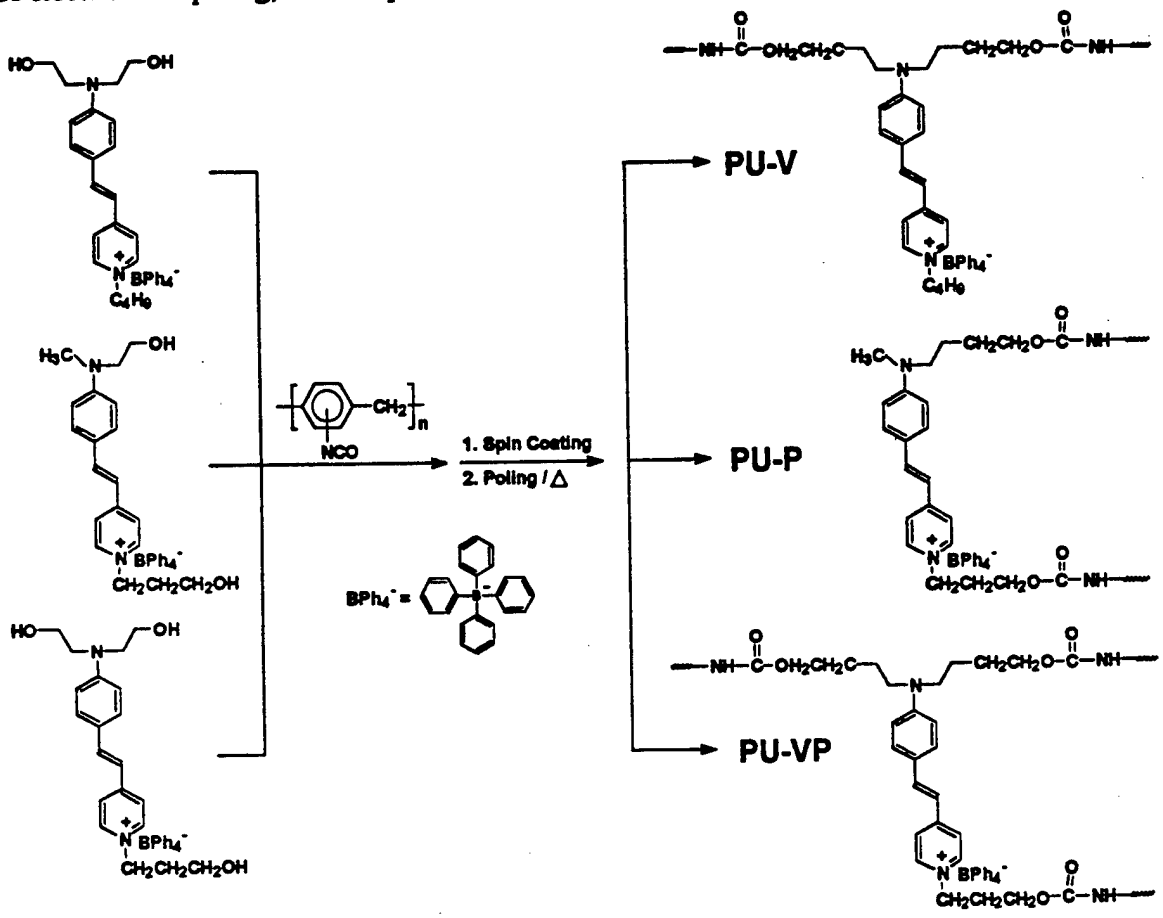

Reference

1. Lee, K.-S., Samoc, M. and Prasad, P. N., In *Comprehensive Polymer Science*; Aggarwal, S.L, Russo, S., Eds.; Pergamon Press: Oxford, U. K., 1992; 1st Suppl. Vol.
2. Burland, D. M., Miller, R. D. and Walsh, C. A., *Chem. Rev.* 1994, **94**, 31.
3. Becker, M. W., Sapochak, L. S., Ghosen, R., Xu, C. Z., Dalton, L. R., Shi, Y. Q. and Steier, W. H., *Chem. Of Mater.*, 1994, **6**, 104.
4. Peng, Z. H. and Yu, L. P., *Macromolecules*, 1994, **27**, 2634.
5. Moon, K. J., Shim, H. K., Lee, K.-S., Zieba, J. and Prasad, P. N., *Macromolecules*, 1996, **29**, 861.

Novel Molecular Design for Photonic Application

Ki Hong Park, Sang-Yeon Shim, and Nakjoong Kim
Division of Polymer Research,
Korea Institute of Science and Technology,
Seoul 130-650, KOREA
(Tel: +82-2-958-5291, Fax: +82-2-958-5309, E-mail: kimn@kistmail.kist.re.kr)

Nonlinear optically (NLO) active polymeric materials have better processability compared to inorganic crystal materials, but their thermal and long term stability of NLO activity must be improved for practical device applications. Especially, the gradual decay of second-order NLO coefficient of poled polymers has been one of the most important issues. We have demonstrated the remarkable enhancement of NLO stability by an introduction of crosslinkable polymer matrix such as polyglycidyl methacrylate copolymers having self-crosslinkable moieties[1] or polymaleimide copolymer having high glass transition temperature[2-3]. Furthermore, we recognized that not only the thermal stability of polymer matrix but also that of NLO chromophores itself are important issues to be studied. Especially, if a high glass temperature polymer matrix is used, the corresponding chromophore endurable at high poling temperature is absolutely demanded. Therefore, our current study focuses on the development of novel NLO chromophores with good thermal stability. The combinations of thermally stable polymer matrix with thermally stable chromophores may provide the promising second-order NLO materials.

Usually, NLO chromophores have contained a stilbene or azobenzene type unit as a π-conjugated bridge because those chromophores have high hyperpolarizability (β) and can be easily synthesized. Considering the thermal- and photo-stability for the practical photonic application, several new chromophores possessing fused ring structure have been proposed for the improvement of thermal stability. The key point of our novel molecular design is an introduction of aromatic benzoxazole unit to general chromophore structures. The benzoxazole unit was adopted because aromatic polybenzoxazoles is one of the most thermally stable polymers comparable to well-known aromatic polyimide. We successfully synthesized several novel benzoxazole type NLO chromophores (Bzo 1 ~ Bzo 9), which show good solubility and thermal stability, and reasonably high $\mu\beta$ values.

In our earlier works, we have demonstrated that the electro-optic coefficients, r_{33}, of the poled polymethyl methacrylate copolymers and polyurethane having benzoxazole type chromophores were sufficiently high comparable to those having stilbene or azobenzene type chromophores[4-5]. The improved thermal stability of benzoxazole chromophores was well evaluated by IR, UV-visible spectroscopy, and thermogravimetric analysis. Moreover, the poled polymers having benzoxazole chromophores exhibited remarkably improved temporal stability of r_{33}, implying that these benzoxazole type NLO chromophore might have been a potential moiety for more stable photonic device applications.

In this presentation, we report some successful achievement of the optimization and stabilization of NLO activity of poled polymers having these novel benzoxazole chromophores synthesized.

References

1. T. S. Lee, S. Y. Park, D. H. Choi, and N. Kim, ***Mol. Cryst. Liq. Cryst.***, **267**, 59 (1995).
2. D. H. Choi, S. Song, T. S. Lee, S. Y. Park, and N. Kim, ***J. Appl. Polym. Sci.***, **59**. 9 (1996).
3. D. H. Choi, S. Song, W. S. Jahng, and N. Kim, ***Mol. Cryst. Liq. Cryst.***, **280**, 17 (1996).
4. K. H. Park, W. S. Jahng, S. J. Lim, and N. Kim, ***Mol. Cryst. Liq. Cryst.***, **280**, 27 (1996).
5. K. H. Park, W. S. Jahng, S. J. Lim, S. Song, D. -H. Shin, and N. Kim, ***Reactive Polymers,*** to be published (1996).

O-9

Quadratic hyperpolarizability of push-pull molecules: experimental and analytical investigations.

M. Blanchard-Desce[a], V. Alain[a], A. Fort[b], J. Muller[b] and M. Barzoukas[b]

[a] *Département de Chimie, Ecole Normale Supérieure, (URA 1679 CNRS), 24 rue Lhomond, F-75231 Paris Cedex 05, France*
[b] *Institut de Physique et Chimie des Matériaux de Strasbourg, Groupe d'Optique Nonlinéaire et d'Optoélectronique (UM 046 CNRS), 23 rue du Loess, 67037 Strasbourg Cedex, France.*

Push-pull molecules that present donor-acceptor (D/A) end groups interacting via a conjugated linker can exhibit large static quadratic hyperpolarizabilities $\beta(0)$. We have analysed correlations between structure and hyperpolarizability, within the two-state approximation, by using a simple description of push-pull molecules wherein both the ground and excited states are described as linear combinations of neutral and charge-separated limiting-resonance forms:

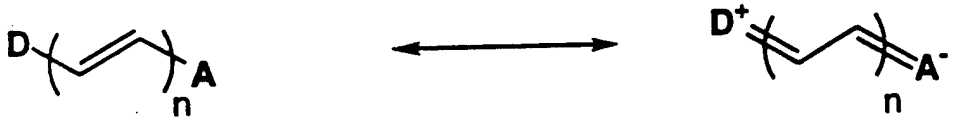

We have defined a parameter *MIX*, that measures the mixing between the two limiting-resonance forms and can be viewed as a generalization of the Bond Length Alternation formalism developed by Marder for push-pull polyenes. We have established an analytical relationship between the quadratic hyperpolarizability and *MIX* that indicates that there is an *optimum mixing between the limiting-resonance forms*, independent of the molecular system, that yields a maximized quadratic hyperpolarizability $\beta_{max}(0)$.

Thus, several series of push-pull molecules of increasing length have been investigated experimentally by performing EFISH experiments, as well as dipole measurements and NMR studies. By examining the experimental results, we have shown that not only *MIX, but also* $\beta_{max}(0)$*, is affected by the structure and size of the conjugated linker, as well as the nature of the D and A end groups*. Results also help understand the length behavior derived from EFISH data for series of push-pull polyenes and emphasize the role of D and A groups in determining β length dependency.

Light Induced Orientation in Azo-Polyimide Polymers up to 325 °C Below the Glass Transition Temperature

Zouheir Sekkat[1], André Knoesen[1], Jonathan Wood[2], Wolfgang Knoll[2,4], Willie Volksen[3], Robert D. Miller[3]

1 Department of Electrical and Computer Engineering, University of California, Davis, Davis California 95616.

2 Max-Planck-Institut für Polymerforschung, Ackermannweg 10, 55128 Mainz, Germany.

3 IBM Research Division, Science and Technology, 650 Harry Road, K13/801, San Jose, California 95120-6099

4 Frontier Research Program, The Institute of Physical and Chemical Research (RIKEN), Wako, Saitama 351-01, Japan.

This talk will report on light-induced nonpolar orientation of side-chain polyimides (glass transition temperature up to 350 °C) containing no flexible connectors or tethers to nonlinear optical azo dye chromophores with the electron-donor part of the chromophore incorporated as a part of the polymer backbone. This impressive photo-induced orientation occurs at room temperature, i.e. at least 325 °C below the Tg of one of the polymers we investigated. Further, it will be shown that after photo-induced ordering this polymer must be heated to 350 °C, to induce a main-chain movement and to erase the orientation; while the direction of the orientation of the chromophores can be easily controlled at room temperature by choosing the appropriate polarization of the irradiating light! This light-induced orientation process will be shown to be useful for storing images in waveguides. Light-induced polar orientation or photoassisted poling of such polyimide materials will be discussed also. This photoisomerization induced orientation phenomenon will be discussed in the light of the polymer molecular structure.

Spectral Content of Hyper-Rayleigh Scattering from Organic Materials

S.F. Hubbard, R.G. Petschek, and K.D. Singer
Case Western Reserve University, Department of Physics,
Cleveland, OH 44106-7079

Hyper-Rayleigh scattering (HRS) has attracted much attention recently as a method of measuring the first hyperpolarizability of nonlinear optical chromophores [1]. It offers many advantages over the traditional electric field-induced second harmonic (EFISH) generation technique most of which stem from the lack of externally applied electric field in HRS. HRS results are independent of the permanent dipole moment of a molecule, and the technique has been applied to materials which possess only higher order multipolar contributions to the nonlinearity [2]. HRS involves focusing an intense laser beam into a solution containing nonlinear optical chromophores and measuring the amount of radiation incoherently scattered at exactly twice the frequency of the input beam. Many nonlinear optical chromophores fluoresce in the visible spectrum, and multiphoton fluorescence competes with the hyper-Rayleigh response. We have studied this competition by spectrally resolving light scattered near the second harmonic from two well-known organic molecules.

Our experimental setup used a pulse-compressed Nd:YAG-synchronously pumped optical parametric oscillator with a parametric amplifier to produce intense picosecond pulses tunable in the near-IR. Light scattered from the sample was collected at 90° and focused into a motor-driven grating monochromator which scanned wavelengths near the second harmonic of the fundamental.

The spectral content of hyper-Rayleigh scattering was studied with solutions of disperse red-1 (DR1) and p-nitroanaline (pNA) in acetone at fundamental wavelengths of 1350nm and shorter. The height of the hyper-Rayleigh peak is expected to increase with the energy of the fundamental, and this behavior was observed in pNA/acetone solutions. Fig. 1 shows the spectra recorded with DR1 at several fundamental wavelengths as indicated and the UV-vis absorption tail in teh same spectral region. As the fundamental wavelength moved onto the linear absorption tail, a broad two-photon fluorescent emission appeared at wavelengths longer than the harmonic. When the harmonic was slightly into the absorption band of the chromophore, the hyper-Rayleigh line was extinguished while the two-photon fluorescence continued to increase with incident energy.

Concentration dependent HRS was used to determine the hyperpolarizabilities of DR1 and pNA in acetone at several wavelengths in the near-IR. The height of the hyper-Rayleigh peak was measured as a function of concentration to reveal a linear dependence, and the quadratic dependence on incident intensity was verified. With pNA, there were no effects

of fluorescence at any of the four operating wavelengths. DR1 produced fluorescence which also had a quadratic dependence on the intensity.

Results of the HRS experiments on DR1 are shown in Fig. 2 along with a two-level dispersive model curve based on the average static hyperpolarizability measured. The two-level model produces zero-frequency hyperpolarizabilities of $7 \cdot 10^{-30}$esu for pNA and $47 \cdot 10^{-30}$esu for DR1. Both of these results are in excellent agreement with previously published EFISH results [4].

The hollow points in Fig. 2 indicate that calculated β based on a narrow-band filter using only the sharp peak (triangles) and a wide-band filter which includes the HRS peak and fluorescence (squares). The upward deviation of the broad-band β values indicates that spectral content must be considered in HRS experiments. The anomolously rapid fall-off for the narrow-band numbers is attributed to dephasing of the virtual excited state which favors the fluorescence cross-section over HRS and, in fact, eliminates the HRS signal even very far from the resonance peak.

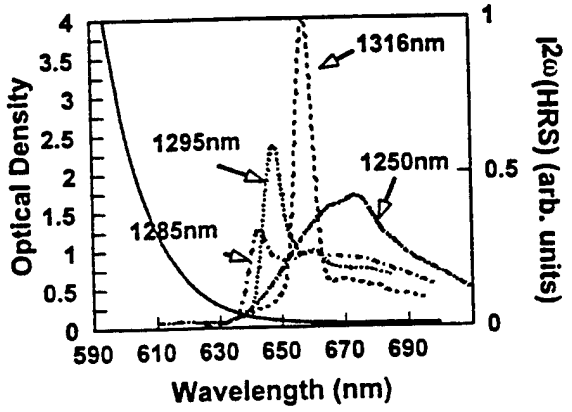

Figure 1

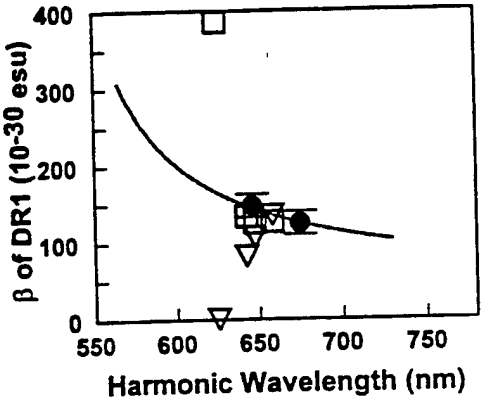

Figure 2

This work was supported by the National Science Foundation under the Science and Technology Center ALCOM No. DMR89-20147.

---

[1] K. Clays and A. Persoons, *Phys. Rev. Lett.*, **66**, 2980 (1991).

[2] J. Zyss and I. Ledoux, *Chem. Rev.*, **94**, 77 (1994).

[3] S. Cyvin, J. Rauch, and J. Decius, *J. Chem. Phys.*, **43**, 4083 (1965).

[4] K. Singer, J. Sohn, L. King, H. Gordon, H. Katz, and C. Dirk, *J. Opt. Sci. Am. B*, **6**, 1339 (1989).

Femtosecond hyper-Rayleigh scattering on thin polymeric films

Koen Clays, Geert Olbrechts, Erik Put, André Persoons[1]
Laboratory of Chemical and Biological Dynamics,
Center for Research in Molecular Electronics and Photonics,
Department of Chemistry, University of Leuven, Celestijnenlaan 200D, B-3001 Leuven, Belgium, tel. +32/16/32.75.08, fax. +32/16/32.79.82
[1]also at *Optical Sciences Center, University of Arizona, Tucson, Arizona 85721, USA*

Naoki Matsuda
Department of Analytical Chemistry,
National Institute of Materials and Chemical Research, 1-1, Higashi,
Tsukuba, Ibaraki 305 Japan, tel. +81/298/54.46.42 fax. +81/298/54.44.87

The generally observed discrepancy between the theoretically infinite coherence length in phase-matched waveguides and the effective interaction length for frequency doubling[1,2] has led us to investigate another limiting parameter for coherent second-harmonic generation in corona-poled thin polymeric films.

The first parameter limiting the efficiency of frequency conversion is the coherence length, *i.e.* the length over which the generated second harmonic stays in phase with the fundamental. Different phase-matching schemes have been devised. In positive, *resp.* negative, uniaxial birefringent crystals, angle tuning or temperature tuning can be used to make the extra-ordinary refractive index of fundamental, *resp.* second harmonic equal to the ordinary refractive index of second harmonic, *resp.* fundamental.[3] The compromise between a tight focus and a long confocal parameter results in a linear relation between conversion efficiency and interaction length. In waveguides, modal dispersion can be used to phase-match a fundamental mode with lower mode number with a second-harmonic mode with higher mode number. The main advantage of waveguides is the guiding of the light along the waveguide, resulting in a quadratic interaction length dependence for the conversion efficiency. The lowering of the field overlap integral with modal dispersion can be overcome by special design of the nonlinear susceptibility. When holding on to matching between modes with different mode numbers, the susceptibility has to be varied perpendicular to the plane of the waveguide.[2,4,5] Periodic poling along the propagation direction in the waveguide results in a quasi phase-matched structure.[1] The result of these different phase-matching schemes is always an infinitely long coherence length for a specific wavelength. Phase-matching curves (second-harmonic intensities as a function of fundamental wavelength) do show intensities peaked around the design wavelength, but the width of the curve indicates effective interaction lengths always much shorter than the physical dimension of the phase-matched structure. Another limiting mechanism has to be responsible for this deviation between the sub-micrometer interaction length and the infinite coherence length.

The coherence length is determined by the dispersion of the refractive index. In this first-order field of optics, symmetry does not come into play. Second-harmonic generation is a second-order nonlinear optical phenomenon. As for all even-order processes, symmetry is very important. Second-harmonic generation is a forbidden process in centrosymmetric media in the dipole approximation and, as such, very inefficient. Only non-centrosymmetric molecules show a second-order molecular hyperpolarizability and it is only when these molecules are oriented in a non-centrosymmetric fashion that this structure can frequency-double light efficiently. At the molecular level, this means that only dipolar and octopolar molecules should be considered for second-order NLO effects. To induce this non-centrosymmetry at the bulk level, different methods have been elaborated. Single crystal growth, Langmuir-Blodgett deposition, and poling of doped or functionalized polymers are currently in use to result in a macroscopically non-centrosymmetric structure. Only single crystal growth results in a constant relative orientation of the molecules in the crystal. The other structures are characterized by an order parameter, describing the degree of orientation in the film. Because of the sensitivity to symmetry, the efficiency of second-harmonic generation is largely determined by the constancy of this orientation. We have developed a measurement scheme to determine the degree of spatial orientational correlation between the chromophores doped in a thin polymeric film. This degree of correlation, quantified as a spatial correlation length, is shown to increase by poling. The longer correlation length after poling results from the higher degree of correlation between the chromophores, induced by the poling effect.

To deduce a value for the correlation length, as a quantifiable parameter for the degree of spatial correlation, the fluctuation in incoherent second-harmonic scattered light is measured as a function of position. Incoherent second-order scattering, or hyper-Rayleigh scattering (HRS), is used, to be able to study the influence of poling over the widest possible range of poling voltages, *i.e.* from unpoled samples also. These samples are

on average centrosymmetric and would not generate any coherent signal. To be able to observe HRS from solid samples, femtosecond pulses had to be used. The peak power available in the femtosecond pulse (≈100 kW) is obtained from a small value for the total energy (10 nJ) in the pulse. This limits optically induced damage in the spincoated films. The experimental set-up is a slight adaptation of the set-up used for HRS for the determination of hyperpolarizabilities with femtosecond pulses.[6] The detection part, consisting of the film holder, optical condensing system for efficient photon collection and wavelength discrimination, and the photodetector can be moved perpendicular to the fundamental beam, enabling HRS intensity measurements as a function of displacement x. The optical resolution of 5 μm (beam waist at focus in film) is matched to the mechanical resolution of the translation of 3 μm.

The resulting curves of the HRS intensity as a function of position are shown in Fig. 1 for an approximately 1 μm thick film of poly(methylmetacrylate) (PMMA) doped with 4-methoxy-4'-nitrostilbene (MONS) at a loading of 4.3 percent by weight. Three curves are shown for different corona poling conditions. These conditions were chosen based on the onset voltage for corona discharge (7 kV) and the lower limit for corona-induced damage to the film (9.1 kV).

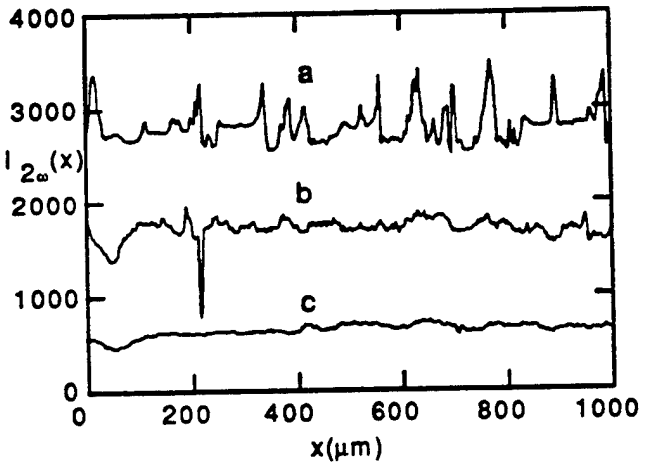

Fig. 1. Second-order (hyper-Rayleigh) scattered light intensities as function of position x...

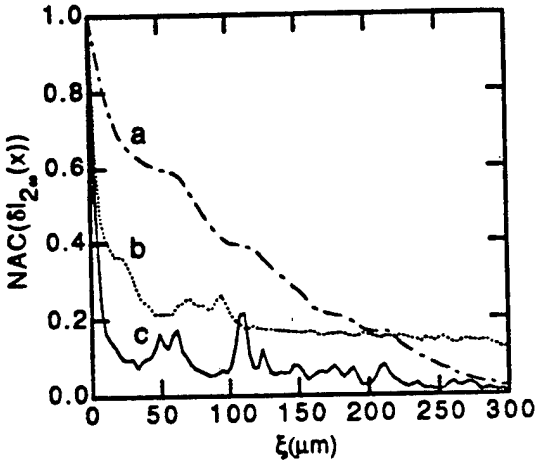

Fig. 2. Normalized autocorrelation functions of the fluctuations of the hyper-Rayleigh scattered light...

...for spincoated PMMA films doped with MONS after corona poling at:
a) 9 kV (high orienting field strength); b) 8 kV (intermediate orienting field strength); c) unpoled.

These data were analyzed towards a single parameter, describing the degree of spatial orientational correlation in the following way.[7] For the measurement of a randomly fluctuating variable with a spatial increment much smaller than the characteristic length of the variation over a total length much longer than this characteristic length, the autocorrelation function (ACF) of the variable is single exponentially decaying from the average of the squared intensities to the square of the average intensity. By subtracting from the variable its average, only the fluctuation itself is taken into account. The ACF then decays to zero. By dividing each point of the ACF by the initial amplitude, a normalized autocorrelation function results, completely characterized by a single correlation length.

Fig. 2 shows normalized autocorrelation functions, derived from the data of Fig. 1. The resulting correlation lengths are 5 μm for the unpoled film (the instrumental resolution), 20 μm for the intermediately poled film, and 121 μm for the fully poled film. The latter value corresponds very well with the values for the effective interaction length in phase-matched structures, as derived from the width of the phase-matching curves.[1,2] This agreement confirms that the limited degree of spatial orientational correlation between nonlinear optical chromophores in poled or self-organized thin films is an important parameter in limiting the effective interaction length in structures that are phase-matched over their complete physical dimensions.

References:

1. G. Khanarian, R.A. Norwood, D. Haas, B. Feuer and D. Karim, Appl. Phys. Lett. 57, 977 (1990).
2. T.L. Penner, H.R. Motschmann, N.J. Armstrong, M.C. Ezenyilimba and D.J. Williams, Nature 367, 49 (1994).
3. D.J. Williams, *Introduction to Nonlinear Optical Effects in Molecules and Polymers* (Wiley, New York, 1991).
4. M. Flörsheimer, M. Küpfer, C. Bosshard, H. Looser and P. Günter, Adv. Mat. 4, 795 (1992).
5. K. Clays, J.S. Schildkraut and D.J. Williams, J. Opt. Soc. Am. B 11, 655 (1994).
6. K. Clays and A. Persoons, Rev. Sci. Instrum. 65, 2190 (1994).
7. G. Olbrechts, E. Put, K. Clays, A. Persoons and N. Matsuda, accepted for publication in Chem. Phys. Lett.

Metal Nanoparticle Field Intensifier Optical Chemical Benches for Linear and Nonlinear Optics

Wenbo Xu[1], Russell Tuling[1], Charlotte Smaglinski[1], M. A. Fardad[1], Chaoyang Dai[2], Todd B. Marder[2], Mark G. Kuzyk[3] and Mark P. Andrews[1]

1. Department of Chemistry, McGill University, Montreal, Quebec, H3A 2K6, Canada
2. Department of Chemistry, University of Waterloo, Waterloo, Ontario, N2L 3G1, Canada
3. Department of Physics, Washington State University, Pullman, WA, USA

Monolayer and quasi-superlattice structures of NLO chromophores are commonly prepared by Langmuir-Blodgett thin film deposition or by chemically induced "self-poling" strategies that invoke chemical bonding across interfaces and within layers. Indeed, molecular self-assembly (MSA) and random grafting of monolayers of mono- and poly-functional organic molecules on macroscopic surfaces offer exciting potential for

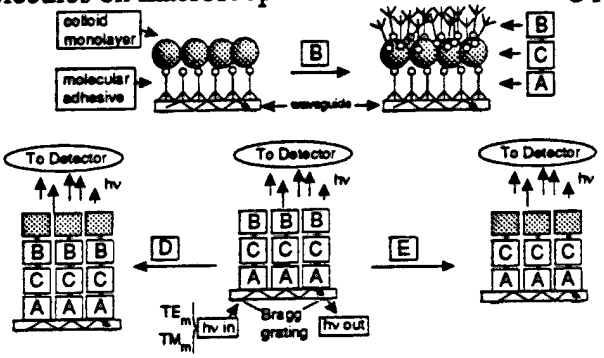

SCHEME 1

developing unusual field responsive supramolecular structures. Schemes 1-3 illustrate new methods we are developing for including metal nanoparticles as resonators that can be used to enhance optical interactions at interfaces for linear and nonlinear optical response. Surface mediated enhancements of optical field interactions at interfaces have been of interest to the scientific community for some time. Our success with metal particle optical field intensifiers to enhance nonlinear optical and Raman processes in fractal silver or gold metal nanoparticle/polymer composites and waveguides led us to consider several new constructions. Under certain conditions, MSA gives quasi-ordered 2D noble metal colloids on optical waveguide surfaces (Scheme 1). Transmission electron microscopy reveals that defected hexagonal array 2D raft growth structures of coinage metal particles are deposited by non-electrophoretic diffusion to the waveguide surface where irreversible binding takes place. Binding is accomplished by reaction with the sulfhydryl termini of ω-thio alkoxysilanes (A=mercaptopropyltrimethoxysilane, Scheme 1) grafted onto the waveguide. MSA of colloids in this manner gives a heterostructure whose evanescent field is enormously enhanced by coupling with surface plasmon excitations. We show how planar and ridge optical waveguides, or more complex optical circuits, can be used as "optical chemical benches" (OCBs) to assemble chromophores at waveguide surfaces. The first part of this

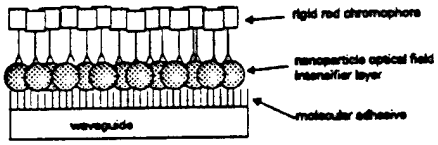

scheme 2

talk describes how the optical chemical bench is assembled layer by layer on a silicon wafer. With X-ray photoelectron spectroscopy we follow the evolution of the sulfur $2p_{1/2,3/2}$ binding energies as the molecular adhesive layer is covered with nanoparticles. Step B in Scheme 1 articulates a post-decoration process where shifts in the S 2p binding energies are traced for 2-
and 4-mercaptopyridine. These molecules were chosen to explore orientational properties that are ultimately important to depositing "self-poled" $\chi^{(2)}$ chromophores on such structures. Accordingly, mercaptopyridine molecules were interrogated by evanescent wave surface enhanced Raman scattering from TE waves propagating in the underlying waveguide. We observe that in-plane totally symmetric ring ($12a_1$, $9a_1$ and $8b_2$) vibrations are preferentially enhanced in intensity. This indicates that the plane of the pyridine ring moiety is oriented roughly perpendicular to the surface of the nanoparticles. Moreover, close analysis of the X-sensitive mixed β(CC)/ν(CS) vibrations supports the conclusion (from XPS) that the molecule is bound through the sulfur atom to the metal.

Enhancement effects are rather sensitive to the state of polarization of the laser beam, with substantial attenuation and photochemistry occurring in the presence of TM-polarized light. This is not surprising since the waveguide to some degree approximates the well known TE/TM metal strip waveguide mode selector. TM modes are well known to couple most strongly with metal plasmon excitations, which may lead to increased photochemistry. To understand the coupling mechanism we have explored a simplified 2D mean field representation of the optical problem of extinction by hexagonal arrays of metal spheres at a dielectric boundary. Failure of Lorentz local field corrections for 2D systems requires that the problem be reformulated for the TE and TM anisotropy of the complex dielectric tensor. A more sophisticated treatment takes retardation effects into account.

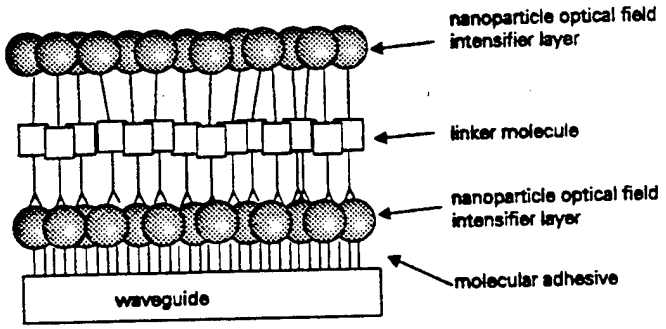

scheme 3

We also describe new waveguide topologies that are defined by depositing new thiol-terminated rigid rod acetylenic NLO chromophores on nanoparticle overlayers (Schemes 1 and 2). A simple and attractive concept is therefore that of self-oriented (self-poled) second order ($\chi^{(2)}$) NLO molecules attached to the colloid array. This construction is used to explore enhancements in the composite material nonlinearity through a local field effect (coupled plasmon excitation). Adsorption of the chromophore on 2D Ag or Au particles gives a noncentrosymmetric chromophore overlayer. This step is a prelude to Scheme 3 where we implement layer-by-layer assemblies of colloid arrays, linked by spacer molecules. We build supported "macrocrystals" of metal nanoparticles with interposed organic chromophores to give new mesoscopic structures that can behave as highly coupled optical resonators. These structures are examined by atomic force microscopy, linear extinction, XPS and enhanced Raman scattering.

Improved Characterization of Chromophores for Photorefractive Applications

Christopher R. Moylan, Robert J. Twieg, I-Heng McComb, and Donald M. Burland
IBM Almaden Research Center, 650 Harry Road, San Jose, California

Rüdiger Wortmann
Institut für Physikalische Chemie, Universität Mainz, W-6500 Mainz, Germany

It was shown three years ago[1] that if electric field-induced second harmonic (EFISH) data for chromophores in solution are reduced using expressions that are consistent between second harmonic generation and the Pockels effect, and are referenced to the best known value of d_{11} for quartz, they can be used to predict the electro-optic coefficients of poled polymers with reasonable accuracy. It has also been shown, however,[2] that the same does not hold for photorefractive polymers based on similar chromophores. Therefore, experiments performed on chromophores for photorefractive applications do not yet have predictive power.

The reason that determination of molecular parameters relevant to the electro-optic effect is not sufficient to predict photorefractive behavior is that the index of refraction grating induced in a photorefractive polymer is not solely, or even primarily, a result of the electro-optic susceptibility of the material and the space-charge field. The anisotropy of the polarizability of a chromophore makes the polymer birefringent to the extent that the chromophores are aligned, and this birefringence is often the primary cause of the material's photorefractive performance. This "orientational enhancement effect" has been previously described.[3] The original treatment defined two coefficients, one for the electro-optic contribution (C_{EO}) and one for the birefringence contribution (C_{BR}). Recently, Wortmann et al. have shown[4] that four molecular terms actually contribute to the photorefractive effect ($\mu\beta$, $\mu^2\alpha$, γ, and $\alpha\alpha$), but that the latter two are generally negligible. Neglecting the smaller terms, the susceptibility is proportional to the chromophore concentration multiplied by

$$\frac{6\mu\beta}{kT} + \frac{4\mu^2(\alpha_{\parallel} - \alpha_{\perp})}{3k^2T^2}.$$

Since the concentration is a material property rather than a molecular one, and since it is typically measured in weight fraction units, we express the concentration N (molecules/cm^3) as $w\rho N_A/M$, where w is the weight fraction, ρ is the polymer density, N_A is Avogadro's number, and M is the molecular weight of the chromophore. Only the last parameter is a molecular property. Simplifying the above expression by eliminating constants that do not depend on the particular chromophore, we arrive at a figure of merit F.

$$F = \frac{9kT\mu\beta + 2\mu^2(\alpha_{\parallel} - \alpha_{\perp})}{kTM}$$

F is the molecular figure of merit for photorefractive chromophores. Interestingly, the same expression is achieved by adding the expressions for C_{EO} and C_{BR} from Reference 3 and performing similar simplifications.

Determination of the usefulness of a given chromophore in photorefractive applications therefore involves not only measurement of $\mu\beta(-2\omega;\omega,\omega)$ by EFISH measurements, determination of μ by separate dielectric measurements, and conversion of $\beta(-2\omega;\omega,\omega)$ at the EFISH wavelength to $\beta(-\omega;\omega,0)$ at the photorefractive use wavelength by means of the two-level model, but also determination of the polarizability anisotropy. This term is equal to $\alpha_{zz} - (\alpha_{xx} + \alpha_{yy})/2$, where the α_{ii} are the three components of the diagonalized polarizability tensor, the z-axis being the one most closely aligned with the molecular dipole moment.

One equation in these three unknowns is obtained by making index of refraction measurements as a function of concentration. These data yield the trace of the polarizability matrix, or $(\alpha_{xx}+\alpha_{yy}+\alpha_{zz})$. A second equation is obtained by measuring the amount of depolarized Rayleigh light scattering from the chromophore as a function of concentration, and calibrating the result to a compound of known polarizability anisotropy (we use diphenylacetylene). These data can be shown[5] to yield the polarizability function $(\alpha_{xx}-\alpha_{yy})^2+(\alpha_{yy}-\alpha_{zz})^2+(\alpha_{zz}-\alpha_{xx})^2$. We have performed both the index and light scattering measurements at the HeNe wavelength of 633 nm, close enough to the Kr^+ laser wavelengths employed in our polymer characterization experiments so that no extrapolation is necessary. The third polarizability component must still be estimated somehow. One method is to use tables of bond polarizabilities[6,7] to estimate the third component. An alternative is to calculate all three components by a semiempirical method and use whichever one is deemed to be the most accurate. We have employed both methods in this work.

The quantity F is evaluated for several chromophores associated with significant photorefractive polymer results, including FDEANST,[8] DTNBI,[9] and DMNPAA.[10] In addition, the figure of merit is evaluated for several members of a new class of chromophores synthesized with the goal of maximizing the polarizability anisotropy. We expect that maximizing $\alpha_{\|}$ (α_{zz}) will also maximize ($\alpha_{\|}$-$\alpha_{\perp}$), and it has been shown[11] that α, β, and γ have a derivative relationship: when one is maximized, the next one is zero. Therefore, a chromophore with an optimized $\alpha_{\|}$ should have a β that vanishes. Rather than designing compounds with large β, therefore, we design compounds with small β as the goal. With this in mind, several cyanomethylene pyran (left) and azine (right) derivatives have been prepared and characterized, and their figures of merit are compared to those of the conventional chromophores, and to material performance.

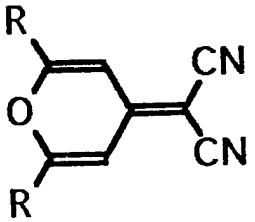

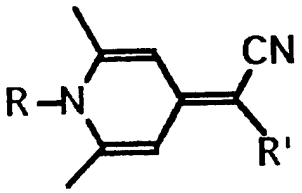

References

1. C.R. Moylan, S.A. Swanson, C.A. Walsh, J.I. Thackara, R.J. Twieg, R.D. Miller, and V.Y. Lee, *SPIE Proc.* **1993**,*2025*,192-201.
2. C.R. Moylan, R.D. Miller, R.J. Twieg, and V.Y. Lee, in *Polymers for Second-Order Nonlinear Optics*, G.A. Lindsay and K.D. Singer, eds; ACS Symp. Ser. vol. 601, ch. 5 (1995).
3. W.E. Moerner, S.M. Silence, F. Hache, and G.C. Bjorklund, *J. Opt. Soc. Am. B* **1994**,*11*,320-330.
4. R. Wortmann, C. Poga, R.J. Twieg, C. Geletneky, C.R. Moylan, P.M. Lundquist, R.G. DeVoe, P.M. Cotts, and D.M. Burland, submitted for publication.
5. K. Eidner and M.F. Vuks, *Opt. Spectrosc. (USSR)* **1978**,*45*,647-649.
6. H.A. Stuart, in Landolt-Börnstein *Atom- und Molekularphysik*, A. Eucken and K.H. Hellwege, eds; Springer-Verlag, Berlin, vol. I-3, p. 513 (1951).
7. R.J.W. LeFèvre, in *Advances in Physical Organic Chemistry*, V. Gold, ed; Academic Press, London, vol. 3, p. 50 (1965).
8. M.C.J.M. Donckers, S.M. Silence, C.A. Walsh, F. Hache, D.M. Burland, W.E. Moerner, and R.J. Twieg, *Opt. Lett.* **1993**,*18*,1044-1046.
9. S.M. Silence, J.C. Scott, J.J. Stankus, W.E. Moerner, C.R. Moylan, G.C. Bjorklund, and R.J. Twieg, *J. Phys. Chem.* **1995**,*99*,4096-4105.
10. K. Meerholz, B.L. Volodin, Sandalphon, B. Kippelen, and N. Peyghambarian, *Nature* **1994**,*371*,497-500.
11. F. Meyers, S.R. Marder, B.M. Pierce, and J.L. Brédas, *J. Am. Chem. Soc.* **1994**,*116*,10703-10714.

Possible Ultrafast All-Optical Switching Mechanism in J Aggregates using Perturbed Free Induction Decay.

Shunsuke Kobayashi and Fumio Sasaki
Electrotechnical Laboratory, 1-1-4 Umezono, Tsukuba, Ibaraki 305, Japan
Tel:(+81)298-58-5449, Fax:(+81)298-58-5459

The optical materials with fast and large nonlinear optical (NLO) responses have attracted much attention in high speed optical computing and data processing applications. A real excitation in NLO materials has to be used to achieve large NLO responses at the expense of switching speed. Several mechanisms are proposed to realize the high speed switching using coherent transient effect in large coherence length excitons.

One of the dye molecule pseudoisocyanine (PIC) forms quasi-one dimensional molecular aggregates called J aggregates. A coherence length of Frenkel excitons in PIC J aggregates is estimated to be nearly a hundred molecules from nonlinear optical properties and superradiant fluorescence decay. We have reported that PIC J aggregates show an extraordinary large NLO susceptibility [1] and also a novel excitation intensity dependent NLO response which could be useful as an optical logic element [2]. Characteristic features of the absorption spectrum of PIC J aggregates are the progression of the sharp bands at 570 nm, 530 nm and 495 nm. The bands at 570 nm (J band) and at 495 nm are assigned to the transitions to the lower and to the upper band edges of exciton, and the band at 530 nm is to the excitons coupled with optical phonons. In this report we propose novel efficient switching mechanisms using a perturbed free induction decay (FID) in Frenkel excitons of molecular aggregates.

Samples were made by dissolving PIC bromide to a concentration of 3 mM in a 1:1 mixture of water and ethyleneglycol (WEG). Details of the aggregate forming procedure were reported previously [1]. All the measurements were carried out at 77 K. The pulses used are the output from a femtosecond optical parametric generator and amplifier (OPG/OPA) pumped by a Ti:Sapphire regenerative amplifier with 1 kHz repetition. The pump pulses are obtained through the sum frequency generation between the output from OPA and that from Ti:Sapphire amplifier. A white light continuum generated by focusing the OPA output in a sapphire plate is used as the probe pulses. The pump wavelength is tuned at 570, 530 and 495 nm. The spectral width and duration of the pump pulses are 8 nm and 200 fs in each wavelength.

The coherent interactions between excitons of PIC J aggregates and the radiation field are measured by using a standard pump-probe method with low density (0.1 $\mu J/cm^2$) 200 fs probe pulses. Figure 1 shows the differential transmittance ($\Delta T/T$) spectra at various negative time delays (the weak probe pulse proceeds the intense pump pulse) probed at J band and pumped at 495 nm with the pump intensity of 7 $\mu J/cm^2$. The oscillatory structures are assigned to the perturbed FID [3] and has been reported in dye solutions [3] and semiconductors [4]. The coherent interaction of femtosecond laser pulses and the polarization in J aggregates produce the oscillatory structures in the differential transmittance spectra at the negative time delay. Passing through zero time delay $\Delta T/T$ spectra changes to the dispersion-type structure characteristics for the one-dimensional Frenkel excitons. Similar to Fig.1 of the 495 nm pump case $\Delta T/T$ spectra pumped at 530 nm and at 570 nm have the

same oscillatory structures irrespective of excitation wavelength. The amplitude of the oscillatory structures are increased with time. The rise-up of the signal indicates the dephasing time (T_2) of the polarization [3] and one can estimate T_2 as 300 fs independent of the pump wavelength.

When the intensities of the pump pulse increase over 30 $\mu J/cm^2$ a sharp dip appears in the middle of the central peak of the oscillation (Fig. 2). The time dependence of the amplitude of the dip is similar to that of the oscillation. The dip can be observed at very early delay time in the central part of the oscillation and disappeared nearly zero time delay.

Such a large $\Delta T/T$ change at certain wavelength region can be used as the all-optical switching which can modulate the weak signal pulses by the strong pump pulses. The dip appeared with the certain threshold of the pump intensity. The switching time is governed by the FID time T_2. The another advantage as the optical switching is that the pump wavelength can be used different from the signal wavelength without loosing switching speed and sensitivity. Such a novel two-color nonlinearities is come from the peculiarities of PIC J aggregates which show several exciton peaks.

Detailed mechanisms of the appearance of the dip in the central part of the oscillation are not clear. Some theoretical works suggest the population inversion effect caused by the strong pump pulses (π pulse). Another possibilities are an optical Stark effect or an phase distortion mechanisms comes from a nonzero optical thickness of the sample.

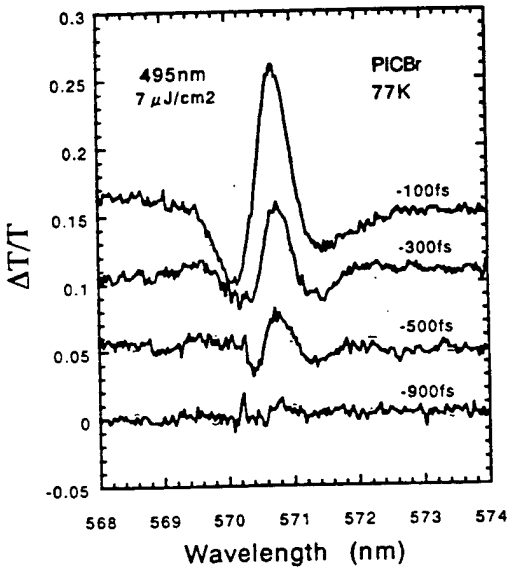

Fig.1. Differential transmission spectra for various negative time delays for PIC J aggregates in WEG at 77 K pumped at 495 nm with 7 $\mu J/cm^2$.

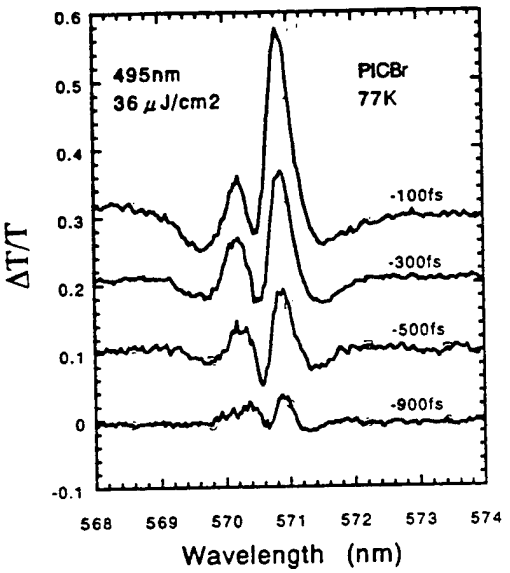

Fig.2. Same as Figure 1 except for the pump intensity with 36 $\mu J/cm^2$.

References.

[1] S.Kobayashi and F.Sasaki, Nonlinear Optics 4, 305 (1993).

[2] F.Sasaki and S.Kobayashi, Appl. Phys. Lett. 63, 2887 (1993).

[3] C.H.Brito Cruz, J.P.Gordon, P.C.Becker, R.L.Fork and C.V.Shank, IEEE J. Quantum Electron. QE-24, 261 (1988).

[4] S.Weiss, M.-A.Mycek, J.-Y.Bigot, S.Schmitt-Rink and D.S.Chemla, Phys.Rev.Lett. 69, 2685 (1992) and references there in.

Effect of meso-nitrogen substitution of symmetric cyanines on third order hyperpolarizabilities

W. Wernicke, M. Pfeiffer, A. Lau, W. Grahn*, H.-H. Johannes*

Max-Born-Institut für Nichtlineare Optik und Kurzzeitspektroskopie
D-12489 Berlin, Germany
**Institut für Organische Chemie, Technische Universität Braunschweig,*
D-38092 Braunschweig, Germany

Replacing the meso CH group in cyanines by a N-atom causes considerable shifts of their lowest ($^1\pi\pi^* \leftarrow S_0$) absorption bands compared to the parent molecule. The bathochromic shifts for even numbers (j) of double bonds in the chain as well as the hypsochromic shifts for odd numbers of double bonds are well described by the free-electron theory /1/. Using this theoretical approach a dramatic influence of nitrogen-substitution on the third order hyperpolarizabilities in the low frequency limit γ_{STAT} was predicted resulting in hyperpolarizabilities with positive signs for odd numbers of double bonds and in negative signs for even numbers /2/. Furthermore for odd and for even j an increase of the modulus of γ_{STAT} by more than an order of magnitude is expected /2/. In contrast to those results, using a Pariser-Parr-Pople (PPP) Hamiltonian only positive and comparatively low hyperpolarizabilities were calculated for the substituted (aza)-compounds /3/.
Up to now some corresponding experimental data are available for trimethines (j=2) only /4/, but an experimental investigation of the chain length dependence was still lacking.

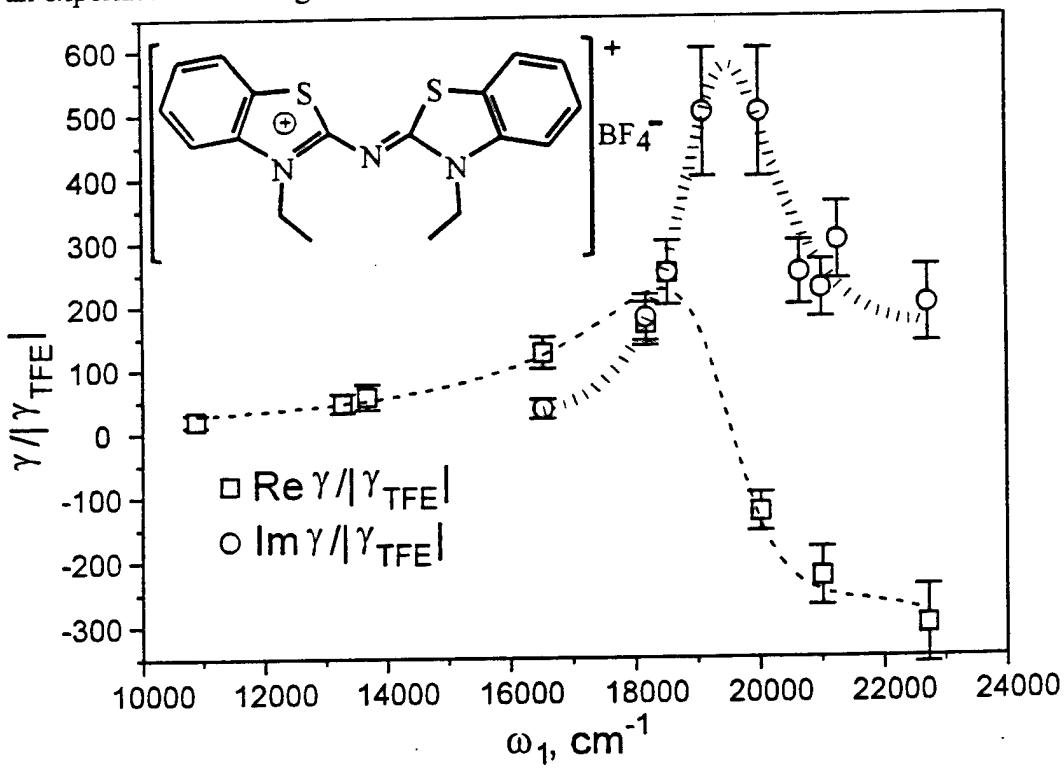

Fig. 1 Measured dispersion of the real part $Re\gamma^{NR}$ (squares) and of the imaginary part $Im\gamma^{NR}$ (circles) of the meso-aza-thiacyanine (trimethine) dye (j=2) dissolved in trifluoroethanol (TFE). Lines: fits of the dispersion curves. The molecular structure of the dye is shown in the insert.

Here we report on static hyperpolarizabilities γ_{STAT} of the homologous series of cyanines with benzthiazole nuclei and of the corresponding series of aza derivatives determined by nondegenerate four wave mixing measurements (CARS,CSRS).
Varying excitation frequencies ω_1 from nearly resonant conditions with respect to the lowest absorption bands to almost off-resonant excitation, dispersion curves of the hyperpolarizabilties γ^{NR} were obtained. As an example in Fig. 1 the dispersion curves of the real part and of the imaginary part of the meso-aza-thiacyanine (trimethine) normalised to the hyperpolarizability of the solvent trifluoroethanol (TFE) are shown. From the four wave mixing dispersion curves hyperpolarizabilities in a static frequency limit γ_{STAT} were extrapolated as has been described in /5,6/. Results are summarised in table 1.

Table 1 Static hyperpolarizabilities γ_{STAT} and absorption maxima λ of the lowest $^1\pi\pi^* \leftarrow S_0$ transition of benzthiazole dyes with different chain lengths (j: number of double bonds, N: number of π electrons) and of their aza-derivatives. (Solvent: TFE)

molecule	j	N	λ [nm]	γ_{STAT} [10^{-36} esu]
trimethine	2	6	420	−7 ±2
aza-trimethine	2	6	375	+4 ±2
pentamethine	3	8	550	−120 ±15
aza-pentamethine	3	8	580	−85 ±15
heptamethine	4	10	645	−700 ±200
aza-heptamethine	4	10	540	−90 ±15

The increase of γ_{STAT} with chain lengths of the unsubstituted cyanines with benzthiazole nuclei follows roughly a $\gamma_{STAT} \sim -N^9$ dependence, which is comparable to the behaviour of the simple bisdimethylamino dyes /5/.
It can be concluded from our measurements that N-atom substitution of the dyes of the benzthialzole series does not result in a drastic increase of the hyperpolarisability $|\gamma_{STAT}|$, but in contrast the modulus $|\gamma_{STAT}|$ slightly decreases.
Furthermore it can be seen, that the hyperpolarizabilities γ_{STAT} of the trimethine dyes (j=2) exhibit a sign reversal due to N-atom substitution and that γ_{STAT} is only slightly effected for j=3. In the aza-heptamethine a drastic decrease of the modulus of γ_{STAT} is observed but its sign remains negative. Therefore taking into account that positive as well as negative terms of comparable magnitude are contributing to the overall hyperpolarizability in polymethines our results show a tendency to an alternation but not a complete sign reversal for j=4.
For a more detailed understanding of the deviations of the dependencies on chain length for the aza derivatives compared to those obtained from π-electron theories theoretical calculations are in progress.

references:

/1/ H. Kuhn; Fortsch. Chem. Org. Nat. **16** (1958) 169; **17** (1959) 404
/2/ S.C. Mehendale, K.C. Rustagi; Opt. Commun. **28** (1979) 359
/3/ I.D.I Albert, P.K. Das, S. Ramesesha; J. Opt. Soc. Am. B. **10** (1993) 1365
/4/ S.H. Stevenson, D.S. Donald, G.R. Meridith; Mat. Soc. Symp. Proc. **109** (1988) 103
/5/ T. Johr, W. Werncke, M. Pfeiffer, A. Lau, L. Dähne; Chem. Phys. Lett. **246** (1995) 521
/6/ T. Johr, W. Werncke, L. Dähne, M. Pfeiffer, A. Lau; Appl. Phys. B (1996) in press

Solitary Waves and Ring-Formation in Polydiacetylene para-Toluene Sulfonate

Brian L. Lawrence, William E. Torruellas, George I. Stegeman
CREOL, University of Central Florida
4000 Central Florida Boulevard, Orlando FL 32816-2700
TEL: (407) 823-6943
FAX: (407) 823-6955

Spatial solitary waves propagate in a nonlinear medium by balancing diffraction with a self-focusing nonlinearity. These waves are of fundamental interest, but are also of technological interest if they are stable under propagation. A Kerr nonlinearity does not lead to stable self-trapping in two transverse dimensions (2D).[1] Methods proposed for stabilizing 2D beams have included saturating mechanisms and quintic nonlinearities.[2,3] Until recently, self-trapped beams had only been observed in vapor systems.[4] However, our measurements indicated that polydiacetylene para-toluene sulfonate (PTS) has $n_2>0$ and $n_3<0$ with low linear loss and negligible nonlinear loss at 1600 nm.[5] In addition, numerical studies using the measured values for n_2 and n_3, interpreted in the context of the variational model of nonlinear Gaussian beam propagation, have predicted self-trapping and ring formation.[6] We now report preliminary experimental demonstrations of 2D spatial solitary waves and ring formation in PTS. These results confirm, for the first time, the existence of the combination of a third-order and a fifth-order nonlinearity, independent of saturation, in a solid-state material, and the ability of this material to support stable self-trapped beams.

Our experiments in PTS crystals show stable self-trapping at moderate intensities and ring formation at higher intensities. Figure 1 shows a cross-section of the solitary wave at the output face of a 1.7 mm PTS crystal and the corresponding numerical simulation for a 1600 nm beam, with an initial waist of 16 microns and an intensity of 500 MW/cm^2 (power = 1.7 kW).

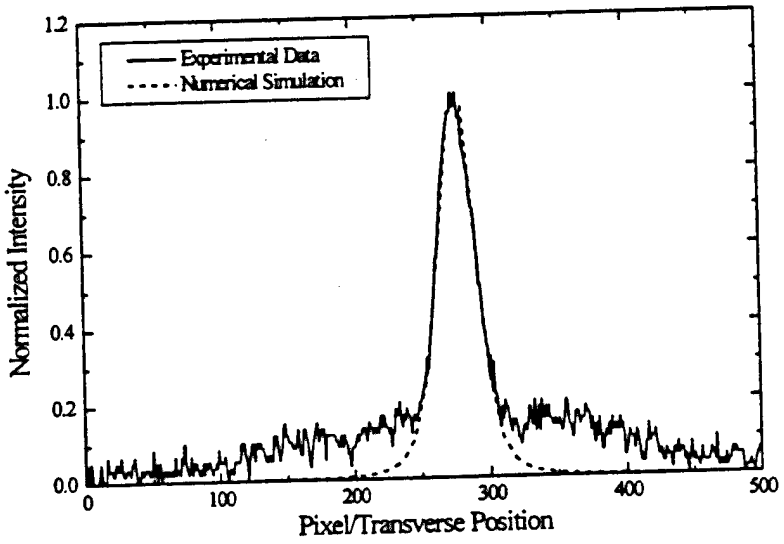

Figure 1: Experimental (solid line) and numerical (dashed line) observation of stable self-trapping in a 1.7 mm PTS crystal at 1600 nm, with an input waist of 16 μm, and an intensity of 500 MW/cm^2 (power =1.7 kW).

Figure 2 shows a cross-section of the ring formation occurring in the same crystal and the accompanying simulation for the same initial conditions as in figure 1, but with an intensity of 9 GW/cm^2 (power = 43 kW). Complete ring formation does not occur due to the pulsed nature of the beam, whereby the higher intensity, center portion of the beam forms the ring, and the lower intensity, temporal wings stay trapped as a solitary wave on axis. The experimental results agree very well with the numerical simulations. Both the solitary wave in figure 1 and the ring in figure 2 have a background that results from portions of the beam that do not form a solitary wave, but instead diffract away, either as portions of the temporal wings of the pulse that are below the threshold for self-trapping or scattering off of defects in the crystal.. To our knowledge, these results are the first experimental demonstration of a quintic nonlinearity, independent of saturation, in a solid-state material system.

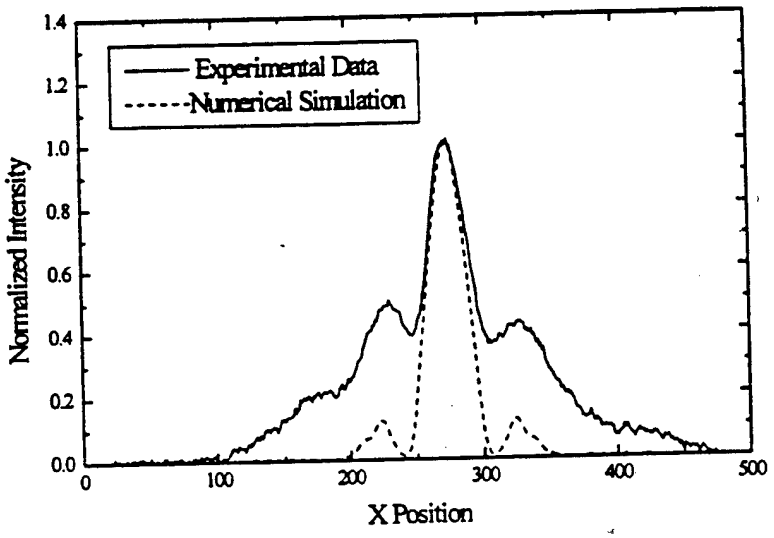

Figure 2: Experimental data (solid line) and numerical calculation (dashed line) of ring formation in a 1.7 mm PTS crystal at 1600 nm, with an input waist of 16 μm, at an intensity of 9 GW/cm^2 (power = 36 kW).

References:

1. P. L. Kelley, Phys. Rev. Lett. **15**, 1005 (1965)

2. J. E. Bjorkholm and A. Ashkin, Phys. Rev. Lett. **32**, 129 (1974)

3. V. E. Zakharov, V. V. Sobolev, and V. C. Synakh, Sov. Phys. JETP **33**, 77 (1971)

4. V. M. Malkin, Physica D **64**, 251 (1993)

5. B. L. Lawrence, M. Cha, J. U. Kang, W. Torruellas, G. Stegeman, G. Baker, J. Meth, and S. Etemad, Electron. Lett. **30**, 447 (1994)

6. E. M. Wright, B. L. Lawrence, W. E. Torruellas, G. I. Stegeman, Opt. Lett., **20**, 2478 (1995)

O-18

Electrical Conduction Processes and High Electric Field Poling in Nonlinear Optical Polymers

Manfred Eich, Robert Blum, Martin Sprave
Telekom Technologiezentrum, P.O. Box 10 00 03, D-64276 Darmstadt, FRG,
Phone: +49-6151-833742, Fax: +49-6151-834960
E-Mail:Eich@fz.telekom.de

ABSTRACT

For optical communication technology electrooptically active materials such as chromophore functionalized second order nonlinear polymers will play an important role. Due to their ultrafast electronic response such materials may be used in phase shifters and in external modulator devices. In order to achieve the macroscopic noncentrosymmetry that is necessary for second order optical nonlinearities these materials have to be poled in strong external electric fields. Electrical properties of the sandwich structures generally used to realize waveguide configurations will determine the maximum electrical poling field strength in the active layer and thus the achievable degree of optical nonlinearity. We have therefore investigated the electrical conduction processes under high electric field poling conditions in thin films of a standard type nonlinear optical side chain polymer (PMMA/DRMA 10 Mol %) covered with gold and ITO electrodes. In addition, sandwich structures composed of this polymer and thin layers of an inorganic low index SiO_x-type buffer material between the polymer and the electrodes were investigated. Poling current was continuously measured during poling experiments and decreases with time (t^{-n} behavior, Fig. 1). Finally the current levels and reaches a steady state value for poling times much longer than 1000s.

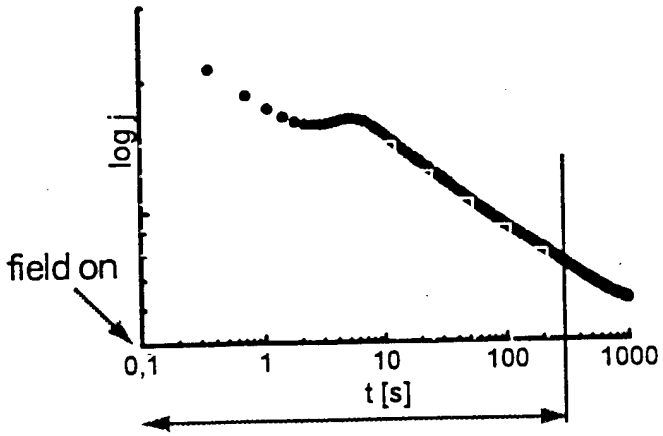

Fig. 1: Current density of a single layer of 10% DR1 functionalized polymethacrylate as a function of time at 90 V/µm and 120°C as a function of time (t^{-n} behavior)

This f^n ($n \leq 1$) dependence indicates a broad distribution and superposition of relaxation times and is often found in amorphous insulators from polymers and inorganic dielectrics and is attributed to trap filling processes. This paper will elucidate in detail the field dependence of the observed current density. Three processes are found: Ohmic conduction at low field strengths (<40 V/μm), interface limited Schottky current for medium field strengths (40 V/μm - 100V/μm) and Fowler-Nordheim tunneling characteristics at poling field strengths exceeding 100 V/μm (Fig. 2).

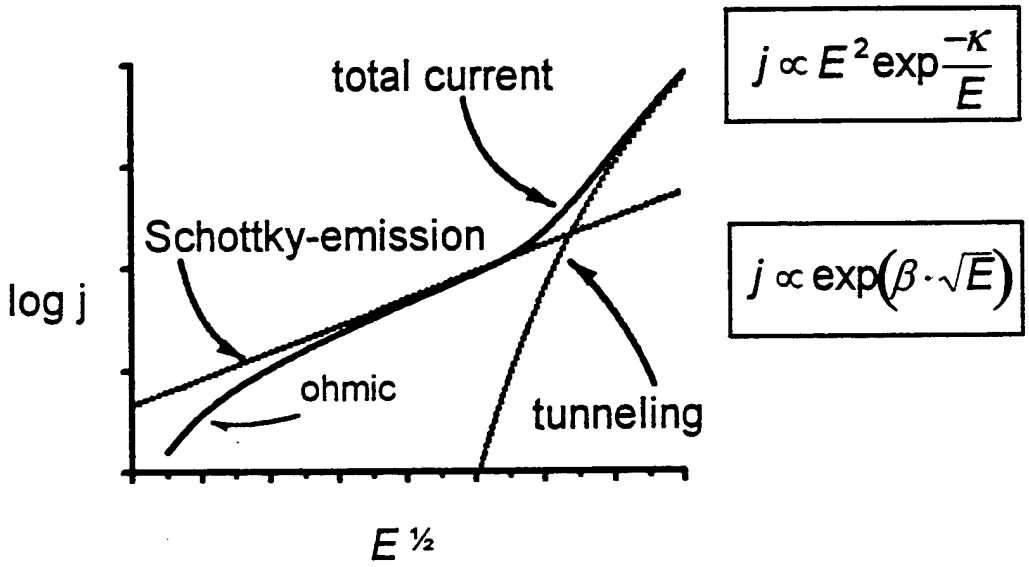

Fig. 2: Typical current density Schottky plot of a NLO polymer. Dotted lines denote theoretical curves for pure Schottky and Fowler-Nordheim emission. The upper right expression represents the Fowler-Nordheim case (tunneling) the lower right expression represents the Schottky case (thermionic emission).

This paper will also discuss how the maximum achievable electrical poling field strength in the polymer can be increased by modification of the electrode-polymer interface. This allows for a significantly higher maximum degree of polar orientational order and hence for a higher achievable electrooptical susceptibility.

Mechanism of DC drift phenomenon in electro-optic polymer waveguide

Heuk Park, Wol-Yon Hwang, and Jang-Joo Kim
Electronics and Telecommunications Research Institute,
P.O.Box 106, Yusong, Taejon, 305-600, Korea

In a Mach-Zehnder intensity modulator, modulation electric signal is applied to one arm and dc bias is applied to the other arm to adjust the operation point of the modulated output light. However, the dc bias required to keep the operation to a certain point is not fixed but drifts with time in many cases. It is called the dc drift phenomenon. The dc drift phenomenon is well known in the inorganic electro-optic (EO) waveguide using Ti:$LiNbO_3$. An equivalent circuit is adopted to interpret the dc drift phenomenon in the Ti:$LiNbO_3$ based EO waveguide. The low resistivity of the buffer layer and the photorefractive effect in the active layer are attributed as the main causes of the dc drift. There are, however, only a few reports on the dc drift phenomenon in EO polymer waveguide devices and the mechanism underlying the phenomenon has not been reported yet. In this paper, we report on the mechanism of the DC drift.

If we apply dc bias V_{dc} to electro-optic waveguide, the induced phase change will be determined by the voltage applied to the core layer V_{core} which is a function of V_{dc} and time. The induced phase shift $\delta\varphi$ is

$$\delta\varphi = \frac{2\pi}{\lambda}\cdot\frac{1}{2}n^3\gamma_{33}\cdot\frac{L}{d}V_{core} \qquad (1)$$

where λ is the wavelength of the guided light, n and γ_{33} the refractive index and the EO coefficient of the core layer, respectively, L the length of the electrode and d the thickness of the core layer. To get the functional form of V_{core}, we adopted an equivalent circuit presented in Fig.1 which is generally used to describe the electrical properties of the multilayer. The calculated functional form of V_{core} is

$$V_{core} = V_{dc}\cdot\xi_{core}\cdot\tau_{rel}\cdot\left[\frac{1}{\tau_{clad}} + 2\xi_{clad}\cdot\left(\frac{1}{\tau_{core}} - \frac{1}{\tau_{clad}}\right)\cdot\exp\left(-t/\tau_{rel}\right)\right] \qquad (2)$$

where $\tau_i = R_i\cdot C_i = \rho_i\cdot\varepsilon_i$ and $\xi_i = \frac{1}{C_i}\Big/\left(\frac{1}{C_{core}} + 2\frac{1}{C_{clad}}\right)$ for the i-th layer. C and R are the capacitance and the resistance, respectively; ρ and ε the resistivity and the permittivity of the material, respectively. The relaxation time of the dc drift, τ_{rel}, is represented by

$$\frac{1}{\tau_{rel}} = \frac{\xi_{core}}{\tau_{clad}} + \frac{2\xi_{clad}}{\tau_{core}}. \qquad (3)$$

The above equations indicates that the voltage applied to the core layer, V_{core}, will change or drift with time if the RC time constants of the core and cladding layer are different each other even thought the V_{dc} is kept constant.

A Mach-Zehnder intensity modulator is used to detect the change of the induced phase shift under the dc bias. A methacrylate copolymer with side chain groups of dimethylamino-nitrostilbene (P2ANS). UV15 (Master bond) was used as the lower and upper cladding layers. The thickness of the cladding layers was 0.65 μm and that of the core layer was 3.5 μm. Photobleaching technique was employed to define the channel waveguides. The waveguide was poled with the poling field of 1.5 MV/cm. The length of the modulation and the bias electrodes is 1.5 cm. The half wave voltage of the modulator V_π is 4.9 V at 1.3 μm.

The phase change induced by dc bias on one arm was directly measured by observing the waveform generated by a triangular electric wave applied to the other arm. The changes of $\delta\varphi$ for the three different values of dc bias (4 V, 8 V and 16 V) are presented in Fig.2. $\delta\varphi$ is normalized to the

initial change for comparison. The application of the dc bias V_{dc} induces an instantaneous change in $\delta\varphi$ by $\pi \cdot V_{dc}/V_\pi$ for each value of the dc bias. Under the dc bias, normalized $\delta\varphi$ decays exponentially and the relaxation time is independent of V_{dc} as expected from Eq.(2) and Eq.(3). The relaxation time is also strongly dependent on the intensity of the guided light and on the exposure to external light. As shown in Fig. 3, the decay becomes faster as the intensity of the guided light (1.3μm) increases. When the device is illuminated by the visible light, the drift becomes faster again. This illumination also reduces the transmittance of the waveguide. After turning off the visible light, the drift gradually becomes slower and the transmittance recovers as presented in Fig. 4.

The effects of the guided light and external light on the dc drift was successfully interpreted by the photoconductivity of the guiding layer. The photoconductivity of P2ANS due to external light was confirmed by the independent photoconductivity measurement. The reduction of the transmittance due to external light can be explained by the photoinduced absorption.

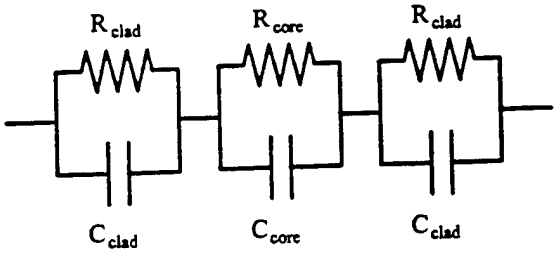

Figure 1. Equivalent circuit of the polymer electro-optic waveguide

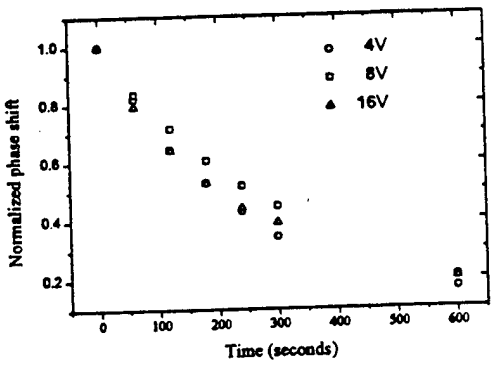

Figure 2. The time dependence of the phase change for different applied voltage.

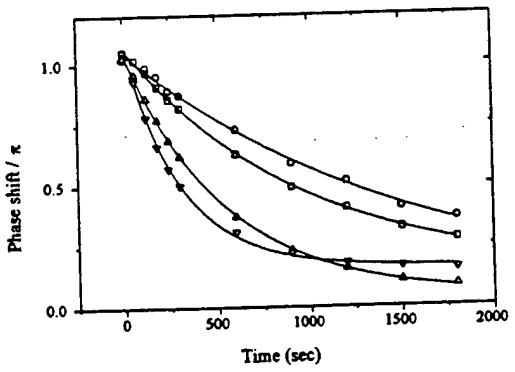

Figure 3. DC drift behavior at different intensity of the guided light.

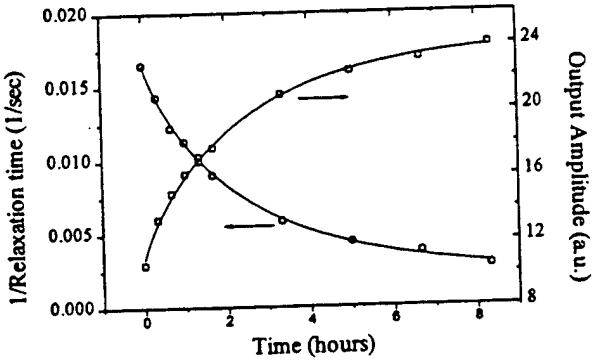

Figure 4. The change of the relaxation time of the DC drift and the transmittance after a few minutes of illumination of the visible light.

Modeling Relaxation Processes in Poled Electro-Optic Polymer Films

R.D. Dureiko and K.D. Singer
Physics Department
Case Western Reserve University, Cleveland, Ohio 44106

The thermal stability of the second order nonlinear optical susceptibility of guest-host and side-chain polymeric systems having glass transition temperatures in the range of $90< T_g <125$ °C was investigated in both the time and frequency domains. Experiments that measured second harmonic(SH) generation as well as transient current in the dye doped polymer systems(namely MMA-DR1, PMMA\DR1, and PMMA\DCM) in the time domain were conducted below the polymer's glass transition temperature, while dielectric and "chi-electric" [1] frequency domain experiments were employed above the glass transition temperature. All optical data was obtained using a 50 fs mode-locked Ti:Sapphire laser.

The decay of the SH and transient current were modeled in the time domain using the standard Kohlrausch- Williams-Watts(KWW) "stretched exponential" function, while in the frequency domain the Havriliak-Negami (HN) function was used to model both the dielectric and chi-electric data. From these models, the relaxation parameter, τ, for the various polymeric systems studied was determined. In separate differential scanning calorimetry (DSC) experiments, the enthalpic relaxation of the polymer system was measured. Our goal was to establish more firmly a universal scaling law for τ as suggested by Kaatz et al. [2]. To this end, the Adams-Gibbs entropic model was used to describe the temperature dependence of τ, that is,

$$\tau = A\exp[\frac{D}{RT\left(1-\frac{T_2}{T_f}\right)}],$$

where T is the temperature, and R is the gas constant. Above T_g, this expression describes Williams-Landel-Ferry behavior, while below T_g, it describes Arrhenius behavior. To determine whether or not this model is universal, a wide variety of systems, such as guest-host, side-chain, and cross-linked, must be studied. Our present studies include two guest-host systems, namely PMMA\DR1 and PMMA\DCM, one side-chain system, MMA-DR1, and two high temperature systems, one which is cross-linked. The Adams-Gibbs plot for three acrylate systems is shown below.

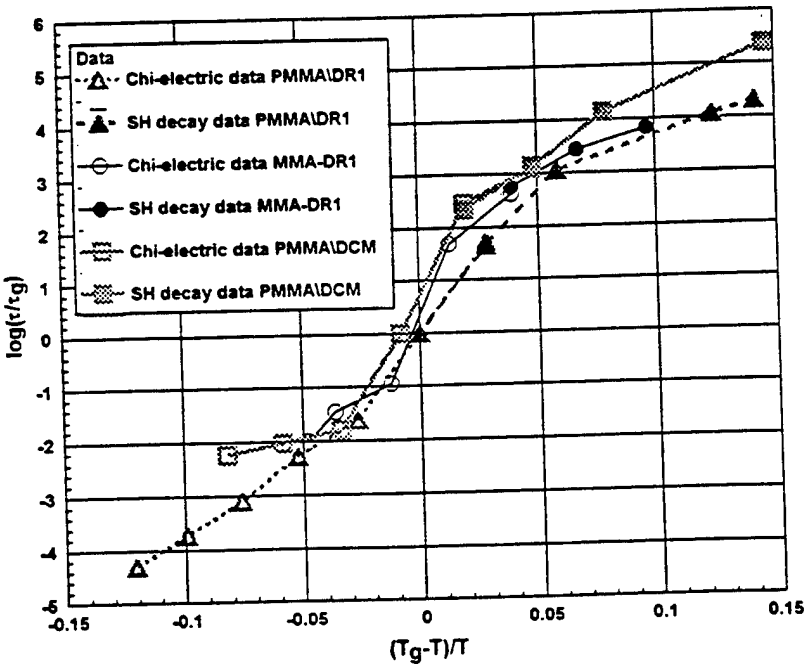

Temperature scaling of normalized relaxation times

* This work was supported by the AFOSR grant No. F49620-93-1-0202.

1. J.A. Cline; W.N. Herman., Tech. Digest, "Organic Thin Films for Photonic Applications", *Opt. Soc. Am.* p. MD39 (1995).
2. Kaatz, P.; Pretre, P.;Meier, U.; Stalder, U.; Bosshard, C.; Gunter, P., *Macromolecules* 29 p. 1666 (1996).

Linear and non-linear optical behaviors of Langmuir-Blodgett multilayers of push-pull tolan derivatives

Hiroo Nakahara, Wei Liang,
Liming Wang ,* Tatsuo Wada* and Hiroyuki Sasabe*
Department of Chemstry, Saitama Universty, Shimookubo 225,
Urawa, Saitama, 338 Japan
* Frontier Research Progarm, The Institute of Physical and Chemical Research (RIKEN), Hirsawa 2-1, Wako, Saitama, 351-01 Japan

Over the past several years much attention has been focused on the second-order nonlinear optical (NLO) phenomena in Langmuir-Blodett (LB) films.[1-3] The LB technique provides an effective approach to a highly ordered films.[4] In normal case, noncentrosymmetric LB multilayers such as Z- and X-types can be obtained by transferring monolayers when the substrate is being withdrowed and a horizontally lifting . However, a convenient LB method usually provides centrosymmetric structured films (Y-type) with an even number of layers where SHG is forbidden. Recently, Y-type LB films with noncentrosymmetric structures have been developed from some amphiphilic molecules with nonlinear optical chromophores, such as 2-docosylamino-5-nitropyridine and N-docosyl-4-nitroaniline.[5] The SHG could be observed in these LB films due to their orientation in plane anisotropy . It is well known the tolan sketeton has an advantage of avoiding the chemically and photochemically induced cis-trans isomerization which can be occured in the corresponding stilbenes.[6] The NLO properties of several push-pull tolans have been studied and found to be highly SHG efficient. In this paper, we report preliminary NLO properties related to the molecular orientation of push-pull tolans in LB multilayers.

4-Amino-4'-nitro-tolan (ANT18) and 4-docosylamino-4'-nitro-tolan (ANT22) as shown in inset of Fig.1, they were synthesized by coupling of 4-docosylaminoiodobenzene with 4-ethynylnitro-benzene using $Pd(PPh_3)Cl_2$/CuI and triethylamine. The monolayer behavior at the air-water interface was investigated by a Lauda film balance and a Brewster angle microscope (BAM). Figure 1 shows the surface pressure - area isotherms of ANT-22 and ANT-18 monolayers on the water surface at 20 °C, spread from toluene solution. ANT-22 and ANT-18 can form stable condensed monolayers, having the limiting areas of 30 and 26 Å^2/molecule at 20°C, respectively, suggesting that the molecules stand nearly vertical together with the alkyl chains. For morphologies of the monolayer of ANT22 at zero surface pressure (57 Å^2/molecule) at 30°C, relatively regular domains of the condensed phase with ordered 'dots' (highly refractive parts) were observed by BAM.

Second harmonic generation was measured for Y-type six layers of ANT-22, which was prepared by the vertical dipping method. A Q-switched Nd-YAG laser (Spectra-physics, GCR-170, repetition rate 10 Hz, pulse width 9 ns) was used. The LB films were irradiated with a Q-switched Nd-YAG laser beam perpendicular to the layer plane. The second harmonic (SH) signal was detected at 532 nm. Figure 2 shows the SH signal *vs.* the angle of incidence for one side of the substrate. The second order nonlinear optical susceptibility $\chi^{(2)}_{p\text{-}p}$ along the dipping direction extracted with respect to the SHG coefficient (d_{11}) of quartz is about 3.31 x 10^{-6} esu. This large nonresonance $\chi^{(2)}_{p\text{-}p}$ value can be ascribed to highly ordered orientation and extended π-conjugation of the chromophore in the film. It was found that $\chi^{(2)}_{p\text{-}p}$ along the dipping direction is approximately five times larger than $\chi^{(2)}_{s\text{-}s}$ perpendicular to it. The larger ratio of $\chi^{(2)}_{p\text{-}p}$ / $\chi^{(2)}_{s\text{-}s}$ in ANT-22 film indecates that the NLO chromophores lie almost flat on the plane of the substrate with orientation preference along the dipping direction. The SH intensity is given by the equation (1)[7]:

$$I^{2\omega} = \frac{2\omega^2 d_{eff}^2 l^2}{c^3 \varepsilon_0 (n^{\omega})^2 (n^{2\omega})} (I^{\omega})^2 \sin c^2 (\frac{\Delta k l}{2}) \qquad (1)$$

where sinc x denotes (sin x)/x, l is the sample thickness, d_{eff} is the effective nonlinear optical susceptibility, n is the refractive index, c is the light speed, and $\Delta k = k_2 - k_1$ is the phase mismatch between the fundamental and the SH waves with the wave vectors k_1 and k_2 respectively.

Polarized UV-Vis. absorption spectra at 45° incidence for monolayer assemblies of ANT-22 gave a linear dichroism(A_P:As = 1.5). showing that the chromophores are oriented with some inclination. In the case of the normal incidence, an in-plane anisotropy was observed and the chromophores were found to be oriented with the transition moments along the dipping axis. This result supports the orientation of chromophroe on the substrate reduced by polarized SHG measurements. The red shift (11nm) in the spectrum for the LB films of ANT-22 compared with that for the chloroform solution of can be due to the intermolecular interaction of chromophores

Further studies concerning the nonlinear optical properties of the LB films, the film morphology and the differences in the molecular orientation of Langmuir-Blodgett films fabricated by the vertical dipping and the horizontal lifting methods are in progress.

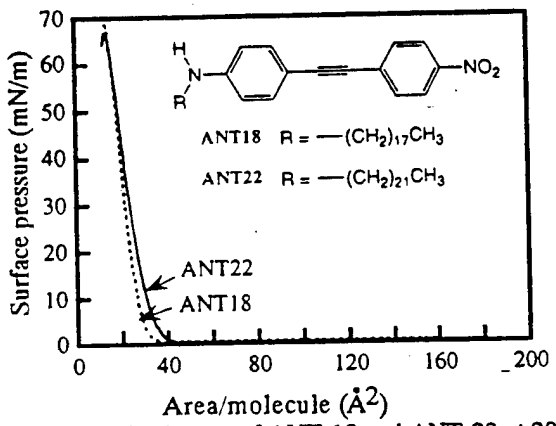

Fig. 1 π-A isotherms of ANT-18 and ANT-22 at 20°C and their chemical structures

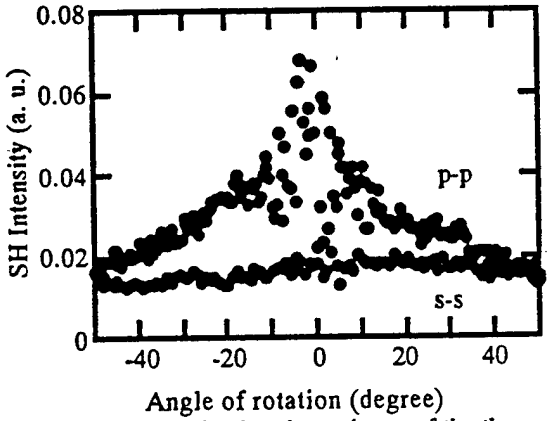

Fig. 2. The polarization dependence of the the second harmonic signal. Both the polarizer and the analyzer were aligned along the dipping axis and the sample was rotated about an axis perpendicular to both the surface normal and dipping direction (p-p). The bottom trace indicates the SH signal for the same rotation when the polarizer and the analyzer were aligned along the y axis

References
1. D. B. Neal, M. C. Petty, G. G. Roberts, M. M. Ahmad, W. J. Feast, I. R. Girling, N. A. Cade, P. V. Kolinsky, I. R. Peterson., Proceeding of ISAF'86, 89-92.
2. Donald Lupo, Werner Prass and Ude Scheunemann, Andre Laschewsky and Helmut Ringsdorf, J. Opt. Soc. Am. B/Vol. 5, 300-308 (1988).
3. G. Decher, B. Tieke, C, Bosshard, and P. Gunter, J. Chem. Soc., Chem. Commun., (1988). 933-934.
4. D. S. Chemla and J. Zyss, eds., Nonlinear Optical Properties of Organic Molecules and Crystals (Academic, New York, 1987), Vols. I and II.
5. W. M. K. P. Wijekoon, B. Asgharian and P. N. Prasad, eds., Thin Solid Films, 208 (1992) 137-144.
6. J. Zyss, I. Ledoux, and J. F. Nicoud, Advances in Molecular Engineering for Quadratic Nonlinear Optics (1993)
7. See e. g., A. Yariv ' Quantum Electronics,' Wiley, New York, 1975

Crystal Engineering for Nonlinear Optics: Self-Assembling of Merocyanine Dyes with Highly Optimized Chromophoric Alignments in Crystalline Solids

Man Shing Wong, Feng Pan, Christian Bosshard, Peter Günter

Nonlinear Optics Laboratory, Institute of Quantum Electronics, ETH-Hönggerberg, CH-8093, Zürich, Switzerland

There has been tremendous progress in understanding and optimizing π-conjugated donor-acceptor chromophores with large second-order molecular hyperpolarizabilities in the area of organic nonlinear optics in the last few years.[1] However, there are only few chromophores with large molecular hyperpolarizabilities such as donor-acceptor stilbenes and tolanes that have been developed into potentially useful crystalline materials. Our interest in molecular crystals stems from the fact that the potential upper limits of macroscopic nonlinearities and long-term orientational stability of molecular crystals are significantly superior to those of polymers. Besides a large molecular hyperpolarizability, chromophores have to arrange non-centrosymmetrically in the crystalline state in order to exhibit second-order nonlinear optical effects. In addition, to be an efficient as well as useful second-order nonlinear optical crystalline material, the orientation of the chromophores in the bulk needs to be optimized. However, there are still no existing means of predicting and controlling molecular packing in crystalline state. 90% of the achiral organic molecules crystallize centrosymmetrically. Furthermore, the crystallinity and crystal properties of the rod-like, highly extended π-conjugation systems are usually poor which is detrimental for practical applications.

We here present a supramolecular synthetic approach to acentrically align and optimize highly hyperpolarizable merocyanine dyes in the crystalline state for various second-order nonlinear optical effects as well as to improve the crystal properties such as crystallinity and crystal quality by co-crystallization with phenolic derivatives.

Unlike the covalently bonded molecular systems, the physical properties of supramolecular assemblies can be easily changed or enhanced by means of modifying the complementary guest molecule. As a result, it provides more design feasibility relative to the traditional synthetic approach as, for example, two molecular components can be tailor-made or modified to adapt one another in order to optimize the desirable supramolecular properties. Furthermore, it is worth mentioning that the physical properties of the assembly and the host molecule in the presence of the guest molecule are often changed or enhanced (e.g. elevation of the melting point and increase of the solubility of the host molecule) which offers advantages for materials development and processing.

Hydrogen bonding, one of the most important non-covalent interactions in nature, has been widely used as an engineering tool in construction of molecular aggregates, host-guest complexes and predefined packing motifs in crystals.[2] Such a relatively strong, directional and selective non-covalent intermolecular affinity will often provide an overwhelming driving force for the formation of molecular aggregates or assemblies in solution which is important for building up supramolecular structures in the crystalline solid.

The merocyanine dye **1** (Fig.1) exhibits an extremely pronounced solvent dependence of the charge transfer absorption band due to a different contribution of the two resonance structures, quinonoid form and zwitterionic form in response to the solvent polarity. It also possesses one of the largest first-order molecular hyperpolarizabilities, $\beta = 4180 \times 10^{-40}$ m^4/V in DMSO ($\lambda = 1.89$ μm), among the stilbenoid structures[3]; therefore, it will be of great interest to develop it into potentially useful crystalline materials. One of our early investigations has shown that the highly electronegative oxygen atom of **1** often forms a rather short hydrogen bond with the phenolic derivative (O-H···O = 2.46 Å) but not with aniline derivatives because of the contribution of the zwitterionic resonance form.[4] The prerequisite for the formation of hydrogen-bonded network

structures is that each molecular component needs to contain more than one functional group that is capable of forming hydrogen bonds; therefore, a hydrogen bond donor, a hydroxyl functionality, was designed and introduced into the merocyanine skeleton as in **2**. Various forms of phenolic derivatives were co-crystallized with equimolar of **2** in methanol by a slow evaporation technique. A qualitative screening of potential co-crystals for further investigation was first performed with the Kurtz and Perry powder test at 1.3 μm. Interestingly, the co-crystals formed from the class I phenolic derivatives in which the electron acceptor is *para*-related to the phenolic functionality together with a substituent either in the *ortho*- or *meta*-position show extremely high tendency of forming acentric co-crystals (50%). Furthermore, there are a few of these acentric co-crystals exhibiting second harmonic generation signals that are two or three orders of magnitudes larger than that of urea standard.

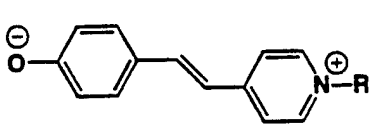

1 : R = CH_3

2 : R = CH_2CH_2OH

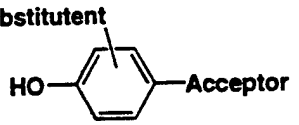

Class I Phenolic Derivatives

Fig.1 Molecular structures of the materials investigated in this work.

In view of several single crystal x-ray structures of these acentric co-crystals, their packing motifs can be distinctively divided into two categories. The group I co-crystals are characterized with anionic and cationic assemblies or aggregates as building blocks. On the contrary, the group II co-crystals are built up of linear, molecular aggregates which give rise to the common key feature of all the highly non-centrosymmetric co-crystals found in this series--a two-dimensional acentric layer structure. In addition, we have found in this newly developed system that the orientation of the merocyanine dye can be changed and tuned within the crystal lattice by a "careful" selection of a guest molecule--phenolic derivative, provided that the linear molecular aggregate and the acentric layer packing motifs are maintained. The best of all, we discovered two novel co-crystals which possess a perfect parallel chromophoric alignment and greatly enhanced crystal properties such as higher crystallinity and better crystal quality for electro-optic applications. Furthermore, we found a highly acentric co-crystal in which the charge-transfer axis of the chromophores makes an angle of about 70° with the polar direction of the crystal which is an attractive candidate for applications in second harmonic generation and optical parametric oscillation.

In conclusion, we have developed a novel approach to align and fully optimize the orientation of a highly extended conjugated chromphore, the merocyanine dye within the crystalline lattice for efficient second-order nonlinear effects. In addition, the newly developed co-crystals shows greatly improved crystal properties compared to its components which presents a large potential for practical applications.

References:

[1] For recent reviews: Ch. Bosshard, K. Sutter, P. Prêtre, J. Hulliger, M. Flörsheimer, P. Kaatz, P. Günter, *Organic Nonlinear Optical Materials*, Gordon and Breach Science Publishers, Amsterdam, **1995**; *Optical Nonlinearities in Chemistry* (Ed.: D. M. Burland) (*Chem. Rev.* **1994**, *94*, No. 1) and the references therein.

[2] For recent reviews: J. M. Lehn, *Supramolecular Chemistry*, VCH, Weinhein 1995; G. R. Desiraju, *Angew. Chem. Int. Ed. Engl.* **1995**, *34*, 2311; J. C. MacDonald, G. M. Whitesides, *Chem. Rev.* **1994**, *94*, 2383 and the references therein.

[3] A. Dulic, C. Flytzanis, *Optics Commun.* **1978**, *25*, 402-406.

[4] F. Pan, M. S. Wong, Ch. Bosshard, P. Günter, *Chem. Comm.* in press.

Photoinduced Anisotropy in Hybrid Organic Sol-Gel Silica Glass Waveguides

Mark P. Andrews and Tanya Kanigan

Department of Chemistry, McGill University, Montreal, Quebec, H3A 2K6, Canada

This poster describes the first observation of Photo-Induced Anisotropy (PIA) that does not involve bond isomerization in a partially organic material derived from an organically modified silicate (ORMOSIL) film. PIA has been defined as the reversible, anisotropic component of a material response which effectively allows birefringent axes to be written at will in a glassy material. In general, glass photosensitivity is a term that describes a wide variety of light-induced modifications of glasses. In photonics, the term is used to describe a process by which a visible or UV laser beam induces a permanent refractive index change. It was first identified in Ge-doped silica in 1978 by Hill[1] who recorded the process through the phase gratings it produced in optical fibers. Later, Lam and Garside[2] showed that the magnitude of the induced refractive index change varied as the square of the laser intensity (for argon 488.0 and 514.5 nm lines); Parent *et al.*[3] showed that the resulting refractive index change was birefringent; and Meltz *et al.*[4] demonstrated that gratings could also be written in fibers with UV radiation externally. These initial experiments involved germanosilicates. The effect has also been reported in several other doped silicates and in fused silica, and has been connected with the phenomenon of self-organized second-harmonic generation in glasses. The refractive index changes observed are very small, typically lying between 10^{-4} and 10^{-6}. These observations have stimulated the development of a model of glass photosensitivity as a two-photon process (when initiated with visible light) involving defects in the silicate glass structure (color centers) with UV absorption bands around 240 nm. Photobleaching of these color centers has been observed to cause a change in the refractive index across the UV and visible regions.

PIA is thus one aspect of the total photosensitive response of glass. In this poster we describe how we use guided waves to induce and examine material changes in ORMOSIL films.

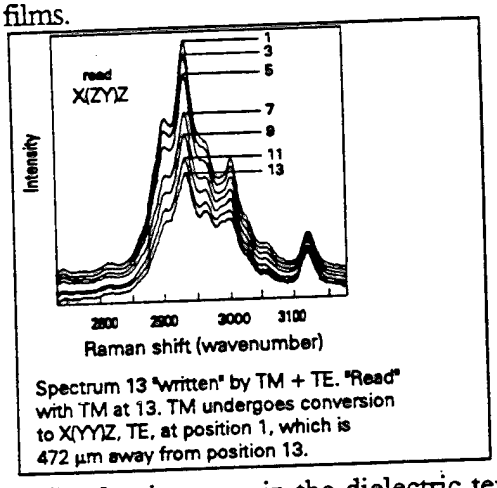

Spectrum 13 "written" by TM + TE. "Read" with TM at 13. TM undergoes conversion to X(YY)Z, TE, at position 1, which is 472 μm away from position 13.

We use PIA to "write" anisotropic photo-transformations in glass films by launching single mode TE_m or TM_m (or TE+TM) guided waves having well defined polarization and electric field profiles. These transformations are distributed in the film according to the mode (node) structure, spatial distribution and state of polarization. This is essentially an "optical poling" experiment in which a polarized light field selects and defines a new set of molecular axes inside the thin film. Collectively, these interact with light in a well defined manner. More succinctly, we use light to induce a well-defined anisotropy in the dielectric tensor of the material. To study this, integrated optics Raman spectroscopy is useful. To illustrate, consider simultaneous excitation of TE + TM

modes in a film. These will generate a net electric field in the XY-plane at some angle to the Y-axis. A refractive index change is induced along the polarization direction, generating off-diagonal dielectric tensor elements. If TM polarized light is launched (Porto's notation, X(ZY)Z), one observes that the photo-poled medium now insinuates TE polarization character (X(YY)Z) into the propagating wave. This can be detected by Raman imaging onto the CCD detector from different spatial regions of the 1D waveguide streak. Observe in the figure above that TM polarized light located 44 μm from the prism edge (position 13) undergoes conversion to TE polarization further along the streak (smaller position numbers). In this experiment the laser beam that "writes" in the anisotropy, also "reads" it out as spectroscopic information.

In thermally cured films, we observe that the laser beam induces a birefringence whose principal axes can be selected with the laser polarization. This birefringence can be reversed by exposing the film to a different laser polarization. By simultaneously exciting TE and TM guided modes, off diagonal elements are introduced into the dielectric tensor, which in turn cause TE↔TM mode conversion, observable in polarized waveguide raman spectra. In uncured films, exposure to TE polarized fields appears to cause irreversible photoalignment of the organic component in addition to photoinduced birefringence. We speculate that this photoalignment occurs preferentially within the plane of the film and involves crosslinking of the unsaturated groups.

1. K. O. Hill, Y. Fuji, D. C. Johnson, and B. S. Kawasaki, *Appl. Phys. Lett.*, **32**, 67 (1978).
2. K. W. Lam, and B. K. Garside, *Appl. Opt.*, **20**, 440 (1981).
3. M. Parent, J. Bures, S. Lacroix, and J. Lapierre, *Appl. Opt.*, **24**, 354 (1985).
4. G. Meltz, W. W. Morey, and W. H. Glenn, *Opt. Lett.*, **14**, 823 (1989).

Optical Limiting Properties of Organic Nonlinear Crystals

P.L. Baldeck, P. Feneyrou, O. Doclot, and D. Block

Laboratoire de Spectrométrie Physique, associé au CNRS
Université Joseph Fourier, BP 87, 38402 Saint martin d'Hères, Cedex, France
e-mail: baldeck@spectro.grenet.fr

Stephane Delysse and Jean-Michel Nunzi
LETI (CEA-Technologies Avancées). DEIN-SPE, Groupe Composants Organiques
Centre d'Etudes de Saclay, F-91191 Gif sur Yvette, France

Optical limiting is a new field of applications for nonlinear organic materials. In particular, the strong two-photon absorption of organic cristals could be used for the design of laser protection devices in the visible spectral range. In this paper, we review our measurements of nonlinear absorption, and discuss the optical limiting potential of organic crystals.

For molecules, in the three-level approximation (with $\mu_{02} << \mu_{01}$), the microscopic two-photon absorption is given by:

$$\mathrm{Im}\{\gamma(-\omega;\omega,\omega,-\omega)\} = \mathrm{Im}\{K\,(-\mu_{01}{}^{4}D_{11} + \mu_{01}{}^{2}\,\Delta\mu_{01}{}^{2}D_{111} + \mu_{01}{}^{2}\mu_{12}{}^{2}D_{121})\} \qquad \text{Eq. (1)}$$

The second and third terms are the two-photon resonant terms. The nonlinear absorption can be optimized by the choice of molecules having the best dipole parameters. Others criteria include the transparency range, a high solubility, and a good photo-stability. For molecules in solution (0.1 mole/liter), good values of the nonlinear absorption coefficient span from 0.1 to 1 cm/GW at the resonance with a spectral range of more than 10000 cm^{-1}. In the first part of this paper, we present measurements of the two-photon absorption spectra of 4-aminobenzonitrile (ABN) and 4-diethylamino-β-nitrostyrene (DEANST) molecules. These spectra compare well with theoretical spectra when the contributions of electronic dipole moments between vibronic states are taken into account.

The macroscopic two-photon absorption can be increased by using packing effects. For example, in crystals one can gain a factor of 50 in concentration, a factor 5 by the augmentation of local field effects, and an alignment factor of 5 if the molecules are parallel. Thus, the nonlinear absorption coefficients of crystals can be two or three orders of magnitude larger than in solutions of the same molecules. In the second part of this paper, we present our measurements of nonlinear absorption in organic crystals (DEANST, DMACB[1], 2A5NPDP[2]...). A best non resonant value of 130 cm/GW has been obtained. Theoretical calculations indicate the possibility of further improvements. They are under investigation.

[1] In collaboration with J. Zyss at CNET.
[2] In collaboration with A. Ibanez and R. Masse at CNRS Grenoble.

The potential of organic crystals based on donor-acceptor π-conjugated molecules for a large third-order nonlinear optical response

Ch. Bosshard, U. Gubler, I. Liakatas, F. Pan, M. S. Wong, and P. Günter

Nonlinear Optics Laboratory, Institute of Quantum Electronics
ETH Hönggerberg, CH-8093 Zurich, Switzerland
Phone: 41-1-633 23 29 Fax: 41-1-633 10 56
E-mail: bosshard@iqe.phys.ethz.ch

There are still only few guidelines on which type of molecules are suitable for third-order nonlinear optics. A complete understanding on how to optimize the third-order nonlinear optical properties and additional properties dealing with applications are still lacking. Up to now, most efforts concentrate on centrosymmetric structures such as π-conjugated polymers or on effects based on the cascading of second-order nonlinearities [1].

We have recently shown that the pure third-order nonlinear optical response of donor-acceptor π-conjugated molecules can also be very large [2]. Such molecules can be of great interest if they can be incorporated into a crystal lattice because of (i) the high molecular density and (ii) a highly ordered structure. As an example, already a factor of five increase in the third-order nonlinearity can be gained from point (ii).

In this contribution we present results on third-order nonlinear optical measurements of a series of functionalized donor-acceptor π-conjugated molecules that form molecular crystals with a favourable parallel arrangement of the chromophores for large third-order nonlinear optical susceptibilities $\chi^{(3)}$.

The materials we will present in this work include the organic salt 4-N,N-dimethylamino-4'-N'-methyl-stilbazolium tosylate (DAST), as well as newly developed molecular crystals - the hydrazone derivative nitrofurylacrolein methoxyphenylhydrazone (NFAMOPH) and several co-crystals based on the merocyanine dye and class I phenolic derivatives (Table.1). All these materials form crystals with an almost completely parallel arrangement of the chromophores.

The second-order hyperpolarizabilities γ of our materials were first studied using third-harmonic generation (fundamental wavelengths of λ=1.907μm and 2.1μm). From the measured values of γ, we then estimated the macroscopic nonlinearity $\chi^{(3)}(-3\omega, \omega, \omega, \omega)$ using the oriented gas model.

As a first example, we measured a value of $\gamma=12.3 \times 10^{-48}$ m^5/V^2 for DAST in methanol at λ=1.907μm. Using the crystallographic data and the refractive indices of DAST we estimate a value of $\chi^{(3)}_{1111}(-3\omega,\omega,\omega,\omega)$ close to $4000 \times \chi^{(3)}_{\text{fused silica}}(-3\omega,\omega,\omega,\omega)$. This is potentially one of the largest nonresonant values of $\chi^{(3)}$. Our newly grown high quality DAST crystals [3] now allow actual measurements of $\chi^{(3)}$ as well as the nonlinear refractive index n_2 in the bulk (using the z-scan technique). Results of these measurements will also be reported. Based on these results we will discuss the different contributions to the Kerr-effect. These are (i) the direct $\chi^{(3)}$, (ii) cascaded second-harmonic generation and difference-frequency mixing, and (iii) cascaded optical rectification and the linear electro-optic effect [4].

Table.1 Molecular structures of some of the materials investigated in this work.

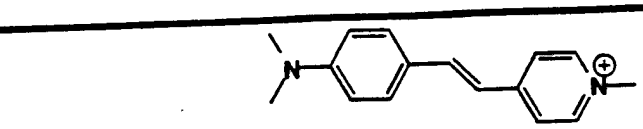

DAST

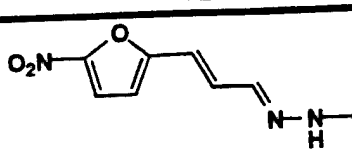

NFAMOPH

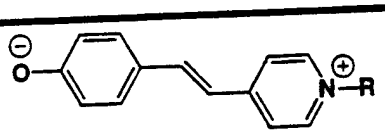

Substitutent

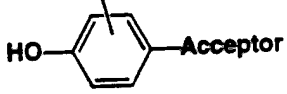

co-crystals

1 : R = CH_3

2 : R = CH_2CH_2OH

Class I Phenolic Derivatives

As a second example we also find a large value of γ for NFAMOPH (γ=8.5 x 10^{-48} m^5/V^2 in 1,4-dioxane). Since NFAMOPH crystallizes in a centrosymmetric point group (with all molecules completely parallel to each other) only γ can contribute to the macroscopic third-order nonlinearity. The oriented gas model yields a large non-resonant value of $\chi^{(3)}_{1111}(-3\omega,\omega,\omega,\omega)$ close to 4500 x $\chi^{(3)}_{\text{fused silica}}(-3\omega,\omega,\omega,\omega)$. Results of bulk measurements are also in progress.

Our investigation shows that highly optimized acentric structures of donor-acceptor π-conjugated molecules yield a large third-order nonlinear optical response not only through the effect of cascading but also due to the pure third-order nonlinearity as will be presented in this work.

In conclusion, our results point out the large potential of molecular crystals for third-order nonlinear optics, a potential that has so far not been fully exploited.

References

1. G. I. Stegeman, M. Sheik-Bahae, E. Van Stryland, and G. Assanto, Opt. Lett. **18**, 13 (1993).
2. C. Bosshard, R. Spreiter, P. Günter, R. R. Tykwinsky, M. Schreiber, and F. Diederich, Adv. Mater. **8**, 231 (1996).
3. F. Pan, M. S. Wong, Ch. Bosshard, and P. Günter, Adv. Mater., in print (1996).
4. C. Bosshard, R. Spreiter, M. Zgonik, and P. Günter, Phys. Rev. Lett. **74**, 2816 (1995).

NON LINEAR OPTICAL PROPERTIES OF LOW BAND GAP MOLECULES : THE ROLE OF ELECTRON- PHONON COUPLING:

C. CASTIGLIONI; M. DEL ZOPPO, P. ZULIANI, G. ZERBI

Dip. di Chimica Industriale e Ingegneria Chimica; Politecnico di Milano; P. L. Da Vinci, 32; 20133 MILANO (Italy)

It is well known that the physics of polyconjugated organic materials is heavily affected by the existence of a mutual relationship between π electron excitations and geometrical distorsion. A typical example is the behaviour of conducting polymers where the electronic defect introduced by doping is strongly coupled with a lattice distorsion; in this case the charge carrier can be described as a structural defect. This is why vibrational spectroscopy is a suitable method to characterize the physics of these systems.

More recently the "vibrational approach" has been extended to the study of the N.L.O. response of organic molecules [1]. It has been shown that, due to the strong electron-phonon coupling, it is possible to obtain directly from the vibrational spectra an estimate of the values of the molecular hyperpolarizabilities β and γ [2].

In this work we present several experimental and theoretical data obtained in our laboratory, which support the above statement. Moreover from the analysis of the experimental (or calculated) spectra it is possible to obtain an insight into the role of the structural parameter in determining the N.L.O. properties[3-5].

Simple thoretical models [6], which give an analytic support to the vibrational approach here discussed, will be also illustrated.

[1]C. Castiglioni, M. Gussoni, M. Del Zoppo, G. Zerbi, Solid State Commun. 82, 13 (1992)
[2] C. Castiglioni, M. Del Zoppo, P. Zuliani, G. Zerbi, Synth. Metals, 74, 171 (1995)
[3] P. Zuliani, M. Del Zoppo, C. Castiglioni, G. Zerbi, S. R. Marder, W.J. Perry, J. Chem. Phys. 103, 9935 (1995)
[4] P. Zuliani, M. Del Zoppo, C. Castiglioni, G. Zerbi, C. Andraud, A. Collet , J. Phys. Chem. 99, 16242 (1995)
[5] M. Del Zoppo, C. Castiglioni, P. Zuliani, A. Razelli, G. Zerbi, M. Blanchard-Desce, J. Chem. Phys., submitted
[6] C. Castiglioni, M. Del Zoppo, G. Zerbi, Phys. Rev. B, in press

Nonlinear Optical Properties of Chromophores in New Crosslinkable Polymer Matrices

Young-Sun Cho, Gyoujin Cho* and Jae-Suk Lee

Dept. of Mater. Sci. and Eng., Kwangju Ins. of Sci. and Tech.(K-JIST), Kwangju, Korea, *Dept. of Chem. eng., Suncheon Nat. Univ., Suncheon, Chonnam, Korea.

Disperse red1 or carbazole containing alkoxysilyl groups was incorporated into new polymer matrices to increase the thermal stability an decrease the relaxation rate of chromophores after poling. Poly[(4-vinylphenyl)dimethyl-2-propoxysilane] and poly [3-(trimethoxysilyl)propyl methacrylate]-co-poly(methyl methacrylate) were prepared and characterized using FT-IR, GPC, DSC, NMR. Crosslinking reaction between the polymer side groups and alkoxysilyl groups of chromophores were traced by FT-IR. The strong absorption of the polymer film at 1170cm^{-1} was completely disappeared due to the Si-O-C stretching, and alternatively a new broad band appeared around 1050cm^{-1} which can be described to the stretching of Si-O-Si bond among alkoxysilyl groups after acid treatment. After crosslinking reaction, maximum peak was red shifted. Before and after polings, both UV absorbance change and relaxation behaviors were checked in chromophore incorporated polymer films. In polymer matrices, the relaxation of the chromophores was not occurred due to the crosslinking reaction between polymer matrices and chromophores. Also, second harmonic generation was measured for the each chromophores/matrices films.

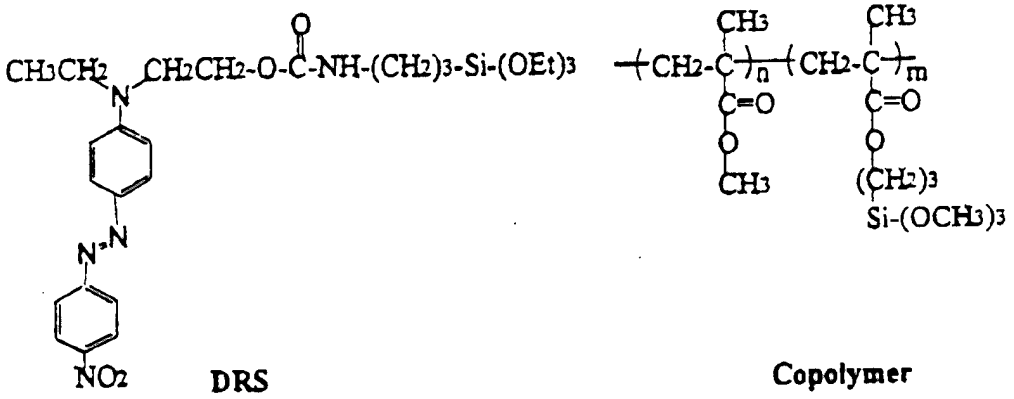

Scheme 1. Chemical structures of NLO chromophore (DRS) and copolymer containing alkoxysilyl groups.

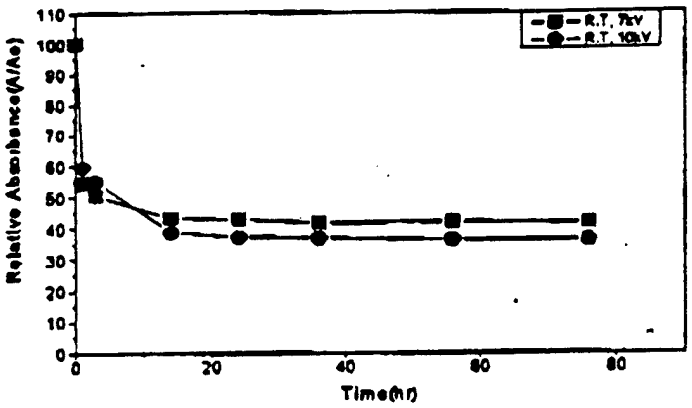

Figure 1. UV absorbance changes for before and after poling of DRS incorporated copolymer films at room temperatures.

Chielectric Relaxation Incorporating Third-order and Electrostriction Effects

J.A. Cline and W.N. Herman
U.S. Navy, NAWCAD, MS07, Warminster, PA 18974
phone: 215-441-2472

The orientational stability of nonlinear optical chromophores in polymer systems has been the subject of extensive research. Here we use a previously developed method[1], which we refer to as chielectric relaxation, to observe chromophore dynamics in a polymer matrix. The method is similar to dielectric relaxation, where $\chi^{(1)}$ is probed by inducing linear polarization in the material using a small sinusoidal electric field, but differs in that here the $\chi^{(2)}$ properties of the material are probed through second harmonic generation (SHG). The chromophore dynamics are observed by inducing molecular orientation in an unordered polymer using a large AC electric field, while in real time observing the induced $\chi^{(2)}$ by monitoring the SHG. Other related techniques that also probe chromophore dynamics have been developed by Ghebremichael et. al.[2,3] and Sugihara et. al.[4] For the data presented here, a thin film of a guest-host polymer system, DR1/PMMA, is sandwiched between two Indium Tin Oxide coated glass slides. The temperature of the sample is controlled by a custom oven, and an AC electric field (300 Volts peak to peak) is applied to the polymer sample. In real time, the second harmonic, fundamental, and electric field signals are collected by analog to digital conversions synchronized with the trigger from the Q-switched YAG laser.

The response of the SHG can be related to the applied electric field, by separating the SHG response into components that are in phase and out of phase with the applied electric field. To first order, the effective $\chi^{(2)}$ is linearly related to the applied electric field[5], thus the SH intensity will be proportional to the square of the applied electric field. If the electric field is represented by $E = E_0 \sin(\Omega t)$, and the SH is then fit to $A^2\sin^2(\Omega t+\phi)$, the resulting curves are shown in Figure 1. We note that this fitting procedure gives an out of phase component that is negative for the low frequency, high temperature points. This implies a nonphysical result that the orientation of the chromophores leads the application of the electric field.

The second harmonic signal resulting from orientational changes of the chromophores was isolated by accounting for other non-orientational effects on the SH signal, specifically the third-order contribution and the electrostriction effect. The third-order contribution to the SH signal originates from the second-hyperpolarizability element γ_{3333} multiplied by the applied electric field. To first order, this effect is instantaneous and in phase with the applied electric field. The electrostriction effect on the SH signal is brought about by a compression of the polymer sandwich due to the attraction of the oppositely charged electrodes, and is most noticeable at high temperature and low frequency. The compressive force decreases the thickness of the polymer film, which reduces the interaction length with the fundamental beam, thus reducing the SH signal. The SH data was fit to a relation of the form $ES(E)*[A_{mo}\sin(\Omega t+\varphi)+A_3\sin\Omega t]^2$, where ES(E) is the electrostriction correction term, $A_{mo}\sin(\Omega t+\varphi)$ is the term due to molecular orientation, and $A_3\sin\Omega t$ is the term due to the instantaneous third-order contribution. The fit results of the orientational component, represented by the term $A\sin(\Omega t+\varphi)$, are shown in figure 2. The nonphysical negative phase shift is no longer present.

In addition to the above results, normalized loss peaks for the chielectric relaxation will be compared to the dielectric case, and the frequency domain behavior will be related to the time domain.

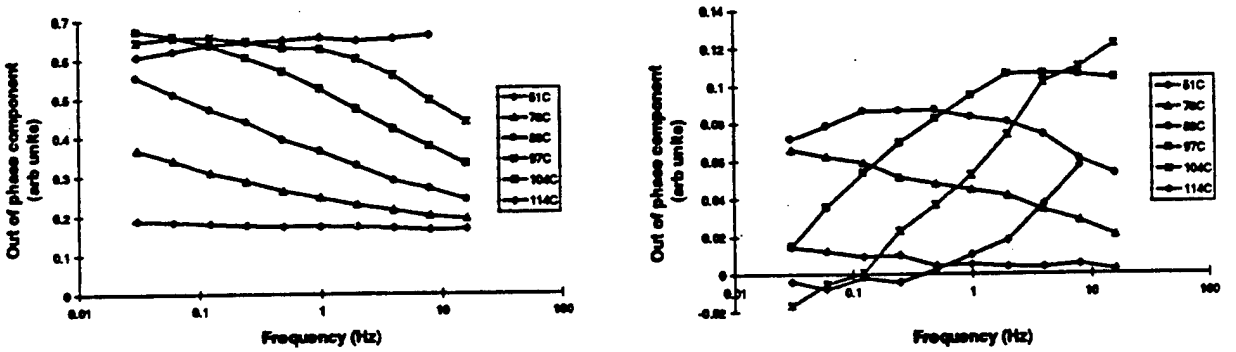

Figure 1. The in phase and out of phase components of the SHG response using the fitting expression $A^2\sin^2(\Omega t+\varphi)$.

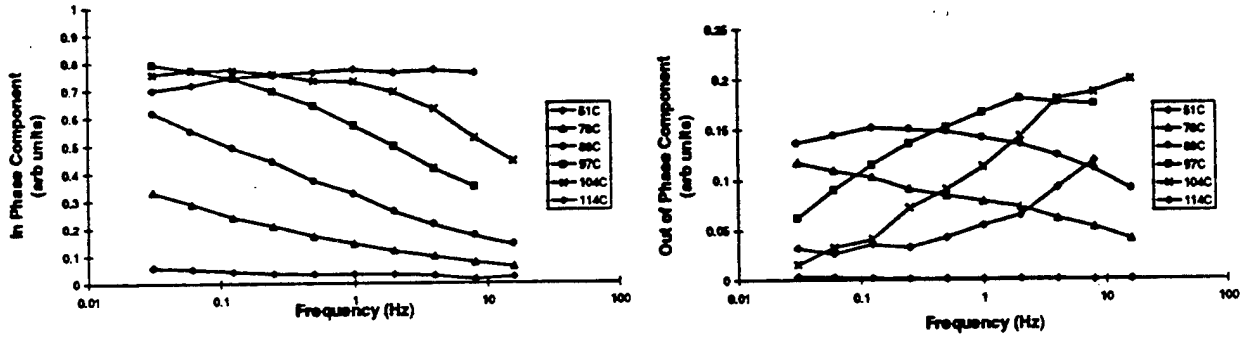

Figure 2. The in phase and out of phase components of the orientational SHG response using a fitting expression that takes into account third-order effects and electrostriction effects.

---

[1] J.A. Cline and W.N. Herman, OSA Technical Digest Series, **21**, 206 (1995).
[2] F. Ghebremichael and M.G. Kuzyk, J. Appl. Phys., **77**(7), 2895 (1995).
[3] F. Ghebremichael and H.S. Lackritz, OSA Technical Digest Series, **21**, 458 (1995).
[4] T. Sugihara, H. Haga, and S. Yamamoto, Appl. Phys. Lett., **66**, 144 (1996).
[5] D.J. Williams, in *Nonlinear Optical Properties of Organic Molecules and Crystals*, D.S. Chemla and J. Zyss, eds. (Academic, New York, 1987), Vol. 1 Chap II-7.

ICONO '3

ABSTRACT FOR CONSIDERATION

QUINOID-TO-BENZENOID EVOLUTION IN SOLVATED NLO CHROMOPHORES

G.H. Cross, M. Szablewski, P.R. Thomas and D. Bloor
University of Durham, Department of Physics, Durham, UK, DH1 3LE

An assembly of evidence describes the evolution in the bond alternation in the conjugated structure of a series of highly dipolar nonlinear optical chromophores. In addition to the evidence from solvatochromism and analysis of the extinction coefficient, measurements from ^1H nmr of the aromatic/quinoid ring system show chemical shifts consistent with evolution to aromatic character as the dielectric constant of the solvent is increased. Measurements of the dipole moment, μ, of these molecules shows the expected increase with solvent dielectric constant although inaccuracies accumulate when attempting to measure μ in high polarity solvents. The dipole moments are high however, even in media with relatively low dielectric constant. For instance in the solid film, doped-PMMA, the dipole moment is found to be around 32 D and this correlates well with measurements made in liquid solution. Considerations of local field models will be discussed, particularly with regard to the apparent need to consider the polarisability ellipsoid representing these highly dipolar molecules. Spherical reaction field models, for example, are inappropriate and in poled films it appears that the *cavity* field (local field) also requires an ellipsoidal description.

Continuum Pump-Probe Experiments in Organic Solutions

A. Dogariu, P. Buck, D.J. Hagan, E.W. Van Stryland

CREOL, University of Central Florida
4000 Central Florida Blvd., P.O. Box 162700
Orlando, FL 32816-2700
(407) 823-6814

We characterize the nonlinear response of several organic solutions applicable for optical limiting using the excite-probe geometry with a femtosecond continuum probe. These experiments show the dynamics and spectral range of utility for these materials which have shown promise for applications in optical limiting devices. The organic dye solutions used exhibit reverse saturable absorption (RSA). RSA materials have larger excited-state absorption cross sections than ground-state cross sections.[1]

The materials studied here are zinc tetra (p-methoxyphenyl) tetrabenzporphyrin (ZnTMOTBP), lead tetrakis(β-cumylphenoxy)phthalocyanine ($PbPc(\beta\text{-}CP)_4$) and silicon naphthalocyanine (SiNc), all RSA materials in the visible. The femtosecond continuum source is based on an argon ion pumped, Kerr lens modelocked, Ti:sapphire oscillator followed by a Cr:LiSAF regenerative amplifier producing milijoule level, 200 fs pulses around 850 nm. A single pulse is used to generate a second harmonic (SH) pump at 425 nm and a femtosecond continuum probe which are then used in a standard pump-probe geometry. The SH is produced in a BBO crystal and the continuum is produced by focusing the 850 nm light into a water cell. Figure 1 shows the normalized transmittance spectrum (the spectrum obtained after excitation divided by the spectrum obtained in the absence of the excitation, i.e., the linear spectrum) of these materials at 10 ns after the excitation with the 425 nm pump.

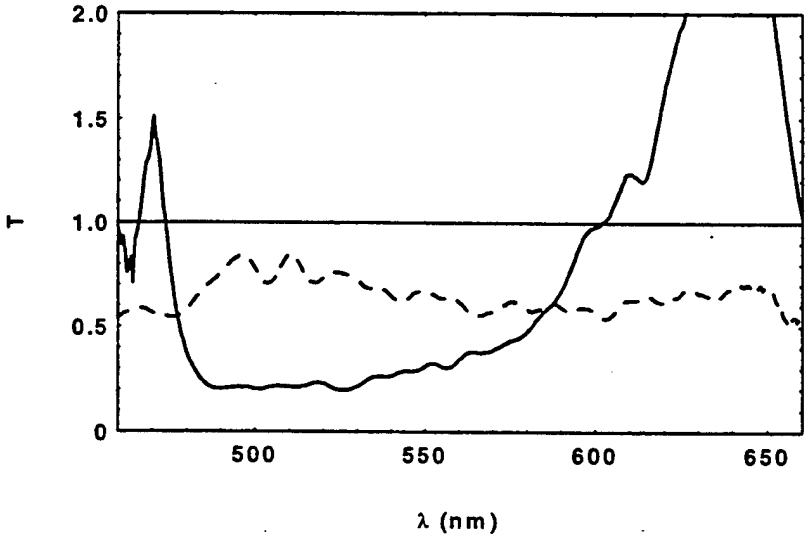

Figure 1. Normalized nonlinear transmittance spectrum for ZnTMOTBP (solid line) and SiNc (dashed line), both 10 ns after excitation.

These experiments show the wavelength and pulsewidth ranges over which effective optical limiting can be obtained for a given material (note the saturation above 600 nm in ZnTMOTBP). As an example, Figure 2 shows the transient absorption spectrum of SiNc time in the visible spectral region.

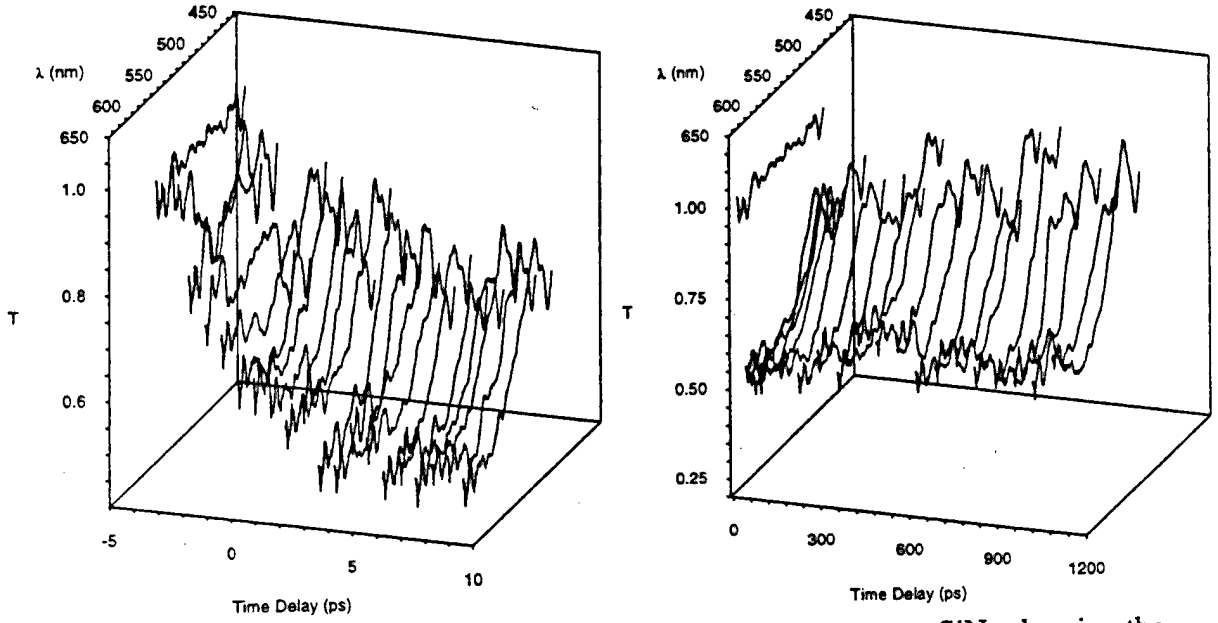

Figure 2. Short (left) and long (right) delay pump-probe experiments on SiNc showing the nonlinear absorption spectrum as a function of time delay.

Using the femtosecond continuum probe, the spectral dependence of the RSA response as a function of time after excitation is revealed. The nonlinear response of these organics is modeled using a five level system that includes both singlet and triplet excited state absorption processes.[2]

References

[1] T. H. Wei, D. J. Hagan, M. J. Sence, E. W. Van Stryland, J. W. Perry, and D. R. Coulter, Applied Physics B54, 46 (1992).
[2] D. J. Hagan, T. Xia, A. A. Said, T. H. Wei, and E. W. Van Stryland, International Journal of Nonlinear Optical Physics, 2, 483 (1993).

Spectral z-scans of substituted phthalocyanides

Per-Otto Arntzen, *Anders Eriksson, Mikael Lindgren
Department of Sensor Technology, Laser Systems Division
National Defense Research Establishment
P. O. Box 1165; S- 581 11 Linköping, Sweden
fax: + 46 13 318287, email: miklin@lin.foa.se
**Department of Physics and Measurement Technology*
Linköping University
S-581 83 Linköping, Sweden

Abstract

The z-scan[1] method was used to perform measurements of the nonlinear absorption coefficient β and the nonlinear refractive index n_2 of various substituted phthalocyanides. Using a tuneable OPO laser, β and n_2 were obtained in a wide wavelength range in the visible and in the near IR.

Because the beam of the laser deployed can deviate considerably from a pure Gaussian TEM_{00}, the analysis method of z-scan was extended to include arbitrary beams entering the sample.

Z-scans at various wavelengths

We perform the z-scan in which the power at the detector plane is measured for a series of different positions of the sample along the beam. The beam is focused so that a larger intensity is enhanced at the waist of the beam. This means that the closer the sample is to the waist of the beam the larger will the nonlinear effects be. The z-scan is recorded at various wavelengths using an OPO laser. Examples of data are shown in Figure 1.

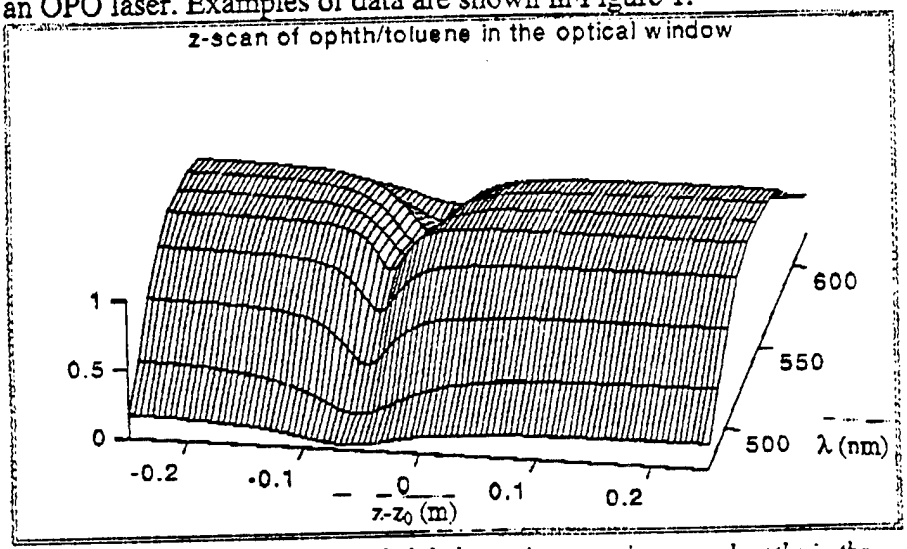

Figure 1. *z-Scans of a substituted phthalocyanine at various wavelengths in the optical window.*

[1] M.Sheik-Bahae, A.A.Said, and E.W.Van Stryland, *Opt. Lett.* **14**, 955 (1989)

Laser beam characterization and reconstruction

In order to analyze the z-scan data it is necessary to know accurately the laser beam parameters and beam quality factor. These were obtained by recording images of the transversal intensity distribution at selected positions along the focussed laser beam,[2] and an appropriate analysis.[3] We show that the intensity distribution of the beam under certain conditions can be reconstructed by a superposition of higher order Gaussian-Hermite (Figure 2) or Gaussian-Laguerre modes. The weigth parameters for the individual contribution of modes is given by a constrained least square fitting of the intensity distribution with a series of Gaussian-Hermite or Gaussian-Laguerre modes (Fig. 2.); the constraints given by the M^2 values.

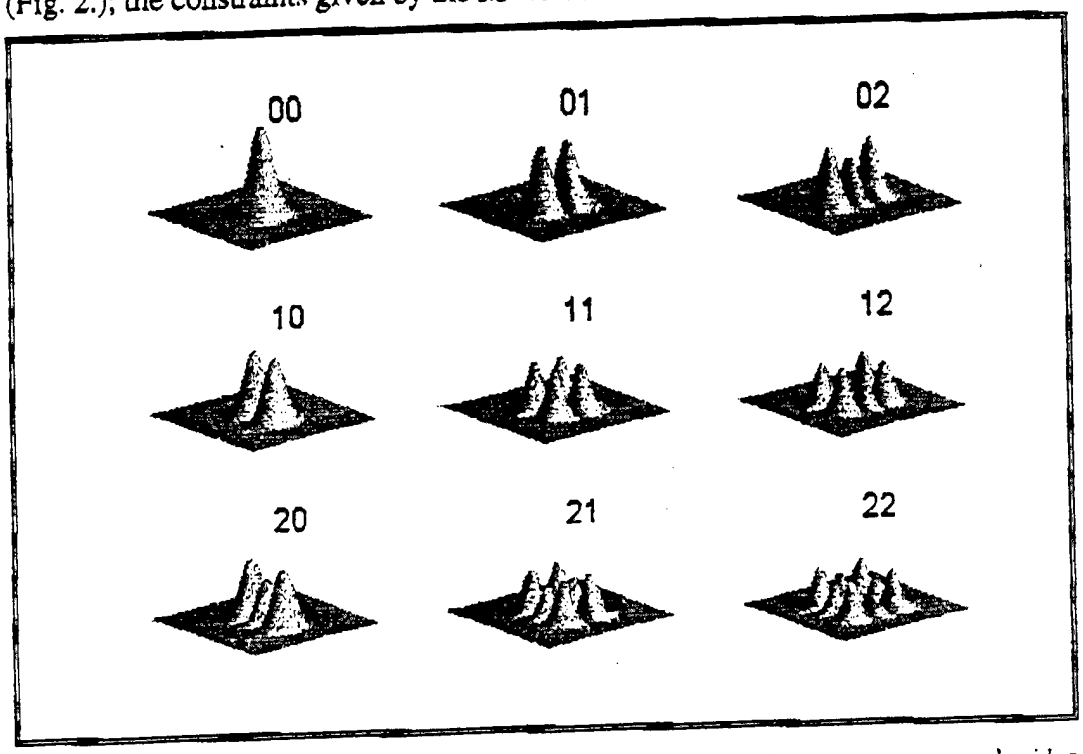

Figure 2. *Intensity distribution of various Gaussian-Hermite modes. Beam parameters and grid: z=0.6 m, Rayleigh length: z_R=0.04 m, wave length: λ=1064 nm, and a grid in x and y coordinates over which the calculation should be performed: -0.006≤ x≤ 0.006 m (40 points), -0.006≤ y≤ 0.006 m (50 points).*

From this mode expansion the intensity distribution at the detector plane, influenced by the nonlinear response of the sample in the z-scan set-up, was calculated.

Analysis of data

Using the methodology outlined above, an arbitrary laser beam can be used to obtain the nonlinear parameters n_2 and β. The experimental data of substituted phthalocyanides were analysed using different laser beam parameters and M^2 values. By repeating the procedure for several wavelengths it was possible to express $n_2(\omega)$ and $\beta(\omega)$.

---

[2] Lindgren et al., *Nonlinear Optics*, 1996, Vol 15, pp 85-88.
[3] See A.E.Siegman, *SPIE*, Vol.1224,Optical Resonators, 1990. D.Weaire et al., *Opt. Lett.* 4, 331 (1979).

Large resonant third-order optical nonlinearities of phthalocyaninatotin(IV) dichloride thin films

S. Ishihara, Y. Imanishi, and M. K. Engel*
Hitachi Research Laboratory, Hitachi, Ltd.
7-1-1 Omika, Hitachi, Ibaraki 319-12, Japan

Phthalocyanine (Pc) derivatives are promising candidates for third-order nonlinear optical applications. Recently, there has been a growing interest in the nonlinear optical properties of metallophthalocyanines with two axial ligands because they have unique crystal structure and sharp absorption peaks.[1-2] In this presentation, we report results on femtosecond degenerate four-wave mixing (DFWM) experiments of phthalocyaninatotin(IV) dichloride ($SnCl_2Pc$) thin films (Figure 1).

The $SnCl_2Pc$ thin films (thickness: 100 nm) were deposited onto a glass substrate in about 10^{-6} torr. Figure 2 shows arrangements of the molecules of the $SnCl_2Pc$ thin film and molecules in β polymorph of CoPcs along a column axis.[3-4] The distance between central metals ($d_{M\text{-}M}$) is 7.9 Å and an angle between the orientation of the molecules and the column axis (θ) is 19 ° in the $SnCl_2Pc$ thin film, while $d_{M\text{-}M}$ is 4.8 Å and θ is 45 ° in β-Pcs. The molecules of the $SnCl_2Pc$ thin film orient more strongly toward the column axis than those of β-Pcs. Figure 3 shows the absorption spectra of $SnCl_2Pc$ in the forms of thin film and solution in α-chloronaphthalene. A sharp and strong peak (Q) of the solution appeared at 700 nm due to π-π* transitions of Pcs, and the shoulders are attributed to the vibrational structures, which are similar to other Pcs solution. The absorption peaks (Q1, Q2) of thin film appeared at about 750 nm and 680 nm, respectively. The absorption spectrum shape of the thin film could be explained by means of a molecular dimers model[5] qualitatively. According to the model, monomer excited level splits into two dimer excited levels (E', E") as shown in the inset of Figure 3. In the arrangements of $SnCl_2Pc$ molecules (θ = 19 °), the transition moment from ground level (G) to E' is much larger than those of G to E", and the intensity of the peak Q1 is intense.

The DFWM experiments were performed in a phase-matched "folded boxcars" configuration with an amplified Ti:sappire laser (pulse width: 70 fs, wavelength: 790 nm). The averaged excitation power density was about 180 $\mu J/cm^2$. Figure 4 shows the evolution of DFWM signals of $SnCl_2Pc$ thin films. The excitation wavelength, 790 nm, lies in the tail of the longer wavelength side of the absorption peak (Q1). The DFWM signal decayed within 1 ps. The $\chi^{(3)}$ of the $SnCl_2Pc$ thin film was determined from the comparison of maximum DFWM signal intensity to that of reference CS_2, for which $\chi^{(3)}$ of 6.8×10^{-13} esu has been reported.[6] The estimated value of $\chi^{(3)}$ was 5.0×10^{-8} esu at 790 nm. The large $\chi^{(3)}$ of $SnCl_2Pc$ has a resonant contribution. We report on dependence of the $\chi^{(3)}$ and decay time on excitation wavelength and dicuss the mechanism of large nonlinearities.

* present address: Kawamura Institute of Chemical Research
631 Sakado, Sakura, Chiba 285, Japan

This work was performed by Hitachi Ltd. under the management of Japan High Polymer Center as a part of Industrial Science and Technology Frontier Program supported by New Energy and Industrial Technology Development Organization (NEDO).

REFERENCE

1. J. W. Wu, J. R. Heflin, R. A. Norwood, K. Y. Wong, O. Zamani-Khamiri, A. F. Garito, P. Kalyanaraman, and J. Sounik, J. Opt. Soc. Am. B6, 707 (1989).
2. B. K. Mandal, B. Bihari, A. K. Sinha, M. Kamath, and L. Chen, Appl. Phys. Lett. 66, 932 (1995).
3. Y. Imanishi, S. Ishihara, M. K. Engel, and S. Kobayashi (unpublished).
4. T. S. Srivastava, J. L. Przybylinski, and A. Nath, Inorg. Chem. 13, 1562 (1974).
5. M. Kasha, H. R. Rawls, and M. A. El-Bayoumi, Pure Appl. Chem. 11, 371 (1965).
6. N. P. Xuan, J. L. Ferrier, J. Gazengel, and G. Rivoire, Opt. Commun. 51, 433 (1984).

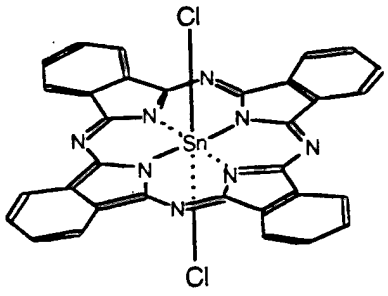

Fig. 1 Chemical structure of $SnCl_2Pc$

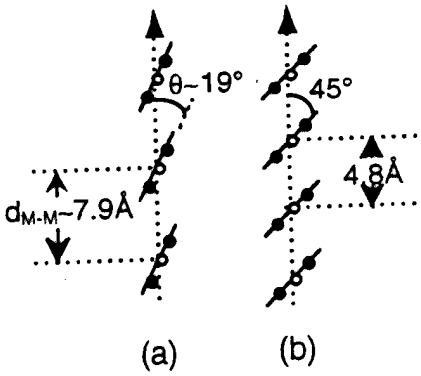

Fig. 2 Schematical representation of the arrangement of molecules in $SnCl_2Pc$ (a) and β-Pcs (b)[3]

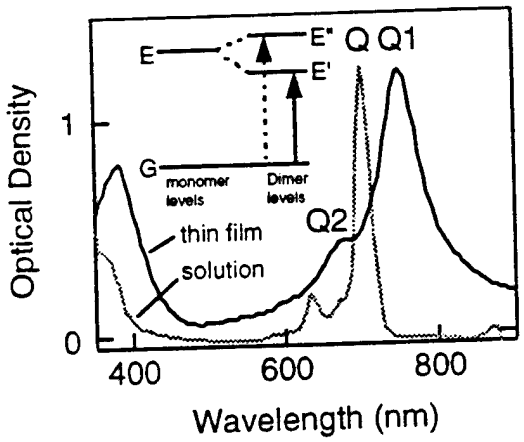

Fig. 3 Absorption spectra of $SnCl_2Pc$ Inset: Exciton band energy diagrams for molecular dimers[5]

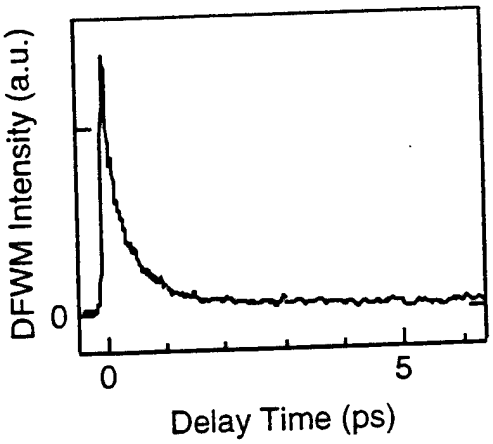

Fig. 4 DFWM signal of $SnCl_2Pc$ thin films

Novel Polyimide Langmuir-Blodgett Films Possessing SHG Chromophore as Pendant Group

Masa-aki Kakimoto and Jung Cheolsoo

Department of Organic and Polymeric Materials, Tokyo Institute of Technology, Meguro-ku, Tokyo 152, Japan

Thermally stable organic SHG materials has been focused because a serious problem of this class of materials is thermal relaxation of the SHG chromophores. Using thermally stable matrix polymers to blend the chromophores has been discussed, and some attempts were successful. Another method is introduction of the chromophores into thermally stable polymers with covalent bonds.

The SHG effect can be seen in organic materials which are the π-conjugating molecules having both electron donating and withdrawing groups at the terminal positions. These molecules can be aligned to order the dipole moment by applying electric potential (poling). There are two important roles to achieve the effective SHG as follows; 1) the SHG chromophores have enough free volume to rotate to align by poling treatment, 2) thermal relaxation of the ordering is enough slow to keep the SHG effect for a long time. Generally, poling is operated over the melting or glass transition temperatures. When the materials are cooled down, almost low molecular chromophores come to crystalline, and this makes the materials opaque. Amorphous polymers are promising materials for SHG matrix or backbone to make the transparent materials. Polyimides which is famous high Tg polymers are generally prepared via precursor polyamic acids whose Tgs are very low. In this paper, we introduce SHG chromophore into the monomer for the polyamic acids. According to the report by Rao (J. Chem, Soc., Chem. Commun., 1993, 1118), thiophen containing conjugating system with tricyanoethenyl as electron withdrawing group shows high SHG susceptibility. The new tetracarboxylic dianhydride 1 having this chromophore as the pendant group is synthesized, and then 1 was reacted with aromatic diamines 2 to make polyamic acids 3 as shown in Eq. (1).

We have studied Langmuir-Blodgett (LB) films of polyimides

possessing a variety of functional groups. The method to make polyimides LB films are called as "The precursor method", where the precursor LB films of polyamic acid alkyl amine salts are prepared, and then they are converted into the polyimide LB films by the chemical or thermal treatment. Polyamic acid 3 was mixed with long alkyl amine to produce LB films of precursor polyamic acid long alkyl amine 4. The LB film of 4 is treated with solution of acetic anhydride and pyridine to convert the polyimide LB film 5.

Characterization including SHG of the LB film of 5 will be reported.

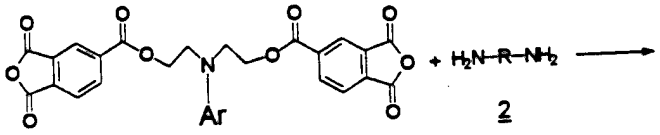

1 2

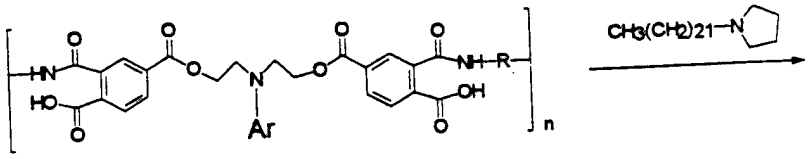

3

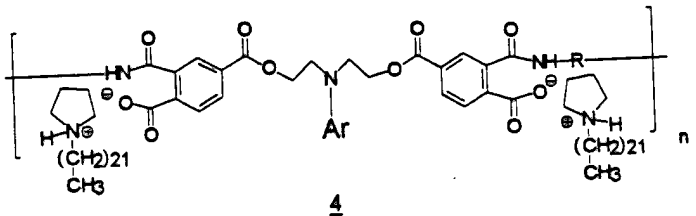

4

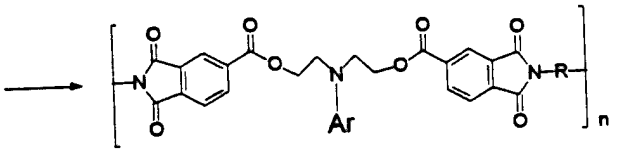

5 (1)

Ar:

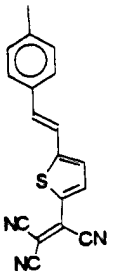

NONLINEAR OPTICAL AND PYROELECTRIC PROPERTIES OF POLAR LANGMUIR-BLODGETT FILMS

T. Srikhirin, D.Y. Minh Nguyen, S.H. Ou, J.B. Lando, J.A. Mann, Jr., L.Zhou, D. Schuele, S. Hubbard, and K.D. Singer

Department of Macromolecular Science, Chemical Engineering, and Physics

Case Western Reserve University

Cleveland, Ohio 44106.

Nonlinear Optical, pyroelectric and dielectric studies were carried out on polar Langmuir-Blodgett films fabricated from side-chain liquid crystalline copolymers containing mesogenic side chains. One of the side chains is a nitrobiphenyl showing second-order nonlinear optical properties while the other, (methoxyethoxy)methoxy biphenyl is incorporated to enhance the spreadability.

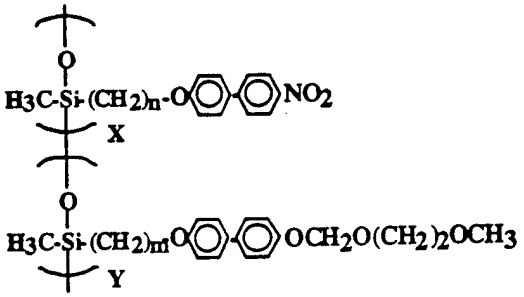

Where m=n= 11, 10, 5, and 4.

X-ray diffraction, second harmonic generation measurements and pyroelectric studies all support the existence of noncentrosymmetric structure for the polymeric multilayer films with the polar axis nearly perpendicular to the substrate. The second harmonic coefficient was found to be 42 pm/V. The copolymeric multilayers with shorter spacers, Cop4, were found to have lower second harmonic response.

An unusual pyroelectric response was observed for Cop11 multilayers. The pyroelectric coefficients were determined to be $2.85 \times 10^{-10} Ccm^{-2} °C^{-1}$ for Cop 11 and

$2.00 \times 10^{-10} Ccm^{-2}\,°C^{-1}$ for Cop 4. Please note that the value given for Cop11 is an average value in the range 18 °C to 35 °C. FTIR-RA studies as a function of temperature show that the aromatic rings of Cop 4 and Cop11 multilayers remain oriented in their liquid crystalline phases. No phase transition is observed for Cop11 in the 18 °C to 35 °C range. The dielectric response was also examined. At the low frequencies the dielectric constant increases with temperature. The dielectric constant ε' of Cop11 is relatively constant below room temperature and changed drastically over the range of unusual pyroelectric behavior in the low frequency range. Thus, an unusual peak is observed in this temperature range. At this time the exact explanation for these effects is being investigated by measuring the piezoelectric response and electric field induced second harmonic generation in this temperature range and by studying Cop5 and Cop10.

The nonlinear optical properties can be enhanced by synthesis with a more efficient electron donor group and a longer conjugation length between the donor and acceptor group e.g.:

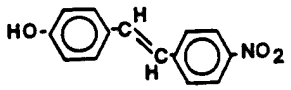

4-Hydroxy-4′-Aminostilbene

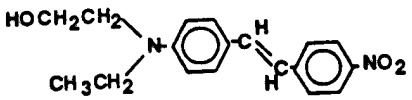

4-(N-Ethyl-N-Hydroxyethylamino)-4′-Nitrostilbene

The mixed monolayer of the 4-hydroxy-4′-nitrostilbene and the MEM biphenyl do form a monolayer. Copolymers will be made.

In addition, molecules that possess both second and third harmonic generation are being synthesized. These polymers consist of a polydiacetylene backbone, contributing to χ^3, and the above chromophore, contributing to χ^2.

**This work is supported by NSF under The S and T Center ALCOM. No DMR 89-20147.

SYNTHESIS AND LIGHT-EMITTING PROPERTIES OF POLY(1,4-PEHNYLENEVINYLENE)/POLY(2-MESYLOXY-1,4-PHENYLENEVINYLENE) COPOLYMERS

Kwang-Sup Lee[1], Kyoung-Soo Kim[1], and Lee-Mi Do[2]
[1]Department of Macromolecular Science, Hannam University,
Taejon 300-791, KOREA.
[2]ETRI, Yusong, Taejon 305-600, KOREA

Poly(p-phenylenevinylene) (PPV) and its derivatized structures can be easily prepared in high molecular weight through the water- or organic-soluble precursor routes[1,2]. The substitution of phenylene ring in PPV with different types of electron-donating or electron-attracting groups can exert a significant influence on the electronic structure of the resulting polymers and thus affecting the electrochemical and optical properties[3]. Most recent interest of PPV derivatives are focused on their application as active materials for the light-emitting diodes (LEDs). The red to yellow-greenish light from PPV derivatives has been reported[4,5]. In the continuing effort to make more blue-shifted PPV derivatives by introducing the electron-attracting groups, we have synthesized copolymers containing both 1,4-phenylenevinylene and 2-mesyloxy-1,4-phenylenevinylene moieties as shown below.

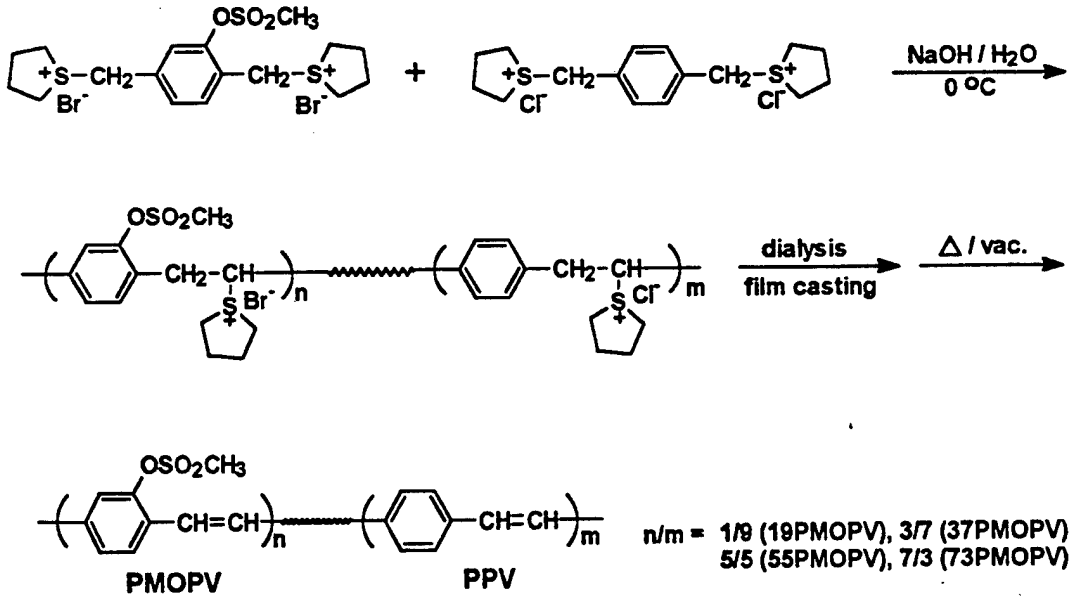

Due to the electron-attracting characteristics of mesyloxy-substituents, poly(2-mesyloxy-1,4-phenylene vinylene) (PMOPV) precursor with high molecular weights can not be obtained by the conventional polymerization process from sulfonium salt monomers. In order to solve this problem, we synthesized a series of PPV-PMOPV copolymers with different compositions.

The absorption maxima and band edges of copolymers are significantly blue-shifted than those of the pure PPV (λ_{max} = 380 nm for 73PMOPV, 410 nm for 19PMOPV). The electrical conductivity of $FeCl_3$-doped copolymer films ranged from 2.7 $\times 10^{-1}$ to 5.3 $\times 10^{-4}$ S/cm depending on copolymer compositions and draw ratios. The photoluminescence (PL) and electroluminescence (EL) spectra of these copolymers have been detected. The emission wavelength of polymer 55PMOPV is drastically shifted as compared to the pure PPV. All copolymers show a relatively broad EL emission peak around 540 nm to 510 nm. The PL spectrum of 55PMOPV exhibited an emission in greenish blue region.

References

1. Wessling, R. A. and Zilbey, R. G. U. S. Patent 3,401,152 (1968); U. S. Patent 3,706,667 (1972).
2. Tokito, S., Murata, T., Tsutsui, T., Saito, S. *Polymer*, **31**, 1137(1990).
3. Bredas, J. L. and Silbey, R. *Conjugated Polymers*; Kluwer Academic Publishers: Dordrecht,
   The Netherlands (1991).
4. Shim, H.-K., Hwang, D.-H. and Lee, K.-S. *Mol. Cryst. Liq. Cryst.*, **267**, 7(1995).
5. Holmes, A. B. et. al, *Synth. Met.*, **55-57**, 4031(1993).

P-14

NONLINEARITIES OF POLYMETHINE DYES IN LIQUID AND POLYMERIC HOSTS

Olga V. Przhonska[1], JinHong Lim[2],
and Eric W. Van Stryland[2]

[1] Institute of Physics, National Academy of Sciences of Ukraine,
Prospect Nauki 45, Kiev-22, 252650, Ukraine
[2] Center for Research and Education in Optics and Lasers,
University of Central Florida, Orlando, Fl. 32816-2700

ABSTRACT

We have investigated nonlinear light absorption of a series of polymethine dyes in liquid and solid (polymeric) media. Depending on the ratio between the absorption cross section from the ground to the first (σ_{01}) and from the first to the higher excited states (σ_{1n}), and on the pumping wavelength, these organic systems demonstrate either photoinduced bleaching (saturation) or photoinduced darkening (reverse saturable absorption). The main effort was directed at studying the optical limiting behavior of the dyes in order to find the best systems for power regulation and protection of optical components from laser-induced damage.

The dyes are distinguished structurally by the length of the π-conjugated system in the polymethine chromophore, the substitute in the polymethine chromophore and of the nature of the end chromophore groups. The measurements were made in absolute ethanol solutions and in solid matrices of polyurethane acrylate (PUA) obtained by the photopolymerization procedure of ref. [1]. The major feature of this polymeric material is the existence at room temperature of a highly elastic state (the glass-transition temperature is $\approx$ 210 K) characterized by a higher mobility of polymeric chain segments compared to the glassy state. This property is responsible for the high resistance to radiation damage and for its self-healing abilities. Hence this polymeric material can be used under intense pumping irradiation with minimal damage which is very important for practical applications.

In our experiments we used two well-developed techniques: Z-scan and pump-probe methods. The measurements were performed using the second harmonic of a mode-locked Nd:YAG laser (532 nm) producing single or multiple pulses of 30 ps duration , with a repetition rate variable from 0.5 to 10 Hz.

The main distinguishing features of these systems are:
- high sensitivity to input irradiance showing the appearance of nonlinear response at less than 0.01 GW/cm^2;
- very broad Z-scan curves for high input, see Fig. 1. Both features are intensified in the polymeric medium which may be connected with the increase of the fluorescence lifetime from the first excited state. For the best system we obtained the value $\sigma_{1n}/\sigma_{01} \approx 80$ that is much higher than for dyes reported previously [2].

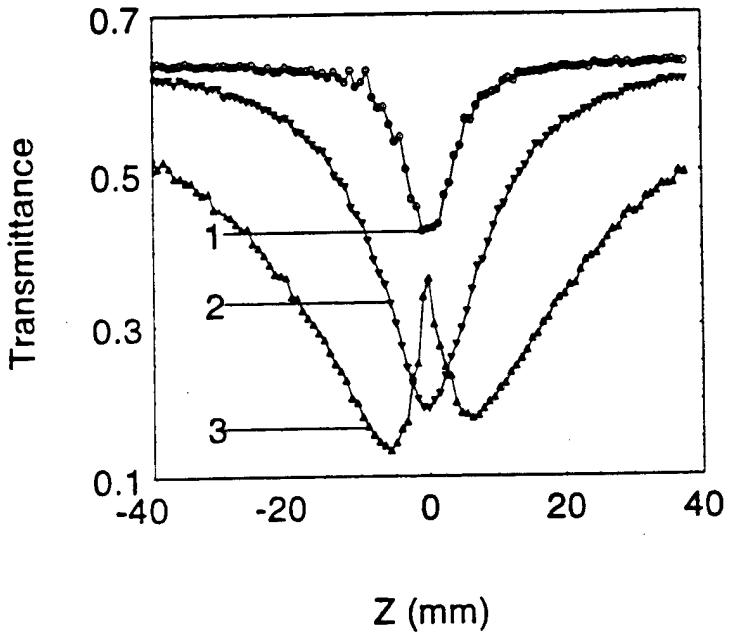

Fig. 1 The nonlinear transmittance (Z-scan) of the indothreecarbocyanine dye in ethanol solution at the energy:
1 - 0.05 μJ,
2 - 0.5 μJ,
3 - 3.5 μJ

At high pump irradiance for most of these systems an unusual behavior of the nonlinear transmittance has been observed: photoinduced darkening was transformed into a bleaching effect (curve 3). This phenomenon is controlled by changing the repetition rate of the laser pulses, and explained by the formation and accumulation of a new product due to photochemical reaction in the excited state of the dye molecule. This is to be distinguished from a similar effect caused by saturation of excited state absorption [3]. We performed a detailed investigation of the dynamics of these processes and numerical simulations of the nonlinear transmittance using a four-level model. Analysis of this model allows us to obtain the correlation between molecular parameters of the dyes and the accumulation effect, and find methods to control this effect.

1. M.V. Bondar, O.V. Przhonska, E.A. Tikhonov, J.Phys.Chem., **96**, 10831-10837 (1992).
2. T.H.Wei, D.J.Hagan, M.J. Sence, E.W.Van Stryland, J.W.Perry, D.R. Coulter, Appl.Phys., **B54**, 46-51 (1992).
3. T.H. Wei, W.P. Zang, G. Zhang, Optik, **98**, 143-146 (1995)

Second harmonic generation of a cross-linked polymer formed in the chiral smectic C phase.

M. Lindgren[#]
Department of Physics and Measurement Technology, Linköping University, 581 83 Linköping, Sweden

M. Trollsås, F. Sahlén, U. W. Gedde, A. Hult
Department of Polymer Technology, Royal Institute of Technology, 100 44 Stockholm, Sweden

D. Hermann, P. Rudquist, L. Komitov, B. Stebler, S. T. Lagerwall
Department of Physics, Chalmers University of Technology, S-412 96 Göteborg, Sweden

Abstract

Pyroelectric polymers were made from liquid crystalline monomer mixtures[*] which possessed a chiral smectic C mesophase with large spontaneous polarization (175 nC/cm^2). The cross-linked polymer was formed by photo-polymerization in the surface stabilized liquid crystalline state. The polymer possessed a second harmonic generation (SHG) signal. Maker-fringes measurements were carried out using a Sunlite OPO laser. For SHG measurements a pump wavelength (idler out-put) ranging between 800 and 1500 nm was used.

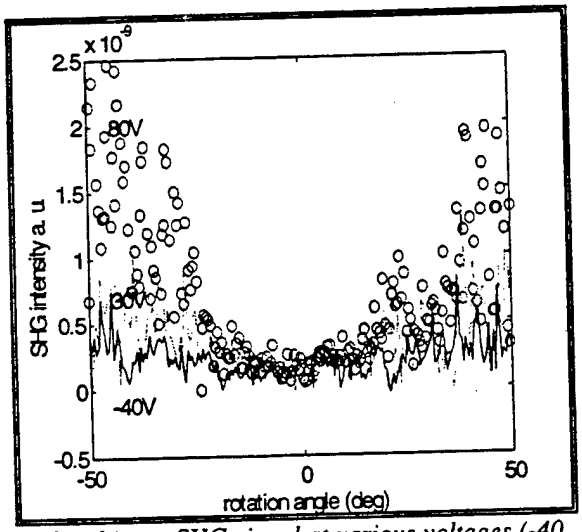

Maker fringes SHG signal at various voltages (-40, 30 and 80V) applied onto the cell (raw data).

At 1100 nm pump wavelength the strength of the SHG signal was found to be approximately one order of magnitude lower than that of a poled PMMA-DR1 polymer of similar thickness.

The application of a voltage over the cell resulted in an increase of the SHG signal. This effect was saturated at 60-80 V. Reversing the polarity of the applied voltage gave no concommitant increase of the SHG signal, which implies that the spontaneous polarization has been "frozen in" in the crosslinked polymer.

New recent results will be presented and discussed. This work is supported by the Swedish National Defense Research Establishment (FOA) and the Swedish Research Council for Engineering Sciences (TFR 240-313: 240-517: 240-691: 251-303: 281-807).

[*]M. Trollsås et al., Macromolecules 1996, 29(7), 2590 : Chemistry of Materials 1996, 8, 382.

[#]*Email: mli@ifm.liu.se*

NONLINEAR OPTICAL RESPONSE OF POLYPHENYLQUINOXALINE SOLUTION

Huimin Liu, Yanyun Wang and Weiyi Jia
Department of Physics, University of Puerto Rico, Mayaguez, PR 00681, U.S.A.

Meng Shen and Shoukuan Fu
Department of Chemistry and Macromolecular Science, Fudan University
Shanghai 200433, P.R.China,

EXTENDED ABSTRACT

Using picosecond Nd:YAG laser as a light source operating at 532nm, the time evolution of nonlinear optical response of Poly[2,2'-(1,4-phenylene)-6,6'-bis-(3-phenyl)quinoxaline] or so-called polyphenylquinoxaline (PPQ) solution has been obtained in degenerate-four-wave-mixing(DFWM) experiment. It was found that the coherent response signal in chloroform, which is often used for estimation of the third-order susceptibility, is actually much weaker than the phonon signal delayed at 0.4 nsec or more. As seen in figure 1, using DFWM technique $\chi^{(3)}$ can be obtained only from the time-resolved spectrum. We calculate $\chi^{(3)}$ value in chloroform in this way, and find to be 4.5×10^{-11} esu, at

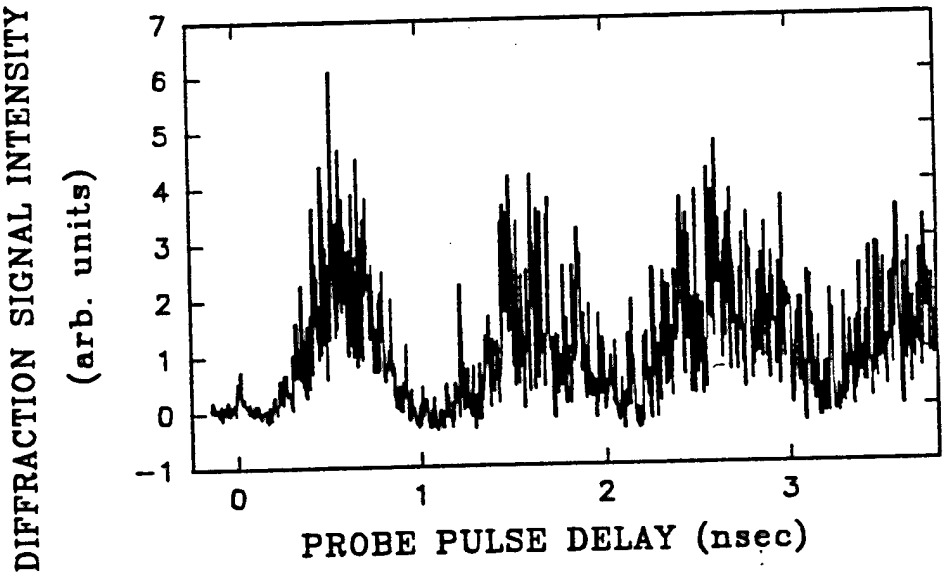

Fig. 1. Time-resolved DFWM spectrum of PPQ - Chloroform solution. A small peak at zero delay is the instantaneous nonlinear optical response signal. The cross angle 2θ between two write beams is 30.4°. The laser pulse width is ~26 psec.

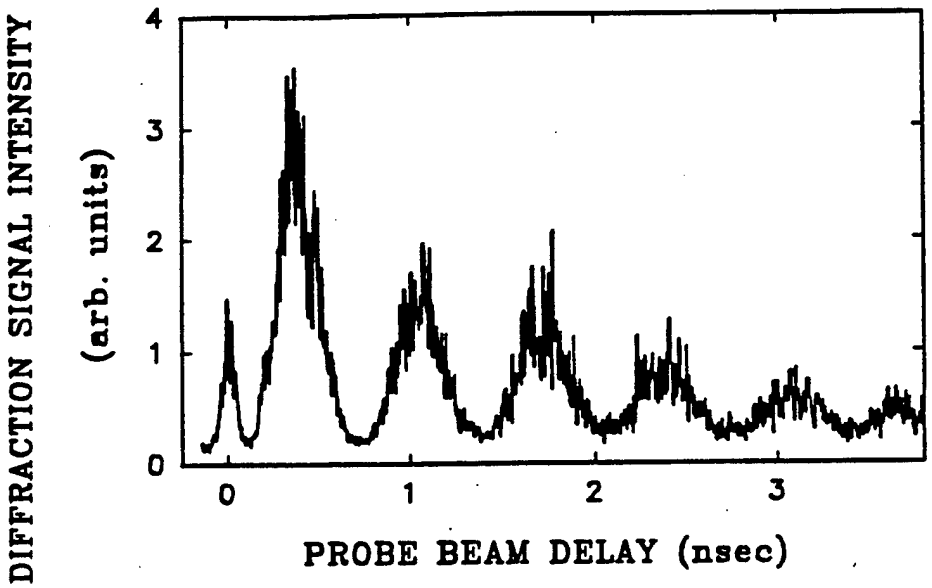

Fig. 2. Time-resolved DFWM spectrum of PPQ - m-Cresol solution. The peak intensity ratio of the coherent signal to maximum phonon signal is about 1/3. The cross angle 2θ and pulse width of laser are the same as figure 1.

least less by a factor of 8 than that reported in the literature.[1] On the other hand, DFWM spectrum of PPQ solution was found to vary with solvent. With PPQ in m-cresol, the DFWM spectrum is composed of an instantaneous coherent optical response signal at zero-delay and a following acoustic phonon signal which is rapidly damped to disappear after 6 nsec. The peak intensity ratio of the coherent signal to maximum phonon signal is about 1/3. The lifetime of the generated acoustic phonon was estimated to be 1.5 ns. With the solvent changes to chloroform, an anomalous enhancement of acoustic phonon signal overwhelms the coherent signal component, and the acoustic phonon in chloroform is much longer-lived. The generated phonon signal was identified as due to the two-photon absorption at 532nm, resulting in thermal effect (heat deposition).[2] Referring to the data obtained we may judge the validity of χ^3 values obtained from FWM measurement for a variety of organic solutions.

References:

1) J. Yan et al., Opt.Lett., 20, 255(1995).
2) H. Liu et al., Phys.Rev.B, 49, 10166(1994).

Synthesis and NLO Properties of High Tg Polymers from Maleimide Substituted with Azo-dye Molecule

Hiro Matsuda, Shinji Yamada
National Institute of Materials and Chemical Research, Tsukuba 305 Japan
Masao Kato, Chikara Ishii, Tatsuhiko Miyoshi
Science University of Tokyo, Noda 278 Japan
Hachiro Nakanishi
Institute of Chemical Reaction Science, Tohoku Univ., Sendai 980-77 Japan

Poled polymer systems have been expected to be a better candidate for electro-optic (EO) device applications. In order to achieve the long term stability of NLO chromophore orientation, side-chain polymers, thermal crosslinked and/or photochemical cross-linked systems have been investigated. Generally, polymer systems with increased glass transition temperature (Tg) show improved temporal stability. In this paper, we report the synthesis of high Tg polymers from maleimide derivatives and their comparatively stable properties of second harmonic generation (SHG) and EO effect.

The new maleimide monomer attached azo-dye molecule was synthesized, however, the homopolymerization could not proceed by radical initiator. Using α-methylstylene as comonomer, the alternating copolymer whose the molecular weight (Mn) and Tg are 1.4×10^4 and 186°C, respectively, was obtained as shown the structure below:

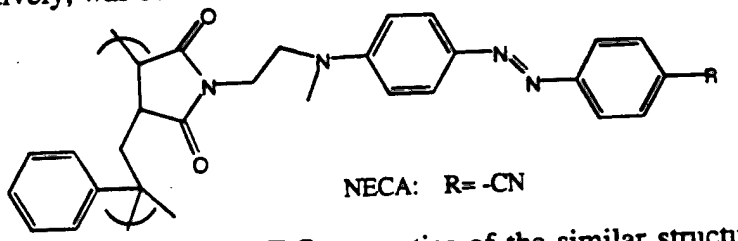

NECA: R= -CN

Allthough the preparetion and NLO properties of the similar structure polymers have already reported[1,2], the introduction of NLO-active azo-dyes into maleimide units was not completed by their polymer reaction. This difficulty was overcome by our new synthetic paths, that is, first synthesized the maleimide monomer with azo-dye. The uniform amorphous film was readily fabricated on a glass substrate by spin-coating 2wt% chloroform solution. The SHG coefficient, d_{33}, at 1.064 μm was found to be 100pm/V at initial stage in the sample to which the optimum corona-poling was applied under 5kV/cm at 160°C. Poled polymer was fairly stable to maintain 54pm/V at room temperature after the quick initial decay, and 25pm/V even after the heat treatment at 80°C for more than 10 days. The EO measurement by the reflection method applying ellipsometry was performed to the poled samples in which a contact poling was carried out using an Al-ITO sandwich cell under 10kV/cm at 150°C. The EO coefficient, r_{33}, at 633nm was measured to be 6 pm/V at a stable state after initial drop. More details on the synthesis and characterization of NECA will be discussed.

References
1) M. Ahlheim and F. Lehr, *Makromol. Chem.*, **195**, 361 (1994).
2) P.Pretre, P.Kaatz, A.Bohren, P.Günter, B.Zysset, M. Ahlheim, M.Stahelin, and F. Lehr, *Macromolecules*, **27**, 5476 (1994).

Glass Transition Temperatures in Guest-Host Systems

Darja Tomić and Alan Mickelson

Guided Wave Optics Laboratory and
Department of Electrical & Computer Engineering
Boulder, Colorado 80309-0425
email mickel@schof.colorado.edu

As work at Lockheed has shown [1], it is presently possible with commercially available polyimides and dyes to form guest-host systems with sufficiently large T_g's to be of interest to electronics manufacturers. A number of commercial polyimides are available with T_g's in the range of 300 °C–400 °C, and these coupled with dyes of decomposition temperatures T_d greater than 200 °C can lead to composite T_g's equal to or greater than 200 °C. As was shown in work at IBM [2], T_g's of 200 °C or greater yield effective room-temperature poling lifetimes of greater than five years, an acceptable lifetime for an electronic system. We are presently looking at a number of guest-host combinations to determine which polymer dye solutions to further study. As the T_g of the composite material is one of the most important of the salient features in making this decision, we wish to determine this parameter before all others. In this work we will present our technique to determine T_g with a minimum amount of material processing.

Figure 1 illustrates our setup for measuring the glass transition temperature. The basic idea for the setup can be illustrated with respect to the typical set of poling curves illustrated in Figure 2. What is shown here is the absorption spectrum of a polymer with dye, in this case a side chain version of a polymethyl merthacrylate (PMMA) backbone with a disperse red 1 (DR1) dye side-chain attached onto this backbone, with a dye weight concentration of roughly 10%. These samples were parallel plate poled at a fixed voltage. The most salient features of the curves is that the absorption spectrum of the side chain thin film is comprised of three features. The first is the backbone absorption peak, whose maximum falls offscale at around $\lambda = 180\,\text{nm}$. Only the tail of the peak can be seen above 200 nm. This exponential tail can also be thought of as a band edge. The two other features are Gaussian bumps. These bumps are due to Gaussian inhomogeneous broadening of the dye absorption lines due to the backbone randomness in the film, convolved with the Lorentzian whose width is determined by the thermal excitation in the film, the value of which is determinable from the band edge decay constant [3].

In an absorption spectrometer, the light is incident normal to the slab. Either corona or parallel plate poling, however, will align the dye molecules perpendicular to the surface. The number of molecules, therefore, aligned with the light polarization direction decreases with an increasing degree of poling. In the present case of Figure 2, to a great extent the degree of poling (order parameter) is determined by the poling voltage. Indeed, the absorption peak is reduced by increasing the poling voltage.

In order to minimize the amount of time spent in determining the T_g of a given material, ideally one would like to be able to spin the material on an ITO-coated sample, corona pole, and then find a readout technique that requires no further material handling. A solution to this problem is given in Figure 1. After the material is poled, it is placed in a spectrometer-like setup but on a controlled temperature jig. By inputting a normally incident, low-intensity light flux tuned near the absorption peak, one can monitor the absorption near the peak. When the jig temperature passes from below T_g to above T_g, the absorption drops and, as one notes from Figure 2, the absorption drop is large, giving 10 or more dBs of signal variation.

Results on various material systems, including side chain PMMA/DR1 and guest-host combinations of DCM/4212, DR1/4212, and DPDR1/4212, will be presented and discussed at the conference.

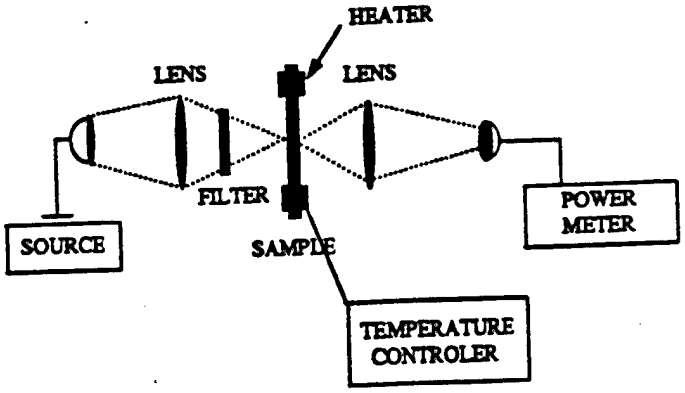

Figure 1. Setup for T_g measurement.

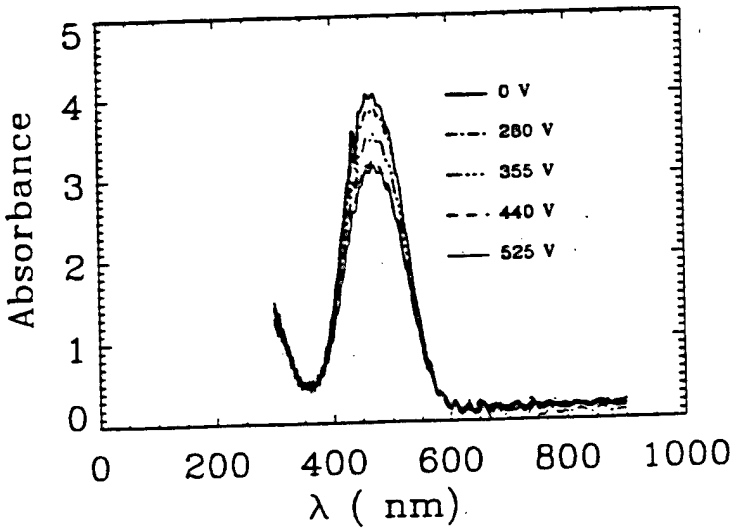

Figure 2. Absorption spectra of poled PMMA/DR1 (film thickness is 1.3 μm) [4].

References:

1. S. Ermer, W. W. Anderson, T. E. Van Eck, D. G. Girton, I. A. Marley, A. Harwit, S. M. Lovejoy, and D. S. Leung, "Progress Toward Practical Electrooptic Devices," *Proc Organic Thin Film for Photonic Applications Conf*, Portland, OR, Paper WA2, 285 (September 11–14, 1995).

2. C. A. Walsh, D. M. Burland, V. Y. Lee, R. D. Miller, B. A. Smith, R. J. Twieg, and W. Volksen, "Orientational Relaxation in Electric Field-Poled Guest-Host and Side-Chain Polymers Below T_g," *Macromolecules* **16**, 3720–3722 (1993).

3. See a separate article in this same volume: A. Mickelson and D. Tomić, "Bleaching of Dye-Doped Polymers."

4. From J. Ma, *Modeling, Simulation, and Characterization of Electrooptic Polymer Waveguide Devices*, Ph.D. Thesis, University of Colorado at Boulder (January 1996).

Bleaching of Dye-Doped Polymers

Alan Mickelson and Darja Tomić

Guided Wave Optics Laboratory and
Department of Electrical & Computer Engineering
Boulder, Colorado 80309-0425
email mickel@schof.colorado.edu

Exposure of a volume of dye-doped polymer to light which spectrally lies within the absorption band of the mixture (here we refer to mixture as either a guest combination or a chemically attached compound) leads to a reduction of the absorption of the dye-polymer mixture. This process is generally referred to as *bleaching*. The accompanying lowering of the index of refraction can be used for waveguide formation in the unexposed (unbleached) regions of the mixture. In this talk, we will discuss some of the salient features of this "bleaching" process.

Figure 1 illustrates a set of bleaching curves—that is, absorbance as a function of wavelength for a fixed thin film thickness of polymer dye mixture, as parameterized by the time of exposure to a visible source of fixed and uniform intensity. The polymer dye mixture here is a guest-host mixture of a guest dicyano methylated nitrostilbene called DCM in an AMOCO 4212 host, the host being a backbone formed from a mer which is essentially a 6FDA polyimide with some oxy-attached phenylenes to either side. The dye weight concentration here is 9%.

Some interesting spectroscopy is illustrated in the curves of Figure 1. The two most obvious features on the curve are the exponential tail, which goes offscale below roughly 300 nm and decays with a roughly 20-nm decay constant toward longer wavelengths, and a broad (>200 nm) peak centered on roughly 460 nm. Interestingly enough, we will show that all of the curves for the various bleaching times can be expressed as simple sums of a dying exponential with an offscale peak and a Gaussian of fixed width and central peak but with an amplitude which varies with bleaching time as an exponential of the square root of the time.

Absorption of a backbone can be thought of as a sum of the absorption of all the associated bonds. The large peak below 300 nm is likely to result from the absorption of the mer-mer bonds. If there were only one bond, one would expect the absorption curve to be Lorentzian, and indeed a Lorentzian tail looks just like an exponential. When multiple conjugated bonds of a long chain are involved, however, the situation is a bit more interesting, as delocalization of the electron wave functions implies that the bond energies must form a band in energy momentum space. Absorption then corresponds to advancing an electron from a valence band to a conduction band and thereby creating a hole in the valence band. The exponential band tail, however, would still appear as in Figure 1.

As to the Gaussian absorption peaks which bleach with a stretch exponential of exponent 0.5, these must basically be due to some broadening of a cis-trans isomerization transition. The unbroadened cis-trans transition should have the form of a Lorentzian feature with thermal broadening on the order of that exhibited by the band edge, here on the order of 20 nm. However, in a spin on guest-host, the guests will tend to be wound into knotted balls of backbone material which exert either stretching or compression on the dye molecule. As the cis-trans energy of a dye molecule is linear in its length (actually linear in the extent of the pi electron wave function which extends from the donor at one end of the molecule to the acceptor at

the other end), one would expect the backbone knotting then to lead to a pure Gaussian broadening of the center frequencies of all of the individual dye molecules. Convolving this broadening with the unbroadened Lorentzian would then give the lineshape. Here the lineshape is Gaussian due to the 200-nm width of this broadening compared to the 20 nm of thermal broadening.

The exponential of $t^{1/2}$ behavior is interesting. Cis-trans isomerization we know to be a totally reversible transition, yet we have seen bleaching to be stable over months and years, meaning that bleaching must be a multiphoton process which involves both cis-trans isomerization together with some process which most likely needs to ionize the cis-excited electron. Ionization of the electron could well have the effect of weakening the stilbene double bond sufficiently that the dye molecule can break in two. However, in the knot regions of the backbone where the dye sits, the excited dye electron is close enough to the backbone to tunnel from dye molecule to backbone and fill an excited hole state. If the tunneling distance from the edge of the cis electron potential well to the backbone varies randomly and if the distribution function of the distances is essentially uniformly distributed, the tunneling process should statistically be a random walk and the time variation should be a square root, as observed.

The results of our bleaching model will be used to fit various bleaching curves for both side chains and guest-hosts, and these comparisons will be presented at the conference.

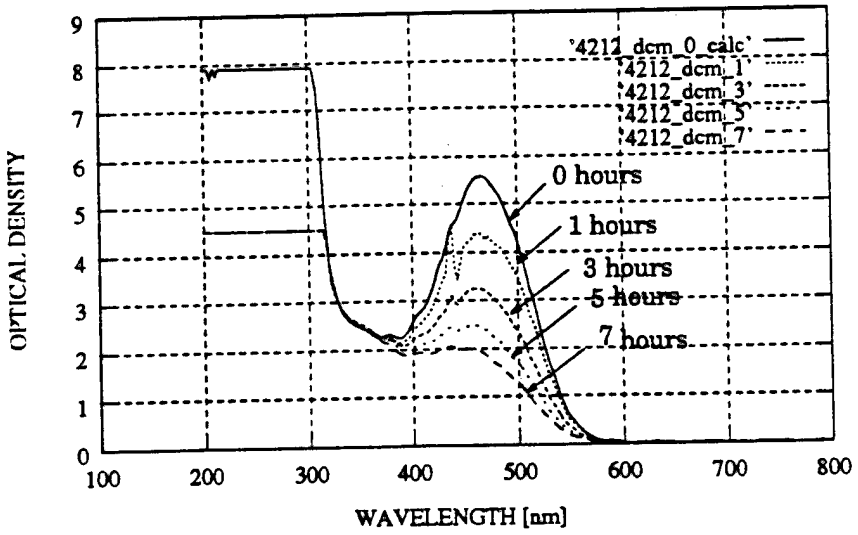

Figure 1. Absorption versus bleaching time.

P-20

Control of orientational order in Langmuir Films

M. Harke, H. Motschmann

Max-Planck Institute of Colloids and Interfaces, Rudower Chaussee 5, 12489 Berlin

Langmuir Blodgett Films have been identified to have potential for second-order nonlinear devices due to a high degree of orientational order and a film architecture controled on a molecular level. The present talk gives a brief review about the current status in this field. The decisive step using this technique is the control of morphology and orientational order within the monolayer. An attractive new method to change both utilizes a gas phase containing organic molecules. It is demonstrated that these molecules are incorporated in the film leading to a significant change in the isotherms, morphology and orientational order. The control of the gas phase gives a decisive parameter to finetune the molecular assembly and to maximize the orientational order. On the basis of a liquid crystal at the air-water interface we discuss the structures obtained in the varius phases and demonstrate the possibility and power offered by this technique. The data obtained are also important to get a better understanding of surface induced order processes in liquid crystals.

Nonlinear Absorption and Light Induced Index Change with a Fast Response Time in the Waveguide of a Novel Organic Quinoid Dye

Hiroshi MURATA
Faculty of Engineering Science, Osaka University
Toyonaka, Osaka 560, Japan

Masayuki IZUTSU
Communications Research Laboratory
Koganei, Tokyo 184, Japan

1. Introduction

Organic materials with third order optical nonlinearity are attracting wide attentions to construct all-optical switching devices by using their large nonlinearity with fast response times. In this report, we present the result of an observation of a large third order optical nonlinearity with a response time < 10ps in a waveguide using a novel quinoid dye.

2. Fabrication of the waveguide

The quinoid dye used for this study is 4,8-dihydroxy-2,6-bis(butylamino)-1,5-naphthoquinone, which was reported to have large third order optical nonlinearity measured by the THG method compared with the conventional dyes [1].

The schematic of the waveguide is shown in Fig. 1. It consists of a base linear waveguide and a thin film of the quinoid dye as the nonlinear material. This structure is suitable for changing the optical nonlinearity in the waveguide selectively by controlling the pattern of the dye films. It is possible to construct all-optical guided-wave devices with the localized nonlinearity we have proposed [2]. A glass waveguide was adopted as the base waveguide, where a 7059 glass stripe was fabricated as a core on a soda glass substrate using the sputtering and the lift-off technique. The core is 1.0μm thick and 4μm wide. A quinoid dye film of 0.1μm thick was fabricated by the vapor deposition on the base waveguide. The length of the dye film is 10mm and the total length of the waveguide is 25mm. The refractive index of the dye film is 2.01 at 850nm measured by the Abeles method.

3. Experiment of the nonlinear optical performances

Changes of the absorption in the waveguide by the light power were measured by using the experimental setup shown in Fig. 2 (a). The light source is a mode-locked Ti:Al_2O_3 laser of the pulse width of about 5ps. The train of pulses from the laser goes through a shutter which reduces the average power to avoid thermal nonlinear effects. Output light power from the waveguide is monitored by a fast (ns) photodiode as well as input light with a moderate time delay. An example of the obtained result is shown in Fig. 2 (b). The saturable absorption is observed clearly at the wavelength of 740nm. The nonlinear absorption coefficient of the dye is calculated from the result as $\alpha_2 = -1 \times 10^{-6}$ cm/W at 740nm.

An experimental setup for the measurement of nonlinear index change is shown Fig. 3 (a). The waveguide was set in the one path of the Mach-Zehnder interferometer and the light induced index change of the waveguide was detected from the output of the interferometer. The two paths of the interferometer were adjusted to have the same path length by monitoring the pulses through the two paths with a synchroscan streak camera. The change of the output was also monitored by the streak camera. Examples of the measured patterns of the output pulses for a low and a high power input cases are shown in Fig. 3 (b) and (c) respectively. In the high power case, the intensity at the center part of the pattern of the pulse is slightly lower than that of the outer part. This means the nonlinear index change was induced corresponding to the transient change of the pulse envelope and the response time of the index change is faster than 10ps. The measured characteristics of the light induced phase shift versus the input power is shown in Fig. 4.

The nonlinear phase shift changes linearly with the input power. The estimated nonlinear index of the dye is $n_2 = -3 \times 10^{-12}$ cm^2/W at 780nm.

4. Conclusion

The measured nonlinear coefficient is three times larger than that from the THG experiment. The observed light induced phase shift over π is enough to drive the all-optical switching devices. The applications to the integrated Mach-Zehnder waveguide and the directional coupler waveguide are now under going.

Acknowledgment

The authors would like to thank Prof. M.Matsuoka for providing the dyes and his useful advice and F.Yoshioka for his valuable assistance of this work. This research was supported in part by the Ministry of Education, Science and Culture under the Grant-in-Aid for Scientific Researches on Priority Areas (No.07246228 and No.08236225).

References

[1] M.Matsuoka, A.Oshida, A.Mizuguchi, Y.Hattori and A.Nishimura, *Nonlinear Optics*, **10**, pp.109-114 (1995). [2] H.Murata and M.Izutsu, *CLEO / Pacific Rim '95* (Jpn. Soc. of Appl. Phys., Chiba, Japan) papers FE2, pp.174-175 (1995).

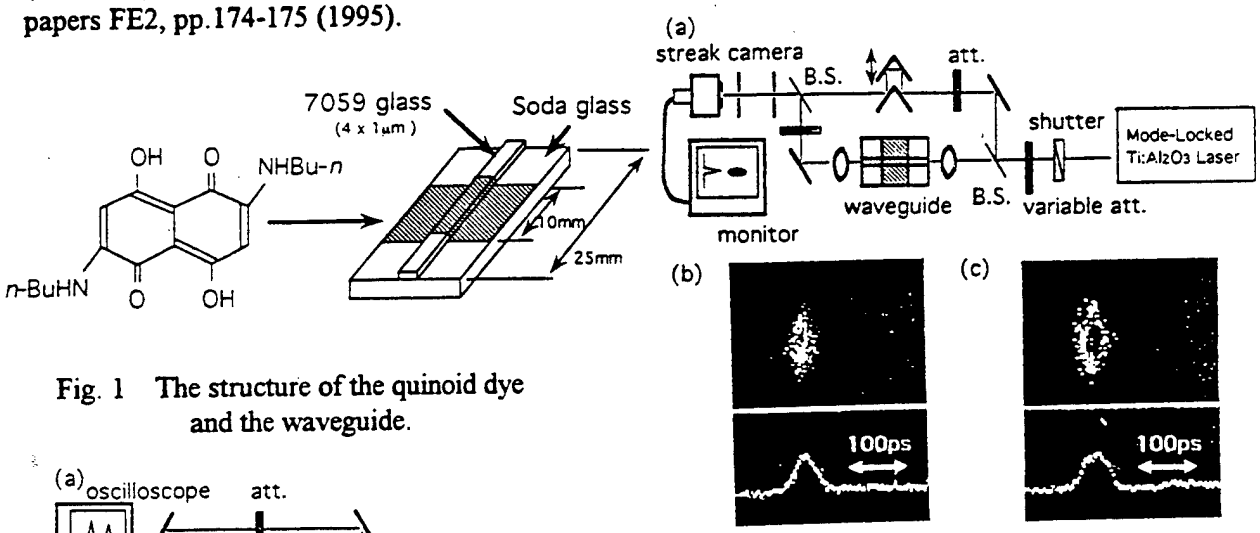

Fig. 1 The structure of the quinoid dye and the waveguide.

Fig. 3 The experimental setup for measuring the nonlinear index change (a) and examples of the observed pattern by a streak camera (b),(c).

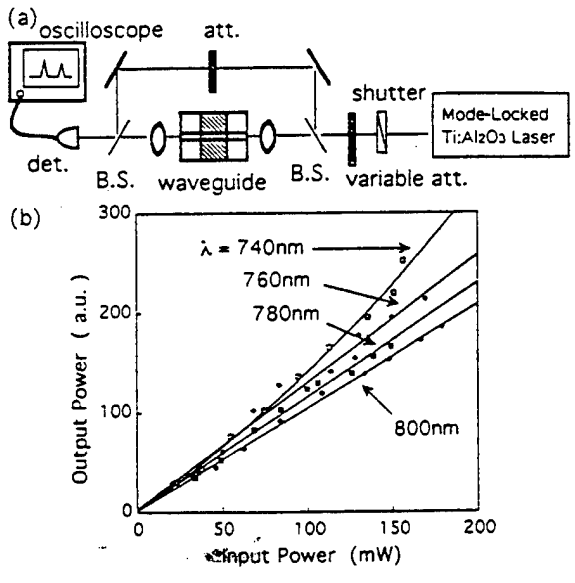

Fig. 2 The experimental setup for measuring the nonlinear absorption (a) and an example of the observed input-output characteristics (b).

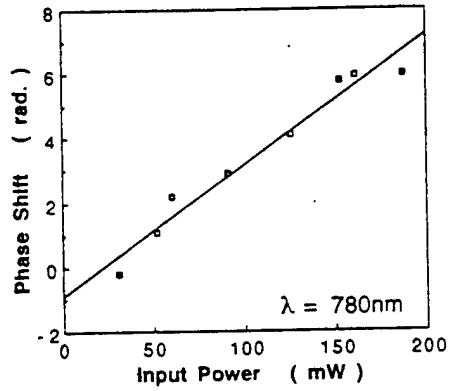

Fig. 4. An example of the change of the induced phase shift by the input power.

P-22

Linear and Nonlinear Optical Properties of Organic Microcrystals

Hachiro Nakanishi
Institute for Chemical Reaction Science, Tohoku University
Katahira, Aoba-ku, Sendai 980-77, Japan

Aiming at obtaining materials which have both high performance as crystals and acceptable optical quality as nearisotropic materials, we have been preparing microcrystals of polydiacetylenes(PDAs) and several dyes and investigating their linear and nonlinear optical properies. Here, recent progress will be introduced.

First, as for the linear properties, it became no doubts that organic microcrystals of π-conjugated chromophers in the liquid dispersion take place a blue shift of absorption and fluorescence maximum with decreasing crystal size even in the range of several tens nm, which is surprizingly about one order larger than that in the case of semiconductors.

Since some PDAs and dyes gave transparent and stable dispersion, their third-order nonlinearities were evaluated. Under Kerr shutter configuration, using the gate beam of 1064nm and the probe beam of 813 nm, the susceptibilities of PDAs and merocyanines, extraporated to 1 M dispersion, were ca. 10 to the -9 esu, and those/absorbance were ca. 10 to the -12 esu · cm at these nonresonant wavelengths. Phthalocyanines as well gave the transparent water dispersion of their microcrystals, and under four wave mixing experiments, the microcrystal dispersion showed completely different behaviours, compared with their solution; i.e., no slow response and saturable absorption in contrast to superposed slow response and induced absorption of solution. Such first response of microcrystals was confirmed by optical parametric oscillator incoherent spectroscopy as well. Details will be presented.

These dispersion of microcrystals in liquids could easily be converted into the dispersion in polymer thin films. Thus, microcrystallization was demonstrated to be one of potential materiallization method of organic third order nonlinear optical materials.

References
1) H. Kasai et al., Jpn. J. Appl. Phys. 31, L1132 (1992).
2) H. Kamatani et al., Mol. Cryst. Liq. Cryst., 252, 233 (1994).
3) R. Iida et al. Mol. Cryst. Liq. Cryst., 267, 95 (1995).
4) H. Kasai et al., Jpn. J. Appl. Phys. 34, L1208 (1995).
5) H. Kasai et al., Jpn. J. Appl. Phy. 35, L221 (1996).
6) T. Yanagawa et al., Opt. Lett. 21, 318 (1996).

Thermally Stable Non-Poled Polymeric Films Doped with Pyrylium Salts Dye

Hideki Nakayama, Atsushi Mizuno*, Okihiro Sugihara*,
Ryoka Matsushima, Naomichi Okamoto

The Graduate School of Electronic Science and Technology, Shizuoka Univ.
*Faculty of Engineering, Shizuoka Univ.
3-5-1 Johoku, Hamamatsu 432 Japan.

Introduction

Many poled polymer films containing the nonlinear optical chromophores are prepared and show high second-harmonic generation. However, the nonlinearity tends to decrease with time because of the orientation relaxation of aligned nonlinear molecules. We synthesize the novel organic ionic material, pyrylium salts dyes and polymer films doped with the chromophores are prepared. These guest-host type polymer films show no absorption in the blue-light region[1,2] and have SHG activity without electric-field poling process. These second-order nonlinearity of the non-poled polymer films is unvaried with no relaxation.

Experiments and Results

The chemical structures of a series of pyrylium salts dye used in this study are shown in Table 1, together with the compound's number for abbreviation. The structures include the same pyrylium group, but different alkyl group and different counterion. To fabricate the dye doped polymer films, each chromophore was dispersed into polymer matrix, poly acrylic acid (PAA:MW=250000), and dissolved in ethanol and the solution was spin-coated onto the transparent microscope slide glass. These films have the characteristic of transparent "Blue Window" in the visible region ranging from 430nm to 470nm. The authors also emphasize the point that these prepared "Blue Window" dye doped polymer films have the SHG activity without electric-field poling process. The nonlinear optical coefficients were measured with the Maker-Fringe method. We use a Q-switched Nd:YAG laser as a fundamental beam and the measured harmonic power was compared with that from the quartz. The d values of these films are listed in Table 1 where dye concentration is 5 wt% and film thickness is 0.6μm. The value of d_{15} are almost the same as d_{31}. In order to investigate the mechanism of such a SHG activity of the non-poled polymer films, we examined the relation between the SH intensity and the film thickness. We found that the d value tends to decrease with the film thickness. From this experimental result, it become evident that SHG active layer exists in the vicinity of the substrate boundary. If the $1^{+}\ \alpha^{-}$ doped polymer film has the same thickness as the SHG active region, the value of second

order nonlinearity becomes d_{33}=12.9 pm/V at the chromophore concentration of 15 wt%. It is notable that the d_{33} values of these films were unvaried without any relaxation at 120℃. Since there exists the nonlinearity without electric-field poling process, no thermal relaxation of aligned dipoles occurs.

Conclusion

We have synthesized novel nonlinear organic ionic materials, pyrylium salt dyes, for blue light SHG devices. We emphasize the point that the prepared chromophore doped polymer films showed the SHG activity without electric-field poling process. The second-order nonlinearity of these non-poled films was thermally stable at 120℃.

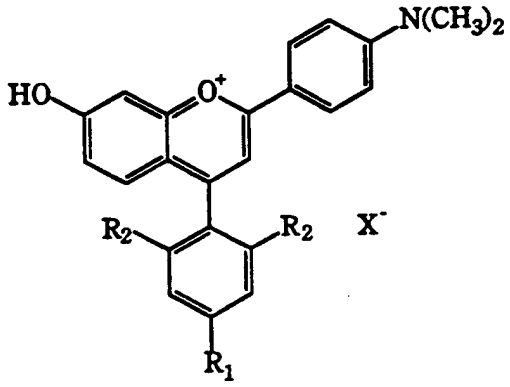

Table 1

Compound	R_1	R_2	X^-	d_{33} (pm/V)	d_{31} (pm/V)
1^+Cl^-	$CH(CH_3)_2$	H	Cl^-	0.43	0.16
1^+B^-	$CH(CH_3)_2$	H	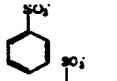	0.26	0.07
$1^+\alpha^-$	$CH(CH_3)_2$	H		0.52	0.18
$1^+\beta^-$	$CH(CH_3)_2$	H	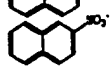	0.34	0.11
2^+Cl^-	CH_2CH_3	H	Cl^- 	0.40	0.13
$2^+\alpha^-$	CH_2CH_3	H		0.20	0.07
3^+Cl^-	$OC_{10}H_{21}$	H	Cl^-	0.57	0.17
4^+Cl^-	CH_3	CH_3	Cl^-	0.68	0.21

References

1) H.Nakayama et al, Opt.Rev.Vol.2,No.4(1995)236.
2) H.Nakayama et al, Nonlinear Optics,Vol.15(1996)407.

Holographic Zone Plate in Bacteriorhodopsin Film for Wavelength Division Beam Splitter

Yoshiko OKADA-SHUDO and François KAJZAR*
Dept. of Electronic Engneering, The Univ. of Electro-Communications
1-5-1, Chofugaoka, Chofu, Tokyo 182 JAPAN
*LETI-DEIN-SPE, CEA Saclay
91191 Gif sur Yvette Cedex FRANCE

Introduction

Molecular electronics and phonics have attracted much attention recently. Among the retinal protain bacteriorhodopsin (bR) [1], which is related to human visual pigment, is considered to be a unique candidate for a molecular device [for referrences see 2,3].

In this paper we propose a wavelength division beam splitter for photonic switching system using the photochromic property of bR. Erasable zone plate (ZP) constracted by the real-time holography in the bR film acts as focussing lens.

Holographic lens in the bR film

The absorption of a visible photon by bR triggers a photocycle [4]. After excitation with yellow light, bR passes through several short-lived intermediates to the M-state which has longest lifetime at the room temperature. The purple color of bR is bleached at M-state. Its light driven photochromic property is used in real-time holographic recording.

Figure 1 shows schematic diagram to generate the circular ZP with 515 nm-line of Ar ion laser, and to read out with 633 nm of He-Ne laser. To obtain the diverging beam, a convex lens is inserted in one of the writing beam. R denotes the distance between the point source and bR film. Circular ZP is recorded by means of the coherent superposition of two wavefronts, plane and spherical. Reading beam travels from the opposite side and irradiates the ZP, which focuses the beam on the focal point. If we input the reading beam with another wavlength, the ZP forms the image of the light source point at the corresponding focal plane. Therefore this ZP functions as a wavelength division beam splitter for multicolor signals.

Deffraction and focussing properties

In this experiment, we use the commercialized bR film (Wacker Chemical Co.Ltd.) which diameter and thickness are 15 mm and 30 μm, respectively. Initial optical density at 570 nm is 2.0 and response time is about 100 miliseconds.

The experimental arrangment employed to reduce the effect of the transmitted beam is off-axis geometry as shown in Fig.2. All three beams are adjusted to be linearly polarized and expanded to a collimated beam of a diameter of 1 cm on the sample. The intensities of the each of the writing beams I_A and I_B and the reading beam I_R are equal to 5 mW/cm². Two writing beams cross at angle of 10° ($\theta = 5°$). Reading beam incident on the ZP with Bragg angle θ_B (= 6.1° at 633 nm) focuses on the focal point, and its spotsize (FWHM) is 30 μm.

In case of inputting signal with several wavelengths from the same direction simultaneously, the incident angle does not always correspond to Bragg angle of each wavelength. Figure 3 represents the diffraction efficiency I/I_R as a function of the difference between incident angle and Bragg angle at 633 nm. The difference within 3°, the diffraction efficiency is reduced to half the maxmum value, while the spotsize remains as 30 μm. This result has clarified that the

holographic ZP can divide the signals which covered wide range of wavelength, because this difference come to about 300 nm in wavelength.

Conclusions

In conclusion, we have proposed a wavelength division beam splitter using biological photochromes bacteriorhodopsin (bR) film. We have demonstrated reading beam focused by the circular zone plate (ZP) which has generated by real-time holographic method.

While bR has a considerable light induced anisotropy, therefore bR film is able to record both intensity and polarization holograms [5-7]. It is planned, however, to consider the polarization holographic ZP for photonic switching system using polarization encoding in the near future.

References

[1] Oesterhelt, D., and Stoeckenius, W., *Nature* (London), *New Biol.*, *233*, 1149 (1971).
[2] Birge, R. R., *Annu Rev. Phys. Chem.*, *41*, 683 (1991).
[3] Bräuchle, C., Hampp, N., and Oesterhelt, D., *Adv. Mater.*, *3*, 420 (1991).
[4] Varo, G., and Lanyi, J. K., *Biochemistry*, *30*, 5008 (1991).
[5] Nikolova, L., and Todorov, T., *Opt. Acta.*, *31*, 579 (1984).
[6] Korchemskaya, E. Ya., Soskin, M. S., and Taranenko, V. B., *Sov., J., Quantum Electron.*, *17*, 450 (1987).
[7] Okada , Y., Yamaguchi, I., Otomo, J., and Sasabe, H., *Jpn. J Appl. Phys.*, *32*, 3828 (1993).

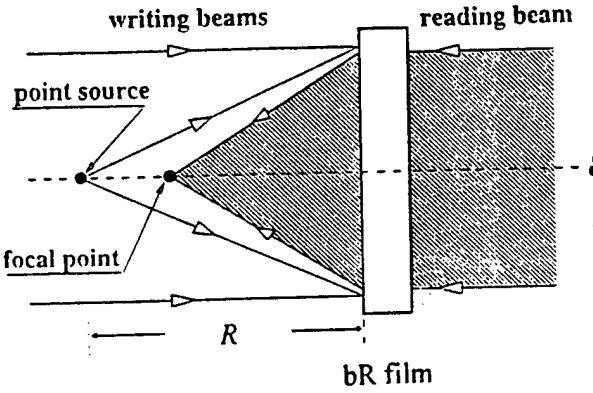

Fig. 1. Schematic diagram to generate the circular ZP.

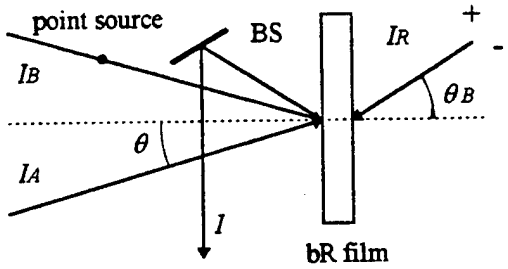

Fig. 2. Experimental arrengment.

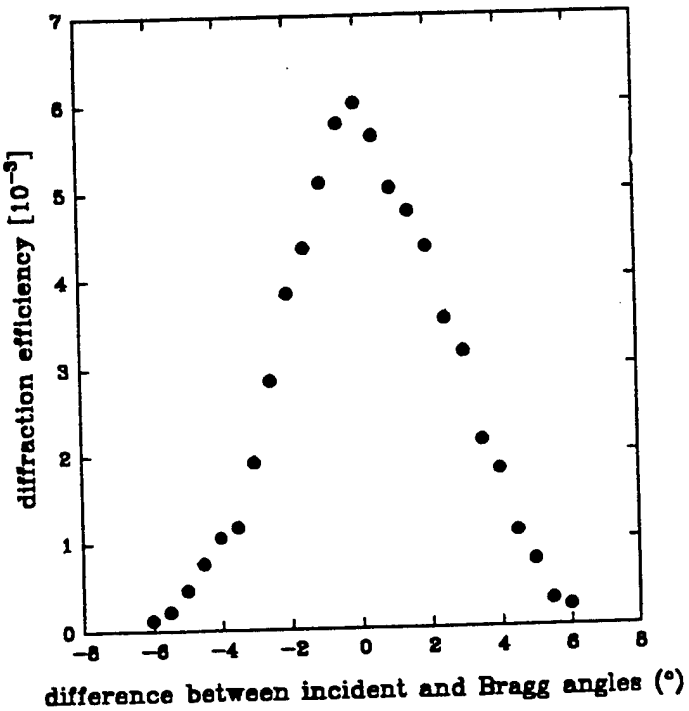

Fig. 3. Diffraction efficiency as a function of the difference between the incident and Bragg angles.

Growth, Electro-optical and Nonlinear Optical Properties of the Organic Salt 4-N,N-dimethylamino-4'-N'-methyl-stilbazolium tosylate (DAST)

F. Pan, Ch. Bosshard, S. Follonier, R. Spreiter, U. Meier, M. S. Wong, and P. Günter
Nonlinear Optics Laboratory, Institute of Quantum Electronics
ETH Hönggerberg, CH-8093 Zürich, Switzerland

4-N,N-dimethylamino-4'-N'-methyl-stilbazolium toluene-p-sulfonate (DAST) is an organic salt crystal in which the stilbazolium as the nonlinear optically active part is one of the most efficient organic chromophores. DAST crystals were already reported to have very large nonlinear optical susceptibilities[1]. The lack of reasonably large and optically homogeneous DAST crystals has prevented any accurate electro-optical characterization in earlier investigations of DAST. In this work, large size DAST crystals were employed to determine the optical quality as well as linear, nonlinear optical, and electro-optical properties.

DAST single crystals were grown from purified material by controlled temperature lowering of a seeded saturated methanol solution. Typically single crystals of dimensions of about $20x20x5mm^3$ were successfully grown. Three different optical samples with dimensions of up to about $axbxc=3x3x3mm^3$ were prepared by polishing (100), (010) and (001) faces, respectively, with a flatness of about $\lambda/4$-$\lambda/2$ (wavelength of Na line). Polarized microscopic studies showed a homogeneous extinction between crossed polarizers confirming the good optical quality of our samples.[2]

The absorption edge for light polarized along the dielectric x_1-, x_2- and x_3-axes (defined here for an absorption coefficient of $5cm^{-1}$) are at λ=700nm, 650nm and 590nm, respectively. The dispersion of the principal refractive index n_1 was re-measured and extended to wavelengths down to 700nm and up to 1535nm.

The electro-optical measurements were performed with a continuously tunable Ti:sapphire laser in the spectral range of 700nm up to 920nm, with a diode pumped YLF laser at 1313nm, and at 1535nm (model 1.5-EHA from Amoco).[3] The interferometric measurements were in good agreement with experiments by field-induced birefringence with crossed polarizers ($\pm 45^o$). As expected from the molecular arrangement, the electro-optical coefficients r_{11} and r_{21} were found to be quite large with values of 47±8pm/V and 21±4pm/V at λ = 1535nm, and 77±8pm/V and 42±5pm/V at λ = 800nm, receptively. The largest effective electro-optic coefficients, $(n^3r)_{eff}$, are $n_1^3 r_{11}$ = 450±70pm/V and 1050±100pm/V at 1535nm and 800nm, respectively (for (010) plates). We found that our experimental results deviate from the expected theoretical expectations both in magnitude and in the wavelength dispersion. This observed discrepancy is currently under investigation. In addition, our values for r_{11} are considerably smaller than the reported measured one of e.g. r_{11} =400 pm/V at λ =820nm.[1]

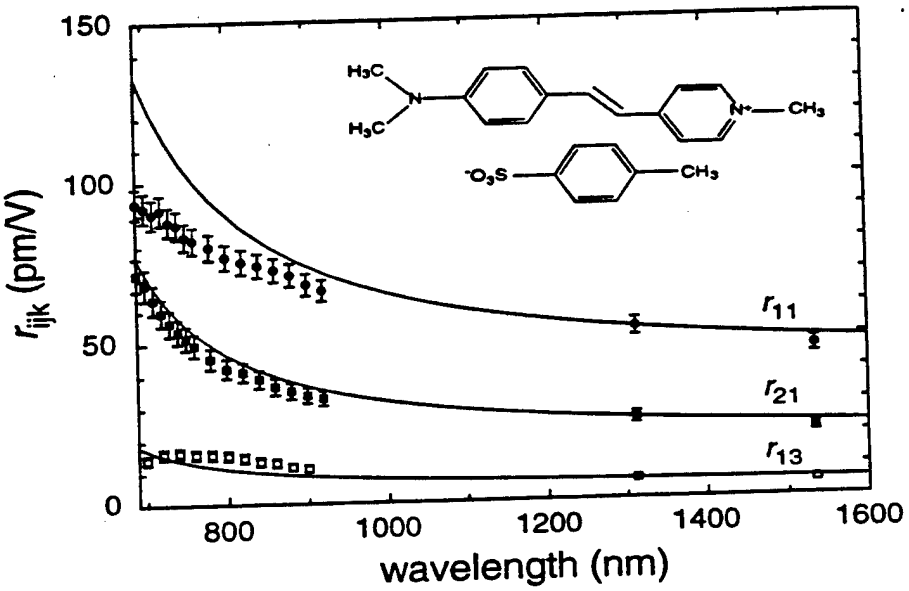

Fig.1 Dispersion of the electro-optic coefficient r_{11} (●), r_{21} (■) and r_{13} (□) of DAST. The experimentally measured dispersion of the electro-optic coefficients were fitted by a theoretical dispersion calculated according to the Sellmeier function and the function based on the two-level model (solid line).

A standard Marker fringe technique was employed to confirm the quality of our samples. We measured the largest nonlinear optical coefficient along the polar x_1-axis, d_{11}, with c- and b-plates of DAST at λ=1542nm. Within the experimental error, these value are in agreement with the data reported before, d_{11}=840±200 pm/V (d_{11}=0.4 pm/V of quartz as a reference value)[4]. In addition, using a (100) plate, type-I phase-matching was observed for second-harmonic generation with an effective nonlinear optical coefficient of d_{eff}= 8±2pm/V at λ=1542nm.[2] Furthermore, by using our refractive index data, the interesting phase matching conditions were found at 1.5 and 1.3μm. Results on phase-matching experiments using appropriately cut samples will also be reported.

References

1 S. R. Marder, J. W. Perry, and C. P. Yakymyshyn, Chem. Mater. **6,** 1137-1147 (1994).

2 F. Pan, M. S. Wong, C. Bosshard, and P. Günter, Adv. Mater. **8** (No. 7), (1996).

3 F. Pan, G. Knöpfle, C. Bosshard, S. Follonier, R. Spreiter, M. S. Wong, and P. Günter, Appl. Phys. Lett. (July, 1996).

4 C. Bosshard, G. Knöpfle, P. Prêtre, S. Follonier, C. Serbutoviez, and P. Günter, Opt. Eng. **34,** 1951-1960 (1995).

Second Harmonic Chiral Organic Molecular Dipoles with Gigantic Nonlinearities for Imaging Electric Fields Associated with Cellular Membrane Potentials.

Peleg G.[1] , Lewis A.[1] , Loew L.[2] .
[1]Division of Applied Physics., The Hebrew University of Jerusalem, Jerusalem, (ISR). [2]Department of Physiology, University of Connecticut Health Center, Connecticut, (USA).

In this report we develop a new and unique methodology, based on the nonlinear optical property of second harmonic generation, for measuring the membrane potential of cellular membranes. The cellular membrane potential is an excellent measure of the physiology and a sensitive monitor of communication within and between cells. The magnitude of the electric field across a biological membrane with a nominal thickness of 4.5 nm is on the order of 10^5 V/cm. We show that second harmonic generation is a singular optical technique to measure such electrical fields across membranes.

Previously the optical methodologies that have been employed have been based on linear optics such as fluorescence and absorption. These methods suffered from several limitations in their applicability for monitoring cellular membrane potentials. These limitations include: (1) the relatively poor sensitivity of the linear absorption and fluorescence of potential sensitive dyes to membrane potential; (2) the background contribution of the non-membrane bound dye molecules; (3) the relatively high cross -section for bleaching the dyes in normal oxygenated physiological conditions; (4) the damaging photoreactions of some potential sensitive dyes such as merocyanine 540; (5) the highly scattering nature of visible light that prevents penetration into the depths of biological media; and (6) the limitations on microscopic resolution that can be obtained with conventional visible light microscopy without signal limiting confocal techniques.

Many of these problems are overcome in this paper by the application of a non-linear optical process to monitor membrane potential. Specifically, the second order non-linear optical process, second harmonic generation, is shown to be very sensitive to membrane potential. In addition, second order processes require symmetry breaking surfaces (Shen, 1989), such as cell membranes (Huang et al., 1989), and thus, only dye molecules with a distribution between the two layers of a bilayer membrane that lack a center of inversion will produce the directed signals associated with second harmonic generation. Furthermore, the infrared excitation does not affect photoexcitable molecules in and around cells when their one or two photon absorptions occur out of the wavelength regimes that can be significantly excited by the 1.06 μ wavelength of this laser. Also, this radiation can penetrate deeper into cellular media without causing destructive photodamaging effects. Finally, the use of non-linear processes in this context results in naturally high resolution in x,y and z and, as has recently been suggested, this resolution can approach 75 nm for appropriate geometries of excitation and detection (Hell, 1994).

The molecular probes that we use for investigating the electric fields in a cell membrane have been specifically designed to anchor into the cell membrane and to have gigantic induced dipoles.The probes are anchored in a coherent order and asymmetrically in the interface which is the cell membrane. No contribution from floating dye is detected. The dyes were designed by the use of molecular orbital calculations that allowed the prediction of the molecular structures that would give the largest light induced dipole alterations, (Huang et. al., 1988). This, together with the chirality of the molecules not only results in large $\chi^{(2)}$ but also ensures a very special response to changes in membrane potential.

We performed nonlinear scattering and microscopical imaging of the stained cells and thus used both the surface selectivity and both the improved resolution of the SHG process. The light source was a 1.064 μ Nd:YAG operated in a Q-Switched - Mode Locked. We used a photomultiplier detector together with a boxcar averager&chanel integrator to collect the SHG signal. The microscope was equipped with a special designed 3D piezo stage that could automatically scan the stained cell membranes. The wavelengths of the nonlinear effects were scanned using a compact monochromator attached to the photomultiplier.

Photostability of Organic Dye-Doped Polymer Optical Fiber

G. D. Peng, Z. Xiong and P. L. Chu

School of Electrical Engineering, University of New South Wales
Kensington, NSW 2052, Australia

Photostability of dye-doped polymer optical fibre is experimentally investigated. It is found that photobleaching induced by the irradiation of an Ar laser output could be partially even fully reversible, depending on experimental conditions. Also, a spectrally asymmetrical decay in the fluorescence spectra, which is associated with irreversible photobleaching, has been observed. Various factors which may lead to the above observation will be discussed.

The unique nonlinear optical properties, such as large nonlinearities and fast response times, of organic materials have attracted considerable research attention for a long time. Organic dyes, especially when they are incorporated in solid-state polymeric matrix, are very promising nonlinear optical materials for a wide range of applications, e.g. optical modulation, all-optical switching, optical amplification and laser.

Optical fibre provides the best configuration for nonlinear device applications where light is confined in a small area for long propagation length. This facilitates the accumulation of sufficient nonlinear effect to activate a particular process. Previously, organic dye-doped polymer optical fibres were fabricated for applications in all-optical switching [1] and in optical amplification [2,3]. One of the main concern in developing polymeric nonlinear optical materials is their photostability. It is well known that organic dyes could be bleached under intense irradiation, and that solid-state dye-doped polymer materials usually have limited lifetime. However, the photobleaching mechanism is not well understood and it may vary from one case to another. Definitely, photobleaching is a fundamentally important problem and needs to be investigated with great efforts, both theoretically and experimentally.

We carried out experiments to investigate the photostability of the dye-doped polymer fibres. In our experiment, an Ar laser of more than 30mW output is used as light source and its output is launched into a single-mode silica fibre coupler with a splitting ratio of 6:94. The higher power output end of the coupler is butt-connected to the doped polymer fibre under test. This connection between the coupler and polymer fibre is made permanent. The lower power output end of the coupler is monitored with a power meter, to ensure constant power launching into the coupler and then to the polymer fibre. Monochromator and lock-in detection technique are used to collect the fluorescence over appropriate wavelength range. The fluorescence decay of various fibre samples and under various conditions are systematically investigated to study the photobleaching behaviour of the dye molecules in the polymer fibres.

Some interesting photobleaching behaviours have been observed. For example, we observed that, under many circumstances, the photobleaching is not readily reversible. In these cases, if there is a self-healing effect to the photobleaching, it is not significant. Importantly, we also observed cases that photobleaching is significantly reversible. As a typical case shown in Fig.1, the fluorescence of a rhodamine B-doped polymer fibre of 20cm length is collected at different times, when it is under constant irradiation of 514nm with optical intensity about 280W/cm^2. It

is obvious that the fluorescence is gradually decaying as the irradiation time is increasing. However, when we stopped irradiating the fibre for a period of 16 hours, we observed that its fluorescence intensity (curve d in Fig.2) was mostly recovered to its pre-irradiation level (curve a in Fig 1. and 2). In this particular case, a full reverse of the photobleaching processing is observed. The possible physical or chemical process associated the reversible photobleaching will be discussed.

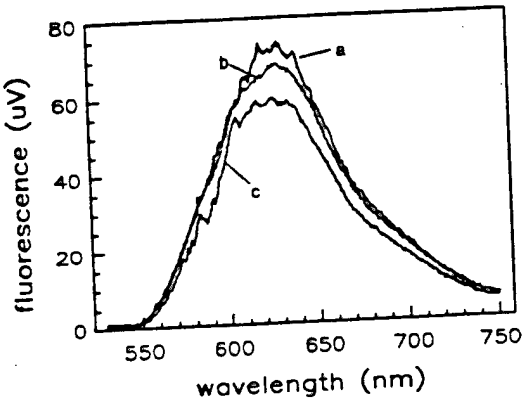

Fig.1 Fluorescence decay for various irradiation times: (a) 0 hour; (b) 3 hours; (c) 6 hours.

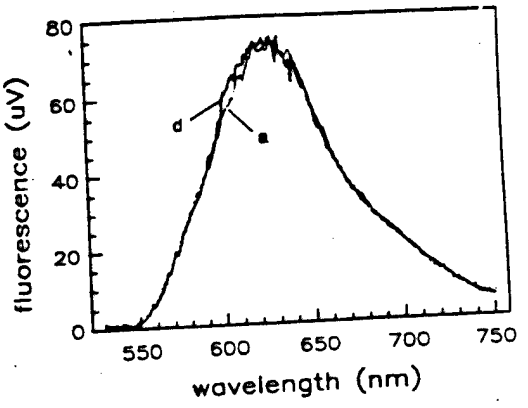

Fig.2 Comparison of fluorescence intensity: (a) before irradiation, i.e. (a) in Fig.1; (d) after 6 hours irradiation and then 16 hours without irradiation

Another finding from the experiment is the observation of an asymmetrical change (degradation) in the fluorescence spectra. Shown in Fig.3 is the fluorescence of a partially bleached rhodamine B fibre (the fluorescence is about 50% that of a fresh fibre), irradiated at optical intensity of about 420W/cm^2, for various times. It is clear that the fluorescence around 600nm decays significantly slower than that 680nm. This behaviour indicates that, now the irradiation induced structure change at the molecule level, hence their energy levels. Different from the situation in Fig.1, no appreciable reversible photobleaching is observed. Further investigation is to establish the relation between the spectral change of fluorescence and structural change of molecules. It is hoped the factors affecting photobleaching are identified and optimal conditions for specific applications of dye-doped fibre are found.

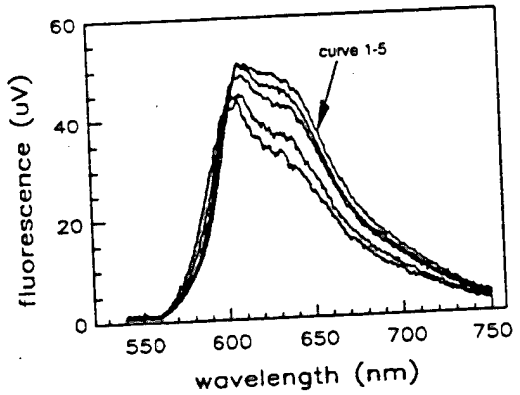

Fig.3 Fluorescence decay for various irradiation times: (1) 0 hour; (2) 1.5 hours; (3) 3 hours; (4) 6 hours; (5) 10 hours.

References

[1] M. G. Kuzyk, U. C. Paek and C. W. Dirk, "Guest-host polymer fibre for nonlinear optics", Appl. Phys. Lett. 59(8), 902-904, 1991

[2] A. Tagaya, Y. Koike, T. Kinoshita, E. Nihei, T. Yamamoto and K. Sasaki, "Polymer optical fibre amplifier", Appl. Phys. Lett. v.63, p.883

[3] G. D. Peng, P. L. Chu, Z. Xiong, T. Whitbread and R. P. Chaplin, "Dye-doped step-index polymer optical fibre for broadband optical amplification, accepted for publication, 1996

Optical Dispersion in a Second Order Nonlinear Optical Polymer

P. Prêtre, L.-M. Wu, D. Yankelevich and A. Knoesen

Dept. of Electrical and Computer Engineering, University of California, Davis
Davis, CA 95616

Phone: (916) 754 9249, Fax (916) 752 8428, e-mail: pretre@ece.ucdavis.edu

We have investigated anomalous dispersion effects in dye doped nonlinear optical (NLO) polymers. The linear optical dispersion of biphenyl-amino-tricyano-vinyl-aniline (PhTCV) as guest molecule in different host materials was measured by variable angle spectroscopic ellipsometry. Dispersion of the electro-optic response was determined using Fabry-Pérot etalon devices.

PhTCV shows an almost negligible absorption at the second harmonic wavelength of ultra-short pulse Ti:Sapphire lasers; see figure below for an absorption spectrum. These types of chromophores are therefore very interesting for the diagnostics of such laser sources with pulse lengths on the order of 10 fs. To generate an undistorted pulse by second harmonic generation a short interaction length is required, limited by a pulse preservation length (i.e. the maximum interaction length wherein the pulse widths of second harmonic matches the fundamental pulse). Therefore a large second order nonlinearity interacting over this pulse preservation length is preferred. Thin poled NLO polymer films meet the first requirement. We explored anomalous linear optical dispersion effects in order to increase the coherence length of NLO polymers up to the pulse preservation length. At a doping level of 5% by weight, the coherence length of a PhTCV/PMMA guest-host system is approximately 50 - 60 μm at a fundamental wavelength of λ = 800 nm.

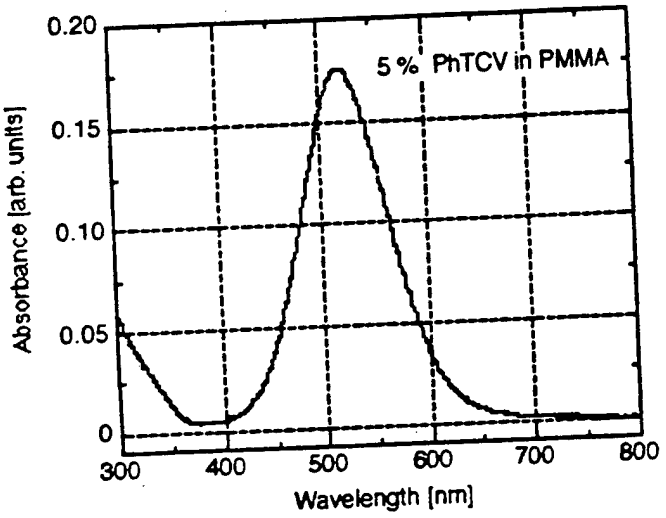

Knowledge of the dispersive behavior of the electro-optic coefficient is of particular interest in resonance enhanced electro-optic modulator devices. An absorption maximum at around 520 nm renders the PhTCV chromophores attractive candidates for modulation close to the absorption band allowing for full exploitation of the intrinsic nonlinear optical properties of organic molecular materials.

P-29 **Relaxation-processes of chromophores in polymer matrices determined by electro-absorption experiments**

S. Saal, S. Großmann, T. Weyrauch, and W. Haase

Technische Hochschule Darmstadt, Institut für Physikalische Chemie, Petersenstraße 20, 64287 Darmstadt, Germany

The relaxation of the dipolar order is an important property of poled NLO-polymers. In order to understand the general behavoiur of poled polymers the study of the relaxation of chromophores is an important task. To measure the dynamics of the chromophores dielectric spectroscopy has some disadvantages since this method is sensitive to all dipole groups in the sample. The electroabsorption technique, however, is selectively sensitive to the chromophores.

Assuming a rigid sample the electroabsorption spectroscopy allows one to determine the difference of the dipole moment $\Delta\mu$ and the difference in polarizability $\Delta\alpha$ between optical ground and excited state due to the quadratic Stark effect in isotropic samples. In poled polymers the linear Stark effect is also observable. It has been shown that the polar order parameter $\langle\cos\theta\sin^2\theta\rangle$ may be determined by the electroabsorption technique, which allows for the measurement of the relaxation of the polar order.

In the case of a non-rigid sample in addition to the Stark effect a contribution to the electroabsorption occurs due to the orientation of the molecules in the electric field, which was shown in first experiments comparing the electroabsorption spectra determined by application of an ac and a dc field simultaneously and an ac field only. The orientation of the chromophores by the electric modulation field is observable in the quadratic-in-field measurements by two means:

(i) a contribution proportional to the absorption spectrum due to the linear dichroism of the molecules

(ii) an apparent change of $\Delta\alpha$ due to the polar orientation of the chromophores.

These contributions may be distinguished by the analysis of the spectral dependence of the elctroabsorption effect.

Our electroabsorption spectrometer allows for the variation of the modulation frequency in the range of 10 mHz to 10 kHz. Measurements were performed on

guest host systems which consist of 4-amino-4'-nitroazobenzol in polymethacrylat. The samples were prepared by spin coating on ITO covered glass substrates. The second electrode was prepared by sputtering gold layers onto the polymer surface. Typical thickness of the films was about 1µm. The strength of the modulation field was about 50V/µm. The films were aged before the measurements at 100°C to have comparable conditions in all samples.

In Fig. 1 the amplitude of the orientational contribution to the electroabsorption spectra is presented in dependence of temperature and modulation frequency. In Fig. 2 the apparent change in $\Delta\alpha$ is demonstrated.

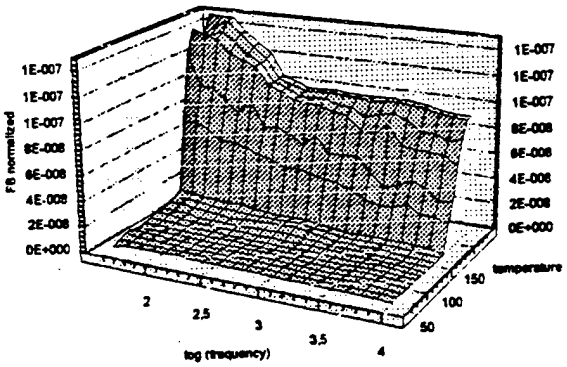

Fig. 1

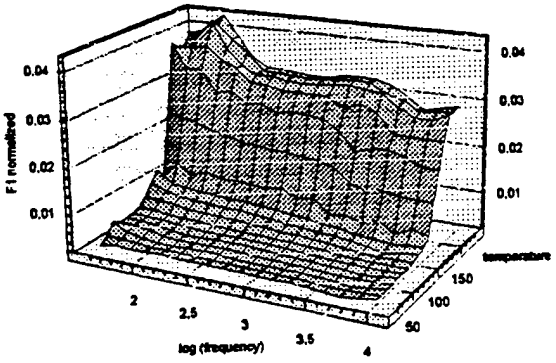

Fig. 2

In Fig. 3 the response of the chromophores to the electric field is shown as function of frequency for a temperature of 110°C. The analysis according to a cole-cole function leads to a chromophore relaxation frequency of 202Hz (Fig. 4).

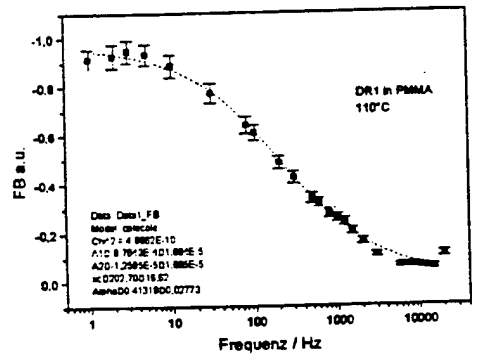

Fig. 3

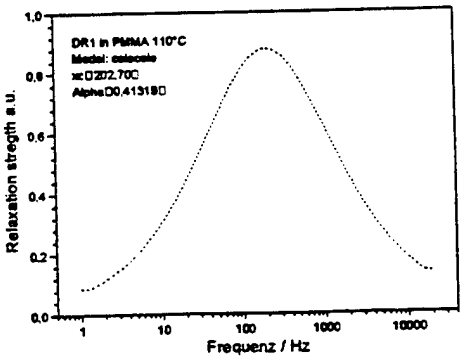

Fig. 4

Thus it could be shown that the relaxation of the chromophores can be measured by this optical method. The technique is sensitive to an amount of less than 1 wt-% of dye.

Femtosecond Z-scan and degenerate four-wave mixing measurements of the real and imaginary part of the third-order nonlinearity of soluble conjugated polymers.

M. Samoc, A. Samoc, B. Luther-Davies, Z. Bao[1)], L.Yu[1)], B. Hsieh[2)], and U. Scherf[3)]

Australian Photonics Cooperative Research Centre, Laser Physics Centre, The Australian National University, Canberra, ACT 2606, Australia

1) Department of Chemistry, The University of Chicago, 5735 S. Ellis Avenue, Chicago, Il 60637, USA
2) Xerox Corporation, The Wilson Center for Research and Technology, 114-39D Webster, NY 14580, USA
3) Max-Planck-Institut fuer Polymerforschung, Ackermannweg 10, D-55128 Mainz, Germany

We have investigated third-order nonlinear optical properties of several π-conjugated polymers with a goal of reliable determination of the parameters characterizing the nonlinearity such as the real and imaginary part of the nonlinear refractive index n_2 and the one-photon loss and two-photon loss merit factors W and T. Most of these measurements were performed at 800 nm using 100 femtosecond pulses from an amplified Ti-sapphire system.

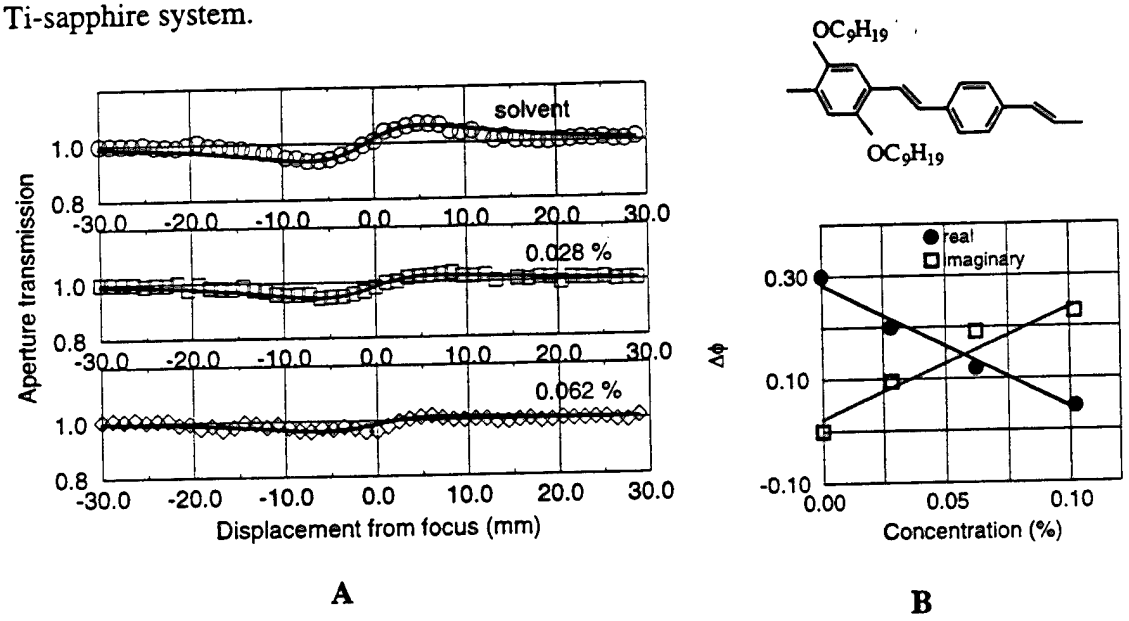

Fig.1 Closed aperture Z-scans (A) on a 1mm cell filled with the solvent (1,1,2,2-tetrachloroethane) and solutions of a soluble PPV polymer with the formula given above. From the dependence of the nonlinear phase change on the concentration of the polymer (B) these measurements give n_{2real}=-2.6x10^{-12} and n_{2imag}=1.1x10^{-12} cm^2/W for the real and imaginary part of n_2 of the polymer.

We describe here results of investigations of several soluble conjugated polymers, namely 2,5-substituted poly(*p*-phenylenevinylenes) including MEH-PPV and a soluble ladder poly(*p*-phenylene) polymer. In particular, Z-scan measurements on polymer

solutions were found to be useful for the determination of the complex nonlinear refractive index. The results could be verified by time-dependent degenerate four-wave mixing studies performed both on solutions and on thin films of the polymers. We find generally a good agreement between the values of n_2 determined from Z-scan and those from DFWM. Examples of the experimental results are shown in Fig.1-3.

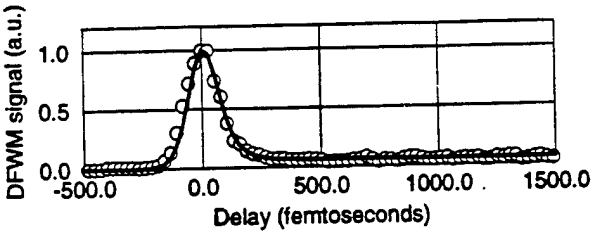

Fig.2 An example of a time-resolved DFWM scan on a 0.5 μm thick film of the same soluble PPV as in Fig.1. The solid line denotes a fit assuming a 100 fs laser pulse and a small contribution of a 30 ps lifetime excited species

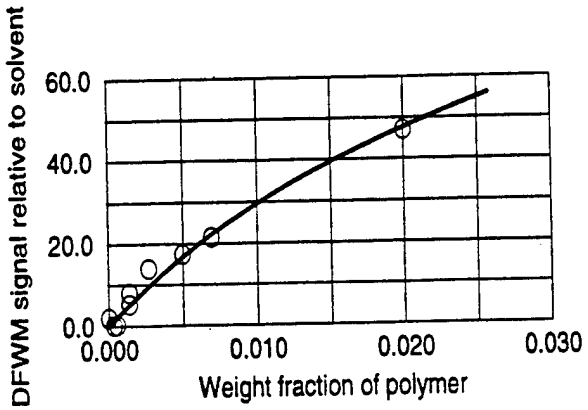

Fig.3 Concentration dependence of the DFWM signal from solutions of a ladder poly(p-phenylene) polymer:

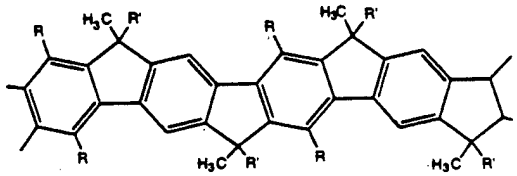

in chloroform at 800 nm. $|n_2|$ of this polymer is $5x10^{-13}$ cm^2/W

The results indicate that the nonlinear refractive index on the order of 10^{-12} cm^2/W can be readily obtained in various conjugated polymers. However, T factors larger than unity are commonly encountered within the two-photon absorption ranges of these compounds. High values of the real and imaginary part of n_2 are also measured by Z-scan and DFWM at 800 nm in base and salt forms of polyaniline [1,2]. Strong one-photon absorption of polyaniline leads, however, to unfavourable values of the one-photon merit factor W. On the other hand, the W factor for the soluble poly-(*p*-phenylenevinylenes) is two to three orders of magnitude better than that for polyaniline.

References

1. M. Samoc, A. Samoc, B. Luther-Davies, J. Swiatkiewicz, C.Q. Jin and J.W. White, Optics Letters, 20,2478 (1995)

2. A. Samoc, M. Samoc, B. Luther-Davies, C.Q. Jin and J.W. White, XX International Quantum Electronics Conference, IQEC'96, Sydney, 14-19 July, 1996

Quantum Chemical Study of Fluorine-Containing Chromophores

S. Schrader, A.H. Otto *, M. Pfeiffer **

Institut für Angewandte Chemie Berlin-Adlershof, Rudower Chaussee 5, D-12484-Berlin
* QC-Center, Johanna-Tesch-Str. 28, 12439-Berlin,
** Max-Born-Institut für Nichtlineare Optik und Kurzzeitspektroskopie, Rudower Chausse 6, 12489 Berlin,

The introduction of fluorine into organic dyes leads to a considerable change of the refractive index. Dependent on the degree of fluorination index changes of more than 0.1 are possible. Therefore fluorination is a powerful tool of index tuning which could be of interest in optimization of photonic devices. The modification of donor-acceptor substituted dyes with fluorine raises the question whether the high values of second order hyperpolarizabilities will be retained or not. In order to obtain a deeper insight into this question a quantum chemical study on the semi-empirical level of some new fluorine containing dyes was carried out, and the results are compared with experimental findings [1]. The studied dyes were (4-trifluoromethyl)phenyl-(4′-dimethylamino)phenyl azomethine (1), (4-dimethylamino)phenyl-(4′-trifluoromethyl)phenyl azomethine (2), (4-dimethylamino)phenyl-(2′,3′,5′,6′-tetrafluoro-4′-trifluoromethyl)phenyl azomethine (3), 4-trifluoromethyl-4′-dimethylamino-azobenzene (4), and 4-trifluoromethyl-4″-dimethylamino bisazobenzene (5).

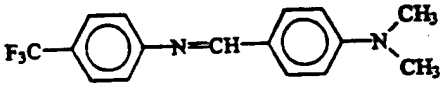

1

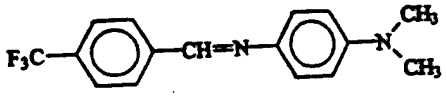

2

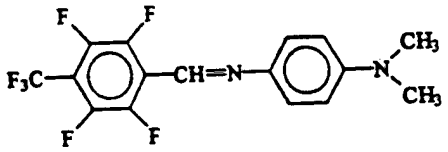

3

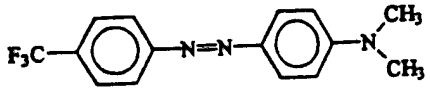

4

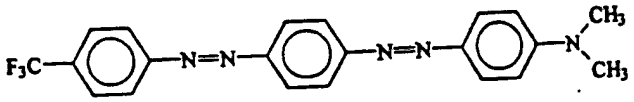

5

Quantum chemical calculations have been performed using three modern methods: MNDO, AM1, and PM3. First their reliability in modelling structural and spectroscopic data for compounds 1-5 was tested. As a result MNDO was excluded from further investigations, since it is unable to locate planar geometries for the considered dyes. Applying AM1 and PM3 a thorough conformational study was carried out with the aim to find for each compound the absolute minimum at the energy hypersurface (e. h. s.).
As a result of this optimization we found that all systems except compound 3 have absolute minimum geometries that possess planarity of the rings. Nevertheless, nonplanar structures also cor-

respond to stationary points on the e. h. s.. For the most stable conformers normal mode frequencies were calculated. While PM3 established minima for all compounds but not for dye no. 5, there were always negative frequencies in the vibrational spectra when AM1 was used. All negative eigenvalues of the Hesse matrix are of the order of 10-20 cm^{-1} or so. For the geometries that are the lowest in energy, single point calculations were performed allowing single excitations and taking into account 14 highest occupied and 14 lowest unoccupied orbitals. This restricted configuration interaction was used to calculate the ultraviolet (electronic) spectrum. A satisfactory agreement was obtained between calculated and measured strongest absorption peaks. The only exception was found, again, for compound 3, were an essential disagreement with the experiment was obtained. Therefore, the absolute minimum structure was changed by the most stable planar geometry and a much better agreement was achieved. The deviation from the experimental values is 5-15%. It seems that PM3 is better in predicting the electronic spectra since AM1 exhibits a second peak that is even somewhat higher in intensity than the "true" peak corresponding to the experimental region.

Calculated dipole moments are, generally, fairly high. They amount to 6-7 D (AM1) and 5-6 D (PM3) and are higher than the experimentally determined values which are equal or less than 4 D for the dyes 1-4. This can be explained by a solvent effect in the experiment. For dye no. 5 the experimental value was about 9 D but the calculated dipole moment reached only lower values between 6 and 7 D depending on the applied method.

Second order hyperpolarizabilities were calculated using MOPAC. The conformations of dye 1-5 optimized in the way described above were used for these calculations. While the calculated values for dye 1-4 (18 .. 22 * 10^{-30} esu) were somewhat less than half the experimental value again the calculated value (32 * 10^{-30} esu) for dye no. 5 was to small by more than a factor of 4 as compared to the experimental value. It is quite clear that the used numerical method did not take the solvent effects into account which can explain this high discrepancy but it also illustrates that deviations are more pronounced for the higher conjugated molecules.

The main conclusion of the present study is that fluorine containing chromophores show second order hyperpolarizabilities as high as the analoguous, well-known donor-acceptor substituted azobenzene or stilbene chromophores. Perfluorination of the acceptor side of the molecule does not lead to twisted structures which would be connected with less conjugation and a much lower hyperpolarizability. Therefore these chromophores can be used for purposes where high hyperpolarizabilities but low refractive indices are necessary. One example are waveguide structures where the figure-of-merit depends on the third power of the inverse refractive index.

[1] S. Schrader, D. Prescher, "Chemical Substitution and Optical Nonlinearities of Organic Chromophores", ICONO'3, 16-20 December 1996, Marco Island, Florida

CHEMICAL SUBSTITUTION AND OPTICAL NONLINEARITIES OF ORGANIC CHROMOPHORES

Sigurd Schrader and Dietrich Prescher*

Institut für Angewandte Chemie Berlin-Adlershof e.V., Rudower Chaussee 5, 12484 Berlin-Adlershof ;
*Universität Potsdam, Inst. f. Festkörperphysik, FG Fluorpolymere, Rudower Chaussee 5, 12484 Berlin-Adlershof

The influence of chemical substitution on linear and nonlinear optical properties of organic chromophores are discussed. Different examples are taken to illustrate the influence of size and the pecularities of the conjugated π-electron system like conjugation length or incorporation of hetero-atoms. Finally property changes by substitution with pendant groups are reviewed. Especially new fluorine-containing chromophores for polymeric guest-host-systems of the type:

$$F_3C - C_6Z_4 - X = Y - C_6H_4 - N(CH_3)_2$$

with	X, Y:	N			
or	X:	N	and	Y:	CH,
or	X:	CH	and	Y:	N,
and	Z:	H	or		F.

are considered. The influence of the fluorinated acceptor moity on the nonlinear optical properties is studied for the azo- and azomethine-chromophores, respectively. In addition, chromophores with perfluorinated benzene ring in the conjugated part of the chromophore were involved in the investigations.

Quantum chemical calculations were carried out in order to correlate molecular geometry with linear and nonlinear optical properties [1]. On a semi-empirical level the most probable conformations were determined, which do not show imaginary eigenvalues in the frequency analysis. These conformations, which are lowest in energy, were used for single point CI-calculations taking the 14 highest occupied and 14 lowest unoccupied orbitals into account. The results give a crude estimate for the lowest energy electronic transition as can be concluded from the comparison with the measured absorption spectra. The calculated transition wavelength always deviates from the measured value by a few nonometers up to some tens of nanometers which can be explained by the influence of the solvent on the molecule during experiment.

Comparing experimentally determined hyperpolarizabilities with values as calculated by semi-empirical methods using MOPAC similar deviations can be recognized. So the quantum chemical calculations give only an estimate of the respective molecular hyperpolarizabilities.

For the fluoro-chromophores molecular hyperpolarizabilities were determined by solvatochromic measurements. It was found that the optical nonlinearities are smaller if the X- and Y-moities differ which is connected to a less conjugated ground state as compared to the case of equal X- and Y-substitution. So the azomethine dyes show static second order hyperpolarizabilities of about 40 * 10^{-30} esu while the azo dye reaches values of about 60 * 10^{-30} esu. The extension of the conjugated system leads to a remarkable increase up to 140 * 10^{-30} esu for the bisazo dye. The corresponding dyes having stilbene like structure have higher hyperpolarizabilities (>70 * 10^{-30} esu) but are photochemically less stable.

[1] S. Schrader, A.H. Otto, M. Pfeiffer, Poster: "Quantum Chemical Study of Fluorine-Containing Chromophores", ICONO'3, 16-20 December 1996, Marco Island, Florida

CHARACTERIZATION OF OMBE-GROWN PTCDA THIN FILMS ON AU(111) SURFACES

F. Sellam, T. Schmitz-Hübsch, M. Hoffmann, R. Staub, T. Fritz, K. Leo
Institut fuer Angewandte Photophysik, Technische Universitaet Dresden, D-01062 Dresden (Germany)

In recent years, there has been an increasing interest in the investigation of molecular beam deposition of organic molecules as a new method for preparation of ultrathin well-ordered organic layers. These films exhibt interesting optical and electronic properties and represent a novel class of materials for molecular electronics.
We report on the growth of monolayers of the organic molecules perylene-3,4,9,10-tetracarboxylic-dianhydride (PTCDA) on Au(111) surfaces by Organic Molecular Beam Epitaxy (OMBE). Gold thin films deposited on freshly cleaved mica (0001) surfaces were investigated in situ by RHEED. The RHEED patterns show typical streaks indicating a smooth, single-crystal surfaces. The PTCDA thin films grown by OMBE onto these surfaces have been characterized in situ by RHEED and STM. The STM-images show an epitaxially grown monolayer and multilayers of flat lying PTCDA molecules with two molecules per unit cell. Similar to graphite [1] one finds two phases of PTCDA. The two phases have different rotation angles with respect to the substrate and differ slightly in their lattice parameters. The detailed crystallographic structure has been determined by means of the Fourier transformation. Additional structural data were obtained by RHEED.
The optical properties of the MBE-grown PTCDA layers were compared with polycristalline PTCDA films prepared in a HV chamber onto amorphous transparent substrates (glass, polymeric sheets). In case of the organic layers on single crystalline Au substrates the absorption was calculated from reflection measurements, using a rather simple model for the optical properties of a thin absorbing layer on a mirror-like non-transparent substrate. Thus a comparison between dye layers on transparent substrates and the highly reflective Au substrates is possible. Both absorption and emission spectra show remarkable differences between the ordered and disordered layers. The differences are discussed in terms of structure [2] and quenching effects caused by the metal.

[1] A. Hoshino, S. Isoda, T. Kobayashi, J. Appl. Phys. **76**, 4113 (1994)
[2] L.-K. Chau, C. D. England, S. Chen, N. R. Armstrong, J. Phys. Chem. **97**, 2699 (1993)

P-34

THE DESIGN OF POLYMERS INCORPORATING DITHIENYLPOLYENE AND THIENYLENE VINYLENE REPEAT UNITS : BIPOLARONIC ENHANCEMENT OF THIRD ORDER NONLINEARITY AND POTENTIAL PHOTONICS APPLICATIONS

Charles W. Spangler[a], Mingqian He[b] and Carl W. Dirk[c]
[a] Department of Chemistry and Biochemistry, Montana State University, Bozeman, MT 59717
[b] Department of Chemistry, University of Southern California, Los Angeles, CA 90089
[c] Department of Chemistry, University of Texas at El Paso, TX 79968

During the past ten years, considerable progress has been made on the oligomeric modeling of polaronic and bipolaronic charge state formation in electroactive polymers such as [2,5-thienylene vinylene]. Dithienylpolyenes containing up to ten double bonds have been synthesized, and when oxidatively doped in solution form extremely stable bipolaron-like dications. These polyenes can solubilized by incorporation of long-chain alkyl substituents on the 3 and 4 positions of each thiophene ring, or by incorporating mesomerically interactive alkylthio groups on the terminal alpha positions of each thiophene ring. For the longest polyenes this represents a potential delocalization pathway of up to 30 atoms. Recent experimental measurements of the third order nonlinearity in the dithienylpolyene series by degenerate four wave mixing (DFWM) for both the neutral and oxidized species have confirmed the previous theoretical prediction of bipolaronic enhancement.

While it is possible to prepare guest-host composites of the dithienylpolyenes in either polycarbonate or polystyrene, yielding optical quality thin films via spin-coating onto silica wafers, the percent active NLO component is usually limited to ca. 20% due to long-term phase separation. This is exacerbated for the doped polyenes due to their ionic character. For these reasons, we have most recently attempted to incorporate these NLO-active chromophores into copolymer structures which maximize the percentage NLO component. In this paper we will describe several such approaches including both polyester, polyurethane and dialkylsilanyl formulations. One question that arose early in this work was whether each and every chromophore could be oxidized to the bipolaronic form. Comparison of the oxidized copolymers to their neutral counterparts, and to the neutral and oxidized model compopunds shows conclusively that each and every dithienylpolyene subunit is oxidized to the bipolaronic form.

One additional problem that was apparent during the original DFWM mixing studies of the third order nonlinearity in the dithienylpolyene series was the relative degrees of resonant enhancement in the neutral and oxidized species as the conjugation length was systematically increased from 3 to 10 double bonds, since the measurements could only be carried out at 532 and 1064 nm. For this reason, we have now calculated the third order hyperpolarizabilities for the neutral and oxidized species in this series at the AM1 level. These calculations confirm that (1) these molecules are among the most nonlinear small molecules yet studied, (2) that the nonlinearity has not yet saturated for the longest polyene studied, and (3) bipolaronic enhancement comparable to that observed experimentally has been confirmed. The combination of these calculations with the previous DFWM results indicate that third order hyperpolarizabilities of ca. 10^{-30} esu are possible for synthetically accessible polyene lengths. For these reasons, the new copolymers discussed above represent an attractive new series of materials with potential applications in such areas as optical limiting and sensor protection derived from reverse saturable absorption (RSA) based on photogeneration of highly absorptive bipolaron states.

Thermally Poled Silica-Based Glass Thin Film with Large Second-Order Nonlinearity

Okihiro Sugihara, Makoto Nakanishi, Naomichi Okamoto, Chikara Egami

Faculty of Engineering, Shizuoka University
3-5-1 Johoku, Hamamatsu 432 Japan

Introduction

Recently second-order nonlinear optical property of thermally poled silica-based glass have been investigated. Silica glass has some advantages over conventional crystallographic material like $LiNbO_3$ and quartz : its higher transparency, lower cost, lower refractive index (relative permittivity), and higher processability. Moreover, large second-order nonlinearity in poled silicate glass thin film[1] and large linear electrooptic property in UV-excited poled fiber[2] were reported.

In this study, highly active second-order nonlinearity one order of magnitude larger than that of quartz is demonstrated from a series of thermally poled silica-based glass thin film. Green and blue light generations by Cerenkov-type phase-matched frequency doubling are realilzed.

Experiments and Results

Glass thin films used to obtain the results in this study were fabricated by sol-gel processing and poled at 300 deg. As a dopant Ge or Ti was mixed with the silica glass. The second-order nonlinearity was measured by the Maker Fringe technique in comparison with d_{11} of quartz crystal using Nd:YAG laser (1064 nm) as a fundamental light source. Figure 1 shows the value of d_{33} as a function of GeO_2 concentration in poled silica film coated on various glass substrates. It indicates that large nonlinearity of d_{33}=7.5 pm/V was obtained at a GeO_2 concentration of 30 % using a Pyrex glass substrate. By changing the condition of poling temperature to 500 deg. the optimum second-order nonlinerity up to d_{33}=12.5 pm/V was achieved. This value is the largest nonlinerity reported from a poled glass material as far as we know. It can be thought that the space charge layer formed in the vicinity of the interface between the glass film and the substrate induces such a large second-order nonlinearity.

Waveguide-type device was also fabricated using thermally poled glass. In

this time rf-sputtered germanosilicate glass thin film was used instead of sol-gel processed film, and a ridge-type channel waveguide was fabricated by photolithography and etching techniques. We have successfully realized the green and blue light generations by Cerenkov-type phase-matched frequency doubling.

Conclusion

Very large second-order nonlinearity of d_{33}=12.5 pm/V was obtained from thermally poled silica-based glass thin film with sol-gel processing. We have also realized the green and blue light generations by Cerenkov-type frequency doubling using poled glass waveguide device. Nonlinear optical property of organic dye doped silica thin film is to be discussed.

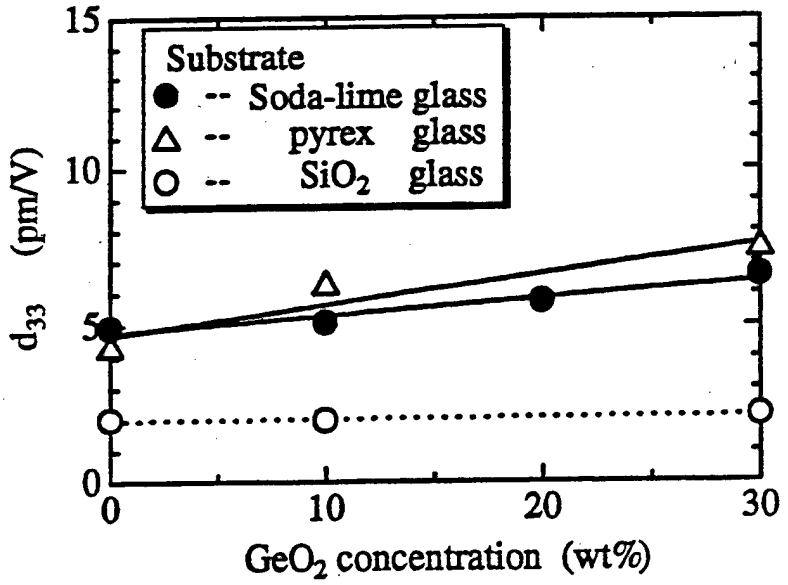

Fig.1 The value of d_{33} as a function of GeO_2 concentration for various glass substrates.

References

(1) T.Hirama, H.Muto, O.Sugihara, and N.Okamoto; Opt.Rev. Vol.3, No.1 (1996) p.17.

(2) T.Fujiwara, D.Wong, Y.Zhao, S.Fleming, S.Poole, and M.Sceats; Electron.Lett. Vol.31, No.7 (1995) P.573.

Syntheses and Nonlinear Optical Properties of Non-aggregated Metallophthalocyanines

Minquan Tian†, Shuichi Yanagi‡, Keisuke Sasaki‡, Tatsuo Wada† and Hiroyuki Sasabe†

†Frontier Research Program, The Institute of Physical and Chemical Research (RIKEN), 2-1 Hirosawa, Wako, Saitama 351-01, Japan

‡Department of Material Sciences, Faculty of Science and Technology, Keio University, 3-14-1 Hiyoshi, Kohoku-ku, Yokohama 223, Japan

In the last decade phthalocyanines have been extensively studied as an important class of third-order nonlinear optical materials because of their two-dimensional π-electron conjugation, exceptionally high thermal and chemical stability, and film-forming properties.[1,2] The magnitude of third-order nonlinear optical susceptibility of metallophthalocyanine films varies by several orders depending on the central metals, peripheral and axial substitution.[2] Among them we found out the vanadyl phthalocyanine films have large third harmonic susceptibilities $\chi^{(3)}(-3\omega; \omega,\omega,\omega)$. The staggered stacking arrangements of VOPc(*t*-bu)$_n$ (*t*-bu: *tert*-butyl, n=0, 1.1) enhanced the resonant and off-resonant $\chi^{(3)}$ values in the condensed state.[3,4] They also show different relaxation behavior of the excited state revealed by femtosecond time-resolved spectroscopy.[5] The molecular aggregation has an important influence on the linear and nonlinear optical properties of metallophthalocyanine films.[6] In this paper, we summarize the syntheses, spectroscopic and nonlinear optical properties of metallophthalocyanines which show no sign of intermolecular aggreagtion even in solid state (Figure 1).

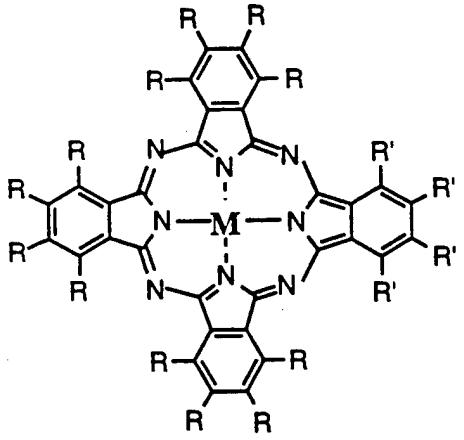

$H_2Pc(TFE)_{16}$: M=H_2, R=R'=CF_3CH_2O
$VOPc(TFE)_{16}$: M=VO, R=R'=CF_3CH_2O
$ZnPc(TFE)_{16}$: M=Zn, R=R'=CF_3CH_2O
$VOPc(TFE)_{12}$: M=VO, R=CF_3CH_2O, R'=H
$VOPc(OEt)_{16}$: M=VO, R=R'=CH_3CH_2O

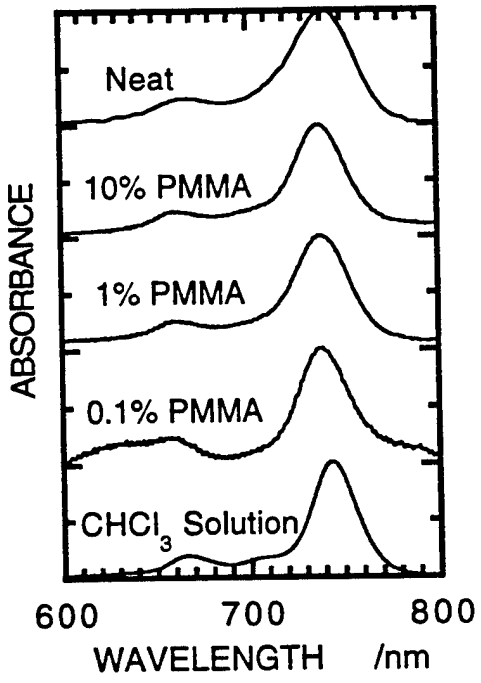

Figure 1. Molecular structures of non-aggregated metallophthalocyanines, and UV-Vis absorption spectra of $VOPc(TFE)_{16}$ in solution and in doped PMMA films.

The target materials were synthesized, and fully characterized by elemental analysis, IR, NMR, FAB-MS and UV-VIS spectroscopic methods. All the analysis results were found to be consistent with the predicted structures. Their aggregation properties were studied by the concentration dependence of absorption and electroabsorption spectra. Figure 1 shows the typical

optical absorption spectra of $MPc(TFE)_{16}$ in solution and in doped poly(methyl methacrylate) (PMMA) films. The Q-band in the optical absorption spectra doesn't change with the concentration of doped $VOPc(TFE)_{16}$, and no significant blue-shift of Q-band was observed from the comparison of the absorption spectra in solution and in solid state. Partially substituted vanadylphthalocyanine ($VOPc(TFE)_{12}$) was newly designed and synthesized by the cross-condensation between phthalonitrile and tetrasubstituted one. We also synthesized non-fluoro substituted compounds ($VOPc(OEt)_{16}$) to examine the influence of fuluoro-substitution on the molecular aggregation. The third-order nonlinear optical susceptibilities ($\chi^{(3)}(-\omega;\omega,0,0)$) of these metallophthalocyanine films were determined by electroabsorption measurement in terms of molecular structure and aggregation.

REFERENCES

1. Z. Z. Ho, C. Y. Ju and W. M. Hetherington III, *J. Appl. Phys.*, **62**, 716 (1987).
2. T. Wada, Y. Matsuoka, K. Shigehara, A. Yamada, A. F. Garito and H. Sasabe, *Proc. Materials Res. Soc. Internatl. Mtg. on Advanced Materials*, MRS Tokyo, **12**, 75 (1989).
3. M. Hosoda, T. Wada, A. Yamada, A. F. Garito and H. Sasabe, *Jpn. J. Appl. Phys.*, **30**, L1486 (1991).
4. M. Hosoda, T. Wada, T. Yamamoto, A. Kaneko, A. F. Garito and H. Sasabe, *Jpn. J. Appl. Phys.*, **31**, 1071-1075 (1992).
5. A. Terasaki, M. Hosoda, T. Wada, H. Tada, A. Koma, A. Yamada, H. Sasabe, A. F. Garito and T. Kobayashi, *J. Phys. Chem.*, **96**, (25), 10534 (1992).
6. T. Wada and H. Sasabe, *Proc. SPIE-Int. Soc. Opt. Eng.*, **2143**, 164 (1994).

Mach-Zehnder interferometer measurement of linear electro-optic coefficient in poled polymer films: coplanar and parallel-plate electrode structures

J.W. Wu

Department of Physics, Ewha Womans University, Seoul 120-750, Korea

Mach-Zehnder interferometer is adopted to measure the Pockels effect in a poled electro-optic polymer thin film. Two sample geometries, coplanar and parallel-plate electrode structures, are compared when the Pockels effects are measured in the interferometer. While the laser beam reflects off the thin film sample serving as one mirror in the interferometer for the parallel-plate electrode sample, in the coplanar electrode structure the beam at the sample arm passes through the polymer thin film spin-coated on top of a clear gap between two electrodes patterned on an optical substrate. Because of the differences in the tensor components interfered, the modulation amplitudes of the interference pattern of each sample geometry are related to the Pockels coefficients of polymer thin film in a different way.

In both sample geometries the modulation amplitudes are measured as a function of the incident light polarization angle, the modulation voltage, and the optical bias. In the parallel-plate electrode structure the Pockels coefficients are determined in a more complicated way than the case of the coplanar electrode structure. In particular, the coplanar electrode structure geometry enables the independent determination of the Pockels coefficients of poled electro-optic polymer film in the ordinary and extra-ordinary optic axes directions.

As an example the tensor ratio r_{33}/r_{13} for a stilbene-dye doped polyimide guest/host polymer film is determined experimentally and compared in two case. While the tensor ratio is measured to be 2.5 for the parallel-plate, it turned out to be 4.6 for the coplanar, higher than the thermodynamic-model value 3. The possible explanation for this discrepancy in the tensor ratio is explained in terms of the surface effects more dominant in the coplanar electrode structure.

Acknowledgement This work is supported kindly by the Korean Science and Engineering Foundation (Grant No. 95-0300-06-01-3).

Third-order Nonlinear Optical Properties of Polydiacetylene Microcrystals

Shinji Yamada, Edward Van Keuren*, Hiro Matsuda
National Institute of Materials and Chemical Research, Tsukuba 305, Japan
Hideyuki Katagi, Hitoshi Kasai, Shyuji Okada, Hidetoshi Oikawa, Hachiro Nakanishi
Institute for Chemical Reaction Science, Tohoku University, Sendai 980-77, Japan
Euan Smith, Ajoy K. Kar, Brian S. Wherrett
Department of Physics, Heriot-Watt University, Edinburgh EH144AS, Scotland

Microcrystals are interesting for the possible enhancement of the nonlinear optical properties due to the quantum confinement effect. Although microcrystals of semiconductors and metals have been intensively studied their preparation and NLO properties, there has so far been little research on organic microcrystals. Polydiacetylene is an especially important class of materials for organic microcrystals since it is among those with the largest third-order NLO properties. Furthermore, the remarkable improvement in the processability and device fabrication thereby can be expected using polydiacetylene microcrystals.

PolyDCHD, which has carbazolyl methyl group attached to the main chain as shown below, were examined in this study. The microcrystals were readily prepared by the reprecipitation of the DCHD monomer followed by the polymerization with the UV-light (254nm) irradiation[1]. The average size of the microcrystals were tuned from about 100nm to about 300nm by controlling the preparation conditions. The polyDCHD/gelatin thin film was fabricated on the glass substrate using spincoating technique for the measurement of NLO properties.

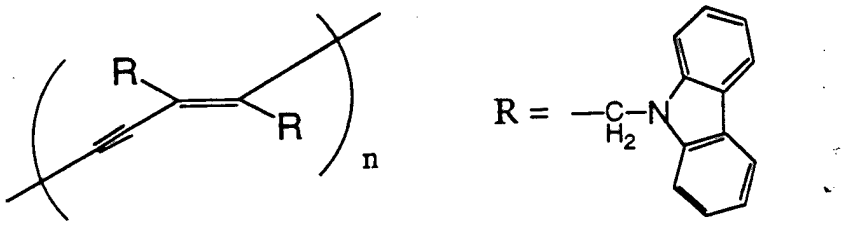

The third-order NLO properties of polyDCHD microcrystals were evaluated using z-scan technique. The tunable pulses from 420nm to 1800nm with about 20ps pulse duration were available from OPG/OPA pumped by the third harmonic (355nm) of a mode-locked Nd:YAG laser. The Gaussian beam was successfully extracted from OPG/OPA output using a spatial filter in the vacuum. The nonlinear refractive index, n_2, was measured to be negative at 580nm. The dispersion of n_2 will be reported.

References

1) R.Iida, H.Kamatani, H.Kasai, S.Okada, H.Oikawa, H.Matsuda, A.Kakuta, and H.Nakanishi, *Mol. Cryst. Liq. Cryst.*, **267**, 95 (1995).

* Present address: Advanced Polymer Research, BASF AG, Yokkaichi 510, Japan

P-39

Electro-optic Effects in Organic/Silica Hybrid Film and Fabrication of Channel Waveguide

Yoo Hong Min and Choon Sup Yoon
Department of Physics, KAIST, Taejon, Korea, 305-701

Hwan-Kyu Kim
Department of Macromolecular Science, Han Nam University, Taejon, Korea, 300-791

Su-Jin Kang
Department of Chemistry, KAIST, Taejon, Korea, 305-701

Inorganic polymer system where organic chromophores with large nonlinear optical coefficients are chemically bonded to silica matirx has been paid a great attention as a novel electro-optic material. Organic/silica hybrid thin film has many advantages over the organic polymer systems; such as low optical propagation loss, temporal stability, chemical and mechanical stabilities. In this paper the optical properties of organic/silica composite film and the fabrication of a single mode channel waveguide will be presented.

Silica composite film was fabricated by sol-gel reaction, where nonlinear optic organic chromophore (DANS diol) was attached to sol-gel monomer (isocyanatopropyl triethoxysilane) by urethane bond (Fig. 1). Both DC contact poling and corona poling were employed to establish the orientation of chromophore molecules in the film and the largest values of electro-optic coefficient r_{33} obtained were 53pm/V at λ=632nm and 16pm/V at λ=1.3 μm. Any appreciable decrease of r_{33} value was not observed at room temperature after 600 hours. At the elevated temperature of 63°C the poled film retained 70% of its initial value after 600 hours (Fig. 2).

The channel waveguide was fabricated by using photobleaching method. The cross-section area was 3.3 × 7 μm^2 and the length 5mm (Fig. 3). The lower cladding and the active core were made of silica composite films containing 30 wt.% and 50 wt.% organic chromophore respectively and AZ4562 positive photoresister was used for the upper cladding. The refractive indices of the lower cladding, core and upper cladding at 1.3 μm wavelength were measured to be 1.59, 1.609, 1.595 respectively.

Laser beam of 1.3 μm wavelength was launched into one end face of the waveguide and the output mode pattern was recorded by CCD camera. Analysis of the intensity distribution of the output beam confirmed that the channel waveguide was a single mode waveguide (Fig. 4).

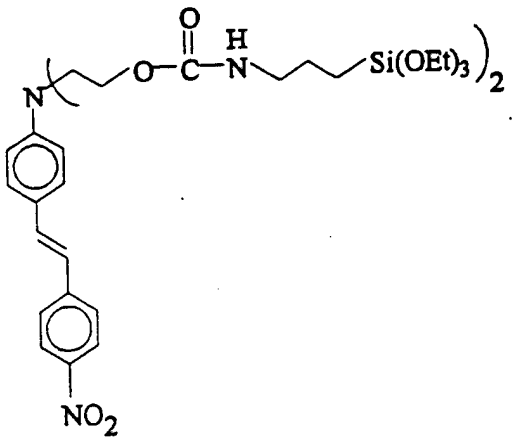

Fig. 1 Structure of sol-gel monomer where organic chromophore, DANS diol is attached to Si atom by urethane bonding.

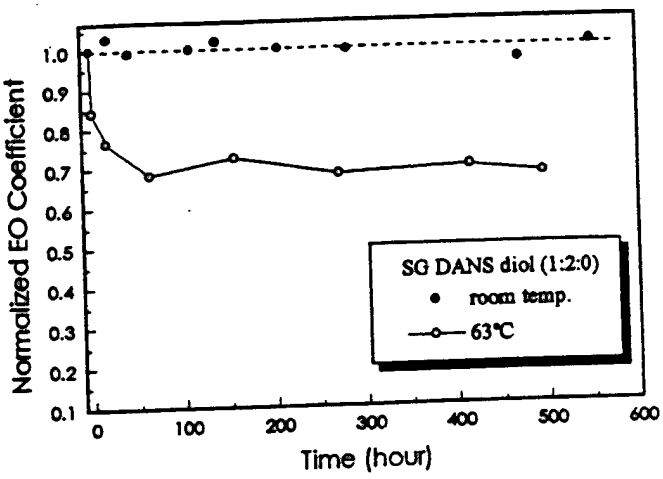

Fig. 2 Temporal stability of the electro-optic coefficient r_{33} as a fuction of temperature.

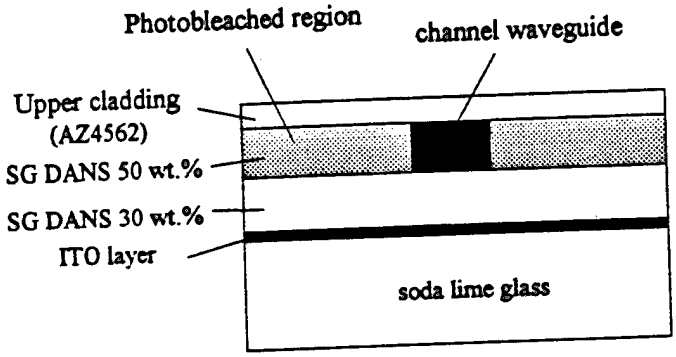

Fig. 3 The cross-section of the channel waveguide.

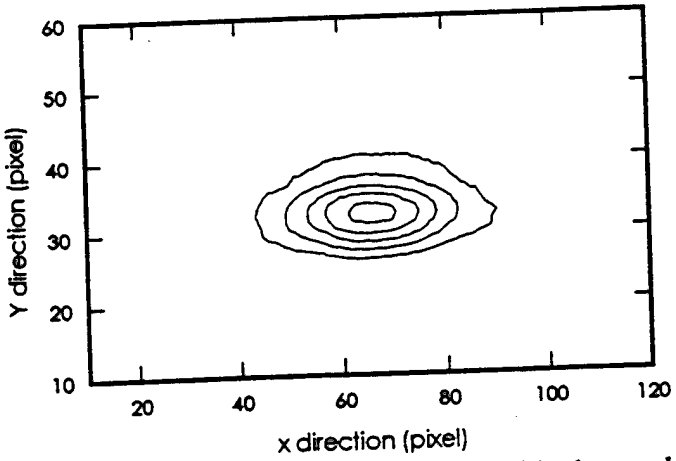

Fig. 4 The mode profile of the sol-gel channel waveguide detected by CCD camera.

Efficient Stimulated Brillouin scattering in organic crystal DLAP

Masashi YOSHIMURA, Hidetsugu YOSHIDA, Hiroaki ADACHI, Yusuke MORI, and Takatomo SASAKI*

Department of Electrical Engineering, Osaka University
2-1 Yamada-oka, Suita, Osaka, 565 Japan
**Institute of Laser Engineering, Osaka University*
2-1 Yamada-oka, Suita, Osaka, 565 Japan

There has been interest in using stimulated Brillouin scattering (SBS) phase conjugate (PC) mirror for correcting of aberrations in laser amplifiers. Over recent years, many experimental and theoretical studies of SBS PC with gaseous and liquid media have been performed, which involved some complicated handling and instability. In order to realize compact all solid state laser system with high quality beams, it is necessary to produce a new SBS solid mirror which has efficient chemical stability and high damage threshold.

In previous work, the organic LAP (L-arginine phosphate monohydrate) and DLAP (deuterated LAP) crystals have been found to show much higher laser damage threshold than KDP (potassium dihydrogen phosphate) and fused silica for focused incident beam of 1.064 μm Q-switched Nd:YAG laser with 1 ns pulse duration [1]. We have found that this phenomenon could be explained by the backward SBS for the first time [2]. This result also indicates the possibility to use organic materials for PC mirror. It is important to evaluate the SBS properties of various organic crystals for the practical application. In this work, we have examined the SBS property of DLAP, and compared with that obtained for LAP.

Figure 1 shows the experimental arrangement. A Nd:YAG single-frequency TEM_{00} Q-switched oscillator radiated linearly polarized 13 ns quasi-Gaussian wavefront pulse with 10 mJ. This output was amplified to ~200 mJ by two 10 $mm^{\phi} \times 100$ mm^{ℓ} Nd:YAG amplifiers. The size of the amplified beam was 1.5 times larger than that of diffraction limited. After going through a variable attenuator (half wave plate/ thin-film polarizer combination) and a Faraday rotator, most of the incident beam polarized b,c axis were focused in DLAP at 1 cm from incident surface with an AR coated focusing lens f=100 mm.

We have measured the transmitted energy and the shapes of the pumping and reflected pulses. Incident surface of DLAP was not coated. Figure 2 shows the SBS reflectivity as a function of input energy. This slope curve indicates the SBS threshold to be 1.7 mJ (c-axis polarization). The reflectivity increases monotonically to the maximum value of 75 % at an input energy of 40 mJ.

DLAP showed much smaller SBS threshold energy of 1.7 mJ than LAP (6mJ). This difference is too large to be explained by the difference in absorption coefficient at 1.064 μm. Therefore, we can consider that the acoustic phonons related to SBS in DLAP would exhibit smaller velocity and longer decay time compared with those in LAP, because of the heavy mass of deuterium, resulting in SBS gain larger and threshold energy smaller.

References:
1. A.Yokotani, T.Sasaki, K.Yoshida, and S.Nakai; Appl. Phys. Lett. **55**, 2692 (1989)
2. H.Yoshida, M.Nakatsuka, T.Sasaki, H.Fujita, K.Yoshida; Opt. Lett. submitted.

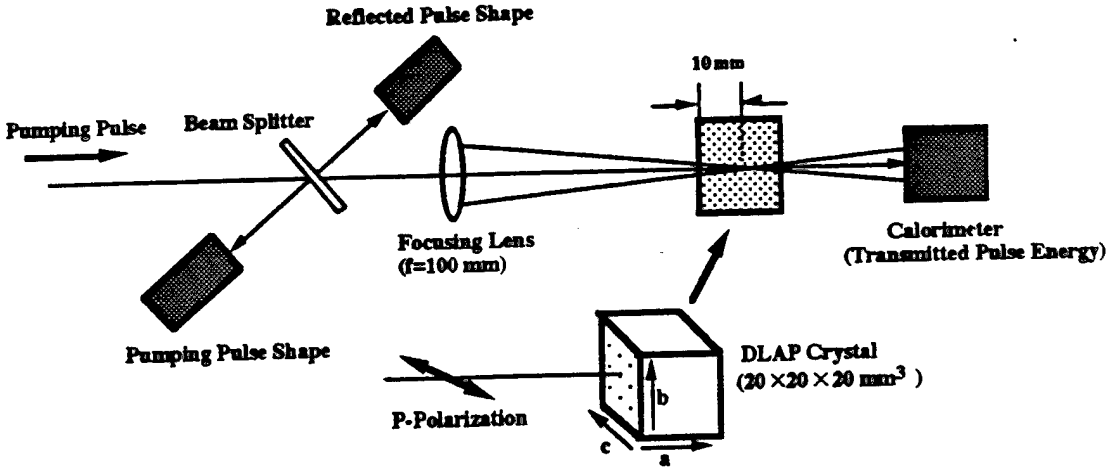

Fig.1 Schematic of experimental arrangement for measuring SBS reflectivity.

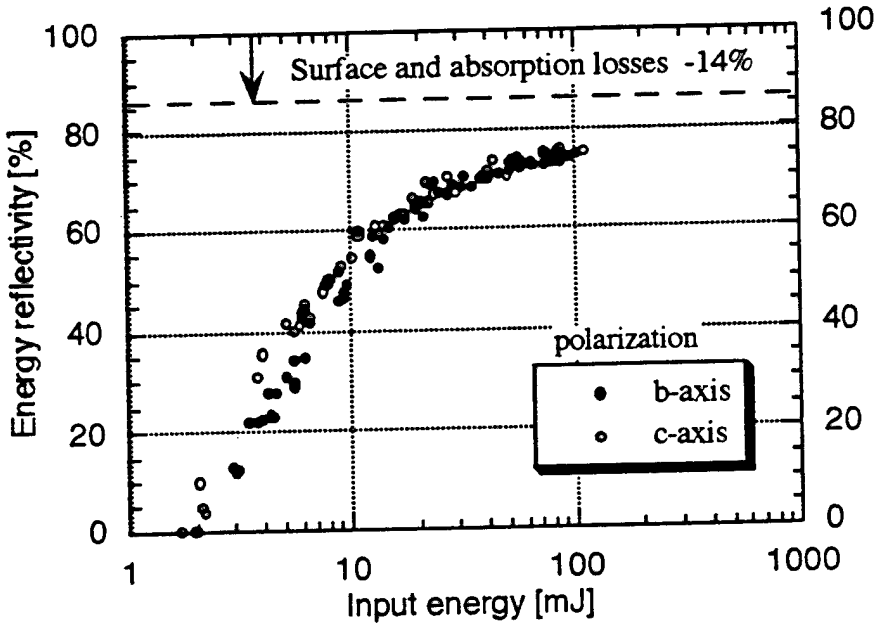

Fig.2 SBS reflectivity for DLAP crystal

OPTICAL NONLINEARITIES OF ONE-DIMENSIONAL METAL COMPLEXES

TOSHIO FUKAYA and TOSHIHIDE KAMATA

1-1, Higashi, Tsukuba, Ibaraki 305 JAPAN
National Institute of Materials and Chemical Research

Abstract It is known that the d^8 transition metal complexes with dionedioximes have square planar configuration and are stacked face to face forming a linear metal chain with large *d*-orbital overlap between metals of adjoining molecules. The formation of linear metal chains can be confirmed by appearance of new absorption band, which does not exist in solute samples. Energy levels of the metal-metal interactions are usually lower than those of metal-rigand interactions, and they appear at visible or infrared region, which depends on the type of materials and the interval of metal chains. We have reported formations of linear metal chains in vacuum evaporated thin films of these metal complexes and their considerably large third-order optical nonlinearities[1]. In those cases, delocalized electrons throughout the linear metal chains and resonance effects at those metal-metal absorption bands are originated to their large optical nonlinearities.

In this paper, we will present recent results about the nonlinear refractive index of the one-dimensional metal complex and discus their brief mechanism using experimental results and MO calculations.

[1] T. Kamata, T. Fukaya, M. Mizuno, H. Matsuda, F. Mizukami, Chem. Phys. Lett., 221(1994)194.

Measurements of Two Photon Absorption and Stimulated Raman Scattering in 4'-Dimethylamino-N-Methyl-4-Stilbazolium Tosylate Crystals

Hoon Shim, Mingguo Liu and George I. Stegeman

CREOL, University of Central Florida
4000 Central Florida Blvd., Orlando FL 32816-2700

The organic salt 4'- Dimethylamino - N - Methyl - 4 - Stilbazolium Tosylate Crystal (DAST) has received considerable attention due to its large nonlinear optical properties, because its second order nonlinearity is well known.[1,2] DAST crystal is monoclinic and positive biaxial. It shows a strong dichroism near the linear absorption edge, with stronger absorption for light polarized along the a-axis which nearly coincides with the X dielectric axis. In this work, we investigated not only the two photon absorption (TPA) coefficients α_2 of a 360 mm thick c-cut DAST crystal using the Z-scan method but the characteristics of stimulated Raman scattering (SRS) which may contribute to the measured value of the two photon absorption coefficients.

The open aperture Z-scan experiments have been performed to measure the dispersion of the two photon absorption coefficient in the wavelength region from 780nm to 920nm.[3] A Kerr lens mode-locked Ti:sapphire laser producing 2~3ps pulses was used as the tunable light source. A typical open aperture Z-scan result with best fit to the data at 830 nm is shown in Fig. 1. The

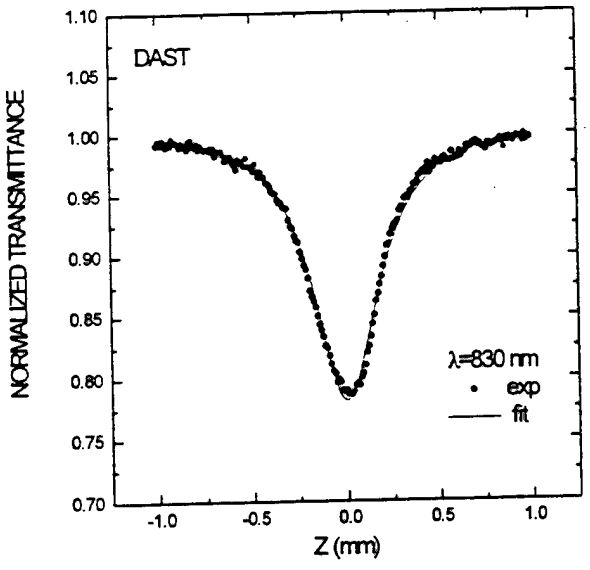

Fig. 1 Typical open aperture Z-scan data of DAST

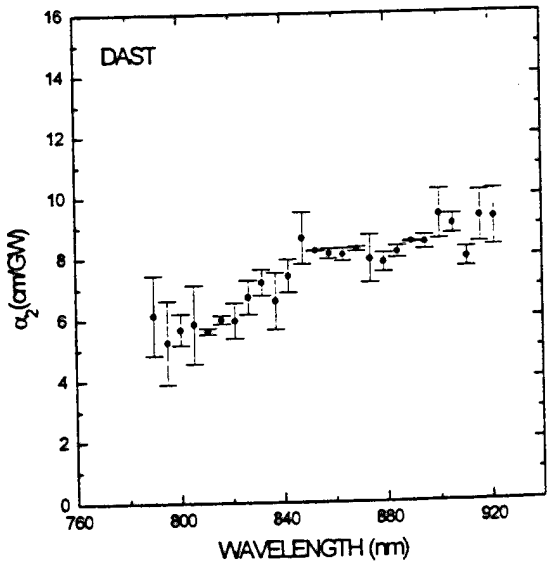

Fig. 2 Two photon absorption spectrum of DAST

two photon absorption coefficients were measured in both cases of the polarization parallel to the a-axis and the b-axis. The pulse energy was also varied and the two photon absorption coefficient was found to be independent of pulse energy within the wavelength region. The measured dispersion of the two photon absorption coefficient α_2 is shown in Fig. 2.

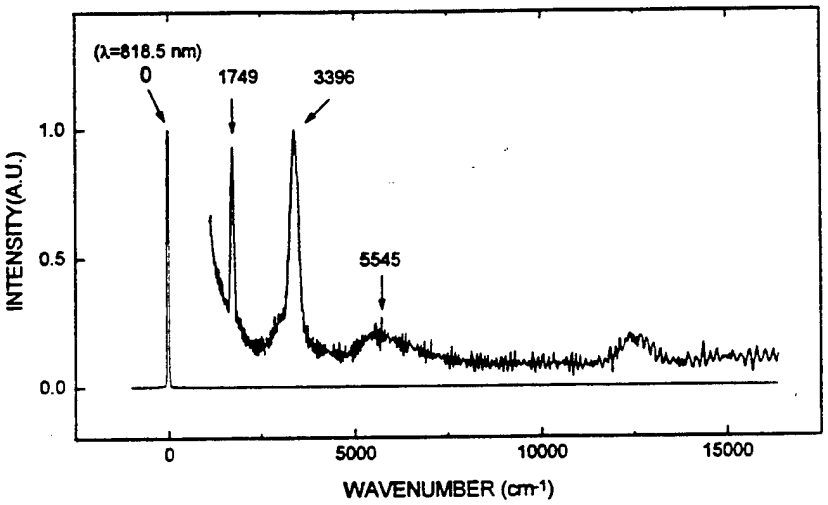

Fig. 3 The spectrum of the scattered lights by stimulated Raman scattering

We also observed several frequency up-shifted anti-Stokes Raman peaks arising from stimulated Raman scattering when an intense light beam was focused at the sample. The spectrum of scattered light for a fundamental wavelength of 818.5nm is shown in Fig. 3. It shows that there are at least two well-defined strong anti-Stokes Raman peaks. We also observed a ring pattern, probably originating from an emission cone of anti-Stokes radiation.

In conclusion, we report measurements of the two photon absorption spectrum of an organic crystal, 4'- dimethylamino - N - methyl - 4 - stilbazolium tosylate, and the stimulated Raman scattering in the wavelength range from 780nm to 920nm.

References:

1. G. Knöpfle, R.Schlesser, R. Ducret, and P. Günter, Nonlinear Optics, **9**, 143 (1995).
2. Seth R. Marder, Joseph W. Perry, and Christopher P. Yakymyshyn, Chem. Mater., **6**, 1137 (1994).
3. Mansoor Sheik-Bahae, Ali A. Said, Tai-Huei Wei, David J. Hagan, and E.W.Van Stryland, IEEE J. Quant. Electron., **24**, 760(1990).

P-43

The third-order nonlinear optical properties of new bis-substituted tetrathiafulvalene derivatives

B. Sahraoui[1,3], G. Rivoire[1], J. Zaremba[3], N. Terkia-Derdra[2], M. Salle[2]
[1] *Laboratoire POMA, Equipe Photonique de Puissance, EP CNRS 130*
[2] *Laboratoire d'Inginerie Moleculaire Materiaux Organique, EP CNRS 66*
Université d'Angers. 2, Boulevard Lavoisier
49045 Angers cedex (France).
e-mail : sahraoui@univ-angers.fr
Tel: 41.73.54.24 Fax: 41.73.53.30
[3] *also in Instytut Fizyki, Uniwersytet M. Kopernika 87-100 Torun - Poland*

The tetrathiafulvalene (TTF) derivatives are the base of organic metals and their charge-transfer salts present remarkable conducting or even superconducting properties. Due to their highly conjugated framework, they fulfill some criteria necessary to reveal large third-order nonlinear optical susceptibilities[1]. In the present work, we compare the third-order optical properties of new bis- substituted tetrathiafulvalene derivatives with the properties of acetylenic and ethylenic analogues of TTF, we have studied previously[2,3].
The bis-substituted TTF derivatives present two major characteristics: (a) they dispose of an extented system π thanks to grafting of two lateral groups of dithiafulvenyles in the skeleton of TTF, (b) The originality of their structure lie in the coexistence of the electrodonor groups (1,3-dithiolylidène) and the electroattractor substitutes (carboethoxy or nitrite) conjugated through the TTF heart. These structural characteristics are susceptible to give rise to the interesting optic properties. Our study is made in order to determine the influence of molecular parameters such as: single and double length alternation, the end group-substitution species and the molecular symmetry on the hyperpolarisability γ enhancement. The bis-substituted TTF derivative which has the largest γ is presented in fig.1. We measure the third-order susceptibilities $\chi^{\langle 3 \rangle}_{ijkl}$ of the samples using the degenerate four wave mixing method and we determine the absorption coefficient of the materials in separate experimental setup. The excitation is provided by 30 ps light pulses at 532 nm. All organic molecules studied reveal large third-order nonlinear optical hyperpolarisability. For the three kinds of TTF derivatives studied - acetylenic, ethylenic and bis-substituted- the best values of γ obtained are respectively 2.410^3, $1.6\ 10^4$ and $44\ 10^4$ times greater than γ of CS_2.

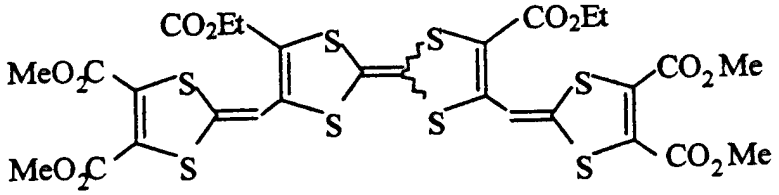

fig.1

References

[1]- Paras N.Prasad, David J. Williams Introduction to nonlinear optical Effects in Molecules & Polymers,
John Wiley & Sons, Inc. (1991)
[2]- M. Sylla, J. Zaremba, R. Chevalier, G.Rivoire, A. Khanous, and A. Gorgues, *Synth. Metals , 59, 111, 1993*
[3]- B . Sahraoui, M. Sylla , J. P. Bourdin , G. Rivoire , J. Zaremba, T.T. Nguyen and M. Sallé, *J. of Modern Optics, vol 42, N° 10, 2095-2107(1995)*

Molecules with Large Two-Photon Absorptivities and Applications in Optical Limiting and Photopolymerization

J. Ehrlich†, A. Heikal#, Z.-Y. Hu#, L-Y. S. Lee#, S. R. Marder†#, J. W. Perry†#, H. Röckel# and X. L. Wu#

† Jet Propulsion Laboratory
California Institute of Technology
Pasadena, CA 91109

Beckman Institute
California Institute of Technology
Pasadena, CA 91125

Molecules exhibiting strong two-photon absorption are currently of considerable interest for a wide range of applications including: two-photon excited fluorescence imaging, three-dimensional optical data storage, stereolithography, and optical limiting, to name a few. From a fundamental point of view, knowledge of molecular two-photon spectra and structure/property relationships are also important for a more complete understanding of the third order polarizabilities of conjugated molecules. However, very little is known or understood about two-photon states and spectra of conjugated molecules or how they correlate with structure.

We have observed large two-photon absorptivities in a class of diphenylpolyene derivatives and have initiated studies to determine their two-photon absorption spectra and to examine structure/two-photon spectra relationships. Given their large two-photon absorptivities and electronic properties, we have also sucessfully utilized these materials for optical limiting and as two-photon initiators of photopolymerization.

We have determined the wavelength dependent two-photon absorptivity of a series of diphenylpolyene derivatives with varying lengths of the polyene bridge, by using direct nonlinear transmission measurements with a nanosecond pulsed dye laser. The wavelength of the maximum two-photon absorptivity for the stilbene like (n, the number of double bonds, = 1) molecule is about 605 nm. Very interestingly, the peak two-photon absorptivity for this molecule is exceptionally large: $\delta = 1.3 \times 10^{-46}$ cm^4 s/photon, which is a factor of 46 greater than that of the dye Rhodamine B at 700 nm (1), which was used as a standard. Furthermore, the value is a factor of 4 greater than that of a bisbenzthiazoledialkoxythiophene compound recently reported by He et al (2). Comparable peak two-photon absorptivities were observed for the n = 2 and n = 3 compounds, although the bands broadened somewhat, and the peaks shifted to longer wavelength with increasing polyene length: 650 nm for n = 2 and 700 nm for n = 3. For all three molecules, the two-photon state energy is greater than that of the lowest energy one photon state, whereas for diphenylhexatriene, in low polarizability solvents, the two-photon state is energetically below the one photon state (3).

Motivated by the large two-photon absorptivities observed, we performed optical limiting experiments on the n = 1 molecule at ~600 nm. Generally, molecular two-photon absorptivities are too small for significant optical limiting of nanosecond duration pulses. As shown in Figure 1, significant optical limiting is observed for the n = 1 molecule for 5 ns, 600 nm pulses. The strong optical limiting by two photon absorption in this material is particularly interesting because the linear transmission is very high, > 95%, for the samples employed. Thus, these molecules hold potential as broadly transparent two-photon optical limiting materials.

Two-photon excitation of a variety of our diphenylpolyene derivatives in the presence of acrylate monomers leads to the formation of polymer. For example, with the two-photon absorbing molecule dissolved at 1% concentration in triacrylate monomer, excitation at ~600 nm with an intensity of ~100 MW/cm^2 leads to formation of a visually observable cross-linked polymer spot on the wall of the vessel. We have written micrometer dimension spots and two and three dimensional patterns of polymer using our two photon absorbers. We have also observed that prolonged exposure of a particular spot at the window/monomer solution interface leads to the development of a fine filament of polymer that extends for several millimeters into the solution. This process is the two-photon analog of the photopolymerization induced optical self-focussing and trapping reported recently by Kewitsch and Yariv (4).

Acknowledgment

This work was performed in part at the Jet Propulsion Laboratory, California Institute of Technology as part of its Center for Space Microelectronics Technology and supported by the Ballistic Missile Defense Organization, Innovative Science and Technology Office and the U. S. Air Force Wright Laboratory (MLPJ), through an agreement with the National Aeronautics and Space Administration. Support at the Beckman Institute, California Institute of Technology from the Office of Naval Research through the Center for Advanced Multifunctional Molecular Assemblies and Polymers, the Office of Naval Research and the Defense Advanced Research Projects Agency is gratefully acknowledged.

References

(1) C. Xu and W. Webb, *J. Opt. Soc. Am.* B, **13**, 481 (1996).
(2) G. S. He, R. Gvishi, P. N. Prasad and B. Rhinehardt, *Opt. Commun.*, **117**, 133 (1995).
(3) B. S. Hudson, B. E. Kohler and K. Shulten, *Excited States*, **6**, 1 (1982).
(4) A. S. Kewitsch and A. Yariv, *Optics Lett.*, **21**(1), 24 (1996).

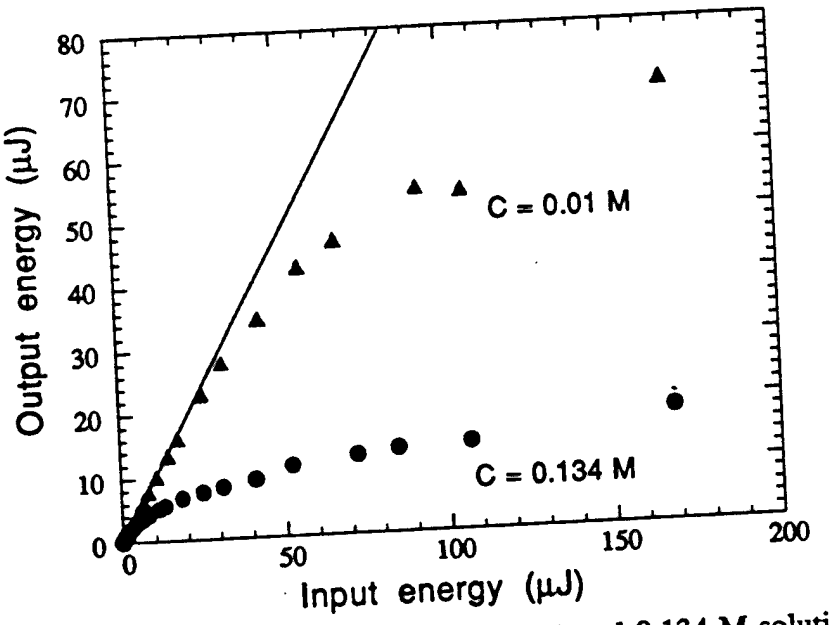

Figure 1. Two-photon optical limiting responses of 0.01 and 0.134 M solutions of a stilbene derivative for ~5-ns, 600 nm pulses. The straight line corresponds to the linear transmission (96%) of the 0.134 M solution. A 1 cm cell was centered on the focus of an ~f/5 optical system (effective interaction length ~200μm) and the total transmitted energy was detected.

Three Dimensional Simulation of Nonlinear Optical Phenomena Using the FDTD Method

Dennis Sullivan
Electrical Engineering Department
University of Idaho
Idaho Falls, Idaho 83402

1. Introduction

Up to this point, research in nonlinear optics has been almost strictly experimental in nature. Excluding approximate solutions to Maxwell's equations, little is known about the detailed interaction of an optical pulse propagating in a nonlinear medium. It is expected that a computer simulation of the exact Maxwell's equations will contribute significantly to this research for two primary reasons:

1. There is a need for explicit understanding of the details of nonlinear electromagnetic propagation.
2. Extremely complex physical models can be simulated and easily altered. This is an enormous advantage over fabricating experimental models.

One method for the simulation of electromagnetic propagation is the finite-difference time-domain method [1]. This is an explicit method to calculate the electromagnetic propagation of light energy by implementing the time domain Maxwell's equations. It has been shown to be capable of simulating nonlinear electromagnetic phenomena [2]. Recently, the application of Z transform theory has quantified the problem of EM interactions in complex dispersive and nonlinear materials [3,4,5].

2. The FDTD Method

The finite-difference time-domain (FDTD) method [6] implements the normalized time-domain formulation of the Maxwell's equations

$$\frac{\partial D}{\partial t} = \frac{1}{\sqrt{\varepsilon_0 \mu_0}} \cdot \nabla \times H \tag{1.a}$$

$$D = \varepsilon_r E + \chi_0^{(3)} E^3 \tag{1.b}$$

$$\frac{\partial H}{\partial t} = -\frac{1}{\sqrt{\varepsilon_0 \mu_0}} \nabla \times E \tag{1.c}$$

The calculation of Ampere's Law (equation 1.a) and Faraday's Law (equation 1.c), are at the heart of the FDTD method. The E and H fields are assumed interleaved around a cell whose origin is at the location I,J,K. Every E field is located 1/2 cell width from the origin in the direction of its orientation; every H field is offset 1/2 cell in each direction except that of its orientation. From 2.a, for instance, the following difference equation can be developed for the Z direction

$$D_z^{n+1/2}(i,j,k+1/2) = D_z^{n-1/2}(i,j,k+1/2) + \frac{\Delta T}{\Delta x \cdot \sqrt{\varepsilon_0 \mu_0}} (H_y^n(i+1/2,j,k+1/2) - H_y^n(i-1/2,j,k+1/2) - H_x^n(i,j+1/2,k+1/2) + H_x^n(i,j-1/2,k+1/2)) \tag{2}$$

where Δx is the cell size and ΔT is the time interval between iterations. Similar difference equations corresponding to 2.c are used to calculate the H fields. These simple, but very effective, difference equations are at the core of the FDTD method, and provide the fundamental algorithm that simulates electromagnetic propagation. A typical problem space consists of tens of thousands of cells. However, the efficiency of the method produces solutions in minutes on today's supercomputers.

The calculation of the constitutive relationship of equation 2.b is not so straight-forward, because it contains the nonlinear term E^3. However, the following approach was developed to handle such nonlinearities [4]: Start by taking a Taylor series expansion of $E^3(t)$ around the time $t = t_{n-1}$ and evaluating it at the time $t = t_n$, an approximation for $E^3(t)$ can be determined, and an explicit expression for E^n can be derived.

$$E^n = \frac{(D^n / \varepsilon_0) + 2\chi_0^{(3)} \cdot \left(E^{n-1}\right)^3}{\varepsilon_\infty + \chi_0^{(3)} 3 \cdot \left(E^{n-1}\right)^2} \tag{3}$$

This and similar formulations of other nonlinear phenomena were used to simulate soliton propagation in silica glass [4].

3. Summary

Three dimensional computer simulation methods are being developed to further the understanding of wave propagation in nonlinear media and aid in the design of innovative nonlinear devices. The method being used, the finite-difference time-domain method, is an extremely robust method which has been proven capable of modeling nonlinear phenomena.

References:

1. K. Kunz, R. Luebbers, *The Finite Difference Time Domain Method for Electromagnetics*, Boca Raton, CRC Press, 1993.
2. P. M. Goorjian, A. Taflove, "Direct time integration of Maxwell's equations in nonlinear dispersive media for propagation and scattering of femtosecond electromagnetic solitions," *Optics Letters*, Vol. 17, pp. 180-182, Feb. 1992.
3. D. M. Sullivan, "A frequency-dependent FDTD method using Z transforms," *IEEE Trans. on Antennas and Propagation*, AP-40, pp. 1223-1230, Oct. 1992.
4. D. M. Sullivan, "Nonlinear FDTD formulations using Z transforms," *IEEE Transactions on Microwave Theory and Techniques*, Vol. MTT-43, pp. 676-682, March, 1995.
5. D. M. Sullivan, "Z transform theory and the FDTD method," *IEEE Trans. on Antennas and Propagation*, accepted for publication.
6. K. S. Yee, "Numerical solution of initial boundary value problems involving Maxwell's equations in isotropic media," *IEEE Trans. on Antennas and Propagation*, AP-17, pp. 585-589, 1966.

This research was supported by grants from the NASA Idaho Space Grant Consortium, the University of Idaho Research Council Seed Grant Program, and a grant for supercomputer time from the San Diego Supercomputer Center.

SCANNING-PROBE ELECTRONIC-STRUCTURE STUDIES OF SELF-ASSEMBLED CONJUGATED MOLECULES

F. Charra[(1)], J. Cousty[(1)], D. Markovitsi[(2)],

(1) *Commissariat à l'Énergie Atomique, DRECAM-SRSIM, Centre d'Études de Saclay, F-91191 Gif-sur-Yvette Cedex, France.*

(2) *CNRS, URA 331, Laboratoire de photochimie, Centre d'Études de Saclay, F-91191 Gif-sur-Yvette Cedex, France.*

Some organic molecules spontaneously form molecularly organized layers at the interface between a solution and an atomically clean solid surface like Highly Oriented Pyrolytic Graphite (HOPG). We have studied such so-called self-assembled layers of several conjugated organic molecules, using scanning probe microscopy techniques, mainly Scanning Tunnel Microscopy (STM).

High-resolution STM images permit a precise determination of the molecular structure of the layer. In particular, some assemblies exhibit symmetry-breaking $\sqrt{3} \times \sqrt{3}$ R 30°overstructures, with identical molecules appearing in sites with different symmetry. Furthermore nanoscale manipulations through interaction with the tip allow the creation of structural defects such as molecular lacunas. The non-linearity of the electronic junction between the metallic tip and the layer allows an electronic spectroscopy of individual molecules. We have observed very important spectroscopic differences depending on the geometry of the molecular site, which reflect a strong influence of the environment on the electronic structure of the conjugated electron system. We discuss the origin of the effect, which can be attributed to combined interactions with neighboring molecules and with conducting substrate. By associating spectroscopic techniques with high-resolution intramolecular imaging we have obtained experimental information on the electron-density spatial distribution of HOMO and LUMO molecular orbitals. Further insights are gained by the association of an optical excitation or detection with the STM.

Theses studies offer a deeper understanding of the electronic structure of individual molecules and electronic processes mediated by the interaction of the molecule with its environment and by optical excitations.

OPTICAL TECHNIQUES FOR PROBING ABSORPTION VARIATIONS INDUCED BY CHARGE INJECTION IN ORGANIC SEMI-CONDUCTOR

P-A. Chollet,[1] F. Charra,[2] A. Lorin,[1] D. Paquet,[1] D. Fichou[3]

CEA-Saclay [1]DEIN/SPE, [2]DRECAM/SRSIM, 91191 Gif Cedex (France)
[3]CNRS-Matériaux moléculaires, 2 rue Henri Dunant 94320 Thiais (France)

Electric field induced charge transport phenomena in organic condensed media occur mostly by intermolecular charge hoping, except in the case when strong intermolecular interactions leads to the formation of genuine valence and conduction bands (charge-transfer systems and conjugated polymers). When the interactions are weak (molecular crystals), the charge may be assigned to given molecules in a reduced or oxydized state, whose absorption spectra is modified. This results in modifications of the optical constants of the material (absorption and refractive index), whose magnitude is related to the volumic concentration of charge species and whose wavelength dependence is connected to the chemical nature and ionizarion degree of the species. These optical modifications can be optically studied from the modifications of the macroscopic optical reflection or transmission of the sample. Since the sample has to be sandwitched between a contact and a blocking electrodes in order to apply the electric field and store charges, one of which being transparent, the interpretation has to be done through a complete analysis of the stratified multilayer structure.

It is interesting to apply the above technique to sexithiophene (6T) thin films which have been used in organic electronic devices. In the reflection technique with one metallic electrode, a collimated monochromatic probe beam can examine the depth profile by scaning the incidence angle. It has been observed that the behavior depends on the nature of the metallic electrode, in connection with the relative work function of the metal and organic semiconductor. Direct injection occurs with gold while injection needs to be photo-assisted in the case of aluminium. Moreover the wavelength dependence of the electric-field induced absorption modulation indicates clearly the formation of charged radical cation $6T^{+*}$. The incidence angle dependence enables to locate the formation of those ionized species in a small layer not thicker than 20 nm. Under the application of a periodic field the whole cycle consists of an excitation formation, charge separation, charge storage in the radical cation $6T^{+*}$ (which is tested by the probe beam) and charge erasure.

SECOND HARMONIC GENERATION IN THERMALLY POLED INORGANIC GLASSES

H. Takebe, P. G. Kazansky*, Philip St. J. Russell*, and K. Morinaga

Department of Materials Science and Technology
Graduate School of Engineering Sciences
Kyushu University
Kasuga, Fukuoka 816, Japan

*Optoelectronics Research Centre
University of Southampton
Highfield, Southampton SO17 1BJ, United Kingdom

Inorganic glasses naturally are not possessing the second order nonlinearity (SON) due to inversion symmetry of the glass matrix. In recent years a number of groups around the world have been exploring, with some success, the use of various poling techniques to break this cento-symmetry and induce substantial second-order nonlinearity in glasses [1]. Levels of nonlinearity of order 1 pm/V have been achieved, with some indications that higher values may be possible [2]. Considering that metre-long interaction length are feasible in optical glass fibre (compared to few cm in ferroelectric crystals), and that the dispersion of refractive index is weak, nonlinearities of this order place glass in the unexpected position of a serious potential rival to such as lithium niobate, potassium titanyl phosphate (KTP) and lithium triborate (LBO) [3]. A better understanding of the mechanisms of glass poling, which is not fully understood, may help improve the value of SON in poled glasses and discover new inorganic glass materials with large SON's.

During thermal poling in fused silica, typically samples 1 mm thick are heated to 280°C with an applied voltage of 4 kV for 15 min. After cooling and removing the electric field, the SON is observed only near the anodic surface. We have systematically studied the effects of poling conditions [4] in particular poling voltage and time on SHG in thermally poled fused silica and discovered that the SH signal is proportional to the square of the applied voltage and that the speed of the poling process increases with the applied voltage. Prior treatment of the samples is found to effect the poling process, and the optimum poling conditions are observed to depend on the poling atmosphere. Effects of impurities such as oxygen deficient centres (ODC), Na, and OH on poling phenomenon in silica glass were also studied. The mechanisms and material conditions for creating permanent SON's in various oxide glasses, e.g., fused silica, sol-gel derived silica, tellurite glasses, are discussed in the light of of new results.

References

1. R. A. Myers, N. Mukherjee, and S. R. J. Brueck, Opt. Lett., **15**, 1733 (1991).
2. T. Fujiwara, D. Wong, Y. Zhao, S. Fleming, S. Pool and M. Sceats, Electron. Lett. **31**, 573 (1995).
3. P. G. Kazansky, V. Pruneri and P. St. J. Russell, Opt. Lett., 20, 843 (1995).
4. H. Takebe, P. G. Kazansky, P. St. J. Russell, and K. Morinaga, Opt. Lett., **20**, 468 (1996).

Nonlinear Optical Properties of Novel Low Bandgap Polythiophenes

W. Schrof, S. Rozouvan, T. Hartmann, H. Mohwald, V. Belov, E. Van Keuren*
BASF AG, Polymer Research Laboratory, D-67056, Ludwigshafen, Germany
* BASF Advanced Polymer Research, Yokkaichi, Mie 510, Japan

The large third order nonlinear optical susceptibilities, fast response times, and numerous possibilities for chemical alteration have stimulated a great deal of interest in polyene materials such as polyacetylene and polythiophene as potential materials for all-optical switching applications. Recently, we have developed a method for producing novel substituted polythiophene derivatives based on the Stille coupling reaction of >bis(trimethyltin)thiophene and dihalothieno(3,4-b]pyrazine monomers.

By varying both substituent groups with different electron donating and accepting character attached to the pyrazine ring as well as the number of substituted vs. unsubstituted units and the degree of polymerazation, soluble materials could be obtained with tailor-made absorption behavior in the near infrared. In contrast to polyacetylene stable conjugated polymer films with good optical quality could be casted or spin-coated. The polymers were analyzed using MALDI (matrix assisted laser desorption and ionization), absorption, and Raman spectroscopy. The nonlinear optical properties were determined by femtosecond degenerate four wave mixing experiments (DFWM) and frequency tunable third harmonic generation (THG). All films showed ultrafast response times in the order of less than one ps to several ps. By optimizing the structures with respect to substituents and conjugation, large values for both values $\chi^{(3)}$ (up to 10-8 esu) and figures of merit $\chi^{(3)}/a$ (higher than 10-13 esu were reached. THG dispersion measurements were also carried out, showing resonance effects of the one- and two-photon states in the wavelength range from 400 to 800nm.

Third Order Nonlinearity Measurements in a Dye-Doped Polymer Fiber at 1.32 μm

Y. Baek and G. I. Stegeman
Center for Research and Education in Optics and Lasers, University of Central Florida
4000 Central Florida Boulevard, Orlando, FL 32816

D. W. Garvey and M. G. Kuzyk
Department of Physics, Washington State University
Pullman, Washington 99164-2814

Abstract : The nonlinear refractive index and two photon absorption coefficients n_2 and α_2 of an ISQ doped polymer fiber were measured to be 1.5×10^{-13} cm^2/W and 0.17 cm/GW with a pulse modulated Mach Zehnder interferometer at 1.32 μm.

Squaraine dyes (ISQ) have attracted interest recently as third order nonlinear materials.[1-4] Low loss, single mode polymer fibers with squaraine-doped cores have been fabricated offering the possibility of all-optical switching in fiber devices at low powers.[2] To be a good candidate for such devices, the material should satisfy the two photon figure of merit (defined as $T = \alpha_2\lambda/n_2$ which should be less than unity where n_2 is nonlinear refractive index coefficient defined by $\Delta n=n_2 I$ and the two photon absorption coefficient α_2 is defined by $\Delta\alpha = \alpha_2 I$). This figure of merit quantifies whether a 2π nonlinear phase shift is achievable over one nonlinear absorption length. Here we report the measurements of the third order nonlinearities of an ISQ doped polymer fiber which show that this material is promising for all-optical devices at 1.32 μm.

The fabrication process for the dye-doped polymer fiber is described in detail elsewhere.[2] A single mode ISQ/PMMA fiber with 0.1 % concentration by weight was studied. The diameter of the core is 13 μm and the 1/e width of the mode is assumed to be equal to the core diameter. The linear loss is estimated to be 0.3 dB/cm. Both 6.5 cm and 12 cm long fibers were used in the experiment. The end surfaces were either polished or rendered smooth for end fire coupling by touching them with a 100W bulb.

We performed nonlinear phase shift measurements using a pulse modulated Mach Zehnder interferometer.[5] A modelocked Nd:YAG laser operating at 1.32 μm with 90 psec pulses, full width at half maximum intensity, was used in the experiment. A single full high power pulse was extracted with an electro-optic pulse slicer at the rate of 2 kHz from the 72 MHz modelocked pulse train and all the other pulses were suppressed by a factor of 50~100 to eliminate thermal contributions. The experimental setup for the Mach Zehnder interferometer is shown in Figure 1. A matched pair of wedge plates are placed in the reference arm. Translation of one wedge causes a slow change in the optical path length of the reference arm without beam displacement, leading to a time-varying sinusoidal fringe pattern. With the boxcar averagers. gates were set up on the high pulse signal and on the background pulse signal immediately preceding it. Because the low

background pulse is not intense enough to induce a nonlinear phase shift, there will be a shift between the high power fringe pattern and the low power one due to the electronic n_2. From the magnitude of the shift between the low and high intensity fringe pattern, we can derive the nonlinear phase shift. The nonlinear refractive index coefficient was measured in this way to be 1.5 ($\pm$1.0)$\times 10^{-13}$ cm^2/W. The measurement of the two photon absorption coefficient required Q-switched and mode-locked operation to increase the peak power. The nonlinear absorption coefficient α_2 was measured to be 0.17 ($\pm$0.05) cm/GW. From the above results we can evaluate the figure of merit to be 0.15, i.e. less than unity. Therefore the figure of merit for a useful device is satisfied, making this material a promising candidate for all-optical switching.

In conclusion, we have measured the third order nonlinearities of the ISQ doped polymer fiber at the communication wavelength of 1.32 μm.

References :

1. M. G. Kuzyk, J. E. Sohn, and C. W. Dirk, J. Opt Soc. Am. B **5**, 842 (1990); M. G. Kuzyk, and C. W. Dirk, Phys. Rev. A 41, 5098 (1990)
2. M. G. Kuzyk, U. C. Paek, and C. W. Dirk, Appl. Phys. Lett. **59**, 902 (1991)
3. C. Poga, M. G. Kuzyk, and C. W. Dirk, J. Opt. Soc. Am. B **11**, 80 (1994)
4. D. W. Garvey, Q. Li, M. G. Kuzyk, C. W. Dirk, and S. Martinez, Opt Lett **21**, 104 (1996)
5. K. B. Rochford, R. Zanoni, G. I. Stegeman, W. Krug, E. Miao, and M. W. Beranek, Appl. Phys. Lett. **58**, 13 (1991)

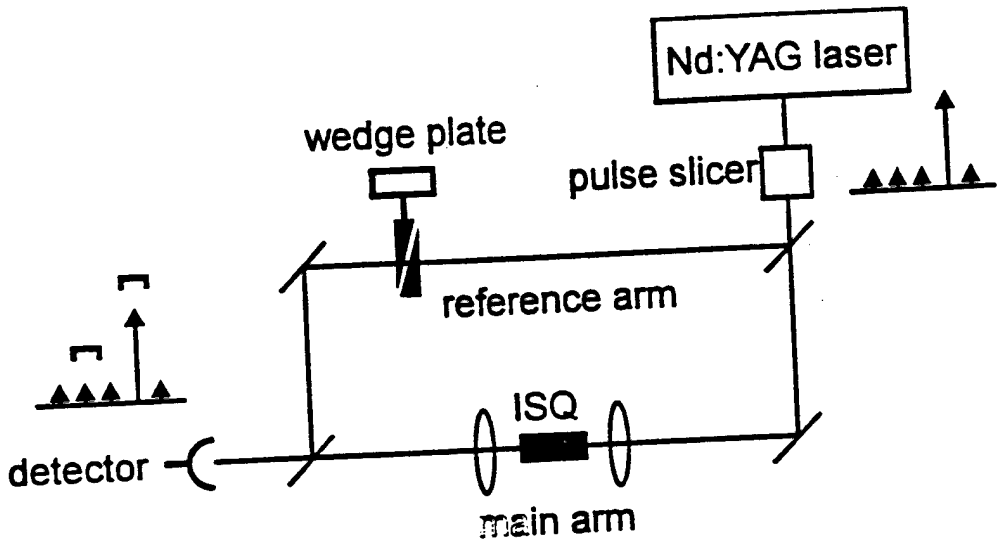

Figure 1 Experimental set up for Mach Zehnder interferometer

ESSENTIAL STATE ANALYSIS OF SQUARAINES USING QUADRATIC ELECTROABSORPTION

K.S. Mathis[1] and M.G. Kuzyk

Department of Physics, Washington State University, Pullman, WA 99164-2814

C.W. Dirk, S. Martinez, H. Selnau, Jr., P. Craig, and L. Green

Department of Chemistry, University of Texas, El Paso, Texas, 79968-0513

The imaginary part of the third order nonlinear optical susceptibility is evaluated for several squaraine dyes to determine the characteristics of their excited states. Quadratic electroabsorption (QEA) and linear absorption spectroscopy are used for this evaluation as well as to determine mechanisms (reorientational, cis-trans isomerization) responsible for the nonlinear optical properties of these dye-doped polymers. The value of $\chi^{(3)}$ (in which we use an optical field to probe the effect of a static field) is of importance in evaluating the applicability of these thin-film dyes to all-optical devices. The nonlinear responses are compared to various models, including three- and four-level models, to help determine which models are most suitable for predicting nonlinear behavior.

Keywords: squaraines, dye-doped polymers, quadratic electroabsorption

1. INTRODUCTION

The three-level model has been shown to be an effective way to characterize the quadratic electroabsorption response of solute squaraine molecules that are imbedded in a solid poly(methyl methacrylate) polymer solution[1]. The theoretical three state model includes a one-photon state and a two-photon state (whose transition moments and energies depend on the particular dye). The four-level model, which includes another two-photon state in addition to the states used for the three-level model, is shown to be ineffective as a means of fitting the experimental data. Indeed, the dipole moment μ_{13} related to this additional fourth state, which has recently been found necessary to describe third harmonic generation of squaraines in chloroform[2], is inconsistent with our experimental QEA data. Investigations of a four-level model, which includes two one-photon states (both close in energy to the one-photon state of the three-level model) and a two photon state (with an excited state energy and a transition moment given by the three-level model), used to fit the measured QEA response are addressed for ISQ (a previously measured squaraine) and a new pyryllium squarylium dye (designated PYSQ). This is prompted by the shoulder that appears at the top of the PYSQ absorption spectrum. It is speculated that this hump is a signature of an additional one-photon state.

[1]Present Address: France Telecom, CNET, CDP/EQM, 196 avenue Henri Ravera, 92225 BAGNEUX, France
mathis@bagneux.cnet.fr

Another small shallow hump appearing in the absorption spectra of some squaraines is thought to be indicative of some underlying mechanism such as molecular reorientation or vibronic levels. By including the term $Im[\alpha(\omega)\alpha(0)]$ with the three-level model, it was determined that addition of this term resulted in little or no improvement in the theoretical fit, implying that molecular reorientation can be ignored. In contrast, by taking cis-trans isomerization into account (or the linear addition of two separate three-level models), the quadratic electroabsorption spectrum is more closely described theoretically than with the original three level model. Two squaraines (ISQ and BSQ) are known to exist as a mixture of isomers[3]. By applying this cis-trans model to BSQ, the theory results in a considerably better fit for this squaraine (as seen in Figure 1).

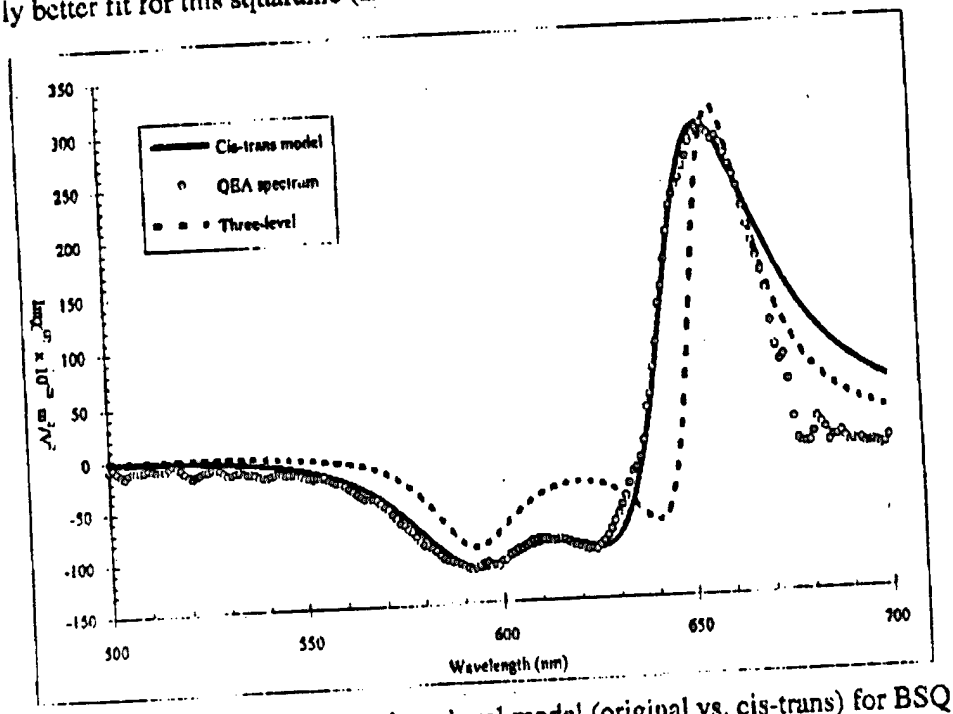

Figure 1: Comparison of the three-level model (original vs. cis-trans) for BSQ

State n	Transition Moment $\mu_{n,n-1}$ (D)	Energy E(λ) [eV (nm)]	Half-Width Γ (meV)
1 (C)	11.40	1.93 (642.5 ± 1)	67 ± 3
2 (C)	3.75	2.12 (579.5 ± 1)	80 ± 4
1' (T)	11.10	1.92 (643.5 ± 1)	65 ± 3
2' (T)	3.63	2.09 (593.0 ± 1)	71 ± 3

Table 1: Parameters used in the cis (C) trans (T) isomerization model for BSQ

Similarly, but not to such an extent, cis-trans isomerization provides a closer description for ISQ than the three-level model alone. For squaraines that do not exist as a mixture of isomers (such as TSQ), the three-level model presents a simple and acceptable fit to the nonlinear QEA spectrum.

REFERENCES

1. C. Poga, T.M. Brown, M.G. Kuzyk, JOSA B, **12**, No. 4, 535 (1995)
2. J.H. Andrews, J.D.V. Khaydarov, K.D. Singer, Opt. Lett., **19**, 984 (1994)
3. C.W. Dirk, W.C. Herndon, et al, J. Am. Chem. Soc., **117**, 2214 (1995)

ACKNOWLEDGEMENTS

We thank the Air Force Office of Scientific Research for generously supporting this work.
We also thank Dr. C. Poga for the valuable discussions.

SECOND ORDER HYPERPOLARIZABILITIES OF TETRATHIAFULVALENE AND DITHIAFULVENE DERIVED CROMOPHORES

B. Villacampa[1], J. Garín[2], L.Sánchez[3], J.Orduna[2], R. Alcalá[1], N. Martín[3]

[1]Dpto. Física de la Materia Condensada. [2]Dpto. Química Orgánica.
Universidad de Zaragoza. C/Pedro Cerbuna, 12. 50009 Zaragoza. Spain
[3]Dpto.Química Orgánica I. Universidad Complutense de Madrid.
Ciudad Universitaria. 28040 Madrid. Spain

Abstract

The second-order hyperpolarizabilities of tetrathiafulvalene and dithiafulvene derivatives have been measured at 1.38 μ by using the Electric Field Induced Second Harmonic (EFISH) generation technique. The nature of the acceptor group (formyl *vs.* dicyanomethylene), the substituents on the donor moiety, and the conjugated spacer group have been varied in order to ascertain the effect of these factors on the μβ values of the molecules.

Experimental details

Two series of compounds have been prepared and studied. For the first one (compounds **1** to **3**) a tetrathiafulvalene (TTF) acts as the donor group, whereas a dithiafulvenyl moiety is present in the second one (compounds **4** and **5**).

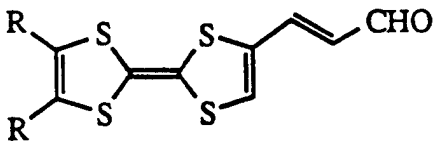

1

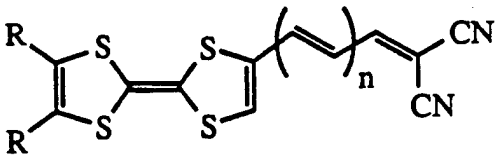

2 n = 0
3 n = 1

a R = H
b R-R = $S(CH_2)_2S$

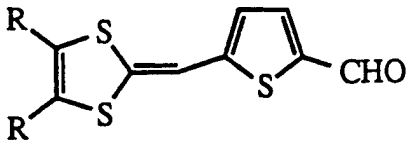

4

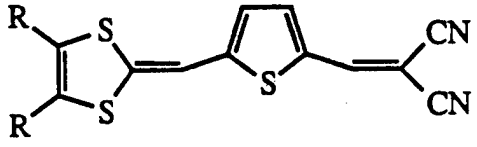

5

a R = H
b R-R = $S(CH_2)_2S$
c R = SCH_3

Compounds **1** have been prepared as previously described [1, 2]. Compounds of type **2** and **3** were synthesized by Knoevenagel reaction of the corresponding formyl derivative. In a similar way, **5** were prepared from **4**, synthesized in turn from Akiba's reagents.

Second order hyperpolarizabilities values of these compounds have been obtained by using the EFISH technique. The light source was a Q-switched Nd-YAG laser operating at 1064 nm with frecuency doubling, together whit a dye laser and a compressed hydrogen-gas Raman cell. The measurements of $\mu\beta$ have been performed in a non linear optical (NLO) spectrometer from SOPRA, with the usual experimental configuration. All the compounds were solved in 1,4-dioxane. The μ values of the molecules were obtained from dielectric constant measurments using the Guggenheim method.

Results

The nonlinear optical properties of a range of compounds bearing a dithiafulvenyl group have been previously studied [3, 4] but compounds **1-3** represent the first examples where second-order optical nonlinearities have been observed in a chromophore in which the TTF core acts as the electron donor.

$\mu\beta$ values up to $1000 \cdot 10^{-48}$ esu have been obtained at 1.38 μ. The measurements show that the change of formyl by dicyanomethylene as the acceptor group results in higher $\mu\beta$ values. The introduction of a ethylenedithio ring as sustituent on the donor group leads to an enhacement of the electronic polarization. These experimental results confirm the trend suggested by preliminar semiempirical calculations.

The rather big red shifted absorption bands in some of the compounds (centered near 600 nm in the dicyanomethylene substituted ones) makes it necessary to complet the measurements at 1.9 μ in order to avoid the near resonance effects of second harmonic absorption in the solutions.

References

[1] J. Garín, J. Orduna, S. Uriel, A.J. Moore, M.R. Bryce, S. Wegener, D.S. Yufit, J.A.K. Howard, *Synthesis*, 489 (1994).

[2] R. Andreu, J. Garín, J. Orduna, M. Savirón, S. Uriel, *Tetrahedron Lett.*, 36, 4319 (1995).

[3] M. Blanchard-Desce, I. Ledoux, J.-M. Lehn, J. Malthête, J. Zyss, *J. Chem. Soc., Chem. Commun.*, 737 (1988).

[4] A. K.-Y. Jen, V. P. Rao, K. J. Drost, K. Y. Wong, M. P. Cava, *J. Chem. Soc., Chem. Commun.*, 2057 (1994).

P-53

Third-Harmonic Spectra of Symmetric and Asymmetric Squaraines

James H. Andrews
Department of Physics & Astronomy
Youngstown State University, Youngstown, Ohio 44555-3616
John D.V. Khaydarov*, and Kenneth D. Singer
Department of Physics
Case Western Reserve University, Cleveland, Ohio 44106-7079
*Currently with *Continuum, Inc., Santa Clara, CA 95051*
Diana L. Hull and Kathy C. Chuang
NASA Lewis Research Center, Cleveland, Ohio 44135-3191

We measured the third-harmonic spectral dispersion for a series of squaraine dyes in chloroform. By fitting the experimental dispersion of the third order susceptibility, γ, to a modified three-level sum-over-states model, we determine the strength and location of the lowest lying two-photon-like transition. For these dyes, we find that the lowest two-photon-like state appears just above the dominant linear absorption peak in energy and that the transition moment to that state makes a significant contribution to the nonlinearity, as do transition moments to one or more higher-lying two-photon-like states in the ultraviolet. We also determine the strength of the dipole moment difference between the ground and first excited state dipole moments of the two noncentrosymmetric squaraine dyes studied. In this abstract, we only report our results for one of the asymmetric dyes.

INTRODUCTION

In molecular materials, such as highly-nonlinear squaraine dyes, the nonlinearity is known to be a function of the dipole transition moments and dipole moment differences between the myriad of electronic states of the material. For both the first and second hyperpolarizabilities, β and γ, one of the most useful simplifications for understanding the structure-property relationships is the observation that the susceptibility is typically dominated by a very limited number of quantum states. For example, the two-level model for β has been used successfully for modeling many smaller conjugated systems such as para-nitroaniline and other substituted benzene molecules.

For many materials, including third-order centrosymmetric materials, the two-state model is inadequate and the contributions from additional excited states must be included. Also, although the two-level model for β has been extensively used in the study of the response of organic dyes, relatively little research has focused on the relationship between β and γ for noncentrosymmetric materials or on the limitations of the two-level model. The same molecular excited states contribute for both β and γ, but in different combinations and with different frequency dependence. The transition moments and dipole moment differences are the same in each case, though their relative importance depends on nonlinear process involved. Experimentally locating and characterizing the most significant excited states using nonlinear optical techniques to probe purely electronic contributions is then of considerable interest for understanding such systems. Third harmonic spectral dispersion measurements are well suited to the study of excited states of these molecular materials because frequencies can be chosen to selectively probe resonant enhancements through intermediate transitions without necessarily involving significant linear absorption at either the input or the detected harmonic frequencies.

MODEL, DATA, AND FITS

In the simplest empirically reasonable approach to third-order systems, a modified three-level model allowing additional higher lying intermediate states (states n in Eq. (1) below), but only one significant excited state in the linear absorption, the expression for γ for third harmonic generation

becomes

$$\gamma_{xxxx}(-3\omega;\omega,\omega,\omega) = \frac{\mu_{01}^2}{4\hbar^3}\left(\Delta\mu_{10}^2 D_{111} - \mu_{01}^2 D_{11} + \left(\sum_n \mu_{1n}^2 D_{1n1}\right)\right), \quad (1)$$

where the states n are pure two-photon states, state 0 is the ground state, and μ_{ab} is the transition moment between states a and b and $\Delta\mu_{ab}$ is their dipole moment difference and the D_{lmn} and D_{ln} are the resonant denominators involving the excited state energies $\hbar\omega_{n0}$ and widths $\hbar\Gamma_{n0}$.

To study the spectral dispersion of the third harmonic generated in low concentration solutions of dye, we recorded third harmonic Maker fringes for the dye-chloroform solutions and for pure chloroform at each wavelength. The ratio of the amplitude of the fringes from the squaraine-chloroform solutions and from the pure chloroform reference for one of our dyes, C16-ISQ-BSQ, is plotted in Fig. 1, together with our least squares fit. A ratio of unity on this graph implies that the presence of the dye at this concentration does not change the amplitude of the third harmonic fringes from the amplitude obtained for pure chloroform. We can infer the location and strength of a significant two-photon resonance in the dye solution from our fit to the shape of the dispersion to the predictions of Eq.(1). By using the linear absorption spectrum to determine μ_{01}, ω_{01} and Γ_{01}, we find that the dispersion of the third harmonic in this region is very sensitive to the location and strength of the 2^1Ag two-photon transition which is seen in the change in sign of the third-harmonic response between 1.15 and 1.3 μm fundamental.

The contribution from the dipole moment difference is seen in the secondary oscillation in the ratio of the third harmonic at around 1.27 μm fundamental (see arrow in Fig.). This secondary resonance is consistent with the contribution of the $\Delta\mu_{01}^2 D_{111}$ term in Eq. (1). Our best fit was then obtained by assuming that this dye is weakly noncentrosymmetric ($\Delta\mu_{01}^2 = 4 \pm 1.5$ Debye). The contribution to D_{111} at $2\omega = \omega_{01}$ approximately reproduces the features at 1.27 μm shown in the figure. Since, the linear absorption peak for this molecule is about 635 nm, this feature is located at the frequency appropriate to an intermediate transition between the ground state and the first excited state, which is only permitted for noncentrosymmetric systems and is modeled using the $\Delta\mu_{01}^2 D_{111}$ term in Eq. (1).

J. H. Andrews acknowledges support from the NASA Lewis Research Center in the form of a Graduate Researchers Fellowship. This work has also been supported in part by AFOSR grant no. F49620-93-1-0202.

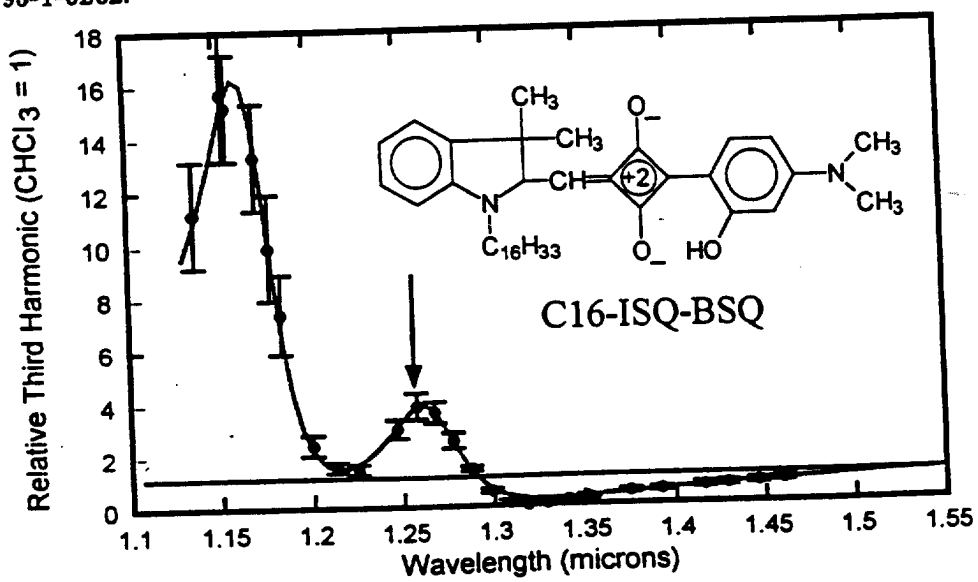

Figure 1: Ratio of C16-ISQ-BSQ solution third harmonic fringe amplitudes to chloroform.

Third-Harmonic Spectra of Symmetric and Asymmetric Squaraines

James H. Andrews
Department of Physics & Astronomy
Youngstown State University, Youngstown, Ohio 44555-3616
John D.V. Khaydarov*, and Kenneth D. Singer
Department of Physics
Case Western Reserve University, Cleveland, Ohio 44106-7079
*Currently with *Continuum, Inc., Santa Clara, CA 95051*
Diana L. Hull and Kathy C. Chuang
NASA Lewis Research Center, Cleveland, Ohio 44135-3191

We measured the third-harmonic spectral dispersion for a series of squaraine dyes in chloroform. By fitting the experimental dispersion of the third order susceptibility, γ, to a modified three-level sum-over-states model, we determine the strength and location of the lowest lying two-photon-like transition. For these dyes, we find that the lowest two-photon-like state appears just above the dominant linear absorption peak in energy and that the transition moment to that state makes a significant contribution to the nonlinearity, as do transition moments to one or more higher-lying two-photon-like states in the ultraviolet. We also determine the strength of the dipole moment difference between the ground and first excited state dipole moments of the two noncentrosymmetric squaraine dyes studied. In this abstract, we only report our results for one of the asymmetric dyes.

INTRODUCTION

In molecular materials, such as highly-nonlinear squaraine dyes, the nonlinearity is known to be a function of the dipole transition moments and dipole moment differences between the myriad of electronic states of the material. For both the first and second hyperpolarizabilities, β and γ, one of the most useful simplifications for understanding the structure-property relationships is the observation that the susceptibility is typically dominated by a very limited number of quantum states. For example, the two-level model for β has been used successfully for modeling many smaller conjugated systems such as para-nitroaniline and other substituted benzene molecules.

For many materials, including third-order centrosymmetric materials, the two-state model is inadequate and the contributions from additional excited states must be included. Also, although the two-level model for β has been extensively used in the study of the response of organic dyes, relatively little research has focused on the relationship between β and γ for noncentrosymmetric materials or on the limitations of the two-level model. The same molecular excited states contribute for both β and γ, but in different combinations and with different frequency dependence. The transition moments and dipole moment differences are the same in each case, though their relative importance depends on nonlinear process involved. Experimentally locating and characterizing the most significant excited states using nonlinear optical techniques to probe purely electronic contributions is then of considerable interest for understanding such systems. Third harmonic spectral dispersion measurements are well suited to the study of excited states of these molecular materials because frequencies can be chosen to selectively probe resonant enhancements through intermediate transitions without necessarily involving significant linear absorption at either the input or the detected harmonic frequencies.

MODEL, DATA, AND FITS

In the simplest empirically reasonable approach to third-order systems, a modified three-level model allowing additional higher lying intermediate states (states n in Eq. (1) below), but only one significant excited state in the linear absorption, the expression for γ for third harmonic generation

becomes

$$\gamma_{xxxx}(-3\omega;\omega,\omega,\omega) = \frac{\mu_{01}^2}{4\hbar^3}\left(\Delta\mu_{10}^2 D_{111} - \mu_{01}^2 D_{11} + \left(\sum_n \mu_{1n}^2 D_{1n1}\right)\right), \quad (1)$$

where the states n are pure two-photon states, state 0 is the ground state, and μ_{ab} is the transition moment between states a and b and $\Delta\mu_{ab}$ is their dipole moment difference and the D_{lmn} and D_{ln} are the resonant denominators involving the excited state energies $\hbar\omega_{n0}$ and widths $\hbar\Gamma_{n0}$.

To study the spectral dispersion of the third harmonic generated in low concentration solutions of dye, we recorded third harmonic Maker fringes for the dye-chloroform solutions and for pure chloroform at each wavelength. The ratio of the amplitude of the fringes from the squaraine-chloroform solutions and from the pure chloroform reference for one of our dyes, C16-ISQ-BSQ, is plotted in Fig. 1, together with our least squares fit. A ratio of unity on this graph implies that the presence of the dye at this concentration does not change the amplitude of the third harmonic fringes from the amplitude obtained for pure chloroform. We can infer the location and strength of a significant two-photon resonance in the dye solution from our fit to the shape of the dispersion to the predictions of Eq.(1). By using the linear absorption spectrum to determine μ_{01}, ω_{01} and Γ_{01}, we find that the dispersion of the third harmonic in this region is very sensitive to the location and strength of the 2^1Ag two-photon transition which is seen in the change in sign of the third-harmonic response between 1.15 and 1.3 μm fundamental.

The contribution from the dipole moment difference is seen in the secondary oscillation in the ratio of the third harmonic at around 1.27 μm fundamental (see arrow in Fig.). This secondary resonance is consistent with the contribution of the $\Delta\mu_{01}^2 D_{111}$ term in Eq. (1). Our best fit was then obtained by assuming that this dye is weakly noncentrosymmetric ($\Delta\mu_{01}^2 = 4 \pm 1.5$ Debye). The contribution to D_{111} at $2\omega = \omega_{01}$ approximately reproduces the features at 1.27 μm shown in the figure. Since, the linear absorption peak for this molecule is about 635 nm, this feature is located at the frequency appropriate to an intermediate transition between the ground state and the first excited state, which is only permitted for noncentrosymmetric systems and is modeled using the $\Delta\mu_{01}^2 D_{111}$ term in Eq. (1).

J. H. Andrews acknowledges support from the NASA Lewis Research Center in the form of a Graduate Researchers Fellowship. This work has also been supported in part by AFOSR grant no. F49620-93-1-0202.

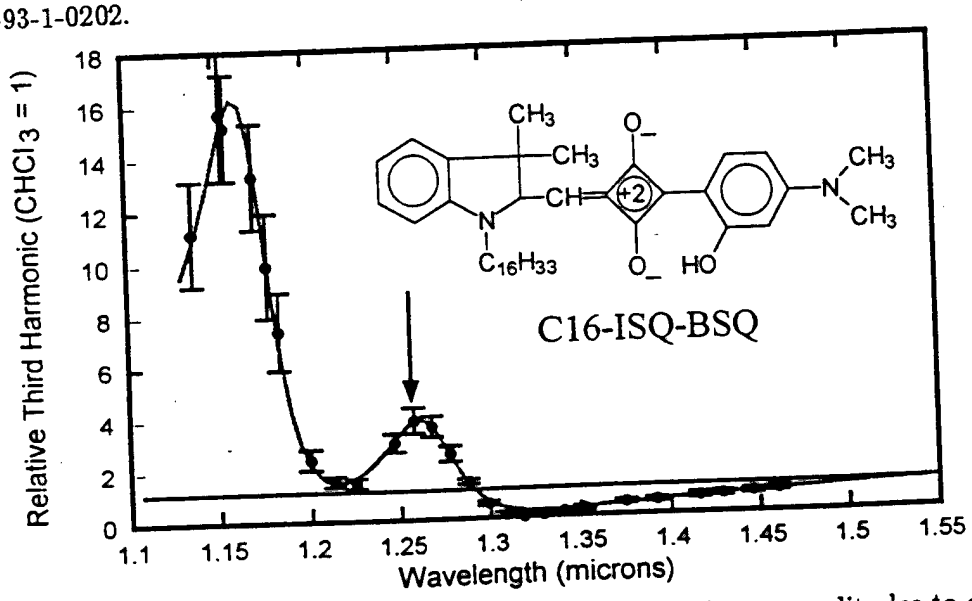

Figure 1: Ratio of C16-ISQ-BSQ solution third harmonic fringe amplitudes to chloroform.

Potential of organic and organo-mineral crystals in low threshold near infrared optical parametric oscillators

S. Khodja, D. Josse and J. Zyss*
France Telecom, CNET-Paris B, Laboratoire de Bagneux
196 Avenue Henri Ravéra, BP107, 92225 Bagneux Cedex, FRANCE
**) Present address: CREOL University of Central Florida*
Orlando, FL 32816

SUMMARY

Conception and elaboration of new nonlinear optical materials with optimized properties are crucial towards the development and practical use of optical parametric amplificators (OPA's) and oscillators (OPO's) towards various signal processing applications.

Among currently developed nonlinear crystals, organic molecular crystals stand-out in view of their high nonlinearity and high damage threshold in the pulsed regime. Adequate spectral tailoring is achieved in the case of the paranitroaniline family for pumping in the visible with emission in the wavelength range encompassing optical fiber transmission windows. The remarkable properties of the N-(4-Nitrophenyl)-L Prolinol (NPP) crystal [1] result from the optimized arrangement of the chromophore units in the monoclinic unit cell which has enabled to demonstrate OPO's with very low threshold (0.5 $MWcm^{-2}$)[2-3] in the nanosecond regime, tuned by either angle or pump wavelength variation[3] over a broad spectral range from 0.9 μm to 1.7 μm [2-3].

Moreover, the concept of organo-mineral materials has been shown to combine the favourable structural properties of inorganics with the enhanced nonlinearities of organics[4]. Strong ionic and hydrogen bonding interactions between organic cations and mineral anions overcome the usual drawbacks of more traditional Van-der-Waals structures. A successful outcome of this approach is 2-amino-5-nitropyridinium-dihydrogen-phosphate (2A5NPDP)[5] which has been precisely tailored towards near-infrared applications. The potential of 2A5NPDP has been taken advantage of in an original non-critical configuration versus both

angle and signal wavelength to demonstrate efficient optical parametric interactions, we believe for the first time in this family materials. High gain parametric emission and amplification (from 10^6 to 10^9) in the picosecond regime and optical parametric oscillation with low threshold (6 $MWcm^{-2}$) high conversion efficiency in the nanosecond regime have been demonstrated in this non-critical configuration, at strategic 1.5 μm and 1.3 μm telecommunication wavelengths.

References

[1] See for example "Molecular Nonlinear Optics: Materials, Physics and Devices" J. Zyss (ed.) (Academic Press, Boston,1993); J. Zyss, J. Phys. D: Appl. Phys. **26**, B198 (1993).

[2] S. X. Dou, D. Josse, and J. Zyss, J. Opt. Soc. of Am. **10**, 1708 (1993).

[3] D. Josse, S. Khodja, J. Badan, I.D.W. Samuel and J. Zyss, Appl.Phys. Lett. **64**, 3655(1994).

[4] R. Masse and J. Zyss, Mol. Eng. **1**, 141 (1991); R. Masse, M. Bagieu-Beucher, J. Pecaut, J-P Levy and J. Zyss, Nonlin. Opt. **5**, 413 (1993).

[5] Z. Kotler, R. Hierle, D. Josse, J. Zyss and R. Masse, J. Opt. Soc. Am. B **9**, 534 (1992).

P-55

60GHz millimeter wave detection by electro-optic effect of DAST crystal

T.Taniuchi, N.Mashio, Y.Konno, H.Ito, D.Dawn and T.Yoneyama
Research Institute of Electrical Communication
Tohoku University
2-2-1 Katahira, Aoba-ku, Sendai 980-77, JAPAN

Organic crystals which have a large electro-optic coefficient and a small dielectric constant are very attractive material for the high speed modulation and detection. In this paper, we demonstrate for the first time the coherent detection of 60GHz millimeter wave by using DAST(4-dimethylamino-N-methyl-4-stilbazolium tosylate) as an electro-optic sensing material. The electro-optic coefficient r_{11} of DAST crystal has been reported to be more than 130pm/V at 820nm[1,2].

DAST crystals with dimensions up to 10x10x2mm^3 have been successfully grown in our group from methanol solution by slowly lowering the temperature at a rate of 0.2℃/h . The wavelength of the absorption edge(E ∥ a) of the grown DAST crystal is 720nm.

For the electro-optic(EO) sensing, high quality DAST crystal of 3x3x0.2mm was selected by measuring the extinction ratio of the cross polarization. High reflecting(HR) dielectric mirror was evaporated on one side of the DAST crystal. The experimental set up is shown in Fig.1. Continuous wave Nd:YAG laser at 1064nm was used as a light source and was incident on the DAST crystal through a polarization beam splitter(PBS). The reflected optical signal, which was modulated by the electric field, was separated by PBS and detected by Si photodiode. The output signal(Vout) was detected through a lock-in amplifier.

For the calibration of this EO sensing system, coplanar electrodes of aluminum, which were separated by 1.5mm, were evaporated on the other side of the DAST crystal. The sensitivity was first calibrated by applying the DC voltage(Vdc) across the electrodes. The obtained sensitivity(Vout/Vdc) was 12.4 μ V/V by forcusing the Nd:YAG laser in between the electrodes.

A gunn diode oscillator which puts out 60GHz cw signal at approximately 140mW was used as the millimeter wave source, and the millimeter wave chopped at 230Hz was radiated through a 40mm long dielectric antenna made by Teflon. In our experiment, the output signal of 14.5 μ V was obtained when the dielectric antenna was placed at a distance of 1mm from the DAST crystal. Therefore, the electric field strength of 60GHz millimeter wave was estimated to be about 1.2V/mm. The dependence of output signal on distance between the dielectric antenna and the DAST crystal was measured as shown in Fig.2. The solid line is the fitting curve following the relation, Vout $\propto Z^{-0.5}$. We have also successfully measured the directivity of the dielectric antenna by transverse scanning of the dielectric antenna.

In conclusion, we have demonstrated the coherent detection of 60GHz millimeter wave by DAST as an electro-optic sensing material. To realize the higher sensitivity, the development of growing high quality DAST crystals with thickness more than 2mm are required. The electro-optic sensing techniques using organic crystals have many advantages for the coherent detection of the microwave, millimeter and terahertz waves.

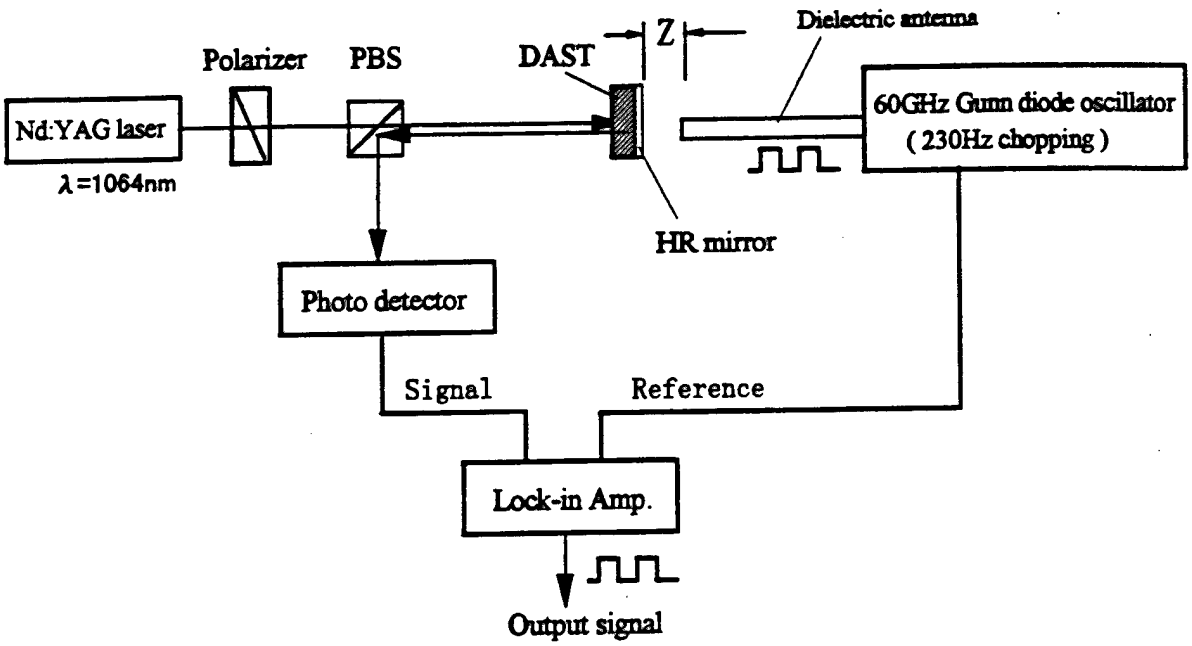

Fig.1 Experimental setup for 60GHz millimeter wave detection using DAST crystal

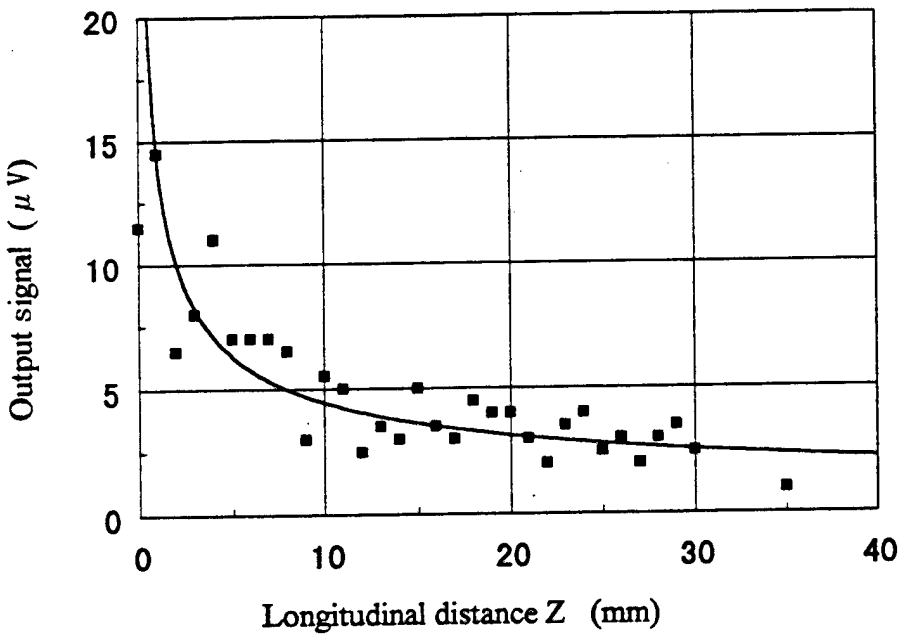

Fig.2 Output signal as a function of the distance between the DAST crystal and the dielectric antenna.

Acknowledgement
The authors are greatly indebted to Professor H. Nakanishi and Dr. S. Okada of Institute for Chemical Reaction Science,Tohoku University, for the synthesis of DAST and their useful discussions about crystal growth and characterization.

References
1)J.W.Perry,S.R.Marder,K.Perry and E.T.Sleva, SPIE Vo.1560 Nonlinear Optical Properties of Organic Materials (1991)
2) G.Knopfle,R.Schlesser,R.Ducret and P.Gunter, Nonlinear Optics, Vol.9, pp.143-149 (1995)

Vibration Suppression in a Sheet with a Fabry-Perot Photomechanical Device.

D. J. Welker
Sentel Technologies, L.L.C., Box 41-1, NE 1615 Eastgate Blvd., Pullman, WA 99163

M. G. Kuzyk
Department of Physics, Washington State University, Pullman, WA 99164-2814

A photomechnical material changes shape in response to light. There are many mechanisms, each with their own characteristic response time, that can lead to a change in the shape of a material in response to light illumination.[1,2] This effect has been used to demonstrate several novel devices: A long photomechanical polymer fiber, when used with an external interferometer, has been used to make an all-optical device that stabilizes the position of a mirror.[3,4] A short photomechanical polymer fiber with reflecting ends that forms a Fabry-Perot cavity (called a mesoscale photomechanical unit (MPU)) has been shown to be multistable - that is, it has several length states for a given level of light illumination.[5] An MPU has also been demonstrated to act as an all-optical modulator, in which one beam can be modulated by a second beam that changes the length of the device thereby changing the intensity of the first beam.[6]

In this report, we show that a mesoscale photomechanical unit that is attached to a plastic sheet can actively suppress vibrations in the sheet. This shows that the MPU is truly sensitive to mechanical vibrations and is capable of acting on an external mass of material. A taut plastic reflective membrane is held around its perimeter by a metal ring. A Disperse Red 1 (DR1) dye/doped poly(methyl methacrylate) MPU of 1 cm length and 110 μm diameter is attached to a reflective membrane. The experimental apparatus is shown schematically in Figure 1. Light is launched into the MPU from above while a second laser is reflected from the bottom mirror so that its deflection angle can be determined. The elastic modes of the membrane are excited by external mechanical vibrations and monitored by the change in deflection angle. A measure of detector #2 voltage is directly related to movements in the membrane. The MPU stabilizer, then, must act on the membrane to stabilize vibrations in the system. Note that detector #1 monitors the light entering the MPU. Detector #3 is used as a reference detector. An acoustical source can be used to drive the membrane.

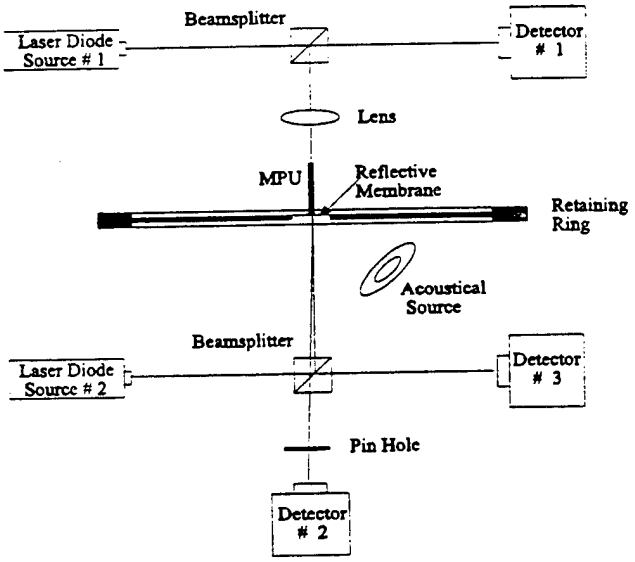

Figure 1. Crossectional view of a vibrational damping experiment.

In a previous experiment the movement of the membrane was monitored interferometrically and the source of mechanical agitation to the membrane included environmental noise from air currents, table vibrations, thermal variations, and acoustical noise - which carry a broad fourier spectrum of frequencies. The average amount of active damping provided

by the MPU was 5.6 dB from 0 to 500Hz and 2.7 dB from 0 to 5KHz. Figure 2 shows the Fast Fourier transform of the interferometer output with the MPU powered and unpowered.

These results are encouraging because we believe that they define a lower limit on the degree of stabilization for the following reasons. First, the MPU that was used in these tests had no reflectors so that the cavity finesse is much lower than possible when metal reflectors are deposited. Our characterization experiments on MPUs clearly show that the higher reflectivities achievable by metalization would result in much more dramatic stabilization. Secondly, the interferometric method of determining the degree of vibration suffers from offset biasing. Depending on the tuning of the interferometer, the degree of stabilization can appear much less than the actual degree of mechanical stabilization. An analysis of the interferometer shows that the degree of stabilization at any frequency is a lower limit. Based on this alone, the average degree of stabilization may be 10dB. Third, these experiments use ambient noise to determine the stabilization efficiency. Because the noise amplitudes are low, the system may be near its most stable level. With a controlled source of vibration, the degree of stabilization could be evaluated more accurately. Finally, note also that when the light is turned off, the MPU provides some degree of passive stabilization, but the data show the degree of active stabilization beyond that of the passive system. The overall degree of stabilization due to the MPU is most likely better than shown by preliminary measurements.

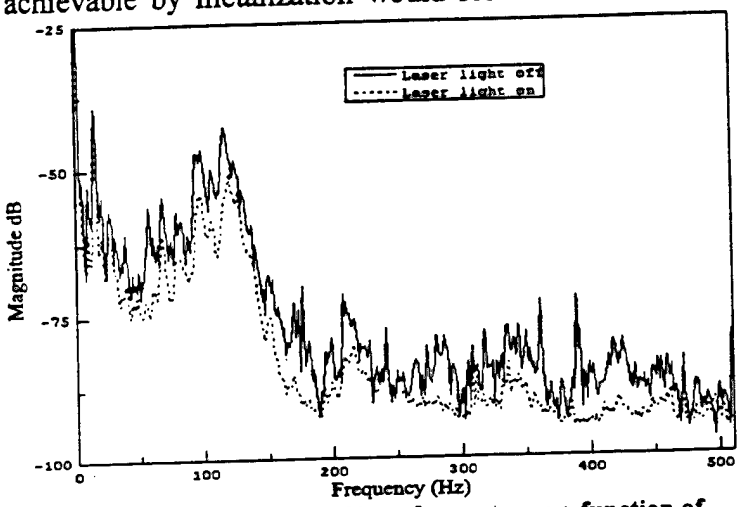

Figure 2. Output spectrum of interferometer as a function of frequency.

More controlled experiments are in progress in which vibrations are excited with a monochromatic acoustical source. The vibration spectrum can then be measured as a function of driving frequency.

In conclusion, we have demonstrated active stabilization of a plastic sheet with an MPU in which vibration suppression is at least 5dB from 0 to 500Hz, and at least 3dB from 500Hz to 5kHz.

The authors wish to acknowledge the Army Research Office for supporting this work under an STTR Phase I contract DAAH04-96-C-0006.

References

[1] D. J. Welker and M. G. Kuzyk, Proceedings of Second International Conference on Intelligent Materials, p. 1308 (Technomic, Lancaster, 1994).

[2] S. Zhou and M. G. Kuzyk, Proceedings of Second International Conference on Intelligent Materials, p. 1375 (Technomic, Lancaster, 1994).

[3] D. J. Welker and M. G. Kuzyk, Appl. Phys. Lett. **64**, 809 (1994).

[4] M. G. Kuzyk, D. J. Welker, and S. Zhou, Nonlinear Optics **10**, 409 (1995).

[5] D. J. Welker and M. G. Kuzyk, Appl. Phys. Lett. **66**, 2792 (1995).

[6] D. J. Welker and M. G. Kuzyk, Appl. Phys. Lett., **69**, 13 (1996).

Second Order Nonlinear Optical Properties of Poled Polymers Consisting of Two-dimensional Charge Transfer Molecules

T. Watanabe, S. Miyata
Tokyo University of Agriculture and Technology
Nakamachi, Koganei-shi, Tokyo 184, Japan

T. Isoshima, T. Wada, H. Sasabe
The Institute of Physical and Chemical Research
Hirosawa, Wako-shi, Saitama, 351-01, Japan

S. C. Lee
Kum-oh National University of Technology
Sin Pyung, Kumi, Kyungbuk, 730-070, Korea

1. Introduction

The organic molecules which possess pi-conjugated systems containing donor and acceptor groups show the large optical nonlinearities. Recently poled polymer systems are of scientific and practical interests due to the their ultra fast response upto 60 GHz, good processability and large optical nonlinearity. Especially rapid development of optical communication technologies needs high-speed digital switching, improved network, and high density recording. In order to obtain second order nonlinear optical (NLO) materials, the lack of inversion symmetry in a medium is required. In general amorphous polymer films do not possess noncentrosymmetry after spin-coating or casting. The additive noncentrosymmetric structure order is induced by using electric field poling. Most of researches focused their attention on the one-dimensional charge transfer characteristic NLO dye which is introduced into polymer backbone as side chain group. These molecules possess large β_{xxx} component and other tensor components are almost negligible. On the other hand, Yamamoto et al. developed two-dimensional charge transfer characteristic (2D-CT) NLO dye, which consisted of two one-dimensional charge transfer NLO dye connected via methylene bridge. Typical conformation of these molecules is similar to the Greek character Λ and it is well known to as Λ shaped molecule. β_{xyy} component of Λ shaped molecules are larger than that of β_{xxx} component. After this research different kinds of molecules with 2D-CT characteristic were reported by Nalwa et al. Recently, the NLO properties of polyarylamine and polyurea consisting of 2D-CT were also studied by Tao et al. The advantages of these main-chain polymer are as follows. 1) Poling is relatively easy compared with head to tail type main chain polymer since the net dipole moment is perpendicular to the polymer chain, reorientation of main-chain is not necessary. 2) There is relatively small β relaxation due to side chain free structure. 3) The large number of chromophore density can be expected. In this presentation we report second-order NLO properties of main chain polymer consisting of two-dimensional charge transfer molecules. Especially we focus our attention on the relationship between βxyy components and d coefficients.

2. Experimental

The chemical structure of main chain polymer used in this experiment is shown in Formula 1. The nonlinear optical coefficients were measured according to the Maker-fringe method using Q-switched pulse Nd:YAG laser (1064 nm, 10 ns). The molecular hyperpolarizabilities were theoretically calculated by MOPAC-PM3 method. The polymer was abbreviated as DADNB-8.

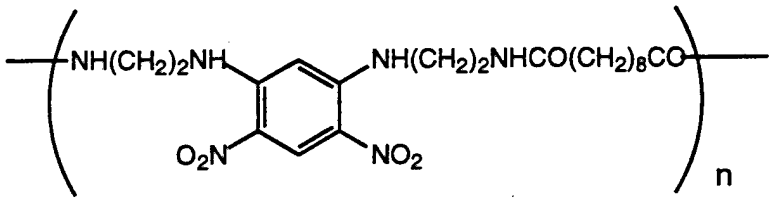

Formula 1

3. Results and discussions

Chromophore of DADNB-8 polymer has amino groups located para position as well as ortho position to nitro groups. Where x is parallel to the dipole moment and y is perpendicular to x and in the plane. The CT interaction between the two pairs of donor and acceptor lead to 2-D nonlinearity. β_{xyy} components of this molecule is about 3 times larger than that of β_{xxx} component, whereas β_{xzz} is negligible. This large β_{xyy} components allow to exhibit an unique nonlinear optical properties when films were drawn and poled. The d_{33}, d_{31} and d_{15} of DADNB-8 were found to be 9.6, 2.5 and 3.6 pm/V, respectively. In general d_{31} is equal to d_{15} due to Kleinman symmetry, however DADNB-8 does not satisfy Kleinman symmetry. The relationship between nonlinear optical coefficients and first-order hyperpolarizability was described by oriented gas description.

$$d_{33} \propto \left(\frac{\mu E}{5kT}\beta_{xxx} + \frac{\mu E}{5kT}\beta_{xyy} + \frac{\mu E}{5kT}\beta_{xzz} \right) \quad (1)$$

$$d_{31} \propto \left(\frac{\mu E}{15kT}\beta_{xxx} + \frac{2\mu E}{15kT}\beta_{xyy} - \frac{\mu E}{15kT}\beta_{yxy} + \frac{2\mu E}{15kT}\beta_{xzz} - \frac{\mu E}{15kT}\beta_{zxz} \right) \quad (2)$$

$$d_{15} \propto \left(\frac{\mu E}{15kT}\beta_{xxx} + \frac{1}{2}\left(\frac{3\mu E}{15kT}\beta_{yxy} - \frac{\mu E}{15kT}\beta_{xyy}\right) + \frac{1}{2}\left(\frac{3\mu E}{15kT}\beta_{zxz} - \frac{\mu E}{15kT}\beta_{xzz}\right) \right) \quad (3)$$

According to the oriented gas description, the difference of d_{31} and d_{15} may ascribe to β_{xyy} and β_{yxy} components. In order to confirm this point, β components of DADNB-8 were calculated by using MOPAC-PM3 method. We found that β_{yxy} of DADNB-8 is 1.1 times larger than β_{xyy}. This difference was only observed when the nonlinear optical coefficients were measured in resonant area. In fact, DADNB-8 shows the small absorption around 532 nm. Same dispersion of β_{xyy} and β_{yxy} in p-nitroaniline was already reported by Garito. While there is no report of breaking of Kleinman symmetry in poled polymer consisting of one-dimensional charge transfer molecules, since the β_{xyy} and β_{yxy} components are relatively too small compared to β_{xxx} component. The decay of d coefficient for DADNB-8 was also studied. We found that relaxation time is over 1,000 hours at 100 . C. Main chain polymer consisting of 2D-CT molecules will be promising materials for EO modulator due to their good optical nonlinearity and temporal stability.

References.

1. H. Yamamoto, S. Katogi, T. Watanabe, H. Sato, S. Miyata and T. Hosomi, Appl. Phys. Lett., **6 0**, 935(1992)
2. H. S. Nalwa, T. Watanabe and S. Miyata, Opt. Mater., **2**, 73(1993)

ELECTROLUMINACENT MATERIALS BASED ON 2,5-BIS-(4-ALKOXY PHENYLENE VINYLENE)THIOPHENES

Mingqian He, Dmitri Voloschenko and L.-C. Chien,* Chemical Physics and Liquid Crystal Institute, Kent State University, Kent, OH 44242. S. Blumstengel, R. Dorsinville, A. Edwards, I. Sokolik, Electric Engineering Department of City College of CUNY, New York, NY 10031.

Bis-(phenylene vinylene)]thiophene (BPTs), was investigated as the central core unit in mesogenic molecules **1**.

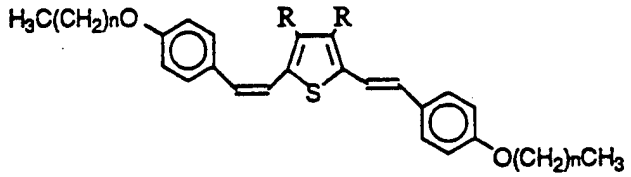

R = H, C_4H_9; n = 5-11

Of particular interest was whether the BPT unit could be self-constrained into a trans-conformation, and thus organize into a liquid crystalline phase. A homologues series of BPTs have been synthesized and found to exhibit the nematic and smectic C mesophases. Their physical and mesomorphic properties as well as light emitting characteristics will be reported.

This research was supported in part by the NSF ALCOM Center Grant DMR89-20147.

Enhanced Nonlinear Photoprocesses and Scaling and Singularities of Local Fields in Nanocomposite Materials

Mark I. Stockman*, Lakshmi N. Pandey#, and Thomas F. George§

*Department of Physics and Astronomy, Georgia State University, Atlanta, GA 30303-3083
#Departments of Physics and Chemistry, Washington State University, Pullman, WA 99163
§Departments of Physics and Chemistry, University of Wisconsin-Stevens Point, Stevens Point, WI 54481-3897

Clusters and nanocomposites belong to so called nanostructured materials. Properties of such materials may be dramatically different from those of bulk materials with identical chemical composition. Confinement of atoms, electrons, phonons, electric fields, etc., in a small spatial region modifies spectral properties (shifts quantum levels, changes transition probabilities), and also changes the interaction between the constituent particles. In this paper we concentrate on an important source of the modification of properties, namely on local fields.

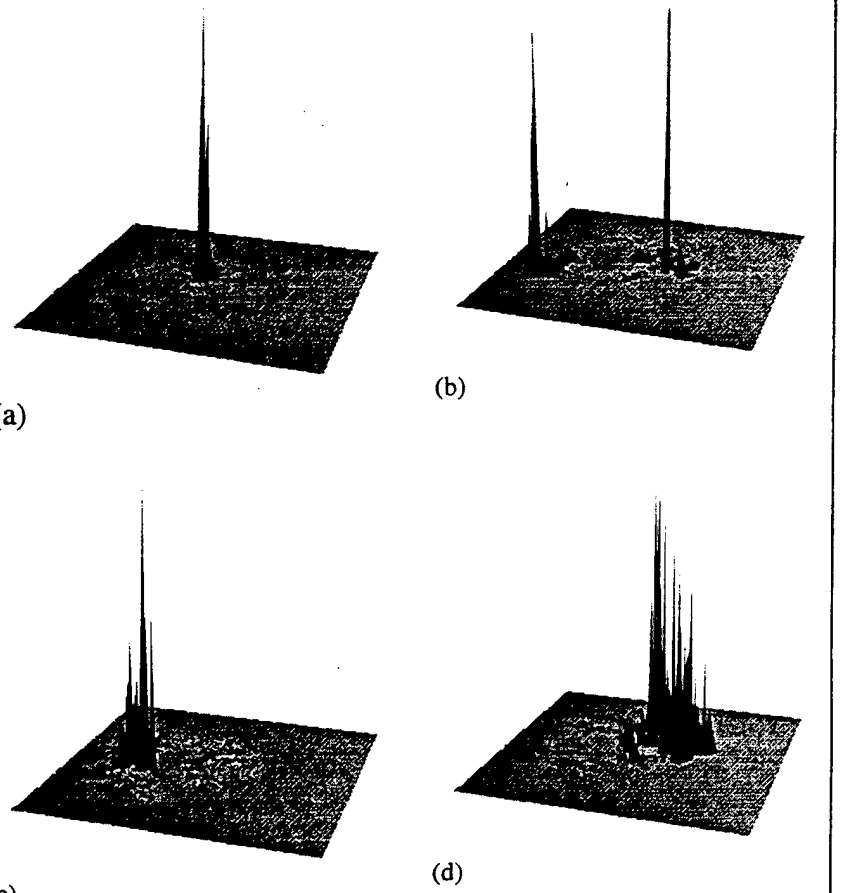

Fig. 1. Spatial intensity for four eigenmodes of an 1000-monomer cluster-cluster aggregate for the values of the spectral parameter X [from (a) to (c)]: -1.28, -1.20, -0.097 and -0.099. The intensity profile is shown over a two-dimensional projection of the cluster.

Electromagnetic radiation interacts with nanoparticles by exciting their eigenmodes. Such eigenmodes are traditionally called surface plasmons. The surface plasmons are eigenvectors of the dipole-dipole interaction.[1] An optical wave with wavelength on order on a (sub)micron scale is very smooth on the nanometer scale of the monomer size. Despite this smoothness, the randomness of the material on the nanometer scale brings about a very singular response, strongly fluctuating in space.[2] An example of such a response is shown in Fig. 1. The sharp peaks seen in this figure are localized on a nanometer scale rather then the micrometer scale as in optical

focusing. These regions of high local fields are responsible for various enhancement effects of nonlinear optical responses, such as nonlinear polarizabilities, photomodification, plasma formation and so on. We called the pattern of the eigenmode localization seen in Fig. 1 as inhomogeneous localization.

To statistically characterize the inhomogeneous localization, we introduce the pair correlation function of the local-field intensity $G_X(r)$ (see Ref.2 for details):

$$G_X(r) = \frac{\sum_n \left[\frac{1}{(X - w_n)^2 + \delta^2} \sum_{i,\alpha;j,\beta} \delta\left(r - \left|\mathbf{r}_i - \mathbf{r}_j\right|\right) (n|i\alpha)^2 (n|j\beta)^2 \right]}{\sum_n \frac{1}{(X - w_n)^2 + \delta^2}}. \qquad (1)$$

We have calculated this function numerically for a large statistical set of randomly generated cluster-cluster aggregates, see Fig. 2. For a spectral wing ($R_0^3|X| >> 1$), this function scale. However, the scaling exponent is negative (-2.3). This indicate that the eigenmodes have an essential singularity at the small scale. In particular, no material object can have such a scaling of density. This is evident for the autocorrelation function of the cluster density shown in Fig. 2. This negative exponent is a reflection of the singular spikes of the intensity seen in Fig. 1.

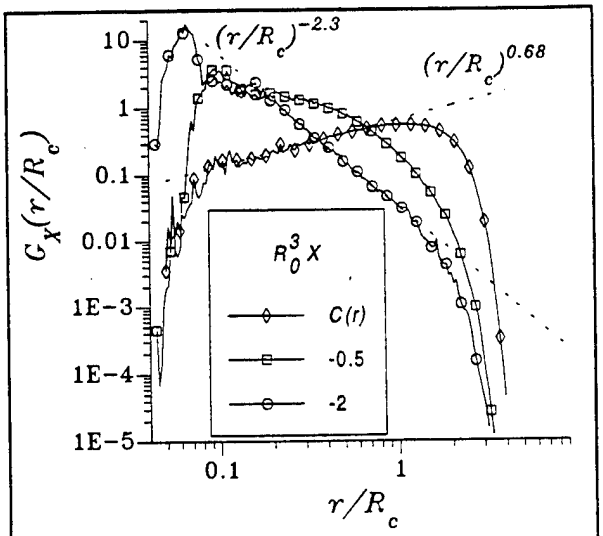

Fig. 2. Autocorrelation function $G_X(r)$ of local-field intensities found for an ensemble of 1000 clusters containing 300 monomers each. For comparison, the density autocorrelation function $C(r)$ is also shown.

On the other hand, the drop-off of the correlation function (within the cluster size) is weak (power-law). This implies that there is no finite localization radius and, correspondingly, no strong localization of the eigenmodes. Instead a new pattern of localization takes place, the inhomogeneous localization.

The observed localization pattern has wide implication for various nonlinear-optical properties. In particular, it has implications for enhanced nonlinear susceptibilities. Second, different incoherent nonlinear phenomena, such as miltiphoton absorption, are enhanced due to the presence of "hot spots" in the distribution of local intensities (see Fig. 1). Finally, very nonlinear and threshold phenomena such as melting, breakdown, plasma formation, etc., will start at the sites of the hot spots.

REFERENCES

1. V.A.Markel, L.S.Muratov, M.I.Stockman, and T.F.George, *Theory and Numerical Simulation of Optical Properties of Fractal Clusters*, Phys. Rev. B **43**, 8183 (1991).
2. M.I.Stockman, L.N.Pandey, and T.F.George, *Inhomogeneous Localization of Polar Eigenmodes in Fractals*, Phys. Rev. B **53**, 2183 (1996).

Femtosecond optical Kerr study of heavy atom effects on the third-order optical nonlinearity of thiophene homologues

Kenji Kamada*, Minoru Ueda, Toru Sakaguchi, Koji Ohta and Toshio Fukumi
Osaka National Research Institute, AIST, MITI, Ikeda, Osaka 563, Japan

The structure-property relationship of molecular third-order nonlinearity is an important subject for obtaining high third-order nonlinearities for future applications of optical switching and optical bistability. Contrary to the case of molecular second-order nonlinearity, the structure-property relationship of molecular third-order nonlinearity has not been well understood yet. In such context, we have been interested in the structure-property relationship and heavy atom effects on third-order molecular nonlinearity of organic and organometalic materials.

On discussing the structure-property relationship, it is important to identify the physical origins contributing to observed macroscopic nonlinearity. The experimentally observed third-order nonlinear optical nonlinearity which causes light-induced refractive index change usually consist of both 'electronic' and 'nuclear' nonlinearities. Electronic nonlinearity arises from *nonlinear electronic distortion* and it is directly associated with the molecular second hyperpolarizability under the Born-Oppenheimer approximation. In contrast, nuclear nonlinearities arise from *linear polarizability changes* caused by molecular orientation and intermolecular interaction, which are induced by incident laser beam. To distinguish individual origins, an effective method is to study time evolution of the nonlinear optical responses. Electronic nonlinearity shows instantaneous response, whereas nuclear nonlinearities show delay due to the inertial nature of nuclear motion against femtosecond impulsive excitation. For this reason, femtosecond time-resolved nonlinear spectroscopy, such as Optical Kerr Gate experiment (OKG) and Impulsive Stimulate light Scattering (ISS), is a good tool to investigate the difference between electronic and nuclear nonlinear responses.

Previously we reported the ultrafast nonlinear optical behavior of thiophene molecule by means of femtosecond Optical Heterodyne Detected (OHD)-OKG experiment[1]. For elucidating heavy atom effects on the third-order nonlinearity of heterocyclic compounds, we extend the study to three thiophene homologues involving furan, thiophene and selenophene that contain calcogen atoms of O, S and Se, respectively[2]. In this paper, we report 'electronic' second hyperpolarizabilities for the above three homologues and discuss heavy atom effect on them. The ultrafast third-order nonlinear responses of the homologues were measured by using OHD-OKG experiment with 60-90 fs laser pulses from a Ti:sapphire laser operating at 82 MHz repetition. From the observed Kerr traces, electronic hyperpolarizabilities were

extracted by the method based on Fourier transform analysis. The Fourier transform analysis was first introduced by McMorrow[3] for interpreting information on molecular dynamics in frequency domain from time domain optical Kerr data. We applied the method for extracting electronic nonlinearity because frequency-independent component in the real part of complex Fourier transformed data is correspond to instantaneous, i.e. electronic, contribution to observed nonlinearity. This analysis can be easily performed on a personal computer with sufficient precision.

From the results, we found that the hyperpolarizabilities of the homologues were in the order of $\sim 10^{-36}$ esu, but the values gradually increased with increasing atomic number of the heteroatom. Also we examined wavelength dispersion of hyperpolarizability at two incident wavelength of 750 and 790 nm and found that the hyperpolarizability did not change from one wavelength to the another. We conclude that the increase in hyperpolarizability is not due to the difference in wavelength dispersion among the homologues. It mainly arises from the difference in static hyperpolarizability.

The electronic hyperpolarizability originates not only from localized electrons on heteroatom but also from delocalized electrons on conjugate system which is affected by presence of heteroatom. However, the conjugation systems of the homologues are so small not likely to affect the third-order nonlinearity so much. Actually, the aromaticity of the homologues reported previously[4] shows that the conjugation is not enhanced by increasing atomic number of the heteroatom. This suggest that contributions from localized electrons on the heteroatom must be dominant in this case.

The present results is important as a part of elucidation of heavy atom effect on third-order hyperpolarizability, which gives a guideline to molecular design of nonlinear optical materials. The further extended study for the homologue containing larger atom and comparison with *ab initio* molecular orbital (MO) calculations are now in progress.

References

1 K. Kamada, M. Ueda, T. Sakaguchi, K. Ohta and T. Fukumi, Chem. Phys. Lett. 249 (1996) 329; K. Kamada, M. Ueda, T. Sakaguchi, K. Ohta and T. Fukumi, European Optical Society Topical Meetings Digest Series, 7 (1996) 249.

2 K. Kamada, M. Ueda, T. Sakaguchi, K. Ohta and T. Fukumi, Chem. Phys. Lett. in printing.

3 D. McMorrow, Opt. Commun. 86 (1991) 236.

4 F. Fringuelli, G. Marino and A. Taticchi, Adv. Heterocycl. Chem. 21 (1977) 119.

High T_g Syndioregic Polymers in Langmuir-Blodgett-Kuhn Films for Second Harmonic Generation

M. J. Roberts, G. A. Lindsay, R. A. Hollins, P. Zarras, J. D. Stenger-Smith, A. P. Chafin, Rena Yee, Eric Nickel, and R. G. Gratz[1]

U.S. Navy, Code 4B2200D, NAWCWPNS, China Lake, CA 93555-6001
[1]Department of Chemistry, Mary Washington College, Fredericksburg, VA

We report here recent progress toward the goal of processing polymers near room temperature to produce all-polymeric nonlinear optical films which may ultimately find application as active waveguides. Our previously reported work[1] has utilized the Langmuir-Blodgett-Kuhn (LBK) technique to produce such films but the noncentrosymmetric order with those materials was lost when heated above 80 °C. The low thermal stability was directly correlated with the chemical structure of the previous materials, namely, the presence of low melting alkyl chains.

Surprisingly, new polymers (Figure 1) designed for spin-casting were found to yield noncentrosymmetric ordered LBK films (Figure 2). The glass transition temperature (T_g) of the bulk polymer is about 240°C, and the upper limit on short term thermal baking stability is about 320°C.

Many materials intended to utilize the LBK methodology for the fabrication of optical waveguides have suffered from low thermal stability of the noncentrosymmetric order. Known strategies to increase the thermal stability of LBK films include interlayer and/or intralayer covalent bonding (ie. crosslinking), incorporation of mesogenic groups to impart liquid crystallinity, removable alkyl groups, and using side-chain chromophores attached to polyimides[2] (high T_g polymer).

LBK films were made using a circular heterolayer trough (NIMA, Coventry). The trough was kept in a glove box continuously purged with nitrogen gas during the film depositions at 24 °C. The substrates were glass slides (Fisher, Cat. # 12-550A) cleaned with H_2SO_4/H_2O_2 and hydrophobicized over refluxing hexamethyldisilazane. A chloroform solution of the polymer was spread at the nitrogen/water interface in one compartment. The polymer layer was compressed a symmetrically at a barrier speed of 10 cm^2/min to a surface pressure of 12 mN/m. The layers were deposited on the downstroke at 3 mm/min (x-type dipping).

Future work will include attempts to deposit thicker films and, if successful, studies of the temporal stability of the noncentrosymmetric order will be performed.

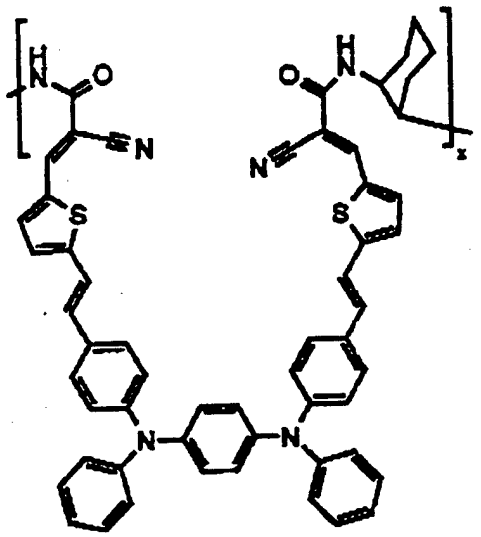

Figure 1. Syndioregic nonlinear optical polymer.

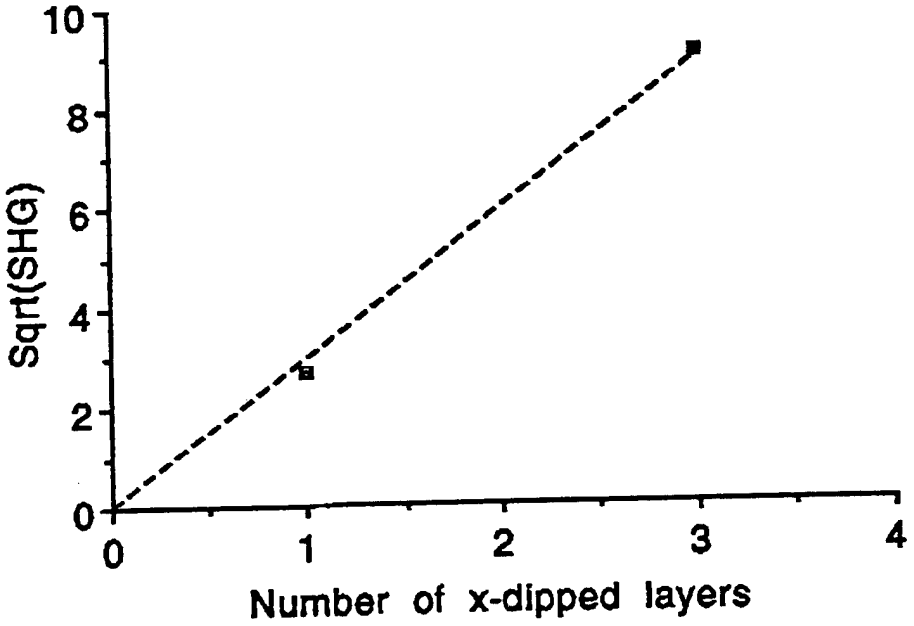

Figure 2. Increase of the SHG as a function of the number of layers.

References

(1) G. Lindsay, K. Wynne, W. Herman, A. Chafin, R. Hollins, J. Stenger-Smith, J. Hoover, J. Cline, J. Roberts *Nonlinear Optics*, volume 15, 139-146, 1996.
(2) T. Yamada, S. Yokoyama, K. Kajikawa, K. Ishikawa, H. Takezoe, A. Fukuda, M. Kakimoto, Y. Imai *Langmuir*, volume 10, 1160-1163, 1994.

Author Index

Author Index

Author Index

Author Index

Author Index

Author Index

Author Index

Author Index

Author Index